PROGRESS
IN PHYSICS

PROGRESS IN PHYSICS

Electronic version of this journal:
http://www.ptep-online.com
http://www.geocities.com/ptep_online

To order printed issues of this journal, contact the Editor in Chief.

Chief Editor
Dmitri Rabounski
rabounski@yahoo.com

Associate Editors
Prof. Florentin Smarandache
smarand@unm.edu
Dr. Larissa Borissova
lborissova@yahoo.com
Stephen J. Crothers
thenarmis@yahoo.com

Department of Mathematics, University of New Mexico, 200 College Road, Gallup, NM 87301, USA

This journal is powered by LaTeX

A variety of books can be downloaded free from the Digital Library of Science:
http://www.gallup.unm.edu/~smarandache

OCTOBER 2006   VOLUME 4

CONTENTS

Information for Authors and Subscribers

Progress in Physics has been created for publications on advanced studies in theoretical and experimental physics, including related themes from mathematics. All submitted papers should be professional, in good English, containing a brief review of a problem and obtained results.

All submissions should be designed in LaTeX format using *Progress in Physics* template. This template can be downloaded from *Progress in Physics* home page http://www.ptep-online.com. Abstract and the necessary information about author(s) should be included into the papers. To submit a paper, mail the file(s) to Chief Editor.

All submitted papers should be as brief as possible. Commencing 1st January 2006 we accept brief papers, no larger than 8 typeset journal pages. Short articles are preferable. Papers larger than 8 pages can be considered in exceptional cases (such as discoveries, etc.) to the section *Special Reports* intended for such publications in the journal.

All that has been accepted for the online issue of *Progress in Physics* is printed in the paper version of the journal. To order printed issues, contact Chief Editor.

This journal is non-commercial, academic edition. It is printed from private donations.

————————————

New Effect of General Relativity: Thomson Dispersion of Light in Stars as a Machine Producing Stellar Energy

Dmitri Rabounski

E-mail: rabounski@yahoo.com

Given a non-holonomic space, time lines are non-orthogonal to the spatial section therein, which manifests as the three-dimensional space rotation. It is shown herein that a global non-holonomity of the background space is an experimentally verifiable fact revealing itself by two fundamental fields: a field of linear drift at 348 km/sec, and a field of rotation at 2,188 km/sec. Any local rotation or oscillation perturbs the background non-holonomity. In such a case the equations of motion show additional energy flow and force, produced by the non-holonomic background, in order to compensate the perturbation in it. Given the radiant transportation of energy in stars, an additional factor is expected in relation to Thomson dispersion of light in free electrons, and provides the same energy radiated in the wide range of physical conditions from dwarfs to super-giants. It works like a machine where the production of stellar energy is regulated by radiation from the surface. This result, from General Relativity, accounts for stellar energy by processes different to thermonuclear reactions, and coincides with data of observational astrophysics. The theory leads to practical applications of new energy sources working much more effectively and safely than nuclear energy.

1 Introduction. The mathematical basis

We aim to study the effects produced on a particle, if the space is non-holonomic. We then apply the result to the particles of the gaseous constitution of stars.

To do this we shall study the equations of motion. To obtain a result applicable to real experiment, we express the equations in terms of physically observable quantities. Mathematical methods for calculating observable quantities in General Relativity were invented by A. Zelmanov, in the 1940's [1, 2, 3]. We now present a brief account thereof.

A regular observer perceives four-dimensional space as the three-dimensional spatial section $x^0 = \text{const}$, pierced at each point by time lines $x^i = \text{const}$.* Therefore, physical quantities perceived by an observer are actually *projections* of four-dimensional quantities onto his own time line and spatial section. The spatial section is determined by a three-dimensional coordinate net spanning a real reference body. Time lines are determined by clocks at those points where the clocks are located. If time lines are everywhere orthogonal to the spatial section, the space is known as *holonomic*. If not, there is a field of the space non-holonomity — the non-orthogonality of time lines to the spatial section, manifest as a three-dimensional rotation of the reference body's space. Such a space is said to be *non-holonomic*.

By mathematical means, four-dimensional quantities can be projected onto an observer's time line and spatial section by the projecting operators: $b^\alpha = \frac{dx^\alpha}{ds}$, the observer's four-dimensional velocity vector tangential to his world-line, and $h_{\alpha\beta} = -g_{\alpha\beta} + b_\alpha b_\beta$. For a real observer at rest with respect

to his reference body ($b^i = 0$), the projections of a vector Q^α are $b^\alpha Q_\alpha = \frac{Q_0}{\sqrt{g_{00}}}$ and $h^i_\alpha Q^\alpha = Q^i$, while for a tensor of the 2nd rank $Q^{\alpha\beta}$ we have the projections $b^\alpha b^\beta Q_{\alpha\beta} = \frac{Q_{00}}{g_{00}}$, $h^{i\alpha} b^\beta Q_{\alpha\beta} = \frac{Q^i_0}{\sqrt{g_{00}}}$, $h^i_\alpha h^k_\beta Q^{\alpha\beta} = Q^{ik}$. Such projections are invariant with respect to the transformation of time in the spatial section: they are *chronometrically invariant quantities*.

In the observer's spatial section the chr.inv.-tensor

$$h_{ik} = -g_{ik} + b_i b_k = -g_{ik} + \frac{g_{0i} g_{0k}}{g_{00}}, \qquad (1)$$

possesses all the properties of the fundamental metric tensor $g_{\alpha\beta}$. Furthermore, the spatial projection of it is $h^\alpha_i h^\beta_k g_{\alpha\beta} = -h_{ik}$. Therefore h_{ik} is the *observable metric tensor*.

The chr.inv.-differential operators

$$\frac{{}^*\partial}{\partial t} = \frac{1}{\sqrt{g_{00}}} \frac{\partial}{\partial t}, \qquad \frac{{}^*\partial}{\partial x^i} = \frac{\partial}{\partial x^i} - \frac{g_{0i}}{g_{00}} \frac{\partial}{\partial x^0}, \qquad (2)$$

are different to the usual differential operators, and are non-commutative: $\frac{{}^*\partial^2}{\partial x^i \partial t} - \frac{{}^*\partial^2}{\partial t \partial x^i} = \frac{1}{c^2} F_i \frac{{}^*\partial}{\partial t}$ and $\frac{{}^*\partial^2}{\partial x^i \partial x^k} - \frac{{}^*\partial^2}{\partial x^k \partial x^i} = \frac{2}{c^2} A_{ik} \frac{{}^*\partial}{\partial t}$. The non-commutativity determines the chr.inv.-vector for the gravitational inertial force F_i and the chr.inv.-tensor of angular velocities of the space rotation A_{ik}

$$F_i = \frac{1}{\sqrt{g_{00}}} \left(\frac{\partial \mathrm{w}}{\partial x^i} - \frac{\partial v_i}{\partial t} \right), \quad \sqrt{g_{00}} = 1 - \frac{\mathrm{w}}{c^2}, \qquad (3)$$

$$A_{ik} = \frac{1}{2} \left(\frac{\partial v_k}{\partial x^i} - \frac{\partial v_i}{\partial x^k} \right) + \frac{1}{2c^2} \left(F_i v_k - F_k v_i \right), \qquad (4)$$

where w is the gravitational potential, and $v_i = -c \frac{g_{0i}}{\sqrt{g_{00}}}$ is the linear velocity of the space rotation†. Other observable

---

*Greek suffixes are the space-time indices $0, 1, 2, 3$, Latin ones are the spatial indices $1, 2, 3$. So the space-time interval is $ds^2 = g_{\alpha\beta} dx^\alpha dx^\beta$.

†Its contravariant component is $v^i = -c g^{0i} \sqrt{g_{00}}$, so $v^2 = h_{ik} v^i v^k$.

properties of the reference space are presented with the chr. inv.-tensor of the rates of the space deformations

$$D_{ik} = \frac{1}{2\sqrt{g_{00}}} \frac{\partial h_{ik}}{\partial t} = \frac{1}{2} \frac{{}^{*}\partial h_{ik}}{\partial t} \qquad (5)$$

and the chr.inv.-Christoffel symbols

$$\Delta^{i}_{jk} = h^{im}\Delta_{jk,m} = \frac{1}{2} h^{im} \left(\frac{{}^{*}\partial h_{jm}}{\partial x^{k}} + \frac{{}^{*}\partial h_{km}}{\partial x^{j}} - \frac{{}^{*}\partial h_{jk}}{\partial x^{m}} \right) \quad (6)$$

built just like Christoffel's usual symbols $\Gamma^{\alpha}_{\mu\nu} = g^{\alpha\sigma}\Gamma_{\mu\nu,\sigma}$ using h_{ik} instead of $g_{\alpha\beta}$.

Within infinitesimal vicinities of any point in a Riemannian space the fundamental metric tensor can be represented as the scalar product $g_{\alpha\beta} = \vec{e}_{(\alpha)}\vec{e}_{(\beta)}$ of the basis vectors, tangential to curves and non-orthogonal to each coordinate line of the space. Hence $g_{\alpha\beta} = e_{(\alpha)}e_{(\beta)}\cos(x^{\alpha}; x^{\beta})$. Therefore the linear velocity of the space rotation

$$v_{i} = -c \frac{g_{0i}}{\sqrt{g_{00}}} = -ce_{(i)} \cos(x^{0}; x^{i}) \qquad (7)$$

shows how much the time line inclines to the spatial section, and is the actual value of the space non-holonomity.

The observable time interval $d\tau$ and spatial displacements are the projections of the world-displacement dx^{α}:

$$d\tau = \frac{1}{c} b_{\alpha} dx^{\alpha} = \sqrt{g_{00}} \, dt - \frac{1}{c^{2}} v_{k} dx^{k}, \qquad (8)$$

while the observable spatial displacements coincide with the coordinate ones $h^{i}_{\alpha} dx^{\alpha} = dx^{i}$. The observable spatial interval is $d\sigma^{2} = h_{ik} dx^{i}dx^{k}$, while $ds^{2} = c^{2}d\tau^{2} - d\sigma^{2}$.

Using these techniques, we can calculate the physically observable projections of any world-quantity, then express them through the observable properties of the space.

2 A global non-holonomity of the background space — an experimentally verifiable fact

Can such a case exist, where, given a non-holonomic space, the linear velocity of its rotation is $v_{i} \neq 0$, while the angular velocity is $A_{ik} = 0$? Yes, it is possible. If v_{i} has the same numerical value $v_{i} = \bar{v}_{i} = \text{const}$ at each point of a space, we have $A_{ik} = 0$ everywhere therein. In such a case, by formula (7), there is a stationary homogeneous *background field of the space non-holonomity*: all time lines, piercing the spatial section, have the same inclination $\cos(x^{0}; x^{i}) = -\frac{\bar{v}_{i}}{ce_{(i)}}$ to the spatial section at each its points.

Is such a background truly present in our real space? If yes, what is the "primordial" value $\bar{v}_{i} = \text{const}$? These questions can be answered using research of the 1960's, carried out by Roberto di Bartini [4, 5].

In his research di Bartini used topological methods. He considered "a predicative unbounded and hence unique specimen A. [...] A coincidence group of points, drawing elements of the set of images of the object A, is a finite

symmetric system, which can be considered as a topological spread mapped into the spherical space R^{n}" [5].

Given the spread R^{n}, di Bartini studied "sequences of stochastic transitions between different dimension spreads as stochastic vector quantities, i. e. as fields. Then, given a distribution function for frequencies of the stochastic transitions dependent on n, we can find the most probable number of the dimension of the ensemble" [5]. He found extrema of the distribution function at $n = \pm 6$, "hence the most probable and most improbable extremal distributions of primary images of the object A are presented in the 6-dimensional closed configuration: the existence of the total specimen A we are considering is 6-dimensional. [...] a spherical layer of R^{n}, homogeneously and everywhere densely filled by doublets of the elementary formations A, is equivalent to a vortical torus, concentric with the spherical layer. The mirror image of the layer is another concentric homogeneous double layer, which, in turn, is equivalent to a vortical torus coaxial with the first one. Such formations were studied by Lewis and Larmore for the $(3+1)$-dimensional case" [5].

For the $(3+1)$-dimensional image, di Bartini calculated the ratio between the torus diameter D and the radius of the circulation r which satisfies the condition of stationary vortical motion (the current lines coincide with the trajectory of the vortex core). He obtained $E = \frac{D}{r} = 274.074\,996$, i. e.

$$\frac{R}{r} = 137.037\,498. \qquad (9)$$

Applying this bizarre result to General Relativity, we see that if our real space satisfies the most probable topological shape, we should observe two fundamental drift-fields:

1. A field of the constant rotating velocity 2,187.671 km/sec — a field of the background space non-holonomity.

This comes with the fact that the frequency distribution Φ_{n} of the stochastic transitions between different dimensions "is isomorphic to the function of the surface's value $S_{(n+1)}$ of a unit radius hypersphere located in an $(n+1)$-dimensional space (this value is equal to the volume of an n-dimensional hypertorus). This isomorphism is adequate for the ergodic concept, according to which the spatial and time spreads are equivalent aspects of a manifold" [5].

In such a case the radius of the circulation r (the spatial spread's function) is expressed through a velocity v just like the torus' radius R (the time spread's function) is expressed through the velocity of light $c = 2.997\,930 \times 10^{10}$ cm/sec. Thus, we obtain the analytical value of the velocity $\bar{v}_{i}$:

$$\bar{v} = \frac{2c}{E} = \frac{cr}{R} = 2.187\,671 \times 10^{8} \text{ cm/sec}, \qquad (10)$$

Because the vortical motion is stationary, the linear velocity $\bar{v}_{i}$ of the circulation r is constant everywhere within it. In other words, $\bar{v}_{i} = 2,187.671$ km/sec is the linear velocity of the space rotation characterizing a stationary homogeneous

field of the background space non-holonomity: there in the space all time lines have the same inclination to the spatial section at each of its points

$$\cos\left(x^0;x^i\right) = -\frac{\bar{v}}{c} = -\frac{1}{137.037498} = -0.0072972728. \quad (11)$$

The background non-holonomity should produce an effect in v_i-dependent phenomena. Hence the non-holonomic background should be an experimentally verifiable fact.

In such an experiment we should take into account the fact that all v_i-dependent physical factors should initially contain the background space rotation $\bar{v}_i = 2,187.671$ km/sec. Therefore, the background cannot itself be isolated; it can be shown only by the changes of the quantities expected to be affected by local perturbations of the background.

2. A field of constant linear velocity 348.1787 km/sec — a field of the background drift-velocity.

This comes from the fact that the background becomes polarized while "the shift of the field vector at $\frac{\pi}{2}$ in its parallel transfer along closed arcs of radii R and r in the affine coherence space R^n" [5]. Hence, we find that the unpolarized component of the field $\bar{v}_i = 2,187.671$ km/sec is a field of a constant dipole-fit velocity

$$\bar{v} = \frac{\bar{v}}{2\pi} = 3.481787 \times 10^7 \text{ cm/sec}. \quad (12)$$

In other words, it should be a global-drift field of the constant dipole-fit linear velocity $\bar{v} = 348.1787$ km/sec, represented in the circulation r (three-dimensional spread).

Our analytically obtained value 348.1787 km/sec is in close agreement with the linear drift-velocity 365 ± 18 km/sec extracted from the recently discovered anisotropy of the Cosmic Microwave Background.

The Cosmic Microwave Background Radiation was discovered in 1965 by Penzias and Wilson at Bell Telephone Lab. In 1977, Smoot, Gorenstein, and Muller working with a twin antenna Dicke radiometer at Lawrence Berkeley Lab, discovered an anisotropy in the Background as the dipole-fit linear velocity 390 ± 60 km/sec [9]. Launched by NASA, in 1989, the Cosmic Background Explorer (COBE) satellite produced observations from which the dipole-fit velocity was extracted more precisely at 365 ± 18 km/sec. The Wilkinson Microwave Anisotropy Probe (WMAP) satellite by NASA, launched in 2001, verified the COBE data [10].

As already shown by Zelmanov, in the 1940's [1], General Relativity permits absolute reference frames connected to the anisotropy of the fields of the space non-holonomity or deformation — the globally polarized fields similar to a global gyro. Therefore the drift-fields analytically obtained above provide a theoretical basis for an absolute reference frame in General Relativity, connected to the anisotropy of the Cosmic Microwave Background.

In the next Section we study the effects we expect on a test-particle due to the background space non-holonomity.

3 A test-particle in a non-holonomic space. Effects produced by the background space non-holonomity

Free particles move along the shortest (geodesic) lines. The equations of free motion are derived from the fact that any tangential vector remains parallel to itself when transferred along a geodesic, so the general covariant derivative of the vector is zero along the line. A particle's four-dimensional impulse vector is $P^\alpha = m_0 \frac{dx^\alpha}{ds}$, so the general covariant equations of free motion are

$$\frac{dP^\alpha}{ds} + \Gamma^\alpha_{\mu\nu} P^\mu \frac{dx^\nu}{ds} = 0; \quad (13)$$

their observable chr.inv.-projections, by Zelmanov [1], are

$$\frac{dE}{d\tau} - mF_i v^i + mD_{ik} v^i v^k = 0,$$
$$\frac{dp^i}{d\tau} - mF^i + 2m\left(D^i_k + A^{\cdot i}_{k\cdot}\right)v^k + m\Delta^i_{nk} v^n v^k = 0, \quad (14)$$

where $v^i = \frac{dx^i}{d\tau}$ and $p^i = mv^i$ are the observable velocity and impulse of the particle, m and $E = mc^2$ are its relativistic mass and energy. Each term in the equations is an observable chr.inv.-quantity*. The scalar equation is the chr.inv.-energy law. The vector equations are the three-dimensional chr.inv.-equations of motion, setting up the 2nd Newtonian law.

In non-free motion, a particle deviates from a geodesic line, so the right sides of the equations of motion become non-zero, expressing a deviating force.

We will now fit the chr.inv.-equations of motion according to the most probable topological configuration of the space, as propounded by di Bartini. In such a case we can represent dx^i as $dx^i = v^i dt$ while the time interval is $dx^0 = cdt$. Such a representation coincides with the ergodic concept, where the spatial and time spreads are equivalent elements of a manifold; so the transformation $dx^i = v^i dt$ should be understood to be "ergodic".

Applying the "ergodic transformation", after some algebra we find that in such a space the metric ds^2 takes the form†

$$ds^2 = g_{00} c^2 dt^2 \left\{ \left(1 + \frac{v^2}{c^2\sqrt{g_{00}}}\right)^2 - \frac{v^2}{c^2 g_{00}} \right\}, \quad (15)$$

while the physically observable time interval is

$$d\tau = \left(\sqrt{g_{00}} - \frac{v^2}{c^2}\right) dt = \left\{1 - \frac{1}{c^2}\left(w + v^2\right)\right\} dt, \quad (16)$$

where $v^2 = v_i v^i = h_{ik} v^i v^k$. Looking at the resultant metric from the geometric viewpoint, we note an obvious feature:

> In such a metric space the flow of time is equivalent to a *turn of the spatial section*.

---

*Given a chr.inv.-quantity, we can raise/lower its indices by the chr.inv.-metric tensor h_{ik}: $h_{ik} = -g_{ik} + \frac{1}{c^2} v_i v_k$, $h^{ik} = -g^{ik}$, and $h^i_k = \delta^i_k$.

†Because $v_i = -c\frac{g_{0i}}{\sqrt{g_{00}}}$, $v^i = -cg^{0i}\sqrt{g_{00}}$, $h_{ik} = -g_{ik} + \frac{1}{c^2} v_i v_k$.

In the (3+1)-dimensional vortical torus, the ratio between its diameter D and the radius of the circulation r is the fundamental constant $E = \frac{D}{r} = 274.074\,996$ [4, 5]. Hence the circulation velocity $\bar{v} = \frac{2c}{E} = 2{,}187.671$ km/sec (the linear velocity of the background space rotation) is covariantly constant. On the other hand, locally in the spatial section, the components of the vector $v_i = -c\frac{g_{0i}}{\sqrt{g_{00}}}$ can be different from $2{,}187.671$ km/sec due to the locally non-holonomic perturbations in the background*. In other words, the field v_i is built on two factors: (1) the background remaining constant and uniform $\bar{v}_i = 2{,}187.671$ km/sec at any point or direction in the space, and (2) a local perturbation $\tilde{v}_i$ in the background produced by rotating bodies located nearby.

As a result, within an area in which the non-holonomic background $\bar{v}_i$ is perturbed by a local rotation $\tilde{v}_i$,

$$dx^i = v^i dt = \left(\bar{v}^i + \tilde{v}^i\right) dt. \tag{17}$$

That is, with the same displacement dx^i the turn dt can be different depending on how much the non-holonomic background is perturbed by a local rotation.

The non-holonomic background remaining constant does not produce an effect in the differentiated quantities. An effect is expected to be due only from the expansion of the differential operator $\frac{\partial}{\partial t}$ where we represent dt, according to the metric (15), as a turn of the spatial section. As such, dt should be expressed through the ergodic transformation $dx^i = v^i dt = \left(\bar{v}^i + \tilde{v}^i\right) dt$. Expanding $\frac{\partial}{\partial t}$ in such a way, after algebra, we obtain the corrected formulae for the main physically observable chr.inv.-characteristics of the space that take the background space non-holonomity into account[†]

$$F_i = \frac{1}{\sqrt{g_{00}}}\left\{\frac{\partial \mathrm{w}}{\partial x^i} - \left(1 + \delta^m_n \frac{\tilde{v}^n}{\bar{v}^m}\right)\frac{\partial \tilde{v}_i}{\partial \bar{t}}\right\}, \tag{18}$$

$$A_{ik} = \frac{1}{2}\left(\frac{\partial \tilde{v}_k}{\partial x^i} - \frac{\partial \tilde{v}_i}{\partial x^k}\right) + \frac{1}{2c^2}\left(F_i \tilde{v}_k - F_k \tilde{v}_i\right), \tag{19}$$

$$D_{ik} = \frac{1}{2\sqrt{g_{00}}}\left(1 + \delta^m_n \frac{\tilde{v}^n}{\bar{v}^m}\right)\frac{\partial h_{ik}}{\partial \bar{t}}, \tag{20}$$

$$\Delta^i_{jk} = \frac{1}{2}h^{im}\left(\frac{\partial h_{jm}}{\partial x^k} + \frac{\partial h_{km}}{\partial x^j} - \frac{\partial h_{jk}}{\partial x^m}\right) + $$
$$+ \frac{1}{c^2}h^{im}\left(1 + \delta^m_n \frac{\tilde{v}^n}{\bar{v}^m}\right)\left(v_k D_{jm} + v_j D_{km} + v_m D_{jk}\right), \tag{21}$$

where the differential operator $\frac{\partial}{\partial t}$ is determined in the unperturbed background $\bar{v}_i$, while the additional multiplier sets up a correction for a local perturbation $\tilde{v}_i$ in it.

---

*Note that Minkowski space of Special Relativity is free of gravitational fields ($g_{00} = 1$) and rotations ($g_{0i} = 0$). So all the effects we are considering are attributed only to General Relativity's space.

[†]Here $\delta^m_n = \begin{pmatrix} 1 & 0 & 0 \\ 0 & 1 & 0 \\ 0 & 0 & 1 \end{pmatrix}$ is the unit three-dimensional tensor, the spatial part of the four-dimensional Kronecker unit tensor δ^α_β used for replacing the indices. So δ^m_n replaces the indices in three-dimensional tensors.

If there is no non-holonomic background, but only locally non-holonomic fields due to rotating small bodies, the above formulae revert to their original shape through $\bar{v}^i = 0$ in the transformation $dx^i = v^i dt = \left(\bar{v}^i + \tilde{v}^i\right) dt$. The above transformation is impossible in a holonomic space since therein the spatial coordinates aren't functions of the time coordinate; $x^i \neq f\left(x^0\right)$. So the foregoing is true only if the space is non-holonomic, and the spatial and time spreads are equivalent elements of the manifold.

From the formulae obtained, we conclude that:

> The main physically observable chr.inv.-properties of the reference space, such as the gravitational inertial force F_i, the angular velocity of the space rotation A_{ik}, the rate of the space deformation D_{ik}, and the space non-uniformity (set up by the chr.inv.-Christoffel symbols Δ^i_{jk}) are dependent on the ratio between the value of the local non-holonomity $\tilde{v}_i$ (due to nearby rotating bodies) and the background space non-holonomity $\bar{v}_i = 2{,}187.671$ km/sec.

What effect does this have on the motion of a particle? Let's recall the chr.inv.-equations of motion (14). While a particle is moved along dx^i by an external force (or several forces), the acceleration gained by the particle is determined by the fact that its spatial impulse vector p^i, being transferred along dx^i, undergoes a space-time turn dt expressed by the ergodic transformation (17).

The entire motion of a particle is expressed by the term with $\frac{d}{d\tau}$ in the scalar and chr.inv.-vector equations of motion (14). The remaining terms in the scalar equation express the work spent on the motion by external forces, while the remaining terms in the vector equation account for the forces themselves. Therefore, for the entire motion of a particle, we have no need of expanding $\frac{\partial}{\partial t}$ by the ergodic transformation, for each force acting thereon. We simply need to apply the expansion to the chr.inv.-derivative with respect to the observable time $\frac{d}{d\tau}$ in the equations of motion (14).

By definition (8), $d\tau = \sqrt{g_{00}}\,dt - \frac{1}{c^2}v_k dx^k$, so we have $dt = \frac{1}{\sqrt{g_{00}}}\left(1 + \frac{1}{c^2}v_k \mathrm{v}^k\right)d\tau$. The differential is $d = \frac{\partial}{\partial x^\alpha}dx^\alpha$, so $d = \frac{1}{\sqrt{g_{00}}}\left(1 + \frac{1}{c^2}v_k \mathrm{v}^k\right)\frac{\partial}{\partial t}d\tau + \frac{\partial}{\partial x^k}dx^k$ and, finally

$$\frac{d}{d\tau} = \frac{1}{\sqrt{g_{00}}}\left(1 + \frac{1}{c^2}v_k \mathrm{v}^k\right)\frac{\partial}{\partial t} + \mathrm{v}^k \frac{\partial}{\partial x^k}. \tag{22}$$

Expanding this formula with the ergodic transformation $dx^i = v^i dt = \left(\bar{v}^i + \tilde{v}^i\right) dt$, we obtain it in the form

$$\frac{d}{d\tau} = \left(1 + \delta^m_n \frac{\tilde{v}^n}{\bar{v}^m}\right)\frac{d}{d\bar{\tau}} + \delta^m_n \frac{\tilde{v}^n}{\bar{v}^m}\mathrm{v}^k \frac{\partial}{\partial x^k} + $$
$$+ \frac{1}{c^2\sqrt{g_{00}}}\left(1 + \delta^m_n \frac{\tilde{v}^n}{\bar{v}^m}\right)\tilde{v}_k \mathrm{v}^k \frac{\partial}{\partial \bar{t}} \tag{23}$$

where the non-holonomic background $\bar{v}_i = 2{,}187.671$ km/sec is taken into account. Here $\frac{\partial}{\partial \bar{\tau}}$ and $\frac{\partial}{\partial \bar{t}}$ are also determined in the unperturbed background $\bar{v}_i$.

In particular, if a moving particle is slow with respect to light and the differentiated quantity is distributed uniformly in the spatial section, we have $\frac{1}{c^2}\tilde{v}_k v^k = 0$ and $\frac{\partial}{\partial x^k} = 0$ in the above formula, so we obtain

$$\frac{d}{d\tau} \simeq \frac{1}{\sqrt{g_{00}}}\frac{\partial}{\partial t} = \frac{1}{\sqrt{g_{00}}}\left(\bar{v}^k + \tilde{v}^k\right)\frac{\partial}{\partial x^k} =$$
$$= \left(1 + \delta_n^m\,\frac{\tilde{v}^n}{\bar{v}^m}\right)\frac{d}{d\bar{\tau}}\,. \tag{24}$$

In such a case, by the chr.inv.-equations of motion (14), the total force moving the particle $\Phi^i = \frac{dp^i}{d\tau}$ and the total energy flow $W = \frac{dE}{d\tau}$ expended on the motion are

$$W = \frac{dE}{d\tau} = \left(1 + \delta_n^m\,\frac{\tilde{v}^n}{\bar{v}^m}\right)W_{(0)} = W_{(0)} + \delta_n^m\,\frac{\tilde{v}^n}{\bar{v}^m}\,W_{(0)} \tag{25}$$

$$\Phi^i = \frac{dp^i}{d\tau} = \left(1 + \delta_n^m\,\frac{\tilde{v}^n}{\bar{v}^m}\right)\Phi^i_{(0)} = \Phi^i_{(0)} + \delta_n^m\,\frac{\tilde{v}^n}{\bar{v}^m}\,\Phi^i_{(0)} \tag{26}$$

where $\Phi^i_{(0)}$ and $W_{(0)}$ are the acting force and energy flow in the unperturbed non-holonomic background (before a local rotation $\tilde{v}^i$ was started). The additional force $\delta_n^m\,\frac{\tilde{v}^n}{\bar{v}^m}\,\Phi^i_{(0)}$ and energy flow $\delta_n^m\,\frac{\tilde{v}^n}{\bar{v}^m}\,W_{(0)}$ are produced by the stationary homogeneous field of the background space non-holonomity $\bar{v}_i$ in order to compensate for a perturbation in it caused by a local rotation $\tilde{v}_i$. As a result we conclude that:

> The presence of a background space non-holonomity manifests in a particle as an addition to its acceleration, gained from an external force (or forces) moving it. This additional force appears only if the non-holonomic background is perturbed by a local rotation in the area where the particle moves. (Being unperturbed, the non-holonomic background does not produce any forces.) The force appears independently of the origin of the forces moving the particle, and is proportional to the ratio between the linear velocity of the local rotation $\tilde{v}_i$ and that of the background space rotation $\bar{v}_i = 2{,}187.671$ km/sec.

Such an additional force should appear on any particle accelerated near a rotating body. On the other hand, because the space background rotates rapidly, at $2{,}187.671$ km/sec, such a force is expected only near rapid rotations, comparable with $2{,}187.671$ km/sec.

For instance, consider a high speed gyro as used in aviation navigation technology: 250 g rotor of $1.65''$ diameter, rotating at $24{,}000$ rpm. With current technology, the latter is almost the ultimate speed for such a mechanically rotating system. In such a case the non-holonomic background near the gyro is perturbed as $\tilde{v} = 5.3\times10^3$ cm/sec, i. e. 53 m/sec[*]. So near the gyro, by our formula (26), we expect to have an additional factor of 2.4×10^{-5} of any force accelerating a

---

[*]Mechanical gyros used in aviation and submarine navigation systems have rotations at speeds in the range $6{,}000 - 30{,}000$ rpm. The upper speed is limited by problems derived from friction in such a mechanical system.

particle near the gyro. In other words, the expected effect is very small near such mechanically rotating systems.

The terrestrial globe rotates at 465 m/sec at its equator, so the non-holonomic space background is perturbed there by Earth's rotation by the factor 2.2×10^{-4}. Hence, given a specific experiment performed at the equator, an additional force produced by the non-holonomic background in order to compensate the perturbation in it should be 2.2×10^{-4} of the force acting in the experiment. This effect decreases with latitude owing to concomitant reduction of the linear velocity of the Earth's rotation, and completely vanishes at the poles.

However, the additional force can be much larger if the non-holonomic background is perturbed by particles rotated or oscillated by electromagnetic fields. In such a case a local rotation velocity can even reach that of the background, i. e. $2{,}187.671$ km/sec, in which case the main force accelerating the particle is doubled. In the next Section we consider a particular example of such a doubled force, expected in relation to Thomson dispersion of light in free electrons within stars.

In forthcoming research we show how such an additional force can be detected in experiment, and applied to the development on a device whose motion is based on principles, completely different from those employed in aviation and space technology today. Such a device should revolutionize aviation and space travel.

It is interesting to note that a similar conclusion on the time flow as a turn and additional forces produced by it were drawn by the famous astronomer and experimental physicist, N. A. Kozyrev, within the framework of his "non-symmetrical mechanics" [8]. Kozyrev proceeded from his research on the insufficiency of Classical Mechanics and thermodynamics in order to explain some effects in rotating bodies and also the specific physical conditions in stars. He didn't construct an exact theory, limiting himself to phenomenological conclusions and general speculations. On the other hand, his phenomenologically deduced formula for a force additional to Classical Mechanics is almost the same as our purely theoretical result $\delta_n^m\,\frac{\tilde{v}^n}{\bar{v}^m}\,\Phi^i_{(0)}$ obtained by means of General Relativity in the non-holonomic four-dimensional space of General Relativity, in the low velocity approximation. Therefore this coincidence can be viewed as an auxiliary verification of our theory.

We see that there is no need to change the basic physics as Kozyrev did. Naturally, all the results we have obtained are derived from the background non-holonomity of the four-dimensional space of General Relativity. Classical Mechanics uses a three-dimensional flat Euclidean space that does not contain the time spread and, hence, the non-holonomic property. Classical Mechanics is therefore insufficient for explaining the effects of the background space non-holonomity predicted herein by means of General Relativity. So the additional force and energy flow are new effects predicted within the framework of Einstein's theory.

4 Thomson dispersion of light in stars as a machine producing stellar energy due to the background space non-holonomity

Here we apply the foregoing results to the particles of the gaseous constitution of stars.

The physical conditions in stars result from the comparison of well-known correlations of observational astrophysics and two main equations of equilibrium in stars (mechanical and thermal equilibrium). Such a comparison is made in the extensive research started in the 1940's by Kozyrev. The final version was printed in 2005 [6].

In brief, a star is a gaseous ball in a stable state, because mechanical and thermal equilibrium therein are expressed by two equations: (1) the mechanical equilibrium equation — gravity pushing each cm^3 of the gas to the centre of a star is balanced by the gaseous pressure from within; (2) the thermal equilibrium equation — the energy flow produced within one cm^3 of the gas equals the energy loss by radiation. The comparison of the equilibrium equations with the mass–luminosity relation and the period — average density of Cepheids, a well verified correlation of observational astrophysics, resulted in the stellar energy diagram wherein the isoergs show the productivity of stellar energy sources per second [6]. The diagram is reproduced below. The energy output of thermonuclear reactions gives a surface, whose intersection with the diagram is the dashed arc. Because stars have a completely different distribution in the diagram, it is concluded that thermonuclear synthesis can be the source of stellar energy in only a minority of stars, located along the dashed arc. Naturally, stars in the diagram are distributed along a straight line that runs from the right upper region to the left lower region, with a ball-like concentration at the centre of the diagram. The equation of the main direction is

$$\frac{B}{n_e} = \text{const} = 1.4 \times 10^{-11}\,\text{erg}, \qquad (27)$$

and is the relation between the radiant energy density B and the concentration of free electrons in stars. In other words, this is the energy produced per free electron in stars, and it is constant throughout the widest range of the physical conditions in stars: from dwarfs to super-giants. This is the actual physical condition under which the mechanism that generates stellar energy works, even in the low-temperature stars such as red super-giants like the infrared satellite of ε Aurigae, wherein the temperature is about 200,000° and the pressure about one atmosphere. In other words, the relation characterizes the source of stellar energy. According to the stellar energy relation (27), constant in any kind of star, Kozyrev concluded that "the energy productivity in stars is determined by the energy drainage (radiation) only. [. . .] In contrast to reaction, such a mechanism should be called a machine. [. . .] In other words, stars are *machines* which generate radiant energy. The heat drainage is the power regu-
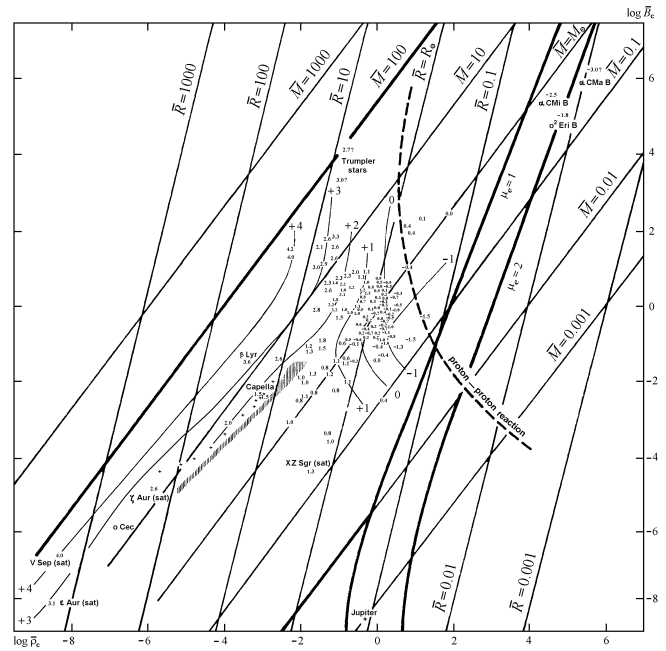

Fig. 1: Diagram of stellar energy: the productivity of stellar energy sources. The abscissa is the logarithm of the density of matter, the ordinate is the logarithm of the radiant energy density (both are taken at the centre of stars in multiples of the corresponding values at the centre of the Sun). Reproduced from [6].

lation mechanism in the machines" [6].

I note that the stellar energy relation (27) — the result of comparing the two main equilibrium equations and observational data — is pure phenomenology, independent of our theoretical views on the origin of stellar energy.

Let's consider the stellar energy relation (27) by means of our theory developed in Section 3 herein. By this relation we have $\frac{B}{n_e} = \text{const} = 1.4 \times 10^{-11}$ erg: the energy produced per electron is constant in any kind of star, under any temperature or pressure therein. So the mechanism producing stellar energy works by a process related to electrons in stars. There is just one process of such a kind — Thomson dispersion of light in free electrons in the radiant transportation of energy from the centre to the surface.

We therefore consider the Thomson process. When a light wave having the average density of energy q encounters a free electron, the flow of the wave energy σcq is stopped in the electron's "square" $\sigma = 6.65 \times 10^{-25}\,\text{cm}^2$ (the square of Thomson dispersion). As a result the electron gains an acceleration σq, directed orthogonally to the wave front. In other words, the electron is propelled by a force produced by the wave energy flow stopped in its square, and in the direction of the wave propagation.

We will determine the force by means of electrodynamics in the terms of physically observable chr.inv.-quantities*. The

---

*The basics of electrodynamics such as the theory of an electromagnetic field and a charged particle moving in it, expressed in terms of chronometric invariants, was developed in the 1990's [11, Chapter 3].

chr. inv.-energy density q and chr.inv.-impulse density J^i are the chr.inv.-projections $q = \frac{T_{00}}{g_{00}}$ and $J^i = \frac{cT_0^i}{\sqrt{g_{00}}}$ of the energy-momentum tensor $T^{\alpha\beta}$ of an electromagnetic field

$$q = \frac{1}{8\pi}\left(E_i E^i + H_{ik}H^{ik}\right), \qquad J^i = \frac{c}{4\pi}E_k H^{ik}, \quad (28)$$

where $E^i = \frac{F_0^{\cdot i}}{\sqrt{g_{00}}}$ and $H^{ik} = F^{ik}$ are the chr.inv.-projections of the electromagnetic field tensor $F_{\alpha\beta}$ — the physically observable electric and magnetic strengths of the field [11]. We consider radiation within stars to be isotropic. In an isotropic electromagnetic field $E_i E^i = H_{ik}H^{ik}$ [11], so

$$q = \frac{1}{4\pi}E_i E^i, \qquad J^2 = h_{ik}J^i J^k = q^2 c^2, . \quad (29)$$

Hence, the wave impulse flow along the x^1 direction the wave travels is

$$J^1 = \frac{qc}{\sqrt{h_{11}}}, \quad (30)$$

while the flow of the wave energy stopped in an electron's surface σ, i. e. the force pushing the electron in the x^1 direction, orthogonal to the wave front, is

$$\Phi^1 = \frac{\sigma q}{\sqrt{h_{11}}} = \frac{\sigma q}{\sqrt{1 + \frac{1}{c^2}v_1 v_1}}. \quad (31)$$

On the other hand, according to our theory, developed in Section 3, the total force Φ^1 acting on an electron and the energy flow W expended on it via the Thomson process should be

$$W = \frac{dE}{d\tau} = W_{(0)} + \delta_n^m \frac{\tilde{v}^n}{\bar{v}^m}W_{(0)}, \quad (32)$$

$$\Phi^1 = \frac{dp^1}{d\tau} = \Phi_{(0)}^1 + \delta_n^m \frac{\tilde{v}^n}{\bar{v}^m}\Phi_{(0)}^1, \quad (33)$$

depending on a local perturbation $\tilde{v}^i$ in the background space non-holonomity $\bar{v}_i = 2,187.671\,\text{km/sec}$.

What is the real value of the local perturbation $\tilde{v}^i$ in Thomson dispersion of light in stars? We calculate the value of $\tilde{v}^i$, proceeding from the self-evident geometrical truth that the origin of a non-holonomity of a space is any motion along a closed path in it, such as rotations or oscillations.

When a light wave falls upon an electron, the electron oscillates in the plane of the wave because of the oscillations of the electric field strength E^i in the plane. The spatial equation of motion of such an electron is the equation of forced oscillations. For oscillations in the x^2 direction, in a homogeneous non-deformed space, the equation of motion is

$$\ddot{x}^2 + \omega_0^2 x^2 = \frac{e}{m_e}E_0^2 \cos\omega t, \quad (34)$$

where ω is the frequency of the wave and ω_0 is the proper frequency of the electron. This equation has the solution

$$x^2 = \frac{eE_0^2 \cos\omega t}{m_e(\omega_0^2 - \omega^2)} \simeq \frac{eE_0^2 \cos\omega t}{m_e \omega^2} \quad (35)$$

so the components of the linear velocity $\tilde{v}^i$ of the local space rotation, approximated by the oscillation, are

$$\tilde{v}^2 = \frac{eE_0^2}{m_e \omega}, \qquad \tilde{v}^1 = 0, \qquad \tilde{v}^3 = 0. \quad (36)$$

The electric field strength E in a light wave, according to (29), is $E = \sqrt{4\pi q} = \sqrt{4\pi B}$ where B is the radiant energy density. Therefore the value of $\tilde{v}^2$ is

$$\tilde{v} = \frac{e\sqrt{4\pi}}{m_e}\frac{\sqrt{B}}{\omega} = \frac{e\sqrt{4\pi\alpha}}{m_e}\frac{T^2}{\omega}, \quad (37)$$

where $\alpha = 7.59\times10^{-15}\,\text{erg/cm}^3\times\text{degree}^4$ is Stefan's constant, T is temperature. Therefore the total energy flow $W = W_{(0)} + \frac{\tilde{v}^2}{\bar{v}^2}W_{(0)} = W_{(0)} + \frac{\tilde{v}}{\bar{v}}W_{(0)}$ and force $\Phi^1 = \Phi_{(0)}^1 + \frac{\tilde{v}^2}{\bar{v}^2}\Phi_{(0)}^1$ acting on an electron orthogonally to the wave plane in the Thomson process should be

$$W = W_{(0)} + \frac{e\sqrt{4\pi}}{m_e \bar{v}}\frac{\sqrt{B}}{\omega}W_{(0)}, \quad (38)$$

$$\Phi^1 = \Phi_{(0)}^1 + \frac{e\sqrt{4\pi}}{m_e \bar{v}}\frac{\sqrt{B}}{\omega}\Phi_{(0)}^1, \quad (39)$$

where $\bar{v} = 2,187.671\,\text{km/sec}$. So the additional energy flow $\Delta W = \frac{\tilde{v}}{\bar{v}}W_{(0)}$ and force $\Delta\Phi^1 = \frac{\tilde{v}}{\bar{v}}\Phi_{(0)}^1$ are twice the initial acting factors W and Φ if the multiplier

$$\frac{\tilde{v}}{\bar{v}} = \frac{e\sqrt{4\pi}}{m_e \bar{v}}\frac{\sqrt{B}}{\omega} \quad (40)$$

becomes close to unity ($\tilde{v}$ becomes close to $\bar{v}$). In such a case the background non-holonomic field produces the same energy and forces as those acting in the system, so the energy flow and forces acting in the process are doubled.

Given the frequency $\nu = \frac{\omega}{2\pi} \approx 5\times10^{14}\,\text{Hz}$, close to the spectral class of the Sun*, we deduce by formula (37) that there in the Sun $\tilde{v}$ reaches the linear velocity of the background space rotation $\bar{v} \simeq 2.2\times10^8\,\text{cm/sec}$, if the radiant energy density is $B = 1.4\times10^{11}\,\text{erg/cm}^3$, which is close to the average value of B in the Sun. From phenomenological data [6], in the central region of the Sun $B \simeq 10^{13}\,\text{erg/cm}^3$ so $\tilde{v} \simeq 2\times10^9\,\text{cm/sec}$ there, i. e. ten times larger than the average in the Sun. In the surface layer where $T \simeq 6\times10^3$, we obtain the much smaller value $\tilde{v} \simeq 2\times10^3\,\text{cm/sec}$.

This calculation verifies the phenomenological conclusion [6] that the sources of energy aren't located exclusively in the central region of a star (as would be the case for thermonuclear reactions), but are distributed throughout the whole volume of a star, with some concentration at the centre. With the above mechanism generating energy by the background space non-holonomity field, the sources of stellar energy should be working in even the surface layer of the

---

*A light wave doesn't change its proper frequency in the Thomson process, so the frequency remains the same while light travels from the inner region of a star to the surface where it determines the spectral class (visible colour) of the star.

Sun, but with much less power.

Because the productivity of such an energy generator is determined by the multiplier $\frac{\tilde{v}}{v} = \frac{e\sqrt{4\pi}}{m_e \tilde{v}}\frac{\sqrt{B}}{\omega}$ (40), in the additional energy flow $\Delta W = \frac{\tilde{v}}{v}W_{(0)}$ and the force $\Delta \Phi^1 = \frac{\tilde{v}}{v}\Phi^1_{(0)}$. So the energy output ε of the mechanism is determined mainly by the radiant energy density B in stars, i.e. the drainage of energy by radiation*. Therefore, given the above mechanism of energy production by the background space non-holonomity, stars are *machines* producing radiation, the power of which (the energy output) is regulated by their luminosity.

By the stellar energy relation (27) determined from observations, the radiant energy density per electron is constant $\frac{B}{n_e} = 1.4 \times 10^{-11}$ erg in any kind of star. Even such different stars as white dwarfs, having the highest temperatures and pressures (the right upper region in the stellar energy diagram), and low-temperature and pressure infrared supergiants (the left lower region therein) satisfy the stellar energy relation. We therefore conclude that:

> Stellar energy is generated in Thomson dispersion of light while light travels from the inner region of a star to the surface. When a light wave is dispersed by a free electron, the electron oscillates in the electric field of the wave. The oscillation causes a local perturbation of the non-holonomic background space of the Universe, so the background non-holonomic field produces an additional energy flow and force in the Thomson process in order to compensate for the local perturbation in itself. Given the physical conditions in stars, the additional energy and forces are the same as those radiated throughout the wide range of physical conditions in stars — from dwarfs to super-giants. Such energy sources work in the whole volume of a star, even in the surface layer, but with some concentration at the centre. Moreover, the power of the mechanism is regulated by the energy drainage (the radiation from the surface). This is a self-regulating machine, actuated by the background space non-holonomity, and is independent of thermonuclear reactions.

This theoretical result, from General Relativity, verifies the conclusion drawn by Kozyrev from his analysis of well-known phenomenological correlations of observational astrophysics [6]. But having no exact theory of stellar energy sources, Kozyrev had no possibility of calculating similar effects under the physical conditions different than those in stars whose temperatures and pressures are hardly reproducible in a laboratory.

With the theory of the phenomenon established, we can simulate similar effects in a laboratory for low temperature and pressure conditions (with less energy output). We can as well discover, in a laboratory, similar additional energy flow and force in processes much more simply realizable than Thomson dispersion of light. So the theoretical results of Sections 3 and 4 can be used as a basis for forthcoming developments of new energy sources.

As is well known, current employment of nuclear energy produces ecological problems because of radioactive waste. Besides that, events of recent years testify that such energy sources are dangerous if atomic power stations are destroyed by natural or human-made causes: the nuclear fuel, even without atomic explosion, produces many heavy particles and other deadly radiations.

We therefore conclude that new energy sources similar to stellar energy sources described herein, being governed by the energy output, and producing no hard radiation, can work in a laboratory conditions much more effectively and safely than nuclear energy, and replace atomic power stations in the near future.

References

1. Zelmanov A. L. Chronometric invariants. Dissertation thesis, 1944. American Research Press, Rehoboth (NM), 2006.

2. Zelmanov A. L. Chronometric invariants and co-moving coordinates in the general relativity theory. *Doklady Acad. Nauk USSR*, 1956, v. 107(6), 815–818.

3. Rabounski D. Zelmanov's anthropic principle and the infinite relativity principle. *Progress in Physics*, 2005, v. 1, 35–37.

4. Oros di Bartini R. Some relations between physical constants. *Doklady Acad. Nauk USSR*, 1965, v. 163, No. 4, 861–864.

5. Oros di Bartini R. Relations between physical constants. *Progress in Physics*, 2005, v. 3, 34–40.

6. Kozyrev N. A. Sources of stellar energy and the theory of the internal constitution of stars. *Prog. in Phys.*, 2005, v. 3, 61–99.

7. Kozyrev N. A. Physical peculiarities of the components of double stars. *Colloque "On the Evolution of Double Stars"*, *Comptes rendus*, Communications du Observatoire Royal de Belgique, ser. B, no. 17, Bruxelles, 1967, 197–202.

8. Kozyrev N. A. On the possibility of experimental investigation of the properties of time. *Time in Science and Philosophy*, Academia, Prague, 1971, 111–132.

9. Smoot G. F., Gorenstein M. V., and Muller R. A. Detection of anisotropy in the Cosmic Blackbody Radiation. *Phys. Rev. Lett.*, 1977, v. 39, 898–901.

10. Bennett C. L. et al. First-year Wilkinson Microwave Anisotropy Probe (WMAP) observations: preliminary maps and basic results. *Astrophys. Journal Suppl. Series*, 2003, v. 148, 1–27.

11. Borissova L. and Rabounski D. Fields, vacuum, and the mirror Universe. Editorial URSS, Moscow, 2001. (2nd revised ed.: CERN, EXT-2003-025).

---

*The frequency ω determining the spectral class of a star undergoes a much smaller change, within 1 order, along the whole range of stars.

Frequency Resolved Detection over a Large Frequency Range of the Fluctuations in an Array of Quantum Dots

Aziz N. Mina[*] and Adel H. Phillips[†]

[*]*Faculty of Science, Cairo University, Beni-Suef Branch, Egypt*
[†]*Faculty of Engineering, Ain Shams University, Cairo, Egypt*
E-mail: adel_phillips@yahoo.com

Quantum noise effects in an array of quantum dots coupled to superconducting leads are studied. The effect of broadband fluctuations on the inelastic rate in such tunable system has been taken into account. The quantum shot noise spectrum is expressed in terms of the time dependent fluctuations of the current around its average value. Numerical calculation has been performed over a wide range of frequencies of the induced photons. Our results show an asymmetry between absorption and emission processes. This research is very important for optoelectronic nanodevices.

1 Introduction

Semiconductor nanostructures based on two dimensional electron gas (2 DEG) could form the basis of future nanodevices for sensing, information processing and quantum computation. Coherent electron transport through mesoscopic system in the presence of a time-varying potential has been a subject of increasing interest in the past recent years [1]. Applying the microwave field with frequency, ω, to an electron with energy, E, the electron wavefunction possesses sideband components with energies $E + n\hbar\omega$ ($n = 0, \pm 1, \pm 2, \dots$). The coherence of sideband components characterizes transport properties of electrons such as photon-assisted tunneling (PAT) [2–6]. Shot noise measurements provide a powerful tool to study electron transport in mesoscopic systems [7]. Shot noise can be enhanced in devices with superconducting leads by virtue of the Andreev-reflection process taking place at the interface between a semiconductor and superconductor [8–10]. A remarkable feature of the current noise in the presence of timedependent potentials is its dependence on the phase of the transmission amplitudes [11]. Moreover, for high driving frequencies, the driving can be treated within a self-consistent perturbation theory [12]. In the present paper, a shot noise spectrum of a mesoscopic device is derived and analyzed over a wide range of frequencies of the induced microwave field.

2 Model of calculations

The present studied mesoscopic device is formed of an array of semiconductor quantum dots coupled weakly to two superconducting leads via tunnel barriers. Electrical shot noise is the time-dependent fluctuation of the current around its average value, due to the discreteness of the charge carriers. The nonsymmetrized shot noise spectrum is given by [13]:

$$P(\omega) = 2 \int_{-\infty}^{\infty} dt\, e^{i\omega t} \langle \Delta\hat{I}(t)\, \Delta\hat{I}(0)\rangle, \qquad (1)$$

where $\Delta\hat{I}(t)$ is the time-dependent fluctuations of the current around its average value [14]. The average current operator is given by [15]:

$$\langle\hat{I}(t)\rangle = \frac{e}{h} \sum_{\alpha,\beta} \int_0^{\infty} d\varepsilon \int_0^{\infty} d\varepsilon'\, I_{\alpha,\beta}(\varepsilon,\varepsilon') \times$$
$$\times\, \hat{a}_\alpha^+(\varepsilon)\, \hat{a}_\beta(\varepsilon')\, e^{i(\varepsilon-\varepsilon')t/\hbar}, \qquad (2)$$

where $\hat{a}_\alpha^+(\varepsilon)$ and $\hat{a}_\alpha(\varepsilon)$ are the creation and annihilation operators of the scattering states $\psi_\alpha(\varepsilon)$ respectively. $I_{\alpha\beta}(\varepsilon,\varepsilon')$ is the matrix element of the current operator between states $\psi_\alpha(\varepsilon)$ and $\psi_\beta(\varepsilon')$. The indices α and β (Eq. 2) denote mode number (m) as well as whether it concerns electron $\alpha = (m, e)$ or hole $\alpha = (m, h)$ propagation, due to Andreev reflection processes at semiconductor-superconductor interface [16]. The scattering states $\psi_\alpha(\varepsilon)$ and $\psi_\beta(\varepsilon')$ are determined by solving the Bogoliubov-deGennes equation (BdG) [17, 18] and are given by:

$$\Psi_{\alpha j}(x,\varepsilon) = \left[A_j \exp(ik_j x)\binom{1}{0} + B_j \exp(-ik_j x)\binom{0}{1} \right] \times$$
$$\times \sum_{n=0}^{\infty} J_n\left(\frac{eV_0}{\hbar\omega}\right) \exp\left[-i\left(\varepsilon + n\hbar\omega\right)t/\hbar\right] \qquad (3)$$

where ω is the frequency of the induced microwave field, J_n is the n-th order Bessel function of first kind and V_0 is the amplitude of the ac-voltage. Eq. (3) represents the eigenfunction inside the quantum dot in the j-th region and the corresponding eigenfunction inside the superconducting leads is given by:

$$\Psi_\alpha(x,\varepsilon) = \left[C \exp(ik'x)\binom{u}{v} + D \exp(-ik'x)\binom{v}{u} \right] \times$$
$$\times \sum_{n=-\infty}^{\infty} J_n\left(\frac{eV_0}{\hbar\omega}\right) \exp\left[-i\left(\varepsilon + n\hbar\omega\right)t/\hbar\right]. \qquad (4)$$

The wave vectors k_j and k' are the wave vectors inside j-th quantum dot and inside the superconducting leads and

they are given by:

$$k_j = \frac{\left(2m^*(V_{\text{eff}} \pm \varepsilon + n\hbar\omega)\right)^{0.5}}{\hbar} \quad (5)$$

and

$$k' = \frac{\left(2m^*(E_F - V_b \pm \sqrt{(\varepsilon + n\hbar\omega)^2 - \Delta^2}\right)^{0.5}}{\hbar} \quad (6)$$

where V_{eff} is expressed as:

$$V_{\text{eff}} = V_b + \frac{U_c N^2}{2} + E_F + e\eta V_g \quad (7)$$

in which V_b is the Schottky barrier height, U_c is the charging energy of the quantum dot, E_F is the Fermi-energy, Δ is the energy gap of superconductor, V_g is the gate voltage and η is the lever arm. The eigenfunctions u and v (Eq. 4) of the corresponding electron/hole due to Andreev reflection process at the semiconductor-superconductor interface are given by:

$$u = \sqrt{\frac{1}{2}\left(1 + \frac{\left((\varepsilon + n\hbar\omega)^2 - \Delta^2\right)^{0.5}}{\varepsilon + n\hbar\omega}\right)} \quad (8)$$

and

$$v = \sqrt{\frac{1}{2}\left(1 - \frac{\left((\varepsilon + n\hbar\omega)^2 - \Delta^2\right)^2}{\varepsilon + n\hbar\omega}\right)}. \quad (9)$$

Now, in order to evaluate the shot noise spectrum, this can be achieved by substituting the current operator Eq. 2 into Eq. 1 and determining the expectation value [19] and after simple algebraic steps, we get a formula for the shot noise spectrum $P(\omega)$ [20] as:

$$P(\omega) = \frac{2eP_0}{h} \sum_{\alpha,\beta} \int_0^\infty d\varepsilon \, |\Gamma(\varepsilon)| \, f_{\alpha FD}(\varepsilon) \times \\ \times \left[1 - f_{\beta FD}(\varepsilon + n\hbar\omega)\right], \quad (10)$$

where P_0 is the Poissonian shot noise spectrum and $f_{\beta FD}(\varepsilon + n\nabla\omega)$ are the Fermi distribution functions.

The tunneling rate, $\gamma(\varepsilon)$ through the barrier must be modified due to the influence of the induced microwave field as [21]:

$$\tilde{\gamma}(\varepsilon) = \sum_{n=-\infty}^{\infty} J_n^2\left(\frac{eV_0}{\hbar\omega}\right) \gamma(\varepsilon + n\hbar\omega). \quad (11)$$

The tunneling rate, $\gamma(\varepsilon)$ is related to the tunneling probability, $\Gamma(\varepsilon)$ [21] as:

$$\gamma(\varepsilon) = \frac{2\pi}{\hbar} \int_{E_F}^{E_F + 2\Delta\hbar\omega} d\varepsilon \, \Gamma(\varepsilon) \rho(\varepsilon) f_{FD}(\varepsilon) \times \\ \times \left(1 - f_{FD}(\varepsilon - \Delta F)\right) \quad (12)$$

in which ΔF is the difference in final and initial free energy

after and before the influence of microwave field. The tunneling probability, $\Gamma(\varepsilon)$, Eq. 10 has been determined by the authors [22, 23] using the transfer matrix method and it is expressed as:

$$\Gamma(\varepsilon + n\hbar\omega) = \frac{1}{\left(1 + C_1^2 C_2^2\right)} \quad (13)$$

where C_1 and C_2 are expressed as:

$$C_1 = \frac{V_{\text{eff}} \sinh(kb)}{2\sqrt{L_1}} \quad (14)$$

and

$$C_2 = 2\cosh(kb)\cos(k'a) - C_3. \quad (15)$$

We have used the following notations:

$$L_1 = (\varepsilon + n\hbar\omega)(V_{\text{eff}} - \varepsilon - n\hbar\omega),$$

$$C_3 = \left(\frac{L_2}{\sqrt{L_1}}\right)\sin(k'a)\exp(2kb), \quad (16)$$

$$L_2 = 2(\varepsilon + n\hbar\omega) - V_{\text{eff}}.$$

The parameters a and b represent the quantum dot size and the width of the barrier.

Now substituting Eq. 13 into Eq. 10 an expression for the frequency dependent shot noise spectrum and it depends on the geometrical dimension of the device under study.

3   Results and discussion

The shot noise spectrum, $P(\omega)$, Eq. 10 has been computed over a wide range of frequencies of the induced microwave field and at different temperatures. We considered a double quantum dots which they are a fully controllable two-level system. These quantum dots are AlGaAs-GaAs heterostructure and the leads are Nb superconductor. The calculations were performed for the cases: absorption of quanta from the environment (Fig. 1) and emission case (Fig. 2). The Schottky barrier height, V_b, was calculated by using a Monte-Carlo technique [24] and found to be equal to 0.47 eV. This value is in good agreement with those found by the authors [25]. As shown in Fig. 1 and Fig. 2, the normalized shot noise spectrum exhibits resonances at certain frequencies for both absorption and emission processes. The present results show that the Coulomb oscillations are modified by frequency of the induced microwave field over a wide range. Also, the Andreev reflection processes at the semiconductor-superconductor interface plays very important role for the appearance of these resonances. Our results show that the interplay between electronic transport and excitation by microwave is a particular interest. As high frequency perturbations are expected to yield a new nonequilibrium situation resulted from additional phase variations in energy states [26, 27, 28].
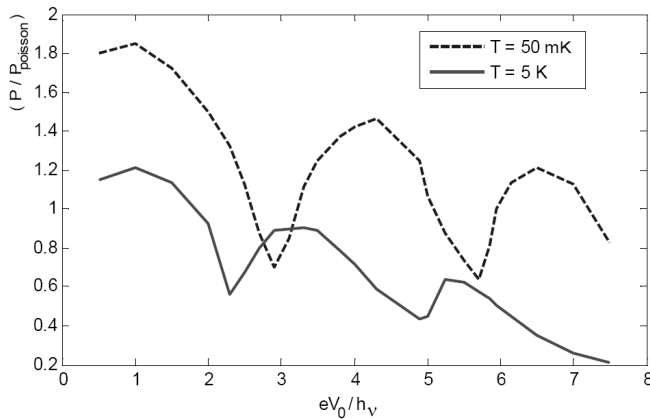
Fig. 1: The dependence of the normalized shot noise spectrum ($P/P_{poisson}$) on the normalized strength of the driving field (absorption case).
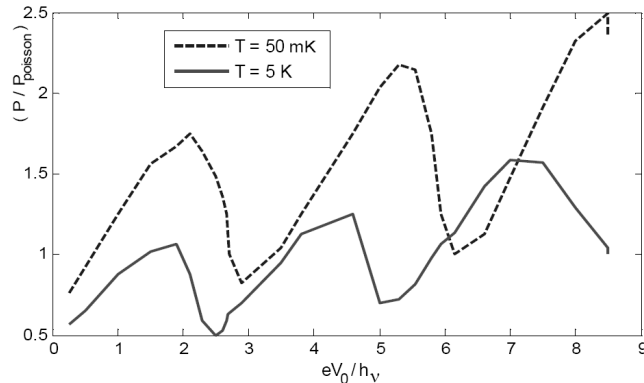

Fig. 2: The dependence of the normalized shot noise spectrum ($P/P_{poisson}$) on the normalized strength of the driving field (emission case).

4 Conclusions

In present paper, an expression for the shot noise spectrum has been deduced. The present studied mesoscopic device is modeled as double quantum dots coupled weakly to superconducting leads. The tunneling through the device is induced by microwave field of wide range of frequencies. The effect of both Andreev reflection processes and the Coulomb blockade had been taken into consideration. The resonances show the interplay between the forementioned effects and the photon induced microwave field. Our results show a concordant with those in the literature.

References

1. Toyoda E., Takayanagi H. and Nakano H. *J. Phys. Soc. Jpn*, 2000, v. 69, 1801.

2. Dayem A. H. and Martin R. J. *Phys. Rev. Lett.*, 1962, v. 8, 246.

3. Tien P. K. and Gordon J. P. *Phys. Rev.*, 1963, v. 129, 647.

4. Kouwenhoven L. P., Jauhar S., Orenstein J., McEuen P. L., Nagamune Y., Motohisa J., and Sakaki H. *Phys. Rev. Lett.*, 1994, v. 73, 3443.

5. Wiel V., Fujisawa W. G., Osterkamp T. H., and Kouwenhoven L. P. *Physica B*, 1999, v. 272, 31.

6. Keay B. J., Zeuner S., and Allen S. J. *Phys. Rev. Lett.*, 1995, v. 75, 4102.

7. Blanter Ya. M. and Buttiker M. *Phys. Rep.*, 2000, v. 336, 1.

8. Nagaev K. E. and Buttiker M. *Phys. Rev.*, 2001, v. B63, 081301(R).

9. Hoffmann C., Lefloch F., and Sanquer M. *Eur. Phys. J.*, 2002, v. B29, 629.

10. Phillips A. H. *Second Spring School on Current Activities of Materials Science*, Assiut University, Assiut, Egypt, 2000.

11. Camalet S., Lehmann J., Kohler S., and Hanggi P. *Phys. Rev. Lett.*, 2003, v. 90, 210602.

12. Brandes J. *Phys. Rev.*, 1997, v. B56, 1213.

13. DeJong M. J. M. and Beenakker C. W. Shot noise in mesoscopic systems. arXiv: cond-mat/9611140.

14. Aguado R. and Kouwenhoven L. P. *Phys. Rev. Lett.*, 2000, v. 84, 1986.

15. DeJong M. J. M. and Beenakker C. W. J. In: *Proceedings of Advanced Study Institute on Mesoscopic Electron Transport*, edited by Sohn L. L., Kouwenhoven L. P. and Schon G., Kluwer, Dordrecht, 1997.

16. Andreev A. F. *Sov. Phys. JETP*, 1964, v. 19, 1228.

17. Furusaki A., Takayanagi H., and Tsukada M. T. *Phys. Rev.*, 1992, v. B45, 10563.

18. Aly A. H., Phillips A. H., and Kamel R. *Egypt. J. Phys.*, 1999, v. 30, 32.

19. Beenakker C. W. J. and Buttiker M. *Phys. Rev.*, 1992, v. B46, R1889.

20. Blanter Ya. M. and Sukhorukov E. V. *Phys. Rev. Lett.*, 2000, v. 84, 1280.

21. Platero G. and Aguado R. Photon-assisted transport in semiconductor nanostructures. arXiv: cond-mat/0311001.

22. Mina A. N. *Egypt. J. Phys.*, 2001, v. 32, 253.

23. Atallah A. S. and Phillips A. H. *Proceedings of The International Conference on Materials Science and Technology*, Faculty of Science, Cairo University, Beni-Suef, Egypt, April 2–4, 2001.

24. Aly A. H. and Phillips A. H. *Phys. Stat. Sol. (B)*, 2002, v. 232, 238.

25. Becker Th., Muck M., and Heiden Ch. *Physica B*, 1995, v. 204, 14286.

26. Fujisawa T. and Hirayama Y. *Appl. Phys. Lett.*, 2000, v. 77, 543.

27. Camalet S., Kohler S., and Hanggi P. arXiv: cond-mat/0402182.

28. Phillips A. H., Mina A. N., Sobhy M. S., and Fouad E. A. Accepted for publ. in *J. Comput. & Theor. Nanoscience*, 2006.

Completing Einstein's Proof of $E = mc^2$

C. Y. Lo

Applied and Pure Research Institute, 17 Newcastle Drive, Nashua, NH 03060, USA
E-mail: c_y_lo@yahoo.com; C_Y_Lo@alum.mit.edu

It is shown that Einstein's proof for $E = mc^2$ is actually incomplete and therefore is not yet valid. A crucial step is his implicit assumption of treating the light as a bundle of massless particles. However, the energy-stress tensor of massless particles is incompatible with an electromagnetic energy-stress tensor. Thus, it is necessary to show that the total energy of a light ray includes also non-electromagnetic energy. It turns out, the existence of intrinsic difference between the photonic and the electromagnetic energy tensors is independent of the coupling of gravity. Nevertheless, their difference is the energy-stress tensor of the gravitational wave component that is accompanying the electromagnetic wave component. Concurrently, it is concluded that Einstein's formula $E = mc^2$ necessarily implies that the photons include non-electromagnetic energy and that the Einstein equation of 1915 must be rectified.

1 Introduction

In physics, the most famous formula is probably $E = mc^2$ [1]. However, it is also this formula that many[(1)] do not understand properly [2, 3]. Einstein has made clear that this formula must be understood in terms of energy conservation [4]. In other words, there is energy related to a mass, but there may not be an equivalent mass for any type of energy [2]. As shown by the Riessner-Nordstrom metric [5, 6], the gravity generated by mass and that by the electromagnetic energy are different because an electromagnetic energy stress tensor is traceless. Thus, the relationship between mass and energy would be far more complicated than as commonly believed.

In Einstein's 1905 derivation,[(2)] he believed [7] that the corresponding was between mass and any type of energy although he dealt with only the light, which may include more than just electromagnetic energy. Moreover, although his desired generality has not been attained, his belief was very strong. On this, Stachel [7] wrote,

> "Einstein returned to the relation between inertial mass and energy in 1906 and in 1907 giving more general arguments for their complete equivalence, but he did not achieve the complete generality to which he inspired. In his 1909 Salzburg talk, Einstein strongly emphasized that inertial mass is a property of all form of energy, and therefore electromagnetic radiation must have mass. This conclusion strengthened Einstein's belief in the hypothesis that light quanta manifest particle-like properties."

Apparently, the publications of the papers of Reissner [6] and Nordstrom [5] have changed the view of Einstein as shown in his 1946 article [4].

Perhaps, a root of misunderstanding $E = mc^2$ is related to the fact that the derivation of this formula [8] has not been fully understood. In Einstein's derivation, a crucial step is his implicit assumption of treating light as a bundle of massless particles. However, because gravity has been ignored in Einstein's derivation, it was not clear that an electromagnetic energy-stress tensor is compatible with the energy-stress tensor of massless particles.

Such an issue is valid since the divergence of an electromagnetic energy-stress tensor $\nabla_c T(E)^{cb}$ (where ∇_c is a covariant derivative) generates only the Lorentz force, whereas the divergence of a massive energy-stress tensor $\nabla_c T(m)^{cb}$ would generate the geodesic equation [9].

Thus, the energy-stress of photons $T(L)_{ab}$ would be

$$T(L)_{ab} = T(E)_{ab} + T(N)_{ab} \qquad (1)$$

or

$$T(N)_{ab} = T(L)_{ab} - T(E)_{ab}$$

where $T(E)_{ab}$ and $T(N)_{ab}$ are respectively the electromagnetic energy-stress tensor and a non-electromagnetic energy-stress tensor. Besides, being intrinsically traceless, $T(E)_{cb}$ would not be compatible with Einstein's formula $\triangle E = \triangle mc^2$. Based on the fact that the electromagnetic energy is dominating experimentally, it is natural to assume as shown later that $T(N)_{ab}$ is in fact the gravitational energy-stress tensor $T(g)_{ab}$.

2 A field equation for the accompanying gravitational wave

Physics requires also that the energy-stress tensor for photons $T(L)_{ab}$ is: (1) traceless, (2) $T(L)_{ab} \approx T(E)_{ab}$ and $\left[T(L)_{tt} - T(E)_{tt} \right] > 0$ on the average, and (3) related to a gravitational wave, i. e. satisfying

$$R_{ab} - \frac{1}{2} g_{ab} R = K T(g)_{ab} = -K \left[T(E)_{ab} - T(L)_{ab} \right], \quad (2)$$

where R_{ab} is the Ricci tensor, and $R = g^{mn} R_{mn}$. Eq. (2) dif-

fers from Einstein equation with an additional term $T(L)_{ab}$ having a coupling of different sign. However, Eq. (2) is similar to the modified Einstein equation,

$$G_{ab} = R_{ab} - \frac{1}{2} g_{ab} R = -K \left[T(m)_{ab} - T(g)_{ab} \right], \quad (3)$$

which is necessitated by the Hulse-Taylor experiment [10, 11]. $T(g)_{ab}$ is non-zero since a gravitational wave carries energy. From Eq. (2), we have $\nabla_c T(L)^{cb} = 0$ since there $\nabla_c T(E)^{cb} = 0$ and $\nabla_c G^{cb} \equiv 0$.

Related to Eq. (2), a crucial question is whether the Einstein equation with only the electromagnetic wave energy-stress tensor as the source is valid. It has been found that such an equation cannot produce a physically valid solution [12]. Historically, it is due to that the Einstein equation does have a physical plane-wave solution that the need of a photonic energy-stress tensor is recognized (see also Sect. 3). One may object that the general form of gravitational energy-stress tensor is not yet known although its approximation for the weak gravity with the massive source is known to be equivalent to Einstein's pseudo-tensor for the gravitational energy-stress [10]. However, for this case, the related gravitational energy-stress tensor is defined by formula (1).

Now the remaining question is whether (2) would produce a gravitational wave. However, we should address first whether an electromagnetic wave has an accompanying gravitational wave. The answer is affirmative because the electromagnetic energy is propagating with the allowed maximum speed in Special Relativity.[3] Thus, the gravity due to the light energy should be distinct from that generated by massive matter [13].

Since a field emitted from an energy density unit means a non-zero velocity relative to that unit, it is instructive to study the velocity addition. According to Special Relativity, the addition of velocities is as follows:

$$u_x = \frac{\sqrt{1 - v^2/c^2}}{1 + u_z' v/c^2} u_x', \quad u_y = \frac{\sqrt{1 - v^2/c^2}}{1 + u_z' v/c^2} u_y',$$
$$\text{and} \ \ u_z = \frac{u_z' + v}{1 + u_z' v/c^2}, \quad (4)$$

where velocity $\vec{v}$ is in the z-direction, (u_x', u_y', u_z') is a velocity w. r. t. a system moving with velocity v, c is the light speed, $u_x = dx/dt$, $u_y = dy/dt$, and $u_z = dz/dt$. When $v = c$, independent of (u_x', u_y', u_z') one has

$$u_x = 0, \ \ u_y = 0, \ \ \text{and} \ \ u_z = c. \quad (5)$$

Thus, neither the direction nor the magnitude of the velocity $\vec{v} \, (= \vec{c})$ have been changed.

This implies that nothing can be emitted from a light ray, and therefore no field can be generated outside the light ray. To be more specific, from a light ray, no gravitational field can be generated outside the ray although, accompanying the light ray, a gravitational field $g_{ab}(\neq \eta_{ab}$ the flat metric) is allowed within the ray.

According to the principle of causality [13], this accompanying gravity g_{ab} should be a gravitational wave since an electromagnetic wave is the physical cause. This would put General Relativity into a severe test for theoretical consistency. But, this examination would also have the benefit of knowing whether Einstein's implicit assumption in his proof for $E = mc^2$ is valid.

Let us consider the energy-stress tensor $T(L)_{ab}$ for photons. If a geodesic equation must be produced, for a monochromatic wave with frequency ω, the form of a photonic energy tensor should be similar to that of massive matter. Observationally, there is very little interaction, if any, among photons of the same ray. Theoretically, since photons travel in the velocity of light, there should not be any interaction (other than collision) among them. Therefore, the photons can be treated as a bundle of massless particles just as Einstein [8] did.

Thus, the photonic energy tensor of a wave of frequency ω should be dust-like and traceless as follows:

$$T^{ab}(L) = \rho P^a P^b, \quad (6)$$

where ρ is a scalar and is a function of $u \, (= ct - z)$. In the units $c = h = 1$, $P^t = \omega$. The geodesic equation, $P^c \nabla_c P^b = 0$, is implied by $\nabla_c T(L)^{cb} = 0$ and also $\nabla_c (\rho P^c) = 0$. Since $\nabla_c (\rho P^c) = \left[\rho g^{bc} g_{bc}' + \rho' \right] (P^t - P^z) = 0$, formula (6) does produces a geodesic equation if Eq. (2) is satisfied.

3 The reduced Einstein equation for an electromagnetic plane wave

Let us consider a ray of uniform electromagnetic waves (i. e. a laser beam) propagating in the z-direction. Within the ray, one can assume that the wave amplitude is independent of x and y. Thus, the electromagnetic potentials are plane-waves, and in the unit that light speed $c = 1$,

$$A_k(x, y, z, t) = A_k(t - z), \ \ \text{where} \ \ k = x, y, z, t. \quad (7)$$

Due to the principle of causality, the metric g_{ab} is functions of $u \, (= t - z)$, i. e.,

$$g_{ab}(x, y, z, t) = g_{ab}(u), \ \ \text{where} \ \ a, b = x, y, z, t. \quad (8)$$

Since, for this case, the coordinates for Special Relativity are also valid for General Relativity [14–16], such a consideration is valid. Let P^k be the momentum of a photon. If a photon is massless, one obtains the conditions,

$$P^z = P^t, \ \ P^x = P^y = 0, \ \ \text{and} \ \ P^m g_{mk} = P_k = 0, \quad (9)$$

for $k = x, y$, and $v \, (= t + z)$. Eq. (9a) is equivalent to

$$g_{xt} + g_{xz} = 0, \quad\quad g_{yt} + g_{yz} = 0,$$
$$\text{and} \ \ g_{tt} + 2 g_{tz} + g_{zz} = 0, \quad (10)$$

or

$$g^{xt} - g^{xz} = 0, \qquad g^{yt} - g^{yz} = 0,$$

$$\text{and} \;\; g^{tt} - 2g^{zt} + g^{zz} = 0.$$

(11)

The transverse of an electromagnetic wave implies

$$P^m A_m = 0,$$

$$\text{or equivalently} \;\; A_z + A_t = 0.$$

(12)

Eqs. (7) to (9) imply that not only the geodesic equation, the Lorentz gauge, but also Maxwell's equation are satisfied. Moreover, the Lorentz gauge becomes equivalent to a covariant expression.

For an electromagnetic wave being the source, Einstein [17] believed the field equation is $G_{ab} = -KT(E)_{ab}$, where $T(E)_{ab} = -g^{mn} F_{ma} F_{nb} + \frac{1}{4} g_{ab} F^{mn} F_{mn}$, while $F_{ab} = \partial_a A_b - \partial_b A_a$ is the field tensor. Since the trace of the energy-stress tensor is zero, $R = 0$. It follows that

$$R_{tt} = -R_{tz} = R_{zz},$$

(13)

because $F^{mn} F_{mn} = 0$ due to Eq. (9). The other components are zero [12]. Then,

$$R_{tt} \equiv -\frac{\partial \Gamma^m_{tt}}{\partial x^m} + \frac{\Gamma^m_{mt}}{\partial t} - \Gamma^m_{mn} \Gamma^n_{tt} + \Gamma^m_{nt} \Gamma^n_{mt} =$$

$$= -KT(E)_{tt} = Kg^{mn} F_{mt} F_{nt}.$$

(14)

After some lengthy algebra [12], Eq. (14) is simplified to a differential equation of u as follows:

$$G'' - g'_{xx} g'_{yy} + (g'_{xy})^2 - G'(g'/2g) = 2GR_{tt} =$$

$$= 2K \left(F^2_{xt} g_{yy} + F^2_{yt} g_{xx} - 2F_{xt} F_{yt} g_{xy} \right),$$

(15)

where

$$G \equiv g_{xx} g_{yy} - g^2_{xy}, \;\; \text{and} \;\; g = |g_{ab}|,$$

the determinant of the metric. The metric elements are connected by the following relation:

$$-g = G g^2_t, \;\; \text{where} \;\; g_t = g_{tt} + g_{tz}.$$

(16)

Note that Eqs. (35.31) and (35.44) in reference [18] and Eq. (2.8) in reference [19] are special cases of Eq. (15). But, their solutions are unbounded [17]. However, compatibility with Einstein's notion of weak gravity is required by the light bending calculation and is implied by the equivalence principle [20].

Equations (9)–(16) allow A_t, g_{xt}, g_{yt}, and g_{zt} to be set to zero. In any case, these assigned values have little effect in subsequent calculations. For the remaining metric elements (g_{xx}, g_{xy}, g_{yy}, and g_{tt}), however, Eq. (15) is sufficient to show that there is no physical solution. In other words, in contrast to Einstein's belief [17], the difficulty of this equation is not limited to mathematics.

4　Verification of the rectified Einstein equation

Now, consider an electromagnetic plane-wave of circular polarization, propagating to the z-direction

$$A_x = \frac{1}{\sqrt{2}} A_0 \cos \omega u, \;\; \text{and} \;\; A_y = \frac{1}{\sqrt{2}} A_0 \sin \omega u,$$

(17)

where A_0 is a constant. The rotational invariants with respect to the z-axis are constants. These invariants are: G_{tt}, R_{tt}, $T(E)_{tt}$, G, $(g_{xx} + g_{yy})$, g_{tz}, g_{tt}, g, and etc. It follows that [12–13]

$$g_{xx} = -1 - C + B_\alpha \cos(\omega_1 u + \alpha),$$

$$g_{yy} = -1 - C - B_\alpha \cos(\omega_1 u + \alpha),$$

$$g_{xy} = \pm B_\alpha \sin(\omega_1 u + \alpha),$$

(18)

where C and B_α are small constants, and $\omega_1 = 2\omega$. Thus, metric (18) is a circularly polarized wave with the same direction of polarization as the electromagnetic wave (17). On the other hand, one also has

$$G_{tt} = 2\omega^2 B^2_\alpha / G \geqslant 0, \quad \text{and}$$

$$T(E)_{tt} = \frac{1}{2G} \omega^2 A^2_0 (1 + C - B_\alpha \cos \alpha) > 0,$$

(19)

where $G = (1 + C)^2 - B^2_\alpha > 0$. Thus, it is not possible to satisfy Einstein's equation because $T(E)_{tt}$ and G_{tt} have the same sign. Therefore, it is necessary to have a photonic energy-stress tensor.

If the photons are massless particles, the photonic energy-stress tensor (6) has a density function [12],

$$\rho(u) = -A_m g^{mn} A_n \geqslant 0$$

(20)

which is a scalar function of $u \, (= t - z)$. Since light intensity is proportional to the square of the wave amplitude, which is Lorentz gauge invariant, $\rho(u)$ can be considered as the density function of photons. Then

$$T_{ab} = -T(g)_{ab} = T(E)_{ab} - T(L)_{ab} =$$

$$= T(E)_{ab} + A_m g^{mn} A_n P_a P_b.$$

(21)

Note that since $\rho(u)$ is a positive non-zero scalar consisting of A_k and/or fields such that, on the average, $T(L)_{ab}$ is approximately $T(E)_{ab}$ and Eq. (2) would have physical solutions, $\rho = -A_m g^{mn} A_n$ is the only choice.

As expected, tensor $T(L)_{ab}$ enables a valid solution for wave (17). According to Eq. (2) and formula (21),

$$T_{tt} = -\frac{1}{G} \omega^2 A^2_0 B_\alpha \cos \alpha < 0,$$

(22)

since $B_\alpha = (K/2) A^2_0 \cos \alpha$. Thus, $T(g)_{tt} = -T_{tt}$ is of order K. It will be shown that $\cos \alpha = 1$.

C. Y. Lo.　Completing Einstein's Proof of $E = mc^2$

To confirm the general validity of (2) further, consider a wave linearly polarized in the x-direction,

$$A_x = A_0 \cos \omega(t - z). \tag{23}$$

Then,

$$T(E)_{tt} = -\frac{g_{yy}}{2G}\,\omega^2 A_0^2 \left[1 - \cos 2\omega(t - z)\right] \ \text{ and}$$

$$T_{tt} = \frac{g_{yy}}{2G}\,\omega^2 A_0^2 \cos 2\omega(t - z). \tag{24}$$

Note that independent of the coupling K, T_{tt} is non-zero. Since the gravitational component is not an independent wave, $T(g)_{tt}(= -T_{tt})$ is allowed to be negative or positive [13]. Eq.(19) implies $(g_{xx} + g_{yy})'$ to be of first order [13], and thus its polarization has to be different.

It turns out that the solution is a linearly polarized gravitational wave and that, as expected, the time-average of $T(g)_{tt}$ is positive of order K [13]. From the viewpoint of physics, for an x-directional polarization, gravitational components related to the y-direction, remains the same. In other words,

$$g_{xy} = 0 \ \text{ and } \ g_{yy} = -1. \tag{25}$$

It follows [10, 11] that $G = -g_{xx}$ and the general solution for wave (18) is:

$$-g_{xx} = 1 + C_1 - (K/2)A_0^2 \cos\left[2\omega(t - z)\right],$$

$$\text{and} \ \ g_{tt} = -g_{zz} = \sqrt{g/g_{xx}}, \tag{26}$$

where C_1 is a constant and g is the determinant of the metric. The frequency ratio is the same as that of a circular polarization. However, there is no phase difference as α in (18). According to the principle of causality, α has a value, and to be consistent with (26) $\alpha = 0$.

However, if $T(L)_{ab}$ were absent, one would have,

$$-g_{xx} = 1 + C_1 - (K/4)\,A_0^2 \left(2\omega^2(t - z)^2 + \right.$$

$$\left. + \cos\left[2\omega(t - z)\right]\right) + C_2(t - z), \tag{27}$$

where C_1 and C_2 are constants. But solution (27) is invalid in physics since $(t - z)^2$ grows very large as time goes by. This would "represent" the effects if Special Relativity were invalid, and the wave energy were equivalent to mass. This illustrates that Einstein's notion of weak gravity, which is the theoretical basis for his calculation on the bending of light, may not be compatible with the Einstein equation with an inadequate source term.

5 Conclusions and discussions

A photonic energy-stress tensor has been obtained to satisfy the demanding physical requirements. The energy and momentum of a photon are proportional to its frequency although, as a classical theory, their relation-ship with the Planck constant h is not yet clear. Just as expected from Special Relativity, indeed, the gravity of an electromagnetic wave is an accompanying gravitational wave propagating with the same speed.[4] Concurrently, for this case, the need of modifying the Einstein equation is accomplished. Then, clearly the gravity due to the light is negligible in calculating the light bending [8].

In this derivation, it is crucial that the spatial coordinates are proven the same in Special and General Relativity [14–16] because the space coordinates must have the Euclidean-like structure.[5] For this case, even the time coordinate is the same, and the plane wave satisfied the Maxwell equation in terms of both Special and General Relativity [16], Thus, Special Relativity and General Relativity are consistent with each other. Einstein's proof is clearly incomplete since the energy-stress tensor of photons is different from that of electromagnetism.

A particle such as the photon has no inertial mass since it is subjected to only absorption and emission, but not acceleration and deceleration. Based on Special Relativity, it has been shown that the electromagnetic energy is distinct from the energy of a rest mass.[6] Interestingly, *it is precisely because of this non-equivalence of mass and energy that photonic energy-stress tensor* (6) *is valid, and the formula* $E = mc^2$ *can be proven.*

One might argue that experiment shows the notion of massless photons is valid, and thus believed the equivalence of mass and electromagnetic energy. However, while the addition of two massless particles may end up with a rest mass, the energy-stress tensor of electromagnetism cannot represent a rest mass since such a tensor is traceless. Thus, the formula[7] $\triangle E = \triangle mc^2$ necessarily implies that $T(L)_{ab}$ must include non-electromagnetic energy. Note that $\left[T(L)_{tt} - T(E)_{tt}\right]$ being non-zero, is independent of the gravitational coupling constant K. This makes it clear that the photonic energy tensor is intrinsically different from the electromagnetic energy tensor.

Although the formula $E = mc^2$ has been verified in numerous situations [1, 18], its direct physical meaning related to gravity was not understood;[8] and thus this formula is often misinterpreted, in conflict with General Relativity [2, 9], as any type of energy being equivalent to a mass [3]. A related natural question is how to measure the gravitational component of a light ray. However, in view of the difficulties encountered in measuring pure gravitational waves, the quantitative measurement of such a gravitational component is probably very difficult with our present level of technology although its qualitative existence is proven by the formula $E = mc^2$.

Both quantum theory and relativity are based on the phenomena of light. The gravity of photons finally shows that there is a link between them. It is gravity that makes the notion of photons compatible with electromagnetic waves.

Clearly, gravity is no longer just a macroscopic phenomena, but also a microscopic phenomena of crucial importance to the formula $E = mc^2$. In Einstein's proof, it has not been shown whether his implicit assumption is compatible with electromagnetism. This crucial problem is resolved with the gravity of an electromagnetic wave. Einstein probably would smile heartily since his formula confirms the link that relates gravity to quantum theory.

Acknowledgments

Endnotes

(1) They include, but not limited to, Fock [21], Hawking [22], Misner, Thorne, & Wheeler [18], Tolman [23], and Will [3].

(2) In 1907 Plank [24] criticized the Einstein argument, and presented his own argument to show that the transfer of heat is associated with a similarly related transfer of inertial mass [7].

(3) In this paper, the convention of the metric signature for Special Relativity is $(1, -1, -1, -1)$.

(4) Some arguments, which were presented differently in the literature [13], are included in this paper for the convenience of the readers. For instance, now the value of α in (18) is obtained.

(5) Einstein called this structure as "in the sense of Euclidean geometry" [8], but failed to understand its physical meaning in terms of measurements [15, 25]. Weinberg [26] has showed, however, that in a curved space the coordinates can be straight.

(6) However, there are theorists such as Tolman [23], who incorrectly saw no difference in terms of gravity between mass and the energy in a light ray.

(7) Einstein's formula $\triangle E = \triangle mc^2$ is proven for radiating energy. Thus, it is applicable to the atomic bomb.

(8) Bodanis [1] gives a good account of how the formula $E = mc^2$ is applied. However, like many others, he also misinterpreted the formula as general equivalence between any type of energy and mass.

References

1. Bodanis D. $E = mc^2$: A biography of the world's most famous equation. The Berkley Publishing Group, New York, 2001.

2. Lo C. Y. *Astrophys. J.*, 1997, v. 477, 700–704.

3. Will C. M. Theory and experiment in gravitational physics. Cambridge Univ. press, Cambridge, 1981.

4. Einstein A. $E = Mc^2$ (from science illustrated 1946) ideas and opinions. Crown, New York, 1954, p. 337.

5. Reissner H. *Annalen der Physik*, 1916, Bd. 50, 106–120.

6. Nordstrom G. On the energy of gravitational field in Einstein's theory. *Proc. Kon. Ned. Akad. Wet.*, 1918, v. 20, 1238.

7. Stachel J., Editor. Einstein's miraculous year. Princeton Press, 1998, p.118.

8. Einstein A., Lorentz H. A., Minkowski H., and Weyl H. The Principle of Relativity. Dover, New York, 1923.

9. Lo C. Y. *Phys. Essays*, 1997, v. 10(4), 540–545.

10. Lo C. Y. *Astrophys. J.*, 1995, v. 455, 421–428.

11. Lo C. Y. *Phys. Essays*, 2000, v. 13(4), 527–539.

12. Lo C. Y. *Phys. Essays*, 1999, v. 12(2), 226–241.

13. Lo C. Y. *Phys. Essays*, 1997, v. 10(3), 424–436.

14. Lo C. Y. *Phys. Essays*, 2002, v. 15(3), 303–321.

15. Lo C. Y. *Chinese J. of Phys.*, 2003, v. 41(4), 1–11.

16. Lo C. Y. *Progress in Physics*, 2006, v. 1, 46.

17. Einstein A. Physics and reality (1936) in ideas and opinions. Crown, New York, 1954, p. 311.

18. Misner C. W., Thorne K. S., and Wheeler J. A. Gravitation. Freeman, San Francisco, 1973.

19. Bondi H., Pirani F. A. E., and Robinson I. *Proc. R. Soc. London A*, 1959, v. 251, 519–533.

20. Lo C. Y. *Phys. Essays*, 1999, v. 11(3), 508–526.

21. Fock V. A. The theory of space time and gravitation. Pergamon Press, 1964.

22. Hawking S. A brief history of time. Bantam Books, New York, 1988.

23. Tolman R. C. Relativity, thermodynamics, and cosmology. Dover, New York, 1987.

24. Planck M. *Annalen der Physik*, 1907, Bd. 22, 180–190.

25. Lo C. Y. *Phys. Essays*, 2005, v. 18(4).

26. Weinberg S. Gravitation and cosmology. John Wiley Inc., New York, 1972, p. 6.

A Source of Energy for Any Kind of Star

Dmitri Rabounski

E-mail: rabounski@yahoo.com

We discuss a recently predicted mechanism whereby energy is produced by the background space non-holonomic field (the global space rotation) in Thomson dispersion of light in free electrons. We compare the mechanism to the relations of observational astrophysics — the mass-luminosity relation and the stellar energy relation. We show that by such a mechanism generating energy in a star, the luminosity of a star L is proportional to its volume, with a progression associated with increasing radius. The obtained relation $L \sim R^{3.4}$ explains why there are no stars of a size close to that of the bulky planets. This also explains the extremely high thermal flow from within Jupiter, which most probably has the same energy sources as those within a star, but with a power much less than that required to radiate like a star. The theory, being applied to a laboratory condition, suggests new energy sources, working much more effectively and safely than nuclear energy.

1 The mechanism that generates energy in stars

By way of introduction, a brief account of my theory of the mechanism producing energy in stars [1] built within the framework of General Relativity, is presented. Then, in the next section, we analyse consequences of the theory in comparison with the correlations of observational astrophysics.

Given a non-holonomic space[*], time lines piercing the spatial section (our proper three-dimensional space) are not orthogonal to the spatial section therein, which manifests as the three-dimensional space rotation. If all time lines have the same inclination to the spatial section at each of its points, there is a field of the background space non-holonomity. Such a non-holonomic background field, if perturbed by a local rotation, can produce a force and energy flow in order to compensate for the perturbation in itself. Such a force and energy flow were deduced on the basis of the equations of motion in a non-holonomic space: they manifest as additions to the total force $\Phi^i_{(0)}$ driving a particle and the total power $W_{(0)}$ spent on the motion

$$W = \frac{dE}{d\tau} = W_{(0)} + \delta^m_n \frac{\tilde{v}^n}{\bar{v}^m} W_{(0)} \,, \qquad (1)$$

$$\Phi^i = \frac{dp^i}{d\tau} = \Phi^i_{(0)} + \delta^m_n \frac{\tilde{v}^n}{\bar{v}^m} \Phi^i_{(0)} \,, \qquad (2)$$

where $\bar{v}^i$ is the constant linear velocity of the background space rotation, while $\bar{v}^i$ is the linear velocity of a local rotation perturbing the background. As obtained within the framework of General Relativity [1], the value of $\bar{v}^i$ is the fundamental constant $\bar{v} = 2.187\,671 \times 10^8$ cm/sec connected to the value $\bar{\mathrm{v}} = \frac{\bar{v}}{2\pi} = 3.481787 \times 10^7$ cm/sec of a dipole-fit velocity $\bar{\mathrm{v}}^i$ characterizing the anisotropy of the rotating background (which is similar to a global gyro). The analytical value $\bar{\mathrm{v}}$ is

---

[*]A four-dimensional pseudo-Riemannian space, which is the basic space-time of General Relativity.

in close agreement with the dipole-fit velocity 365 ± 18 km/sec extracted from the recently discovered anisotropy of the Cosmic Microwave Background Radiation.

Such an additional factor should appear in Thomson dispersion of light in free electrons in stars. When a light wave of average energy density B encounters a free electron, the flow of the wave energy $c\sigma B$ is stopped in the electron's square $\sigma = 6.65 \times 10^{-25}$ cm^2 (the Thomson square of dispersion). As a result the electron gains an acceleration σB, directed orthogonally to the wave front. With this process the electron oscillates in the plane of the wave at the frequency ω of the wave's electric strength E^i oscillating in the plane. Let the wave travel in the x^1-direction, so $E^2 = E$, $E^1 = E^3 = 0$. The oscillation equation gives the linear velocity $\tilde{v}^i$ of the local space rotation, caused by the oscillating electron,

$$\tilde{v}^2 = \frac{eE}{m_e \omega} \,, \qquad \tilde{v}^1 = 0 \,, \qquad \tilde{v}^3 = 0 \,. \qquad (3)$$

Because the density of energy in an isotropic electromagnetic field is $B = \frac{1}{4\pi} E_i E^i$, the additional force and the power produced in the Thomson process by the global non-holonomic background should be

$$\Delta W = \frac{\tilde{v}^2}{\bar{v}^2} W_{(0)} = \frac{e\sqrt{4\pi}}{m_e \bar{v}} \frac{\sqrt{B}}{\omega} W_{(0)} \,, \qquad (4)$$

$$\Delta \Phi^1 = \frac{\tilde{v}^2}{\bar{v}^2} \Phi^1_{(0)} = \frac{e\sqrt{4\pi}}{m_e \bar{v}} \frac{\sqrt{B}}{\omega} \Phi^1_{(0)} \,, \qquad (5)$$

so the output of energy ε produced by the non-holonomic background in the process (within one cm^3 per second) is

$$\varepsilon = \frac{\tilde{v}}{\bar{v}} c n_e \sigma B = \frac{c\sigma e \sqrt{4\pi}}{m_e \bar{v}} \frac{n_e B^{3/2}}{\omega} \,. \qquad (6)$$

In other words, our equation (6) is the *formula for stellar energy*. The factor $\frac{c\sigma e \sqrt{4\pi}}{m_e \bar{v}}$ is constant, while the second fac-
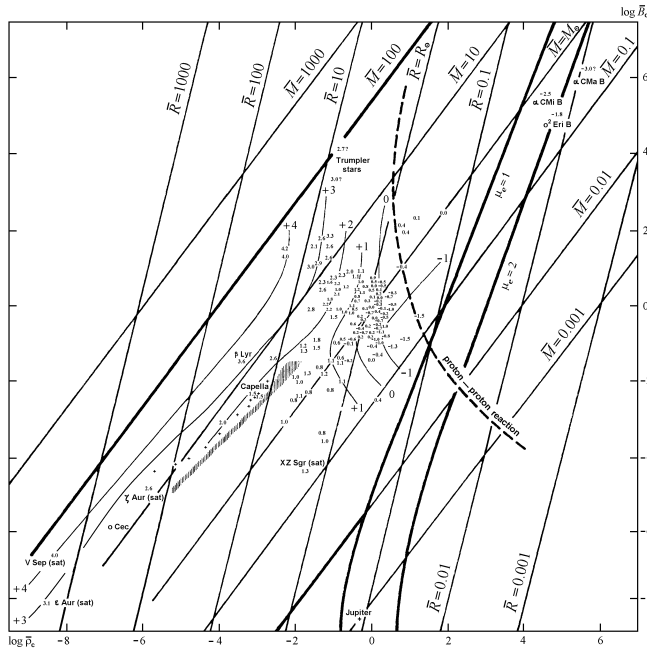
Fig. 1: Diagram of stellar energy: the productivity of stellar energy sources. The abscissa is the logarithm of the density of matter, the ordinate is the logarithm of the radiant energy density (both are taken at the centre of stars in multiples of the corresponding values at the centre of the Sun). Reproduced from [2]. Stars in the diagram are distributed along a straight line that runs from the right upper region to the left lower region, with a ball-like concentration at the centre of the diagram. The equation of the main direction is $\frac{B}{n_e} = 1.4 \times 10^{-11}$ erg (n_e is the concentration of free electrons).

tor depends mainly on the radiant energy density B in a star*.

Given the frequency $\nu = \frac{\omega}{2\pi} \approx 5 \times 10^{14}$ Hz (by the spectral class of the Sun), $\tilde{v}$ reaches the background space rotation $\bar{v} \simeq 2.2 \times 10^8$ cm/sec (so the additional energy flow fully compensates for the radiation) at $B = 1.4 \times 10^{11}$ erg/cm³, which is close to the average value of B in the Sun. The theoretical result coincides with the phenomenological data [2] by which energy is generated throughout the whole volume of a star with some concentration at the centre (in contrast to thermonuclear reactions working exclusively in the central region).

Besides the main direction $\frac{B}{n_e} = $ const, along which stars are distributed in the stellar energy diagram, Fig. 1 testifies that the power of a mechanism that generates energy in stars is regulated by the density of radiant energy, i. e. by the energy loss by radiation. So the real mechanism producing stellar energy works similar to a self-regulated machine and is independent of the inner resources reserved in stars.

Our formula for stellar energy (6) satisfies this condition, because the energy output is regulated by the radiant energy density B. So a mechanism that works by formula (6) at an oscillation velocity $\tilde{v}$ close to $\bar{v} \simeq 2.2 \times 10^8$ cm/sec behaves as an universal self-regulating generator of energy: the out-

---

*And, to a much smaller extent, on ω, which has changes within 1 order of magnitude along the whole range of the spectral classes of stars.
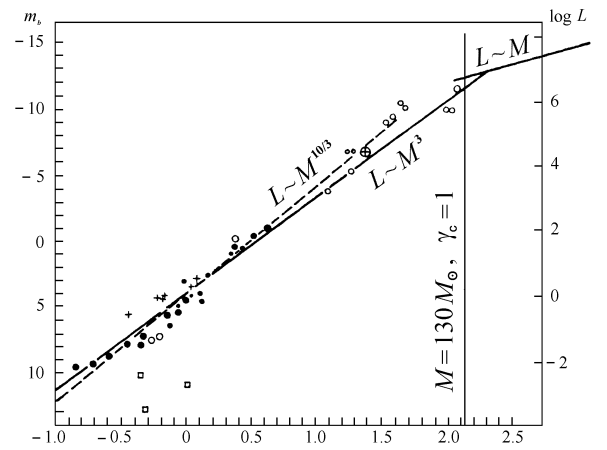

Fig. 2: The mass-luminosity relation. Here points are visual binaries, circles are spectral-binaries and eclipse variable stars, crosses are stars in Giades, squares are white dwarfs, the crossed circle is the satellite of ε Aurigae. Reproduced from [2].

put of energy ε the non-holonomic background produces in order to compensate for a perturbation $\tilde{v}$ in itself is regulated by the density of radiant energy B in the system, while the perturbation in the background $\tilde{v} = \frac{e\sqrt{4\pi}}{m_e \bar{v}} \frac{\sqrt{B}}{\omega}$ is caused by the oscillation of free electrons, also regulated by the radiant energy density B. If the average oscillation velocity of electrons $\tilde{v}$ in a star becomes larger than that of the background $\bar{v} \simeq 2.2 \times 10^8$ cm/sec, temperature increases, and so the star expands until a new state of thermal equilibrium is reached, with a larger luminosity that compensates for the increased generation of energy within. If the average oscillation velocity of electrons becomes less than $\bar{v} \simeq 2.2 \times 10^8$ cm/sec, the star contracts until a new thermal equilibrium with lower luminosity is attained.

If there were no other active factors slowly discharging the inner resources of a star (e. g. nuclear transformations of a different kind, etc), such a mechanism could generate stellar energy eternally, keeping stars in a stable radiating state.

2 Comparing the theory of stellar energy to observational data. The "volume-luminosity" correlation

We now analyse the implications of our formula (6) for stellar energy in comparison to the phenomenological data of observational astrophysics: the stellar energy relation (Fig. 1) and the mass-luminosity relation (Fig. 2).

We consider characteristics of a star in multiples of the corresponding values of the parameters for the Sun. We therefore operate with dimensionless characteristics: mass $\bar{M} = \frac{M}{M_\odot}$, radius $\bar{R} = \frac{R}{R_\odot}$, luminosity $\bar{L} = \frac{L}{L_\odot}$, productivity of energy $\bar{\varepsilon} = \frac{\varepsilon}{\varepsilon_\odot}$, etc. Using this notation, our formula (6) for stellar energy takes the form

$$\bar{\varepsilon} = \frac{\bar{n}_e \bar{B}^{3/2}}{\bar{\omega}} \simeq \bar{n}_e \bar{B}^{3/2}, \tag{7}$$

or, considering the hydrogen constitution of most stars, so that $n_e = \frac{\rho}{m_p}$ (i. e. $\bar{n}_e = \bar{\rho}$),

$$\bar{\varepsilon} = \frac{\bar{\rho}\bar{B}^{3/2}}{\bar{\omega}} \simeq \bar{\rho}\bar{B}^{3/2}. \qquad (8)$$

By the stellar energy relation $\frac{B}{n_e} = \mathrm{const}$ from the stellar energy diagram (see Fig. 1), we have $\bar{B} = \bar{n}_e = \bar{\rho}$ throughout the whole range of stars. We can therefore write the stellar energy formula (8) in the final form

$$\bar{\varepsilon} = \bar{\rho}\bar{B}^{3/2} = \bar{B}^{5/2}. \qquad (9)$$

By the data of observational astrophysics, stars obey the principles of an ideal gas, except for the white dwarfs wherein the gas is in a state on the boundary of degeneration. We therefore obtain by the equation for an ideal gas $p = \frac{\Re T\rho}{\mu}$ (where $\Re$ is Clapeyron's constant, μ is the molecular weight), $\bar{p} = \frac{\bar{T}\bar{\rho}}{\mu}$, or, with a similar molecular composition throughout the whole range of stars, $\bar{p} = \bar{T}\bar{\rho}$. The gaseous pressure p is determined by the state of mechanical equilibrium in a star, according to which the pressure from within is equal to the pressure of a column of the star's contents, so we obtain $\bar{p} = \frac{\bar{M}}{\bar{R}^2}\bar{\rho}\bar{R} = \frac{\bar{M}}{\bar{R}^2}\frac{\bar{M}}{\bar{R}^3}\bar{R} = \frac{\bar{M}^2}{\bar{R}^4}$. Therefore the density of radiant energy in a star is $\bar{B} = \bar{T}^4 = \frac{\bar{M}^4}{\bar{R}^4}$. So the stellar energy formula takes the final form,

$$\bar{\varepsilon} = \bar{B}^{5/2} = \frac{\bar{M}^{10}}{\bar{R}^{10}}. \qquad (10)$$

We analyze this result, taking the mass-luminosity relation into account. According to well verified data of observational astrophysics, stars satisfy the mass-luminosity relation $\bar{L} = \bar{M}^{10/3} \simeq \bar{M}^{3.3}$ (see Fig. 2). The relation $\bar{L} = \bar{M}^3$ can be deduced from theory. Here is how. Thermal equilibrium in a star is characterized by the equation [2]

$$\varepsilon = -\frac{c}{\kappa\rho}\frac{dB}{dr}, \qquad (11)$$

which means that the flow of energy generated in a star is balanced by the flow of radiant energy therein (κ is the coefficient of absorption). In other words, this formula is the *condition of energy drainage* in a star — the condition of radiation. From this formula we have, for stars of approximately the same chemical composition,

$$\bar{\varepsilon} = \frac{\bar{B}}{\bar{\rho}\bar{R}} = \frac{\bar{M}^3}{\bar{R}^2}, \qquad (12)$$

and hence, because the luminosity of a star is $\bar{L} = \bar{\varepsilon}\bar{R}^2$, we obtain the mass-luminosity relation $\bar{L} = \bar{M}^3$.

As a matter of fact, ε determined by the energy drainage condition in a star should coincide with ε determined by the mechanism producing stellar energy — an *energy production condition*. In our theory of stellar energy, such an energy production condition is represented by the stellar energy for-
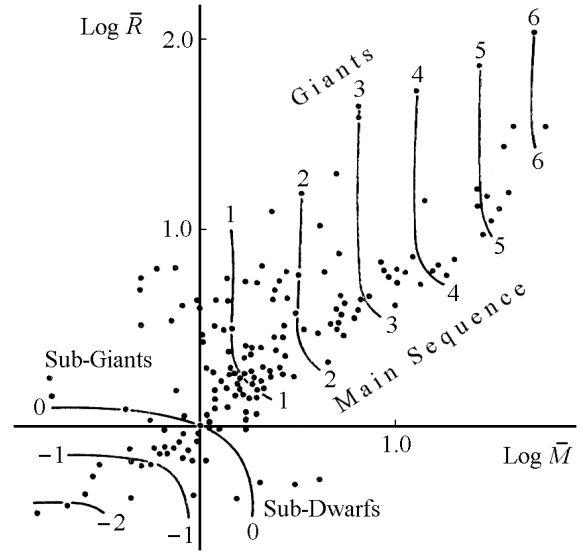

Fig. 3: Diagram of "mass–radius" devised by N. A. Kozyrev, the famous astronomer and experimental physicist, in the late 1970's. The arcs are isoergs of stellar matter. (Courtesy of V. V. Nassonov, Kozyrev's assistant, who had frequent meetings with the author in 1984–1985.)

mula $\bar{\varepsilon} = \bar{n}_e\bar{B}^{3/2} = \bar{\rho}\bar{B}^{3/2} = \bar{B}^{5/2}$.

We therefore substitute the observed mass-luminosity relation $\bar{L} = \bar{M}^{10/3}$ and the theoretical relation $\bar{L} = \bar{M}^3$ into our formula for stellar energy reduced to the absolute mass and radius of a star $\bar{\varepsilon} = \bar{B}^{5/2} = \frac{\bar{M}^{10}}{\bar{R}^{10}}$ (10). Because $\bar{L} = \bar{\varepsilon}\bar{R}^2$, our formula for stellar energy, in common with the observed mass-luminosity relation $\bar{L} = \bar{M}^{10/3}$, gives

$$\bar{L} = \bar{R}^4, \qquad (13)$$

while with the theoretical relation $\bar{L} = \bar{M}^3$ our formula gives a slightly smaller exponent,

$$\bar{L} = \bar{R}^{3.4}. \qquad (14)$$

In other words, for both the observed and theoretical mass-luminosity relation, our formula for stellar energy says that,

> On the basis of stellar energy being generated by the background space non-holonomity field, in Thomson dispersion of light in free electrons, the luminosity L of a star is proportional to its volume $V = \frac{4}{3}\pi R^3$, with a small progression with an increase of radius. We will refer to the newly discovered correlation as the *volume-luminosity relation*.

The predicted volume-luminosity relation $\bar{L} = \bar{R}^4 - \bar{R}^{3.4}$ is derived from the condition of energy production by the non-holonomic space background in Thomson dispersion of light in stars (our theory of stellar energy). If such a correlation (the condition of energy production) is true, the correlation, in common with the energy drainage condition (the mass-luminosity relation $\bar{L} = \bar{M}^3 - \bar{M}^{10/3}$), should produce another correlation; mass-radius $\bar{M} = \bar{R}^{1.1} - \bar{R}^{1.2}$. Fig. 3

D. Rabounski. A Source of Energy for Any Kind of Star

21

shows a diagram devised by Kozyrev in the 1970's on the basis of observational data, along with many other diagrams within the framework of his extensive phenomenological research into stellar energy and the internal constitution of stars. As seen from the diagram, stars are distributed along the average direction $\bar{M} \sim \bar{R}$, which perfectly verifies the expected correlation $\bar{M} = \bar{R}^{1.1} - \bar{R}^{1.2}$ predicted on the basis of our formula for stellar energy. Hence the relation $\bar{M} \sim \bar{R}$ verifies as well the whole theory of the stellar energy mechanism we have built here and in [1].

The deduced volume-luminosity relation clearly depends upon the chemical composition of stars. Naturally, because the gravitational pressure in a star $\bar{p} = \frac{\bar{M}}{\bar{R}^2} \bar{\rho} \bar{R} = \frac{\bar{M}^2}{\bar{R}^4}$ is balanced by the gaseous pressure calculated by the equation for an ideal gas $\bar{p} = \frac{\bar{T}\bar{\rho}}{\bar{\mu}}$, we have $\bar{B} = \bar{T}^4 = \bar{\mu}^4 \frac{\bar{M}^4}{\bar{R}^4}$. On the other hand, Kozyrev has found, from the stellar energy diagram (Fig. 1), that "The main direction wonderfully traces an angle of exactly $45°$. Hence, all stars are concentrated along the line, determined by the equation $B \sim \rho\mu^4$" [2]. We therefore substitute $\bar{n}_e = \bar{\rho} = \frac{\bar{B}}{\bar{\mu}^4}$ and $\bar{B} = \bar{\mu}^4 \frac{\bar{M}^4}{\bar{R}^4}$ into our initial formula for stellar energy $\bar{\varepsilon} = \bar{n}_e \bar{B}^{3/2}$ (7). As a result we obtain the formula for stellar energy in the form, where the molecular weight of the stellar contents is taken into account,

$$\bar{\varepsilon} = \bar{\mu}^6 \frac{\bar{M}^{10}}{\bar{R}^{10}}, \qquad (15)$$

from which, because $\bar{L} = \bar{\varepsilon} \bar{R}^2$, we obtain, with the observed mass-luminosity relation $\bar{L} = \bar{M}^{10/3}$,

$$\bar{L} = \frac{1}{\bar{\mu}^3} \bar{R}^4, \qquad (16)$$

while with the theoretical relation $\bar{L} = \bar{M}^3$ our updated formula (8) gives

$$\bar{L} = \frac{1}{\bar{\mu}^{2.6}} \bar{R}^{3.4}. \qquad (17)$$

As is clearly seen, our deduced relation — the proportionality of the luminosity of a star to its volume $L \sim V \sim R^3$ — is inversely proportional to ~ 3 orders of the molecular weight of the gas consisting a star. The greater the molecular weight of the gaseous contents of a star, the smaller its luminosity for the same volume. For instance, for a star consisting, instead of Hydrogen, of Helium or other heavy elements, the luminosity of such a star should be many times less than a completely hydrogen star of the same size.

3 The same stellar energy formula applied to brown dwarfs and the bulky planets

So the mass-luminosity relation $\bar{L} = \bar{M}^3$ is derived from the energy drainage condition $\bar{\varepsilon} = \frac{\bar{B}}{\bar{\rho}\bar{R}} = \frac{\bar{M}^3}{\bar{R}^2}$. The necessary coincidence with the energy production condition, the stellar energy formula $\bar{\varepsilon} = \bar{n}_e \bar{B}^{3/2} = \bar{\rho} \bar{B}^{3/2} = \bar{B}^{5/2}$, gives a new relation between the observable characteristics of stars — the

Table 1: Brown dwarfs

	$\bar{L} = \bar{M}^{10/3}$	$\bar{L} = \bar{M}^3$	$\bar{L} = \bar{R}^4$	$\bar{L} = \bar{R}^{3.4}$
$\bar{L} = 10^{-4}$	$\bar{M} = 0.06$	$\bar{M} = 0.05$	$\bar{R} = 0.1$	$\bar{R} = 0.07$
$\bar{L} = 10^{-5}$	$\bar{M} = 0.03$	$\bar{M} = 0.02$	$\bar{R} = 0.06$	$\bar{R} = 0.03$

volume-luminosity relation: $\bar{L} = \bar{R}^{3.4}$ for the theoretical relation $\bar{L} = \bar{M}^3$, or $\bar{L} = \bar{R}^4$ for the observed $\bar{L} = \bar{M}^{10/3}$.

In this section we shall look at how our stellar energy formula can be applied to space objects of extremely small luminosity — recently discovered brown dwarfs, and also the bulky planets (Jupiter, Saturn, Uranus, and Neptune) whose radiated energy exceeds that received from the Sun (so they have their own internal sources of energy).

Brown dwarfs

These have masses $\bar{M} \leqslant 0.08$, luminosity $\bar{L} = 10^{-4} - 10^{-5}$, and temperature at the surface $T \approx 700$ K, which determines their observed brown colour.

Proceeding from the luminosity $\bar{L}$ of brown dwarfs, we calculate: (1) their masses $\bar{M}$ by the mass-luminosity relation (the energy drainage condition), and also (2) their radii $\bar{R}$ by the volume-luminosity relation (the energy production condition) that characterizes the generation of stellar energy by the background space non-holonomity in Thomson dispersion of light. The results are given in Table 1.

By the observed mass-luminosity relation $\bar{L} = \bar{M}^{10/3}$, we obtained the masses in the range $\bar{M} = 0.03 - 0.06$ that satisfies the masses $\bar{M} \leqslant 0.08$ required for stars of such class. Brown dwarfs therefore satisfy the condition of energy drainage.

The radii of brown dwarfs $\bar{R} = 0.06 - 0.1$ we calculated by the condition of energy production — the volume-luminosity relation $\bar{L} = \bar{R}^4$ — are within the range of the bulky planets (from $\bar{R} = 0.034$ for Uranus to $\bar{R} = 0.10$ for Jupiter). Hence, from our calculations we conclude that:

> Brown dwarfs are stars of a size similar to Jupiter or Saturn. Their energy source is the same as that in stars of other kinds — the background space non-holonomity that generates energy in Thomson dispersion of light in free electrons. However, in contrast to the bulky planets, the radii of brown dwarfs satisfy the volume-luminosity relation, so the physical conditions therein are such that the stellar energy mechanism produces enough energy to compensate for the radiation from the surface.

The bulky planets

By direct measurements made by NASA's space missions (Pioneer, Voyager, Galileo, Cassini), the bulky planets have $\sim 75 - 90\%$ hydrogen content (see http://www.nasa.gov for the details). So, because of the huge pressure in the central region, enough to ionize hydrogen, we propose the same energy source as that in any star. We can therefore calculate a table similar to that herein for brown dwarfs.

Table 2: The bulky planets

	$\bar{R}$	$\bar{M}$	T_{eff}	T_{ac}	B_{eff}	B_{ac}	$\bar{L}_{\text{p}}$	$\bar{L}=\bar{M}^{x}$	$\bar{L}=\bar{R}^{y}$	$\bar{L}=\bar{R}^{4}$
JUPITER:	0.10	9.5×10^{-4}	125 K	105 K	1.3×10^{4}	0.69×10^{4}	1.0×10^{-9}	$x=3.0$	$y=9.0$	$R=4{,}000\,\text{km}$
SATURN:	0.086	2.9×10^{-4}	95 K	74 K	4.6×10^{3}	1.7×10^{3}	3.4×10^{-10}	$x=2.7$	$y=8.9$	$R=3{,}000\,\text{km}$
URANUS:	0.034	4.4×10^{-5}	57 K	55 K	6.0×10^{2}	5.2×10^{2}	1.5×10^{-12}	$x=2.7$	$y=7.8$	$R=770\,\text{km}$
NEPTUNE:	0.036	5.2×10^{-5}	59 K	38 K	6.9×10^{2}	1.2×10^{2}	1.2×10^{-11}	$x=2.5$	$y=7.4$	$R=1{,}300\,\text{km}$

In Table 2 we use the effective temperature T_{eff} and the temperature T_{ac} acquired from the Sun, determined from the direct measurements made by the NASA satellites. The proper luminosity of each planet $L_{\text{p}}=4\pi R^2 B_{\text{p}}$ is calculated through the density of the proper radiant energy $B_{\text{p}}=B_{\text{eff}}-B_{\text{ac}}=\sigma\left(T_{\text{eff}}^4-T_{\text{ac}}^4\right)$, where $\sigma=5.67\times10^{-5}\,\text{erg/cm}^2\times\text{sec}\times\text{deg}$.

As seen from Table 2, the bulky planets have the luminosity $\bar{L}=\bar{M}^{2.5}$–$\bar{M}^{3.0}$. Many stars have a greater deviation from the average mass-luminosity relation $\bar{L}=\bar{M}^{10/3}$ (see Fig. 2), than the planets. We therefore conclude that,

> The bulky planets satisfy the mass-luminosity relation, which is the condition of energy drainage, so they radiate energy similar to stars.

Another result is provided by the volume-luminosity relation $\bar{L}\sim\bar{R}^{y}$, which characterizes the condition of energy production. The bulky planets have $\bar{L}=\bar{R}^{7.4}$–$\bar{R}^{9.0}$, while the coincidence of the energy drainage with the energy production in stars requires $\bar{L}=\bar{R}^{3.4}$–$\bar{R}^{4.0}$. The last column in Table 2 gives the values of the radii which should result if the energy loss is completely balanced by the energy produced within. So the bulky planets would be like stars. As seen, in such a case the bulky planets would be a bit smaller than the Earth: Jupiter and Saturn would have a size similar to Mars, Neptune would be similar to the Moon, while Uranus would be half the Moon. The obtained result implies that:

> The real radii of the bulky planets are so large that the energy produced within the planets is substantially less than that radiated from the surface: the planets are cooling down, in contrast to stars whose temperature is stable on the average.

So there is no crucial difference between stars and the bulky planets built on the gaseous contents. Looking at the evolution of the bulky planets, we see that as soon as the gravitational pressure compresses the planets down to radii satisfying the volume-luminosity relation $\bar{L}=\bar{R}^{3.4}$–$\bar{R}^{4.0}$, the energy output within the planets becomes balanced by the radiation from the surface, so the planets become stars. In such a case the density of the planets would become enormous.

Such high densities are conceivable, along the whole range of known stars, only within white dwarfs, which are mostly satellites of the most bulky stars. Compare Sirius' satellite ($\bar{R}=0.025$) and Procyon's satellite ($\bar{R}=0.013$), typical white dwarfs, which have a density $\rho\approx10^{4}$. We there therefore conclude that:

Table 3: The bulky planets, if becoming stars

	Radius, $\bar{R}$	Radius, km	Average density
JUPITER:	0.0057	4,000 km	7.1×10^{3} g/cm^3
SATURN:	0.0043	3,000 km	5.0×10^{3} g/cm^3
URANUS:	0.0011	770 km	4.6×10^{4} g/cm^3
NEPTUNE:	0.0019	1,300 km	1.1×10^{4} g/cm^3

> White dwarfs were formerly bulky planets like Jupiter and the great jovian planets, which, containing mostly hydrogen, were compressed by gravitational pressure to such a state that the energy produced within is the same as that radiated from the surface.
>
> So Jupiter and the jovian planets are stars in an early stage of their evolution. As soon as the gravitational pressure compresses each of them to the appropriate radius, they become white dwarfs — star-satellites of the Sun, so that the solar system becomes a multiple-star system.

4 A perspective for the new energy source

Accordingly, our theory that stellar energy is generated by the background space in Thomson dispersion of light in free electrons is readily verified. All that we need to reproduce the mechanism is ionized hydrogen: even if the temperature is much lower than in stars, we should obtain some energy output if the theory is correct. The ionization energy of a hydrogen atom is 13.6 eV; suitable equipment is accessible in even a junior college laboratory. Moreover, proceeding from the above theory, we can predict additional forces and energy output produced by the non-holonomic space background in phenomena other than Thomson dispersion of light. So the stellar energy theory herein, applied to laboratory conditions, predicts new energy sources working much more effectively and safely than nuclear energy.

References

1. Rabounski D. *Progress in Physics*, 2006, v. 4, 3–10.

2. Kozyrev N. A. *Progress in Physics*, 2005, v. 3, 61–99.

The Thermodynamics Associated with Santilli's Hadronic Mechanics

Jeremy Dunning-Davies

Department of Physics, University of Hull, England
Institute for Basic Research, P. O. Box 1577, Palm Harbor, Florida 346822, USA
E-mail: j.dunning-davies@hull.ac.uk

The new mathematics, referred to as iso-mathematics and geno-mathematics, introduced by Santilli to help explain a number of outstanding problems in quantum chemistry as well as in other areas of science such as astrophysics, has been applied successfully in a number of physical situations. This new formalism has, for the first time, provided an irreversible description of thermodynamics via an irreversible differential calculus together with the related mathematics. However, the associated thermodynamics has not been considered so far. That defect is remedied here.

1 Introduction

For many years now, science has harboured the belief that the theories of relativity and quantum mechanics offered the means to solve all outstanding theoretical problems. One person who has felt for many years that these theories are not complete is Ruggero Santilli. He has devoted his life to searching for extensions to these undoubtedly extremely successful theories. He was driven to this by the realisation that, despite a multitude of successes, a number of basic issues remained unresolved by orthodox quantum chemistry. Although a mountain of publications preceded it, the culmination of this work was presented in a monograph, *Foundations of Hadronic Chemistry* [1], which was produced in an attempt to provide possible explanations for a number of problems which had persisted for many years in the general area of quantum chemistry. In this book, he suggests a generalisation, or covering, of quantum chemistry, under the name "hadronic chemistry", which appears to resolve many of the outstanding problems. The suggested solution originates with the assumption that valence forces are nonlinear (in the wavefunction), non-local, and of non-potential type due to the deep overlapping of the wavepackets of valence electrons in singlet coupling. In turn, this "valence force" may not be represented quantitatively via conventional quantum chemistry since the latter is linear, local and potential. The covering of quantum chemistry for the invariant representation of the indicated new valence forces is based on a new mathematics called "iso-mathematics", which is itself based on real-valued (hermitian), nowhere singular yet arbitrary integro-differential units. Being, by fundamental assumption, incapable of representation via a Hamiltonian, these new valence forces are represented with the generalised integro-differential units. In turn, the representation of the new valence forces with a unit ensures the invariance of the theory, since the unit is known to be the basic invariant. The provision of simple means, utilising non-unitary transforms, for the construction of hadronic chemistry ensures that it differs from conventional theories.

In addition, an invariant formulation of irreversibility was presented also. The starting point for this was the historical legacy of Lagrange and Hamilton of representing irreversibility with the external terms in their celebrated equations — terms which are frequently ignored in modern expositions of the subject. For reasons of consistency, Santilli reformulates identically the original analytic equations in a form admitting a Lie-admissible structure in the sense of the American mathematician A. A. Albert. The formulation is extended from the classical to all branches. In this way, irreversibility emerges as originating from the most elementary levels of nature. Therefore, a possible resolution of the problem of reducing a macroscopic irreversible classical system to a finite collection of elementary particles, all in reversible conditions, is offered. This suggested formulation of irreversibility is based on an additional new form of mathematics known as "geno-mathematics". This is characterised by two real-valued, non-singular, non-symmetric, generalised units, interconnected by hermitian conjugates, one of which is assumed to characterise motion forward in time and the other, motion backward in time. The differences between the basic units for the two directions of time guarantee irreversibility for all possible reversible Hamiltonians. Since all potential interactions are reversible, these non-symmetric, generalised units represent the interactions responsible for irreversibility — namely, Lagrange's and Hamilton's external terms. This second set of methods is intended for an invariant representation of open irreversible processes, such as chemical reactions, and is part of the so-called genotopic branch of hadronic mechanics and chemistry.

However, the above generalisations were found not to resolve problems relating to anti-matter. To resolve these problems, it was found necessary to introduce yet more new mathematics. These further forms of mathematics are anti-isomorphic to the proposed iso- and geno-mathematics, have their own channel of quantisation, and the operator images are indeed antiparticles, defined as charge conjugates of con-

ventional particles on a Hilbert space. As far as the applicability of well-known thermodynamics' results is concerned, it is only the thermodynamics of anti-matter via Santilli's isodualities which has been considered [2]. It remains to consider the position of the powerful thermodynamic results in iso-mathematics and geno-mathematics.

2 Iso-thermodynamics

The basic rules for iso-mathematics are laid out clearly in Santilli's book [1] but what must be noted at the outset is the importance of realising that in such typical thermodynamic expressions as TdS, multiplication of T by dS is indicated. Hence,

$$TdS = T \times dS \to \hat{T}\hat{\times}\hat{d}\hat{S} \to T \times \hat{I} \times \hat{K} \times \hat{d}\hat{S} \to T \times \hat{d}\hat{S},$$

where

$$I \to \hat{I} = \frac{1}{\hat{K}} > 0.$$

Then

$$T \times dS \to T \times \hat{d}\hat{S} = T \times \hat{I} \times d\left(S \times \hat{I}\right) = \hat{I} \times TdS.$$

Hence, it follows immediately that,

$$dQ = dU + pdV \to \hat{d}\hat{Q} = \hat{d}\hat{U} + \hat{p} \times \hat{d}\hat{V} \to \hat{I} \times dQ =$$
$$= \hat{I} \times (dU + pdV) \Rightarrow dQ = dU + pdV$$

and

$$dQ = TdS \to \hat{d}\hat{Q} = \hat{T}\hat{\times}\hat{d}\hat{S} \to \hat{I} \times dQ = \hat{I} \times TdS \Rightarrow$$
$$\Rightarrow dQ = TdS.$$

This means that, within the iso-mathematical framework, the equations representing the first and second laws of thermodynamics hold in their familiar forms. A moment's consideration indicates that other familiar thermodynamic relations will also retain the familiar forms; for example, the Euler relation

$$TS = U + pV - \mu N,$$

the Gibbs-Duhem relation

$$SdT - Vdp + Nd\mu = 0,$$

and the expressions for the well-known thermodynamic potentials

$$\text{enthalpy: } H = U + pV,$$
$$\text{Helmholtz Free Energy: } F = U - TS,$$
$$\text{Gibbs Free Energy: } G = U + pV - TS.$$

3 Geno-thermodynamics

As far as the extension to include geno-mathematics is concerned, the basic rules of manipulation are again laid out in Santilli's book [1]. Application of these leads, for the com-bined first and second laws of thermodynamics, to

$$TdS = dU + pdV \to T^> {>} d^> S^> = d^> U^> + p^> {>} d^> V^>$$

which becomes

$$(TI^>) I^{>-1} \left[I^{>-1} d (SI^>) \right] = TdS = I^{>-1} d (UI^>) +$$
$$+ (pI^>) I^{>-1} \left[I^{>-1} d (VI^>) \right] = dU + pdV.$$

However, here the genounit has been assumed constant. If the genounit depends on local variables

$$dS \to d^> S^> = I^{>-1} d (SI^>) = dS + SI^{>-1} dI^>,$$

and similarly for dQ and dW. Hence, in these circumstances the equation representing the second law takes the form

$$T^> {>} d^> S^> = d^> U^> + p^> {>} d^> V^> \to$$
$$\to TdS + TSI^{>-1} dI^> =$$
$$= dU + UI^{>-1} dI^> + pdV + pVI^{>-1} dI^> \Rightarrow$$
$$\Rightarrow TdS = dU + pdV,$$

since $TS = U + pV$.

Hence, even if the genounit does depend on local variables, the form of the equation representing a combination of the first and second laws of thermodynamics retains its familiar form. It may be noted that this is true of all the fundamental equations of thermodynamics when the extension into geno-mathematics is considered, just as was the case for iso-mathematics.

4 Conclusions

The end result of this discussion is simply to conclude that the familiar results of thermodynamics remain valid in their familiar forms in both iso-mathematics and geno-mathematics. These results all follow easily but are, nevertheless, important in that it confirms that the various results of thermodynamics may be used with confidence in conjunction with both iso-mathematics and geno-mathematics. It is worth remembering, however, that Santilli's new formalism achieves an irreversible description of thermodynamics through an irreversible differential calculus together with the related mathematics. Although it is shown here that the familiar thermodynamic results remain applicable in their familiar forms, it should be noted that the overall new formalism may be used to describe departures from the conventional laws which appear in several areas of science. This overall subject is relatively new and so the full extent of this claim is simply not known at present. Hence, it is important to embrace this new material with a truly open mind.

Further, it might be noted that, while a large number of Santilli's applications refer to what are essentially small systems and thermodynamics is a macroscopic theory, exactly how thermodynamics will apply in these cases is not yet completely clear. However, if a lead is taken from the work

of Hill [3], it is readily seen that the familiar equations as modified for application to these small systems remain valid in both iso-mathematics and geno-mathematics.

Finally, it is worth realising that, for all its background as a collection of "facts of experience", thermodynamics in its well-known form continues to be applicable in all situations which arise for consideration. It is certainly a topic which can lay claim to be at the very heart of physics.

References

1. Santilli R. M. Foundations of Hadronic Chemistry. Kluwer Academic Publishers, Dordrecht, 2001; *Il Nuovo Cimento B* (in press) and http://www.i-b-f.org/Hadronic-Mechanics.htm

2. Dunning-Davies J. *Found. Phys. Lett.*, 1999, v. 12, 593–599.

3. Hill T. L. Thermodynamics of small systems. Benjamin, New York, 1963.

A Note on Geometric and Information Fusion Interpretation of Bell's Theorem and Quantum Measurement*

Florentin Smarandache[†] and Vic Christianto[‡]

[†]*Department of Mathematics, University of New Mexico, Gallup, NM 87301, USA*
E-mail: smarand@unm.edu

[‡]*Sciprint.org — a Free Scientific Electronic Preprint Server, http://www.sciprint.org*
E-mail: admin@sciprint.org

In this paper we present four possible extensions of Bell's Theorem: Bayesian and Fuzzy Bayesian intrepretation, Information Fusion interpretation, Geometric interpretation, and the viewpoint of photon fluid as medium for quantum interaction.

1 Introduction

It is generally accepted that Bell's theorem [1] is quite exact to describe the linear hidden-variable interpretation of quantum measurement, and hence "quantum reality". Therefore null result of this proposition implies that no hidden-variable theory could provide good explanation of "quantum reality".

Nonetheless, after further thought we can find that Bell's theorem is nothing more than another kind of abstraction of quantum observation based on a set of assumptions and propositions [7]. Therefore, one should be careful before making further generalization on the null result from experiments which are "supposed" to verify Bell's theorem. For example, the most blatant assumption of Bell's theorem is that it takes into consideration only the classical statistical problem of chance of outcome A or outcome B, as result of adoption of Von Neumann's definition of "quantum logic". Another critic will be discussed here, i. e. that Bell's theorem is only a reformulation of statistical definition of correlation; therefore it is merely tautological [5].

Therefore in the present paper we will discuss a few plausible extension of Bell's theorem:

(a) Bayesian and Fuzzy Bayesian interpretation.

(b) Information Fusion interpretation. In particular, we propose a modified version of Bell's theorem, which takes into consideration this multivalued outcome, in particular using the information fusion Dezert-Smarandache Theory (DSmT) [2, 3, 4]. We suppose that in quantum reality the outcome of $P(A \cup B)$ and also $P(A \cap B)$ shall also be taken into consideration. This is where DSmT and Unification of Fusion Theories (UFT) could be found useful [2, 17].

(c) Geometric interpretation, using a known theorem connecting geometry and imaginary plane. In turn, this leads us to 8-dimensional extended-Minkowski metric.

(d) As an alternative to this geometric interpretation, we submit the viewpoint of photon fluid as medium for quantum interaction. This proposition leads us to Gross-Piteavskii equation which is commonly used to describe bose condensation phenomena. In turn we provide a route where Maxwell equations and Schrödinger equation could be deduced from Gross-Pitaevskii equation by using known algebra involving bi-quaternion number. In our opinion, this new proposition provides us a physical mechanism of quantum interaction, beyond conventional "quantum algebra" which hides causal explanation.

By discussing these various approaches, we use an expanded logic beyond "yes" or "no" type logic [3]. In other words, there could be new possibilities to describe quantum interaction: "both can be wrong", or "both can be right", as described in Table 1 below.

In Belnap's four-valued logic there are, besides Truth (T) and Falsehood (F), also Uncertainty (U) and Contradiction (C) but they are inter-related [30]. Belnap's logic is a particular case of Neutrosophic Logic (which considers three components: Truth, Falsehood, and Indeterminacy (I)) when indeterminacy is split into Uncertainty and Contradiction. In our article we have: Yes (Y), No (N), and Indeterminacy (I, which means: neither Yes nor No), but Indeterminacy is split into "both can be wrong" and "both can be right".

It could be expected that a combined interpretation represents multiple-facets of quantum reality. And hopefully it could bring better understanding on the physical mechanism beneath quantum measurement, beyond simple algebraic notions. Further experiments are of course recommended in order to verify or refute this proposition.

2 Bell's theorem. Bayesian and fuzzy Bayesian interpretation

Despite widespread belief of its ability to describe hidden-variables of quantum reality [1], it shall be noted that Bell's theorem starts with a set of assumptions inherent in its formulation. It is assumed that each pair of particles possesses a particular value of λ, and we define quantity $p(\lambda)$ so that probability of a pair being produced between λ and $\lambda + d\lambda$

---

*Note: The notion "hronir wave" introduced here was inspired from Borges' Tlon, Uqbar, Orbis Tertius.

Alternative	Bell's theorem	Implications	Special relativity
QM is nonlocal	Invalid	Causality breaks down; Observer determines the outcome	Is not always applicable
QM is local with hidden variable	Valid	Causality preserved; The moon is there even without observer	No interaction can exceed the speed of light
Both can be right	Valid, but there is a way to explain QM without violating Special Relativity	QM, special relativity and Maxwell electromagnetic theory can be unified. New worldview shall be used	Can be expanded using 8-dimensional Minkowski metric with imaginary plane
Both can be wrong	Invalid, and so Special Relativity is. We need a new theory	New nonlocal QM theory is required, involving quantum potential	Is not always applicable

Table 1: Going beyond classical logic view of QM

is $p(\lambda)\,d\lambda$. It is also assumed that this is normalized so that:

$$\int p(\lambda)\,d\lambda = 1 \,. \qquad (1)$$

Further analysis shows that the integral that measures the correlation between two spin components that are at an angle of $(\delta - \phi)$ with each other, is therefore equal to $C''(\delta - \phi)$. We can therefore write:

$$|C''(\phi) - C''(\delta)| - C''(\delta - \phi) \leqslant 1 \qquad (2)$$

which is known as Bell's theorem, and it was supposed to represent any local hidden-variable theorem. But it shall be noted that actually this theorem cannot be tested completely because it assumes that all particle pairs have been detected. In other words, we find that a hidden assumption behind Bell's theorem is that it uses classical probability assertion [12], which may or may be not applicable to describe Quantum Measurement.

It is wothnoting here that the standard interpretation of Bell's theorem includes the use of Bayesian posterior probability [13]:

$$P(\alpha \,|\, x) = \frac{p(\alpha)\, p(x \,|\, \alpha)}{\sum_\beta p(\beta)\, p(x \,|\, \beta)} \,. \qquad (3)$$

As we know Bayesian method is based on classical two-valued logic. In the meantime, it is known that the restriction of classical propositional calculus to a two-valued logic has created some interesting paradoxes. For example, the Barber of Seville has a rule that all and only those men who do not shave themselves are shaved by the barber. It turns out that the only way for this paradox to work is if the statement is both *true and false simultaneously* [14]. This brings us to *fuzzy Bayesian approach* [14] as an extension of (3):

$$P(s_i \,|\, \underline{M}) = \frac{p(\underline{M} \,|\, s_i)\, p(s_i)}{p(\underline{M})} \,, \qquad (4)$$

where [14, p. 339]:

$$p(\underline{M} \,|\, s_i) = \sum_{k=1}^{r} p(x_k \,|\, s_i)\, \mu_{\underline{M}}(x_k) \,. \qquad (5)$$

Nonetheless, it should also be noted here that there is shortcoming of this Bayesian approach. As Kracklauer points out, Bell's theorem is nothing but a reformulation of statistical definition of correlation [5]:

$$\mathrm{Corr}\,(A, B) = \frac{\langle |AB| \rangle - \langle A \rangle \langle B \rangle}{\sqrt{\langle A^2 \rangle \langle B^2 \rangle}} \,. \qquad (6)$$

When $\langle A \rangle$ or $\langle B \rangle$ equals to zero and $\langle A^2 \rangle \langle B^2 \rangle = 1$ then equation (6) reduces to Bell's theorem. Therefore as such it could be considered as merely tautological [5].

3 Information fusion interpretation of Bell's theorem. DSmT modification

In the context of physical theory of information [8], Barrett has noted that "there ought to be a set theoretic language which applies directly to all quantum interactions". This is because the idea of a bit is itself straight out of *classical set theory*, the definitive and unambiguous assignment of an element of the set $\{0, 1\}$, and so the assignment of an information content of the photon itself is fraught with the same difficulties [8]. Similarly, the problem becomes more adverse because the fundamental basis of conventional statistical theories is the same classical set $\{0, 1\}$.

Not only that, there is also criticism over the use of Bayesian approach, i. e.: [13]

(a) In real world, neither class probabilities nor class densities are precisely known;

(b) This implies that one should adopt a parametric model for the class probabilities and class densities, and then use empirical data.

(c) Therefore, in the context where multiple sensors can be used, information fusion approach could be a better alternative to Bayes approach.

In other words, we should find an extension to standard proposition in statistical theory [8, p. 388]:

$$P(AB\,|\,C) = P(A\,|\,BC)P(B\,|\,C) \qquad (7)$$

$$= P(B\,|\,AC)P(A\,|\,C) \qquad (8)$$

$$P(A\,|\,B) + P(\bar{A}\,|\,B) = 1\,. \qquad (9)$$

Such an extension is already known in the area of information fusion [2], known as Dempster-Shafer theory:

$$m(A) + m(B) + m(A \cup B) = 1\,. \qquad (10)$$

Interestingly, Chapline [13] noted that neither Bayesian theory nor Dempster-Shafer could offer insight on how to minimize overall energy usage in the network. In the meantime, Dezert-Smarandache (DSmT) [2] introduced further improvement of Dempster-Shafer theory by taking into consideration chance to observe intersection between A and B:

$$m(A) + m(B) + m(A \cup B) + m(A \cap B) = 1\,. \qquad (11)$$

Therefore, introducing this extension from equation (11) into equation (2), one finds a modified version of Bell's theorem in the form:

$$\begin{aligned}|C''(\phi) - C''(\delta)| - \\ - C''(\delta - \phi) + C''(\delta \cup \phi) + C''(\delta \cap \phi) \leqslant 1\,,\end{aligned} \qquad (12)$$

which could be called as modified Bell's theorem according to Dezert-Smarandache (DSmT) theory [2]. Its direct implications suggest that it could be useful to include more sensors in order to capture various possibilities beyond simple $\{0, 1\}$ result, which is typical in Bell's theorem.

Further generalization of DSmT theory (11) is known as Unification of Fusion Theories [15, 16, 17]:

$$\begin{aligned}m(A) + m(B) + m(A \cup B) + m(A \cap B) + \\ + m(\bar{A}) + m(\bar{B}) + m(\bar{A} \cup \bar{B}) + m(\bar{A} \cap \bar{B}) = 1\,,\end{aligned} \qquad (13)$$

where $\bar{A}$ is the complement of A and $\bar{B}$ is the complement of B (if we consider the set theory).

(But if we consider the logical theory then $\bar{A}$ is the negation of A and $\bar{B}$ is the negation of B. The set theory and logical theory in this example are equivalent, hence doesn't matter which one we use from them.) In equation (13) above we have a complement/negation for A. We might define the $\bar{A}$ as the entangle of particle A. Hence we could expect to further extend Bell's inequality considering UFT; nonetheless we leave this further generalization for the reader.

Of course, new experimental design is recommended in order to verify and to find various implications of this new proposition.

4 An alternative geometric interpretation of Bell-type measurement. Gross-Pitaevskii equation and the "hronir wave"

Apart from the aforementioned Bayesian interpretation of Bell's theorem, we can consider the problem from purely geometric viewpoint. As we know, there is linkage between

geometry and algebra with imaginary plane [18]:

$$x + iy = \rho e^{i\phi}\,. \qquad (14)$$

Therefore one could expect to come up with geometrical explanation of quantum interaction, provided we could generalize the metric using imaginary plane:

$$X + iX' = \rho e^{i\phi}\,. \qquad (15)$$

Interestingly, Amoroso and Rauscher [19] have proposed exactly the same idea, i. e. generalizing Minkowski metric to become 8-dimensional metric which can be represented as:

$$Z^\mu = X_{re}^\mu + iX_{im}^\mu = \rho e^{i\phi}\,. \qquad (16)$$

A characteristic result of this 8-dimensional metric is that "space separation" vanishes, and quantum-type interaction could happen in no time.

Another viewpoint could be introduced in this regard, i. e. that the wave nature of photon arises from "photon fluid" medium, which serves to enable photon-photon interaction. It has been argued that this photon-fluid medium could be described using Gross-Pitaevskii equation [20]. In turns, we could expect to "derive" Schrödinger wave equation from the Gross-Pitaevskii equation.

It will be shown, that we could derive Schrödinger wave equation from Gross-Pitaevskii equation. Interestingly, a new term similar to equation (14) arises here, which then we propose to call it "hronir wave". Therefore one could expect that this "hronir wave" plays the role of "invisible light" as postulated by Maxwell long-time ago.

Consider the well-known Gross-Pitaevskii equation in the context of superfluidity or superconductivity [21]:

$$i\hbar \frac{\partial \Psi}{\partial t} = -\frac{\hbar^2}{2m}\Delta\Psi + \left(V(x) - \gamma\,|\Psi|^{p-1}\right)\Psi\,, \qquad (17)$$

where $p < 2N/(N-2)$ if $N \geqslant 3$. In physical problems, the equation for $p = 3$ is known as Gross-Pitaevskii equation. This equation (17) has standing wave solution quite similar to Schrödinger equation, in the form:

$$\Psi(x, t) = e^{-iEt/\hbar} \cdot u(x)\,. \qquad (18)$$

Substituting equation (18) into equation (17) yields:

$$-\frac{\hbar^2}{2m}\Delta u + \left(V(x) - E\right)u = |u|^{p-1}u\,, \qquad (19)$$

which is nothing but time-independent linear form of Schrödinger equation, except for term $|u|^{p-1}$ [21]. In case the right-hand side of this equation is negligible, equation (19) reduces to standard Schrödinger equation. Using Maclaurin series expansion, we get for (18):

$$\Psi(x, t) = \left(1 - \frac{iEt}{\hbar} + \frac{\left(\frac{iEt}{\hbar}\right)^2}{2!} + \frac{\left(-\frac{iEt}{\hbar}\right)^3}{3!} + \ldots\right) \cdot u(x)\,. \qquad (20)$$

Therefore we can say that standing wave solution of Gross-Pitaevskii equation (18) is similar to standing wave

solution of Schrödinger equation (u), except for nonlinear term which comes from Maclaurin series expansion (20). By neglecting third and other higher order terms of equation (20), one gets an approximation:

$$\Psi(x,t) = \big[1 - iEt/\hbar\big] \cdot u(x) \, . \tag{21}$$

Note that this equation (21) is very near to hyperbolic form $z = x + iy$ [18]. Therefore one could conclude that standing wave solution of Gross-Pitaevskii equation is merely an extension from ordinary solution of Schrödinger equation into Cauchy (imaginary) plane. In other words, there shall be "hronir wave" part of Schrödinger equation in order to describe Gross-Pitaevskii equation. We will use this result in the subsequent section, but first we consider how to derive bi-quaternion from Schrödinger equation.

It is known that solutions of Riccati equation are logarithmic derivatives of solutions of Schrödinger equation, and *vice versa* [22]:

$$u'' + vu = 0 \, . \tag{22}$$

Bi-quaternion of differentiable function of $x = (x_1, x_2, x_3)$ is defined as [22]:

$$Dq = -\operatorname{div}(q) + \operatorname{grad}(q_0) + \operatorname{rot}(q) \, . \tag{23}$$

By using alternative representation of Schrödinger equation [22]:

$$\big[-\Delta + u\big] f = 0 \, , \tag{24}$$

where f is twice differentiable, and introducing quaternion equation:

$$Dq + q^2 = -u \, . \tag{25}$$

Then we could find q, where q is purely vectorial differentiable bi-quaternion valued function [22].

We note that solutions of (24) are related to (25) as follows [22]:

- For any nonvanishing solution f of (24), its logarithmic derivative:

$$q = \frac{Df}{f} \, , \tag{26}$$

  is a solution of equation (25), and *vice versa* [22].

Furthermore, we also note that for an arbitrary scalar twice differentiable function f, the following equality is permitted [22]:

$$\big[-\Delta + u\big] f = \big[D + M^h\big]\big[D - M^h\big] f \, , \tag{27}$$

provided h is solution of equation (25).

Therefore we can summarize that given a particular solution of Schrödinger equation (24), the general solution reduces to the first order equation [22, p. 9]:

$$\big[D + M^h\big] F = 0 \, , \tag{28}$$

where

$$h = \frac{D\sqrt{\varepsilon}}{\varepsilon} \, . \tag{29}$$

Interestingly, equation (28) is equivalent to **Maxwell equations**. [22] Now we can generalize our result from the preceding section, in the form of the following conjecture:

Conjecture 1 *Given a particular solution of Schrödinger equation (24), then the approximate solution of Gross-Pitaevskii equation (17) reduces to the first order equation:*

$$\big[1 - iEt/\hbar\big]\big[D + M^h\big] F = 0 \, . \tag{30}$$

Therefore we can conclude here that there is neat linkage between Schrödinger equation, Maxwell equation, Riccati equation via biquaternion expression [22, 23, 24]. And approximate solution of Gross-Pitaevskii equation is similar to solution of Schrödinger equation, except that it exhibits a new term called here "*the hronir wave*" (30).

Our proposition is that considering equation (30) has imaginary plane wave, therefore it could be expected to provided "physical mechanism" of quantum interaction, in the same sense of equation (14). Further experiments are of course recommended in order to verify or refute this

5　Some astrophysical implications of Gross-Pitaevskii description

Interestingly, Moffat [25, p. 9] has also used Gross-Pitaevskii in his "phion condensate fluid" to describe CMB spectrum. Therefore we could expect that this equation will also yield interesting results in cosmological scale.

Furthermore, it is well-known that Gross-Pitaevskii equation could exhibit *topologically* non-trivial vortex solutions [26, 27], which can be expressed as quantized vortices:

$$\oint p \bullet dr = N_v \, 2\pi\hbar \, . \tag{31}$$

Therefore an implication of Gross-Pitaevskii equation [25] is that topologically quantized vortex could exhibit in astrophysical scale. In this context we submit the viewpoint that this proposition indeed has been observed in the form of Tifft's quantization [28, 29]. The following description supports this assertion of topological quantized vortices in astrophysical scale.

We start with standard definition of Hubble law [28]:

$$z = \frac{\delta\lambda}{\lambda} = \frac{Hr}{c} \tag{32}$$

or

$$r = \frac{c}{H}\, z \, . \tag{33}$$

Now we suppose that the major parts of redshift data could be explained via Doppler shift effect, therefore [28]:

$$z = \frac{\delta\lambda}{\lambda} = \frac{v}{c} \, . \tag{34}$$

In order to interpret Tifft's observation of quantized redshift corresponding to quantized velocity 36.6 km/sec and

72.2 km/sec, then we could write from equation (34):

$$\frac{\delta v}{c} = \delta z = \delta \left(\frac{\delta \lambda}{\lambda} \right). \qquad (35)$$

Or from equation (33) we get:

$$\delta r = \frac{c}{H} \delta z. \qquad (36)$$

In other words, we submit the viewpoint that Tifft's observation of quantized redshift implies a quantized distance between galaxies [28], which could be expressed in the form:

$$r_n = r_0 + n\,(\delta r). \qquad (35a)$$

It is proposed here that this equation of quantized distance (5) is resulted from topological quantized vortices (31), and agrees with Gross-Pitaevskii (quantum phion condensate) description of CMB spectrum [25]. Nonetheless, further observation is recommended in order to verify the above proposition.

Concluding remarks

In the present paper we review a few extension of Bell's theorem which could take into consideration chance to observe outcome beyond classical statistical theory, in particular using the information fusion theory. A new geometrical interpretation of quantum interaction has been considered, using Gross-Pitaevskii equation. Interestingly, Moffat [25] also considered this equation in the context of cosmology.

It is recommended to conduct further experiments in order to verify and also to explore various implications of this new proposition, including perhaps for the quantum computation theory [8, 13].

Acknowledgment

References

1. Shimony A. http://plato.stanford.edu/entries/bell-theorem/; http://plato.stanford.edu/entries/kochen-specker/.

2. Smarandache F. and Dezert J. Advances and applications of of DSmT for information fusion. American Research Press, Rehoboth, 2004.

3. Smarandache F. *Bulletin of Pure and Applied Sciences*, Ser. Physics, 2003, v. 22D, No. 1, 13–25.

4. Smarandache F. and Christianto V. Multivalued logic, neutrosophy and Schrödinger equation. Hexis, Phoenix, 2005.

5. Kracklauer A. La theorie de Bell, est-elle la plus grande meprise de l'histoire de la physique? *Annales de la Fondation Louis de Broglie*, v. 25, 2000, 193.

6. Aharonov Y. *et al.* arXiv: quant-ph/0311155.

7. Rosu H. C. arXiv: gr-qc/9411035.

8. Zurek W. (ed.), Complexity, entropy and the physics of information. Santa Fe Inst. Studies, Addison-Wesley, 1990.

9. Schrieffer J. R. Macroscopic quantum phenomena from pairing in superconductors. Lecture, December 11, 1972.

10. Anandan J. S. In: *Quantum Coherence and Reality*. Columbia SC, World Sci., 1994; arXiv: gr-qc/9504002.

11. Goldstein S. Quantum theory without observers − part one. *Physics Today*, March 1998, 42–46.

12. Pitowski I. arXiv: quant-ph/0510095.

13. Chapline G. arXiv: adap-org/9906002; quant-ph/9912019; Granik A. and Chapline G. arXiv: quant-ph/0302013; http://www.whatsnextnetwork.com/technology/index.php/2006/03/.

14. Ross T. J. fuzzy logic with engineering applications. McGraw-Hill, 1995, 196–197, 334–341.

15. Smarandache F. Unification of Fusion Theories (UFT). *Intern. J. of Applied Math. & Statistics*, 2004, v. 2, 1–14.

16. Smarandache F. An in-depth look at information fusion rules and unification of fusion theories. Invited speech at NASA Langley Research Center, Hampton, VA, USA, Nov 5, 2004.

17. Smarandache F. Unification of the fusion theory (UFT). Invited speech at NATO Advance Study Institute, Albena, Bulgaria, May 16–27, 2005.

18. Gogberashvili M. arXiv: hep-th/0212251.

19. Rauscher E. A. and Amoroso R. *Intern. J. of Comp. Anticipatory Systems*, 2006.

20. Chiao R. *et al.*. arXiv: physics/0309065.

21. Dinu T. L. arXiv: math.AP/0511184.

22. Kravchenko V. arXiv: math.AP/0408172.

23. Lipavsky P. *et al.* arXiv: cond-mat/0111214.

24. De Haas E. P. *Proc. of the Intern. Conf. PIRT-2005*, Moscow, MGTU Publ., 2005.

25. Moffat J. arXiv: astro-ph/0602607.

26. Smarandache F. and Christianto V. *Progress in Physics*, 2006, v. 2, 63–67.

27. Fischer U. arXiv: cond-mat/9907457; cond-mat/ 0004339.

28. Russell Humphreys D. Our galaxy is the centre of the universe, "quantized" red shifts show. *TJ Archive*, 2002, v. 16(2), 95–104; http://answersingenesis.org/tj/v16/i2/galaxy.asp.

29. Setterfield B. http://www.journaloftheoretics.com.

30. Belnap N. A useful four-valued logic, modern uses of multiple-valued logic. (D. Reidel, editor), 8–37, 1977.

Developing de Broglie Wave

J. X. Zheng-Johansson* and Per-Ivar Johansson†

Institute of Fundamental Physics Research, 611 93 Nyköping, Sweden
E-mail: jxzj@iofpr.org

†*Uppsala University, Studsvik, 611 82 Nyköping, Sweden*
E-mail: Per-Ivar.Johansson@studsvik.uu.se

The electromagnetic component waves, comprising together with their generating oscillatory massless charge a material particle, will be Doppler shifted when the charge hence particle is in motion, with a velocity v, as a mere mechanical consequence of the source motion. We illustrate here that two such component waves generated in opposite directions and propagating at speed c between walls in a one-dimensional box, superpose into a traveling beat wave of wavelength $\Lambda_d = \frac{v}{c}\Lambda$ and phase velocity $c^2/v + v$ which resembles directly L. de Broglie's hypothetic phase wave. This phase wave in terms of transmitting the particle mass at the speed v and angular frequency $\Omega_d = 2\pi v/\Lambda_d$, with Λ_d and Ω_d obeying the de Broglie relations, represents a de Broglie wave. The standing-wave function of the de Broglie (phase) wave and its variables for particle dynamics in small geometries are equivalent to the eigen-state solutions to Schrödinger equation of an identical system.

1 Introduction

As it stood at the turn of the 20th century, M. Planck's quantum theory suggested that energy (ε) is associated with a certain periodic process of frequency (ν), $\varepsilon = h\nu$; and A. Einstein's mass-energy relation suggested the total energy of a particle (ε) is connected to its mass (m), $\varepsilon = mc^2$. Planck and Einstein together implied that mass was associated with a periodic process $mc^2 = h\nu$, and accordingly a larger ν with a moving mass. Incited by such a connection but also a clash with this from Einstein's relativity theory which suggested a moving mass is associated with a slowing-down clock and thus a smaller ν, L. de Broglie put forward in 1923 [1] a hypothesis that a matter particle (moving at velocity v) consists of an internal periodic process describable as a packet of phase waves of frequencies dispersed about ν, having a phase velocity $W = \frac{\nu}{k} = c^2/v$, with c the speed of light, and a group velocity of the phase-wave packet equal to v. Despite the hypothetic phase wave appeared supernatural and is today not held a standard physics notion, the de Broglie wave has proven in modern physics to depict accurately the matter particles, and the de Broglie relations proven their fundamental relations.

So inevitably the puzzles with the de Broglie wave persist, involving the hypothetic phase waves or not, and are unanswered prior to our recent unification work [2]: What is waving with a de Broglie wave and more generally Schrödinger's wave function? If de Broglie's phase wave is indeed a reality, what is then transmitted at a speed (W) being $\frac{c}{v}$ times the speed of light c? How is the de Broglie (phase) wave related to the particle's charge, which if accelerated generates according to Maxwell's theory electromagnetic (EM) waves of speed c, and how is it in turn related to the EM waves, which are commonplace emitted or absorbed by a particle which changes its internal state? In [2] we showed that a physical model able to yield all of the essential properties of a de Broglie particle, in terms of solutions in a unified framework of the three basic mechanics, is provided by a single harmonic oscillating, massless charge $+e$ or $-e$ (termed a *vaculeon*) and the resulting electromagnetic waves. The solutions for a basic material particle generally in motion, with the charge quantity (accompanied with a spin) and energy of the charge as the sole inputs, predict accurately the inertial mass, total wave function, total energy equal to the mass times c^2, total momentum, kinetic energy and linear momentum of the particle, and that the particle is a de Broglie wave, it obeys Newton's laws of motion, de Broglie relations, Schrödinger equation in small geometries, Newton's law of gravitation, and Galilean-Lorentz-Einstein transformation at high velocities. In this paper we give a self-contained illustration of the process by which the electromagnetic component waves of such a particle in motion superpose into a de Broglie (phase) wave.

2 Particle; component waves; dynamic variables

A free massless vaculeon charge (q) endowed with a kinetic energy $\mathcal{E}_q$ at its creation, being not dissipatable except in a pair annihilation, will tend to move about in the vacuum, and yet at larger displacement restored, fully if $\mathcal{E}_q$ below a threshold, toward equilibrium by the potential field of the surrounding dielectric vacuum being here polarized under the charge's own field [2]. As a result the charge oscillates in the vacuum, at a frequency Ω_q; once in addition uni-directionally driven, it will also be traveling at a velocity v here in a one-dimensional box of length L along X-axis firstly in $+X$-direction. Let axis X' be attached to the moving charge, $X' = X - vT$; let v be low so that $(v/c)^2 \rightarrow 0$,

with c the velocity of light; accordingly $T' = T$. The charge will according to Maxwell's theory generate electromagnetic waves to both $+X$ and $-X$-directions, being by the standard solution a plane wave, given in dimensionless displacements (of the medium or fields in it):

$$\varphi^\dagger(X', T) = C_1 \sin\left[K^\dagger X' - \Omega^\dagger T + \alpha_0\right], \quad \text{(a)}$$

$$\varphi^\ddagger(X', T) = -C_1 \sin\left[K^\ddagger X' + \Omega^\ddagger T - \alpha_0\right], \quad \text{(b)} \quad (1)$$

where $\begin{bmatrix} K^\dagger \\ K^\ddagger \end{bmatrix} = \lim_{(v/c)^2 \to 0} \begin{bmatrix} k^\dagger \\ k^\ddagger \end{bmatrix} = K \pm K_d$, $\begin{bmatrix} k^\dagger \\ k^\ddagger \end{bmatrix} = \frac{K}{1 \mp v/c}$ being wavevectors Doppler-shifted due to the source motion from their zero-v value, K; $\Lambda = 2\pi/K$, and $\Omega = cK$; $\Omega = \Omega_q$ for the classical electromagnetic radiation. On defining $k_d = \sqrt{(k^\dagger - K)(K - k^\ddagger)} = \left(\frac{v}{c}\right)k$, with $k = \gamma K$, $\gamma = \frac{1}{\sqrt{1 - (v/c)^2}}$, we have at classic-velocity limit:

$$K_d = \lim_{(v/c)^2 \to 0} k_d = \left(\frac{v}{c}\right)K; \quad (2)$$

$\begin{bmatrix} \Omega^\dagger \\ \Omega^\ddagger \end{bmatrix} = \begin{bmatrix} K^\dagger c \\ K^\ddagger c \end{bmatrix} = \Omega \pm K_d c$, and α_0 is the initial phase. Assuming $\mathcal{E}_q$ is large and radiated in $J (\gg 1)$ wave periods if without re-fuel, the wavetrain of φ^j of a length $L_\varphi = JL$ will wind about the box L in $J \gg 1$ loops.

The electromagnetic wave φ^j of an angular frequency $\omega^j = k^j c$, $j = \dagger$ or $\ddagger$, has according to M. Planck a wave energy $\varepsilon^j = \hbar\omega^j$, with $2\pi\hbar$ the Planck constant. The waves are here the components of a particle; the geometric mean of their wave energies, $\sqrt{\varepsilon^\dagger \varepsilon^\ddagger} = \hbar\sqrt{\omega^\dagger \omega^\ddagger} = \gamma\hbar\Omega$ gives thereby the total energy of the particle. $\varepsilon_v = \gamma\hbar\Omega - \hbar\Omega = \frac{1}{2}\hbar\Omega_d\left[1 + \frac{3}{4}\left(\frac{v}{c}\right)^2 + \ldots\right]$ gives further the particle's kinetic energy and in a similar fashion its linear momentum p_v (see [2]), and

$$\mathcal{E}_v = \lim_{(v/c)^2 \to 0} \varepsilon_v = \frac{1}{2}\hbar\left(\frac{v}{c}\right)^2 \Omega, \quad (3)$$

$$P_v = \lim_{(v/c)^2 \to 0} p_v = \sqrt{2m_0 \mathcal{E}_v} = \hbar\left(\frac{v}{c}\right)K. \quad (4)$$

The above continues to indeed imply as L. de Broglie noted that a moving mass has a larger $\gamma\Omega/2\pi \ (= \nu)$, and thus a clash with the time-dilation of Einstein's moving clock. This conflict however vanishes when the underlying physics becomes clear-cut [2, 2006c].

3 Propagating total wave of particle

A tagged wave front of say $\varphi^\dagger(X', T)$ generated by the vaculeon charge, of $v > 0$, to its right at location X' at time T, will after a round-trip of distance $2L$ in time $\delta T = 2L/c$ return from left and propagate again to the right to X' at time $T^* = T + \delta T$. Here it gains a total extra phase $\alpha' = K2L + 2\pi$ due to $2L$ (with $\frac{(K^\dagger + K^\ddagger)}{2} = K$) and the twice reflections at the massive walls, and becomes

$$\varphi_r^\dagger(X', T^*) = C_1 \sin\left[K^\dagger X' - \Omega^\dagger T + \alpha_0 + \alpha'\right]. \quad (1a)'$$

$\varphi_r^\dagger$ meets $\varphi^\dagger(X', T^*)$ just generated to the right, an identical wave except for an α', and superposes with it to a

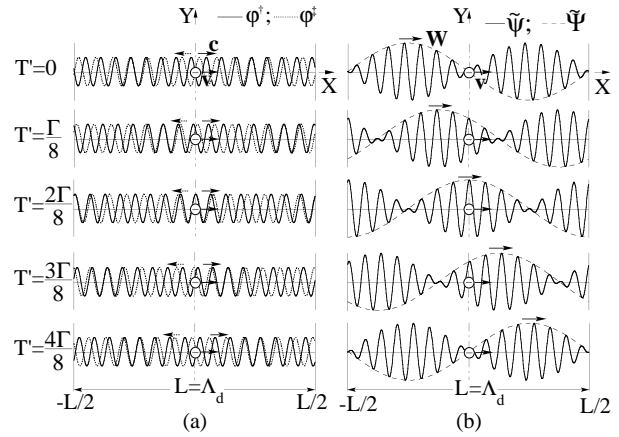Fig. 1: (a) The time development of electromagnetic waves with wave speed c and wavelength Λ, $\varphi^\dagger$ generated to the right of (1a)' and $\varphi^\ddagger$ to the left of (1b) by a charge $(\ominus)$ traveling at velocity v in $+X$ direction in a one-dimensional box of side L. (b) $\varphi^\dagger$ and $\varphi^\ddagger$ superpose to a beat, or de Broglie phase wave $\widetilde{\psi}$ of (5) traveling at phase velocity $W \simeq \frac{c^2}{v}$, of wavelength Λ_d. For the plot: $\Lambda = 0.067\Lambda_d$, and $\alpha_0 = -\frac{\pi}{2}$; $T' = T - \frac{\Gamma}{4}$; $v = \left(\frac{\Lambda}{\Lambda_d}\right)c \ll c$.

maximum if assuming $K2L = N2\pi$, $N = 0, 1, \ldots$, returning the same $\varphi^\dagger$ (assuming normalized). Meanwhile, $\varphi_r^\dagger(X', T^*)$ meets $\varphi^\ddagger(X_1', T^*)$ just generated to the left (Fig. 1a) and superposes with it as $\widetilde{\psi} = \varphi_r^\dagger + \varphi^\ddagger$. Using the trigonometric identity (TI), denoting $\widetilde{\psi}(X', T) = \widetilde{\psi}(X', T^*)$, this is $\widetilde{\psi}(X', T) = 2C_1 \cos(KX' - K_d cT) \sin(K_d X' - \Omega T + \alpha_0)$. With $X' = X - vT$, we have on the X-axis:

$$\widetilde{\psi}(X, T) = \widetilde{\Phi}(X, T)\,\widetilde{\Psi}(X, T), \quad (5)$$

$$\widetilde{\Phi}(X, T) = 2C_1 \cos(KX - 2K_d cT), \quad (6)$$

$$\widetilde{\Psi}(X, T) = \sin\left[K_d X - (\Omega + \Omega_d)T + \alpha_0\right], \quad (7)$$

where $Kv = K_d c$, and

$$\Omega_d = K_d v = \left(\frac{v}{c}\right)^2 \Omega. \quad (8)$$

$\widetilde{\psi}$ expressed by (5) is a *traveling beat wave*, as plotted versus X in Fig. 1b for consecutive time points during $\Gamma/2$, or Fig. 2a during $\Gamma_d/2$. $\widetilde{\psi}$ is due to all the component waves of the particle while its charge is moving in one direction, and thus represents the (propagating) total wave of the particle, to be identified as a *de Broglie phase wave* below.

$\widetilde{\psi}$ has one product component $\widetilde{\Phi}$ oscillating rapidly on the X-axis with the wavelength $\Lambda = 2\pi/K$, and propagating at the speed of light c at which the total wave energy is transported. The other, $\widetilde{\Psi}$, envelops about $\widetilde{\Phi}$, modulating it into a slow varying beat $\widetilde{\psi}$ which has a wavevector, wavelength and angular frequency given by:

$$K_b = K_d, \quad \Lambda_b = \frac{2\pi}{K_b} = \frac{2\pi}{K_d} = \Lambda_d, \quad \Omega_b = \Omega + \Omega_d; \quad (9)$$

$$\text{where} \quad \Lambda_d = \left(\frac{c}{v}\right)\Lambda. \quad (10)$$

As follows (9), the beat $\widetilde{\psi}$ travels at the *phase velocity*

$$W = \frac{\Omega_{\mathrm{b}}}{K_{\mathrm{b}}} = \frac{\Omega}{K_d} + v = \left(\frac{c}{v}\right) c + v\,. \qquad (11)$$

4 De Broglie wave

Transmitted along with its beat wave, of a wavelength Λ_d, with $K_d = 2\pi/\Lambda_d$, is the mass of the particle at the velocity v. The beat wave conjoined with its transportation of the particle's mass represents thereby a periodic process of the particle, of a wavelength and wavevector equal to Λ_d and K_d of the beat wave. K_d and v define for the particle dynamics an angular frequency, $K_d v = \Omega_d$, as expressed by (8). Combining (10) and (4), and (8) and (3) respectively yield just the *de Broglie relations*:

$$P_v = \hbar K_d\,; \qquad (12) \qquad \mathcal{E}_v = \frac{1}{2}\hbar\Omega_d\,. \qquad (13)$$

Accordingly K_d, Λ_d, and Ω_d represent the de Broglie wave-vector, wavelength and angular frequency. The beat wave $\widetilde{\psi}$ of a phase velocity W resembles thereby the *de Broglie phase wave* and it in the context of transmitting the particle mass represents the *de Broglie wave* of the particle.

## 5 Virtual source. Reflected total particle wave

At an earlier time $T_1 = T - \Delta T$, at a distance L advancing its present location X, with $\Delta T = L/v$, the actual charge was traveling to the left, let axis $X''(= X + vT)$ be fixed to it. This past-time charge, said being virtual, generated at location X'' at time T_1 similarly one component wave $\varphi^{\dagger\mathrm{vir}}(X'', T_1^*)$ to the right, which after traversing $2L$ returned from left to X'' at time $T_1^* = T_1 + \delta T$ as $\varphi^{\dagger\mathrm{vir}}_r(X'', T_1^*) = = C_1 \sin(K^\dagger_{-v} X'' - \Omega^\dagger_{-v} T_1^* + \alpha_0 + \alpha')$, where $K^\dagger_{-v} = K - K_d$, $K^\ddagger_{-v} = K + K_d$, and $\Omega^j_{-v} = K^j_{-v} c$ are the Doppler shifted wavevectors and angular frequencies; $\alpha' = (2N + 1)\pi$ as earlier. Here at X'' and T_1^*, $\varphi^{\dagger\mathrm{vir}}_r$ meets the wave the virtual charge just generated to the left, $\varphi^{\ddagger\mathrm{vir}}(X'', T_1^*) = -C_1 \times \times \sin(K^\ddagger_{-v} X'' + \Omega^\dagger_{-v} T_1^* - \alpha_0)$, and superpose with it to $\widetilde{\psi}^{\mathrm{vir}}(X, T_1^*) = \varphi^{\dagger\mathrm{vir}}_r + \varphi^{\ddagger\mathrm{vir}} = 2C_1 \cos(KX'' + K_d c T_1) \times \times \sin\left[-K_d X'' - 2\Omega T_1 - \alpha_0\right]$.

With $J \gg 1$ and being nondamping, $\widetilde{\psi}^{\mathrm{vir}}$ will be looping continuously, up to the present time T. Its present form $\widetilde{\psi}^{\mathrm{vir}}(X'', T)$ is then as if just produced by the virtual charge at time T but at a location of a distance L advancing the actual charge; it accordingly has a phase advance $\beta = = \frac{(K^\dagger - K^\dagger_{-v})}{2} L = K_d L$ relative to $\widetilde{\psi}$ (the phase advance in time yields no never feature). Including this β, using TI and with some algebra, $\widetilde{\psi}^{\mathrm{vir}}(X'', T)$ writes on axis X as

$$\widetilde{\psi}^{\mathrm{vir}}(X, T) = \widetilde{\Phi}^{\mathrm{vir}}(X, T)\,\widetilde{\Psi}^{\mathrm{vir}}(X, T)\,, \qquad (14)$$

$$\widetilde{\Phi}^{\mathrm{vir}}(X, T) = 2C_1 \cos\left[(KX + 2K_d cT\right]\,, \qquad (15)$$

$$\widetilde{\Psi}^{\mathrm{vir}}(X, T) = -\sin\left[K_d X + (\Omega + \Omega_d)T + \alpha_0 + \beta\right]. \qquad (16)$$
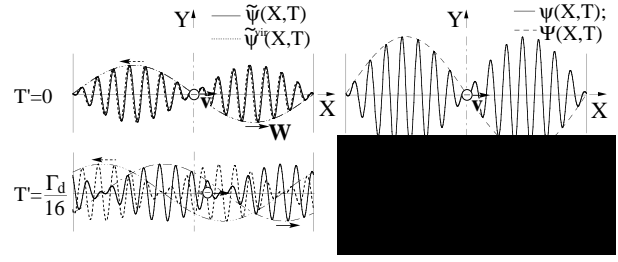
ψ of (18) is a standing beat or standing de Broglie phase wave; it includes all of the component waves due to both the actual and virtual charges and hence represents the (standing) total wave of the particle.

7 Eigen-state wave function and variables

Equation (13) showed the particle's kinetic energy is transmitted at the angular frequency $\frac{1}{2}\Omega_d$, half the value Ω_d for transporting the particle mass, and is a source motion effect of order $\left(\frac{v}{c}\right)^2$. This is distinct from, actually exclusive of, the source motion effect, of order v, responsible for the earlier beat wave formation. We here include the order $\left(\frac{v}{c}\right)^2$ effect only simply as a multiplication factor to ψ, and thus have $\psi' = \psi\left(X,T\right)e^{-i\frac{1}{2}\hbar\Omega_d T}$ which describes the particle's kinetic energy transmission. Furthermore, in typical applications $K \gg K_d$, $\Omega \gg \Omega_d$; thus on the scale of (K_d, Ω_d), we can to a good approximation ignore the rapid oscillation in Φ of (21), and have

$$\Phi(X,T) \simeq C_4 \equiv \text{constant} \qquad (21)'$$

and $\psi(X,T) = C\Psi_X(X)$. The time-dependent wave function, in energy terms, is thus $\Psi(X,T) = \psi'(X,T) = \psi e^{-i\frac{\Omega_d}{2}T} = C\Psi_X(X)e^{-i\frac{\Omega_d}{2}T}$, or

$$\Psi(X,T) = C\sin(K_d X)\, e^{-i\frac{1}{2}\Omega_d T}\,, \qquad (22)$$

where $C = \frac{1}{\int_0^L \psi^2 dX} = \frac{\sqrt{2/L}}{C_4}$ is a normalization constant. With (17) for K_{dn} in (12)–(13), for a fixed L we have the permitted dynamic variables

$$P_{vn} = \frac{n\hbar\pi}{L}\,, \qquad (23) \qquad \mathcal{E}_{vn} = \frac{n^2\hbar^2\pi^2}{2ML^2}\,, \qquad (24)$$

where $n = 1, 2, \ldots$ These dynamic variables are seen to be quantized, pronouncingly for L not much greater than Λ_d, as the direct result of the standing wave solutions. As shown for the three lowest energy levels in Fig. 3a, the permitted $\Psi(X), \equiv \Psi(X, T_0)$ with T_0 a fixed time point, describing the envelopes (dotted lines) of $\psi(X) \equiv \psi(X, T_0)$ which rapid oscillations have no physical consequence to the particle dynamics, are in complete agreement with the corresponding solution of Schrödinger equation for an identical system, $\Psi_S(X)$, indicated by the same dotted lines.

The total wave of a particle, hence its total energy, mass, size, all extend in (real) space throughout the wave path. A portion of the particle, hence the probability of finding the particle, at a given position X in real space is proportional to the wave energy stored in the infinitesimal volume at X, $\mathcal{E}(X) = B\left(\psi(X)\right)^2$, with B a conversion constant [2], $\psi(X)$ as shown in Fig. 3b.

With (23) in $\Delta P_v = P_{v.n+1} - P_{v.n}$ we have $\Delta P_v\, 2L = h$, which reproduces Heisenberg's uncertainty relation. It follows from the solution that the uncertainty in finding a particle in real space results from the particle is an extensive
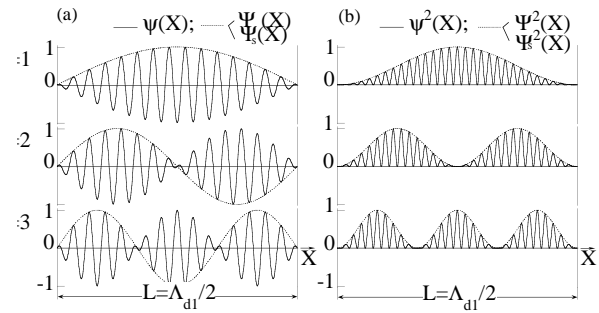

Fig. 3: (a) The total wave of particle $\psi(X)$ of (19) with rapid oscillation, and the de Broglie wave $\Psi(X)$ as the envelop, for three lowest energy levels $n = 1, 2, 3$; Ψ coincides with Schrödinger eigen-state functions Ψ_S. (b) The corresponding probabilities.

wave over L, and in momentum space from the standing wave solution where waves interfering destructively are cancelled and inaccessible to an external observer.

8 Concluding remarks

We have seen that the total wave superposed from the electromagnetic component waves generated by a traveling oscillatory vaculeon charge, which together make up our particle, has actually the requisite properties of a de Broglie wave. It exhibits in spatial coordinate the periodicity of the de Broglie wave, by the wavelength Λ_d, facilitated by a beat or de Broglie phase wave traveling at a phase velocity $\sim c^2/v$, with the beat in the total wave resulting naturally from the source-motion resultant Doppler differentiation of the electromagnetic component waves. Λ_d conjoined with the particle's center-of-mass motion leads to a periodicity of the de Broglie wave on time axis, the angular frequency Ω_d. The Λ_d and Ω_d obey the de Broglie relations. The particle's standing wave solutions in confined space agree completely with solutions for Schrödinger equation for an identical system.

References

1. De Broglie L., *Comptes rendus*, 1923, v. 177, 507–510; PhD Thesis, Univ. of Paris, 1924; *Phil. Mag.* 1924, v. 47, 446.

2. Zheng-Johansson J. X. and Johansson P.-I., Unification of classical, quantum and relativistic mechanics and of the four forces (Foreword by R. Lundin). Nova Science, N.Y., 2006a, 2nd printing (later 2006); *Quantum Theory and Symmetries IV*, ed. by V. K. Dobrev, Heron Press, Sofia, 2006b (one of two papers with R. Lundin); arxiv: phyiscs/0411134(v4); phyiscs/0411245; physics/0501037(v3); Inference of basic laws of classical, quantum and relativistic mechanics from first-principles classical-mechanics solutions (updated title), Nova Science, N.Y., 2006c.

The Classical Theory of Fields Revision Project (CTFRP):

Collected Papers Treating of Corrections to the Book "The Classical Theory of Fields" by L. Landau and E. Lifshitz

CALL FOR PAPERS

The "Course in Theoretical Physics" by L. Landau and E. Lifshitz has for decades served as a set of outstanding textbooks for students and reference for researchers. Many continue to learn their basic physics from this lucid and extensive exposition of physical theory and relevant mathematical methods.

The second volume of this series of texts, "The Classical Theory of Fields", is a mainstay source for physicists learning or conducting research in General Relativity*. However, it has been realised over the years that "The Classical Theory of Fields" contains a number of serious theoretical errors. The errors are in general not peculiar to this book alone, but are fundamental misconceptions that appear routinely in all textbooks on General Relativity, without exception.

Save for the errors alluded to above, "The Classical Theory of Fields" remains an authoritative and skilful exposition of Einstein's theory of gravitation. To enhance its already great standing in the scientific literature, the Editorial Board of Progress in Physics proposes a series of papers dealing with corrections of the now obsolete, although rather standard, erroneous arguments contained in "The Classical Theory of Fields". Any person interested in contributing to this project is invited to submit, for the consideration of the Editorial Board, a paper correcting one or more errors in the book. All papers will undergo review just as any research paper, and be published in Progress in Physics if accepted.

It is envisaged that accepted papers will also be collected together as a supplementary pamphlet to "The Classical Theory of Fields", which will be made available free as a download from the Progress in Physics website. Each author's contribution will bear the author's name, just like any research paper. All authors must agree to free dissemination in this fashion as a condition of contribution.

Should the pamphlet, at any future time, be considered by the Publisher's of the "Course in Theoretical Physics", or any other publisher besides Progress in Physics, as a published supplement packaged with the "Course in Theoretical Physics", all authors will be notified and can thereafter negotiate, if they wish, issues of royalties with the publisher directly. Progress in Physics will still reserve the right to provide the supplementary pamphlet free, from its website, irrespective of any other publication of the supplementary pamphlet by the publishers of the "Course in Theoretical Physics" or any other publisher. No author shall hold Progress in Physics, its Editorial Board or its Servants and Agents liable for any royalties under any circumstances, and all contributors will be required to sign a contract with Progress in Physics to that effect, so that there will be no dispute as to terms and conditions. The Editorial Board of Progress in Physics shall reserve all rights as to inclusion or rejection of contributions.

Those interested in making a contribution should express that interest in an email to the Editors of Progress in Physics who manage this project.

Dmitri Rabounski, Editor-in-Chief
Stephen J. Crothers, Associate Editor
(*the CTFRP organisers*)

---

*The first edition of "The Classical Theory of Fields" was completed in 1939, and originally published in Russian. Four revised editions of the book were later published in English in 1951, 1962, 1971, and 1975. (After Landau was severely injured in a car crash in 1962, Lifshitz alone expanded upon subsequent editions.) As a result the volume of the fourth edition doubled the volume of the first edition. Lifshitz, until his death in 1985, introduced numerous corrections, which are also included in the reprints. "The Classical Theory of Fields" was translated from the Russian, in all its editions, by Prof. Morton Hamermesh (University of Minnesota). Reprints of "The Classical Theory of Fields" are produced by Butterworth-Heinemann (Elsevier) almost annually.

Plausible Explanation of Quantization of Intrinsic Redshift from Hall Effect and Weyl Quantization

Florentin Smarandache* and Vic Christianto†

*Department of Mathematics, University of New Mexico, Gallup, NM 87301, USA
E-mail: smarand@unm.edu

†Sciprint.org — a Free Scientific Electronic Preprint Server, http://www.sciprint.org
E-mail: admin@sciprint.org

Using phion condensate model as described by Moffat [1], we consider a plausible explanation of (Tifft) intrinsic redshift quantization as described by Bell [6] as result of Hall effect in rotating frame. We also discuss another alternative to explain redshift quantization from the viewpoint of Weyl quantization, which could yield Bohr-Sommerfeld quantization.

1 Introduction

In a recent paper by Moffat [1] it is shown that quantum phion condensate model with Gross-Pitaevskii equation yields an approximate fit to data corresponding to CMB spectrum, and it also yields a modified Newtonian acceleration law which is in good agreement with galaxy rotation curve data. It seems therefore interesting to extend further this hypothesis to explain quantization of redshift, as shown by Tifft *et al.* [2, 6, 7]. We also argue in other paper that this redshift quantization could be explained as signature of topological quantized vortices, which also agrees with Gross-Pitaevskiian description [3, 5].

Nonetheless, there is remaining question in this quantized vortices interpretation, i.e. how to provide explanation of "intrinsic redshift" argument by Bell [6]. In the present paper, we argue that it sounds reasonable to interpret the intrinsic redshift data from the viewpoint of rotating Hall effect, i.e. rotational motion of clusters of galaxies exhibit quantum Hall effect which can be observed in the form of "intrinsic redshift". While this hypothesis is very new, it could be expected that we can draw some prediction, including possibility to observe small "blue-shift" effect generated by antivortex part of the Hall effect [5a].

Another possibility is to explain redshift quantization from the viewpoint of Weyl-Moyal quantization theory [25]. It is shown that Schrödinger equation can be derived from Weyl approach [8], therefore quantization in this sense comes from "graph"-type quantization. In large scale phenomena like galaxy redshift quantization one could then ask whether there is possibility of "super-graph" quantization.

Further observation is of course recommended in order to verify or refute the propositions outlined herein.

2 Interpreting quantized redshift from Hall effect. Cosmic String

In a recent paper, Moffat [1, p. 9] has used Gross-Pitaevskii in conjunction with his *phion condensate fluid* model to describe CMB spectrum data. Therefore we could expect that this equation will also yield interesting results in galaxies scale. See also [1b, 1c, 13] for other implications of low-energy phion fluid model.

Interestingly, it could be shown, that we could derive (approximately) Schrödinger wave equation from Gross-Pitaevskii equation. We consider the well-known Gross-Pitaevskii equation in the context of superfluidity or superconductivity [14]:

$$i\hbar \frac{\partial \Psi}{\partial t} = -\frac{\hbar^2}{2m}\Delta\Psi + \left(V(x) - \gamma\left|\Psi\right|^{p-1}\right)\Psi, \qquad (1)$$

where $p < 2N/(N-2)$ if $N \geqslant 3$. In physical problems, the equation for $p = 3$ is known as Gross-Pitaevskii equation. This equation (1) has standing wave solution quite similar to solution of Schrödinger equation, in the form:

$$\Psi(x,t) = e^{-iEt/\hbar} \cdot u(x) \qquad (2)$$

Substituting equation (2) into equation (1) yields:

$$-\frac{\hbar^2}{2m}\Delta u + \left(V(x) - E\right)u = \left|u\right|^{p-1}u, \qquad (3)$$

which is nothing but a time-independent linear form of Schrödinger equation, except for term $\left|u\right|^{p-1}$ [14]. If the right-hand side of this equation is negligible, equation (3) reduces to standard Schrödinger equation.

Now it is worth noting here that from Nottale *et al.* we can derive a gravitational equivalent of Bohr radius from generalized Schrödinger equation [4]. Therefore we could also expect a slight deviation of this gravitational Bohr radius in we consider Gross-Pitaevskii equation instead of generalized Schrödinger equation.

According to Moffat, the phion condensate model implies a modification of Newtonian acceleration law to become [1, p. 11]:

$$a(r) = -\frac{G_\infty M}{r^2} + K\frac{\exp\left(-\mu_\phi r\right)}{r^2}\left(1 + \mu_\phi r\right), \qquad (4)$$

where

$$G_\infty = G\left[1 + \sqrt{\frac{M_0}{M}}\right]. \tag{5}$$

Therefore we can conclude that the use of phion condensate model implies a modification of Newton gravitational constant, G, to become (5). Plugging in this new equation (5) into a Nottale's gravitational Bohr radius equation [4] yields:

$$r_n \approx n^2 \frac{GM}{v_0^2}\left[1 + \sqrt{\frac{M_0}{M}}\right] \approx \chi \cdot n^2 \frac{GM}{v_0^2}, \tag{6}$$

where n is integer $(1,2,3\dots)$ and:

$$\chi = \left[1 + \sqrt{\frac{M_0}{M}}\right]. \tag{7}$$

Therefore we conclude that — provided the higher order Yukawa term of equation (4) could be neglected — one has a *modified* gravitational Bohr-radius in the form of (6). It can be shown (elsewhere) that using similar argument one could expect to explain a puzzling phenomenon of *receding Moon* at a constant rate of $\pm 1.5''$ per year. And from this observed fact one could get an estimate of this χ factor. It is more interesting to note here, that a number of *coral reef* data also seems to support the same idea of modification factor in equation (5), but discussion of this subject deserves another paper.

A somewhat similar idea has been put forward by Masreliez [18] using the metric:

$$ds^2 = e^{\alpha\beta}\left[dx^2 + dy^2 + dz^2 - (icdt)^2\right]. \tag{8}$$

Another alternative of this metric has been proposed by Socoloff and Starobinski [19] using multi-connected hypersurface metric:

$$ds^2 = dx^2 + e^{-2x}\left(dy^2 + dz^2\right) \tag{9}$$

with boundaries: $e^{-x} = \Lambda$.

Therefore one can conclude that the use of phion condensate model has led us to a form of expanding metric, which has been discussed by a few authors.

Furthermore, it is well-known that Gross-Pitaevskii equation could exhibit *topologically* non-trivial vortex solutions [4, 5], which also corresponds to quantized vortices:

$$\oint p \cdot dr = N_v\, 2\pi\hbar. \tag{10}$$

Therefore an implication of Gross-Pitaevskii equation [1] is that topologically quantized vortex could exhibit in astrophysical scale. In this context we submit the viewpoint that this proposition indeed has been observed in the form of Tifft's redshift quantization [2, 6]:

$$\delta r = \frac{c}{H}\,\delta z. \tag{11}$$

In other words, we submit the viewpoint that Tifft's observation of quantized redshift implies a quantized distance between galaxies [2, 5], which could be expressed in the form:

$$r_n = r_0 + n\left(\delta r\right), \tag{12}$$

where n is integer $(1,2,3,\dots)$ similar to quantum number. Because it can be shown using standard definition of Hubble law that redshift quantization implies quantized distance between galaxies in the same cluster, then one could say that this equation of quantized distance (11) is a result of *topological* quantized vortices (9) in astrophysical scale [5]; and it agrees with Gross-Pitaevskii (quantum phion condensate) description of CMB spectrum [1]. It is perhaps more interesting if we note here, that from (11) then we also get an equivalent expression of (12):

$$\frac{c}{H}\,z_n = \frac{c}{H}\,z_0 + n\left(\frac{c}{H}\,\delta z\right) \tag{13}$$

or

$$z_n = z_0 + n\left(\delta z\right) \tag{14}$$

or

$$z_n = z_0\left[1 + n\left(\frac{\delta z}{z_0}\right)\right]. \tag{15}$$

Nonetheless, there is a problem here, i.e. how to explain intrinsic redshift related to Tifft quantization as observed in Fundamental Plane clusters and also from various quasars data [6, 6a]:

$$z_{iQ} = z_f\left[N - 0.1 M_N\right] \tag{16}$$

where $z_f = 0.62$ is assumed to be a fundamental redshift constant, and $N (=1, 2, 3\dots)$, and M is function of N [6a]. Meanwhile, it is interesting to note here similarity between equation (15) and (16). Here, the number M seems to play a rôle similar to second quantum number in quantum physics [7].

Now we will put forward an argument that intrinsic redshift quantization (16) could come from rotating quantum Hall effect [5a].

It is argued by Fischer [5a] that "Hall quantization is of necessity derivable from a *topological quantum number* related to this (quantum) coherence". He used total particle momentum [5a]:

$$p = mv + m\Omega \times r + qA. \tag{17}$$

The uniqueness condition of the collective phase represented in (9) then leads, if we take a path in the bulk of electron liquid, for which the integral of mv can be neglected, to the quantization of the sum of a *Sagnac flux*, and the magnetic flux [5a]:

$$\Phi = q\oint A \cdot dr + m\oint \Omega \times r \cdot dr =$$
$$= \iint B \cdot dS = N_v\, 2\pi\hbar. \tag{18}$$

This flux quantization rule corresponds to the fact that a *vortex* is fundamentally characterised by the winding number N alone [5a]. In this regard the vortex could take the form of cosmic string [22]. Now it is clear from (15) that quantized vortices could be formed by different source of flux.

After a few more reasonable assumptions one could obtain a generalised Faraday law, which in rotating frame will give in a non-dissipative Hall state the quantization of Hall conductivity [5a].

Therefore one could observe that it is quite natural to interpret the quantized distance between galaxies (11) as an implication of quantum Hall effect in rotating frame (15). While this proposition requires further observation, one could think of it in particular using known analogy between condensed matter physics and cosmology phenomena [10, 22]. If this proposition corresponds to the facts, then one could think that redshift quantization is an imprint of generalized quantization in various scales from microphysics to macrophysics, just as Tifft once put it [2]:

> "The redshift has imprinted on it a pattern that appears to have its origin in microscopic quantum physics, yet it carries this imprint across cosmological boundaries".

In the present paper, Tifft's remark represents natural implication of topological quantization, which could be formed at any scale [5]. We will explore further this proposition in the subsequent section, using Weyl quantization.

Furthermore, while this hypothesis is new, it could be expected that we can draw some new prediction, for instance, like possibility to observe small "blue-shift" effect generated by the Hall effect from antivortex-galaxies [23]. Of course, in order to observe such a "blue-shift" one shall first exclude other anomalous effects of redshift phenomena [6]. (For instance: one could argue that perhaps Pioneer spacecraft anomaly's blue-shifting of Doppler frequency may originate from the same effect as described herein.)

One could expect that further observation in particular in the area of low-energy neutrino will shed some light on this issue [20]. In this regard, one could view that the Sun is merely a remnant of a neutron star in the past, therefore it could be expected that it also emits neutrino similar to neutron star [21].

3 An alternative interpretation of astrophysical quantization from Weyl quantization. Graph and quantization

An alternative way to interpret the above proposition concerning topological quantum number and topological quantization [5a], is by using Weyl quantization.

In this regards, Castro [8, p. 5] has shown recently that one could derive Schrödinger equation from Weyl geometry using continuity equation:

$$\frac{\partial \rho}{\partial t} + \frac{1}{\sqrt{g}}\, \partial_i\big(\sqrt{g}\rho v^i\big) \tag{19}$$

and Weyl metric:

$$R_{\text{Weyl}} = (d-1)(d-2)\left(A_k A^k\right) - 2(d-1)\,\partial_k A^k\,. \tag{20}$$

Therefore one could expect to explain astrophysical quantization using Weyl method in lieu of using generalised Schrödinger equation as Nottale did [4]. To our knowledge this possibility has never been explored before elsewhere.

For instance, it can be shown that one can obtain Bohr-Sommerfeld type quantization rule from Weyl approach [24, p. 12], which for kinetic plus potential energy will take the form:

$$2\pi N\hbar = \sum_{j=0}^{\infty} \hbar^j S_j(E)\,, \tag{21}$$

which can be solved by expressing $E = \sum \hbar^k E_k$ as power series in $\hbar$ [24]. Now equation (10) could be rewritten as follows:

$$\oint p \cdot dr = N_v\, 2\pi\hbar = \sum_{j=0}^{\infty} \hbar^j S_j(E)\,. \tag{22}$$

Or if we consider quantum Hall effect, then equation (18) can be used instead of equation (10), which yields:

$$\Phi = q \oint A \cdot dr + m \oint \Omega \times r \cdot dr = \\ = \iint B \cdot dS = \sum_{j=0}^{\infty} \hbar^j S_j(E)\,. \tag{23}$$

The above method is known as "graph kinematic" [25] or Weyl-Moyal's quantization [26]. We could also expect to find Hall effect quantization from this deformation quantization method.

Consider a harmonic oscillator, which equation can be expressed in the form of deformation quantization instead of Schrödinger equation [26]:

$$\left(\left(x + \frac{i\hbar}{2}\,\partial_p\right)^2 + \left(p - \frac{i\hbar}{2}\,\partial_x\right)^2 - 2E\right) f(x,p) = 0\,. \tag{24}$$

This equation could be separated to become two simple PDEs. For imaginary part one gets [26]:

$$\left(x\,\partial_p - p\,\partial_x\right) f = 0\,. \tag{25}$$

Now, considering Hall effect, one can introduce our definition of total particle momentum (17), therefore equation (25) may be written:

$$\left(x\,\partial_p - (mv + m\Omega \times r + qA)\,\partial_x\right) f = 0\,. \tag{26}$$

Our proposition here is that in the context of deformation quantization it is possible to find quantization solution of harmonic oscillator without Schrödinger equation. And

because it corresponds to graph kinematic [25], generalized Bohr-Sommerfeld quantization rule for quantized vortices (22) in astrophysical scale could be viewed as signature of "*super-graph*"*quantization*.

This proposition, however, deserves further theoretical considerations. Further experiments are also recommended in order to verify and explore further this proposition.

Concluding remarks

In a recent paper, Moffat [1] has used Gross-Pitaevskii in his "phion condensate fluid" to describe CMB spectrum data. We extend this proposition to explain Tifft redshift quantization from the viewpoint of topological quantized vortices. In effect we consider that the intrinsic redshift quantization could be interpreted as result of Hall effect in rotating frame.

Another alternative to explain redshift quantization is to consider quantized vortices from the viewpoint of Weyl quantization (which could yield Bohr-Sommerfeld quantization).

It is recommended to conduct further observation in order to verify and also to explore various implications of our propositions as described herein.

Acknowledgment

References

1. Moffat J. arXiv: astro-ph/0602607; [1a] Consoli M. arXiv: hep-ph/0109215; [1b] Consoli M. *et al.* arXiv: physics/0306094.

2. Russell Humphreys D. Our galaxy is the centre of the universe, "quantized" red shifts show. *TJ Archive*, 2002, v. 16(2), 95–104; http://answersingenesis.org/tj/v16/i2/galaxy.asp.

3. Smarandache F. and Christianto V. A note on geometric and information fusion interpretation of Bell theorem and quantum measurement. *Progress in Physics*, 2006, v. 4, 27–31.

4. Smarandache F. and Christianto V. Schrödinger equation and the quantization of celestial systems. *Progress in Physics*, 2006, v. 2, 63–67.

5. Fischer U. arXiv: cond-mat/9907457; [5a] arXiv: cond-mat/0004339.

6. Bell M. B. arXiv: astro-ph/0111123; [6a] arXiv: astro-ph/0305112; [6b] arXiv: astro-ph/0305060.

7. Setterfield B. http://www.journaloftheoretics.com; http://www.setterfield.org.

8. Castro C. and Mahecha J. On nonlinear Quantum Mechanics, Brownian motion, Weyl geometry, and Fisher information. *Progress in Physics*, 2006, v. 1, 38–45.

9. Schrieffer J. R. Macroscopic quantum phenomena from pairing in superconductors. Lecture, December 11, 1972.

10. Zurek W. H. Cosmological experiments in superfluids and superconductors. In: *Proc. Euroconference in Formation and Interaction of Topological Defects*, Plenum Press, 1995; arXiv: cond-mat/9502119.

11. Anandan J. S. In: *Quantum Coherence and Reality, Proc. Conf. Fundamental Aspects of Quantum Theory*, Columbia SC., edited by J. S. Anandan and J. L. Safko, World Scientific, 1994; arXiv: gr-qc/9504002.

12. Rauscher E. A. and Amoroso R. The physical implications of multidimensional geometries and measurement. *Intern. J. of Comp. Anticipatory Systems*, 2006.

13. Chiao R. *et al.* arXiv: physics/0309065.

14. Dinu T. L. arXiv: math.AP/0511184.

15. Kravchenko V. arXiv: math.AP/0408172.

16. Lipavsky P. *et al.* arxiv: cond-mat/0111214.

17. De Haas E. P. *Proc. of the Intern. Conf. PIRT-2005*, Moscow, MGTU Publ., 2005.

18. Masreliez J. *Apeiron*, 2005, v. 12.

19. Marc L.-R. and Luminet J.-P. arXiv: hep-th/9605010.

20. Lanou R. arXiv: hep-ex/9808033.

21. Yakovlev D. *et al.* arXiv: astro-ph/0012122.

22. Volovik G. arXiv: cond-mat/0507454.

23. Balents L. *et al.* arXiv: cond-mat/9903294.

24. Gracia-Saz A. *Ann. Inst. Fourier*, Grenoble, 2005, v. 55(5), 1001–1008.

25. Asribekov V. L. arXiv: physics/0110026.

26. Zachos C. arXiv: hep-th/0110114.

Geometrical Dynamics in a Transitioning Superconducting Sphere

James R. Claycomb[*] and Rambis K. Chu[†]

[*]*Department of Mathematics and Physics, Houston Baptist University, Houston, TX 77074-3298, USA*
E-mail: jclaycomb@hbu.edu

[†]*Bio-Nano Computational Laboratory RCMI-NCRR and Physics Department,*
Texas Southern University, Houston, TX 77004, USA
E-mail: chu_rk@tsu.edu

Recent theoretical works have concentrated on calculating the Casimir effect in curved spacetime. In this paper we outline the forward problem of metrical variation due to the Casimir effect for spherical geometries. We consider a scalar quantum field inside a hollow superconducting sphere. Metric equations are developed describing the evolution of the scalar curvature after the sphere transitions to the normal state.

1 Introduction

The classical Casimir effect [1, 2] may be viewed as vacuum reduction by mode truncation where the presence of conducting boundaries, or capacitor plates, excludes vacuum modes with wavelengths longer than the separation between the conductors. The exclusion of longer wavelengths results in a lower vacuum pressure between the plates than in external regions. The resulting pressure difference, or Casimir force, may act to push the conductors together, effectively collapsing the reduced vacuum phase. This tiny force has been measured experimentally [3, 4] in agreement with the predictions of quantum electrodynamics. Boyer gives the first detailed treatment of the vacuum modes inside a conducting sphere [5] with more a recent account by Milton [6]. The Casimir effect for spherical conducting shells in external electromagnetic fields has been investigated [7, 8]. Applications of the Casimir effect to the bag model have been studied for massive scalar [9] and Dirac [10] fields confined to the interior of the shell. An example of the Casimir effect in curved spacetime has been considered for spherical geometries [11] in de Sitter space [12] and in the background of static domain wall [13]. In this paper we investigate the metrical variations resulting from vacuum pressure differences established by a spherical superconducting boundary. We first consider the static case when the sphere is superconducting and then the dynamical case as the sphere passes to the normal state.

2 The static case

Our idealized massless, thin sphere of radius R_0 has zero conductivity in the normal state. In the superconducting state, the vacuum inside the hollow is reduced so that there exists a pressure difference Δp inside and outside the sphere. In general, all quantum fields will contribute to the vacuum energy. When the sphere of volume V transitions to the superconducting state, a latent heat of vacuum phase transi-

tion $\Delta p V$ is exchanged. The distribution of vacuum pressure, energy density and space-time geometry are described by the semi-classical Einstein field equations taking $c = 1$,

$$R_{\mu\nu} - \frac{1}{2} R \, g_{\mu\nu} = 8\pi G \left\langle T_{\mu\nu} \right\rangle, \tag{1}$$

where $R_{\mu\nu}$ and R are the Ricci tensor and scalar curvature, respectively. $\left\langle T_{\mu\nu} \right\rangle$ is the vacuum expectation of the stress energy tensor. Regulation procedures for calculating the renormalized stress energy tensor are given in [14] for various geometries. The most general line element with spherical symmetry is

$$ds^2 = B\left(r, t\right) dt^2 - A\left(r, t\right) dr^2 - C\left(r, t\right) dr dt - \\ - r^2 d\theta^2 - r^2 \sin^2\theta \, d\phi^2, \tag{2}$$

where A, B, and C are arbitrary functions of time and the radial coordinate. (2) can be written under normal coordinate transformation [15],

$$ds^2 = \tilde{B}\left(r, t\right) dt^2 - \tilde{A}\left(r, t\right) dr^2 - r^2 d\theta^2 - r^2 \sin^2\theta \, d\phi^2. \tag{3}$$

The metric tensor then becomes, dropping tildes,

$$g_{\mu\nu} = \mathrm{Diag}\left(B\left(r, t\right), -A\left(r, t\right), -r^2, -r^2 \sin^2\theta\right). \tag{4}$$

For a diagonal stress energy tensor, the solutions to equation (3) relating A and B are

$$-\frac{1}{r^2} + \frac{1}{r^2 A} - \frac{A'}{rA^2} = 8\pi G \frac{1}{B} \left\langle T_{00} \right\rangle, \tag{5}$$

$$\frac{1}{r^2} - \frac{1}{r^2 A} - \frac{B'}{rAB} = 8\pi G \frac{1}{A} \left\langle T_{11} \right\rangle, \tag{6}$$

$$\frac{A'}{2rA^2} - \frac{B'}{2rAB} + \frac{A'B'}{4A^2B} - \frac{B'^2}{4AB^2} - \\ - \frac{B''}{2AB} = 8\pi G \frac{1}{r^2} \left\langle T_{22} \right\rangle, \tag{7}$$

with a fourth equation identical to (7). The prime denotes ∂_r.

Note that all time derivatives cancel from the field equations when the metric is in standard form and the stress energy tensor is diagonal. When the sphere is in the superconducting state, the scalar curvature $R = g^{\mu\nu} R_{\mu\nu}$ is given by

$$R = \frac{2}{r^2} - \frac{2}{r^2 A} + \frac{2A'}{rA^2} - \frac{2B'}{rAB} + \frac{A'B'}{2A^2 B} + \frac{B'^2}{2AB^2} - \frac{B''}{AB}. \tag{8}$$

In calculating the Casimir force, one properly calculates differences in vacuum pressure established by the conducting boundaries [2]. In the present case, it is only meaningful to consider changes in scalar curvature due to variations in vacuum pressure.

3 The dynamical case

If the sphere passes from the superconducting to the normal state, the pressure should equalize as the vacuum relaxes. The diagonal form of the stress energy tensor results in the cancellation of all time derivatives in the field equations. External electromagnetic fields will contribute off-diagonal terms, however we wish to consider how the pressure equalizes in absence of external fields. The key is that the required time dependence is provided by the zero point field fluctuations. As the simplest example, we consider the massless scalar quantum field with stress energy tensor [14]

$$T_{\mu\nu} = \phi_{,\mu} \phi_{,\nu} - \frac{1}{2} g_{\mu\nu} g^{\alpha\beta} \phi_{,\alpha} \phi_{,\beta}. \tag{9}$$

The non-zero components of $T_{\mu\nu}$ are

$$T_{00} = \frac{1}{2} \dot{\phi}^2 + \frac{B}{2A} \phi'^2, \tag{10}$$

$$T_{11} = \frac{1}{2} \phi'^2 + \frac{A}{2B} \dot{\phi}^2, \tag{11}$$

$$T_{22} = r^2 \left(\frac{1}{2B} \dot{\phi}^2 + \frac{1}{2A} \phi'^2 \right), \tag{12}$$

$$T_{33} = r^2 \sin^2\theta \left(\frac{1}{2B} \dot{\phi}^2 + \frac{1}{2A} \phi'^2 \right), \tag{13}$$

$$T_{01} = \dot{\phi} \phi', \tag{14}$$

where $T_{01} = T_{10}$. The semi-classical field equations become

$$-\frac{1}{r^2} + \frac{1}{r^2 A} - \frac{A'}{rA^2} = 8\pi G \frac{1}{B} \langle T_{00} \rangle, \tag{15}$$

$$\frac{1}{r^2} - \frac{1}{r^2 A} - \frac{B'}{rAB} = 8\pi G \frac{1}{A} \langle T_{11} \rangle, \tag{16}$$

$$-\frac{\dot{A}^2}{4A^2 B} - \frac{\dot{A}\dot{B}}{4AB^2} + \frac{\ddot{A}}{2AB} + \frac{A'}{2r^2 A} - \frac{B'}{2rAB} + \frac{A'B'}{4A^2 B} + \frac{B'^2}{4AB^2} - \frac{B''}{2AB} = 8\pi G \frac{1}{r^2} \langle T_{22} \rangle, \tag{17}$$

$$-\frac{\dot{A}}{rA} = 8\pi G \langle T_{01} \rangle. \tag{18}$$

Equations (15) and (16) are identical to (5) and (6). Two additional equations are identical to (17) and (18). Expressions for A and B may be obtained from equation (18) and (15) or (16), respectively. The scalar curvature is given by

$$R = \frac{2}{r^2} - \frac{2}{r^2 A} - \frac{\dot{A}^2}{2A^2 B} - \frac{\dot{A}\dot{B}}{AB} + \frac{\ddot{A}}{AB} + \frac{2A'}{rA^2} - \frac{2B'}{rAB} + \frac{A'B'}{2A^2 B} + \frac{B'^2}{2AB^2} - \frac{B''}{AB}. \tag{19}$$

Combining equation (19) with (15–17) and (10–12) reveals

$$R = 16\pi G \left\langle \frac{\dot{\phi}^2}{2B} - \frac{\phi'^2}{2A} \right\rangle. \tag{20}$$

When evaluating changes in scalar curvature, the expression for R in absence of the sphere should be subtracted from that obtained for a given quantum field.

4 Conclusion

When a hollow sphere transitions between the normal and superconducting state a latent heat of vacuum phase transition is exchanged. In the dynamical case, zero-point field fluctuations result in off-diagonal components of the stress energy tensor that give rise to time dependent field equations. The analysis presented here may be extended to include massive fields with coupling or spin (0, $\frac{1}{2}$ and 1) as well as other superconducting geometries.

References

1. Casimir H. B. G. On the attraction between two perfectly conducting plates. *Proc. K. Ned. Akad. Wet.*, 1948, v. 51, 793.

2. Milonni P. W. The quantum vacuum: An introduction to Quantum Electrodynamics. Academic Press, London, 1994.

3. Lamoreaux S. K. Demonstration of the Casimir force in the 0.6 to 6 μm range. *Phys. Rev. Lett.*, 1997, v. 78, 5–8.

4. Mohideen U., Roy A. Precision measurement of the Casimir force from 0.1 to 0.9 μm. *Phys. Rev. Lett.*, 1998, v. 81, 4549–4552.

5. Boyer T. H. Quantum electromagnetic zero-point energy of a conducting spherical shell and the Casimir model for a charged particle. *Phys. Rev.*, 1968, v. 25, 1764–1776.

6. Milton K. A. Vector Casimir effect for a D-dimensional sphere. *Phys. Rev. D*, 1997, v. 55, 4940–4946.

7. Milton K. A., DeRaad L. L., Schwinger J. *Ann. Phys.*, 1978, v. 115, 338.

8. Nesterenko V. V., Pirozhenko I. G. Simple method for calculating the Casimir energy for a sphere. *Phys. Rev. D*, 1998, v. 57, 1284–1290.

9. Bordag M., Elizalde E., Kirsten K., Leseduarte S. Casimir energies for massive scalar fields in a spherical geometry. *Phys. Rev. D*, 1997, v. 56, 4896–4904.

10. Elizalde E., Bordag M., Kirsten K. Casimir energy for a massive fermionic quantum field with a spherical boundary. *J. Phys. A*, 1998, v. 31, 1743–1759.

11. Bayin S., Ozcan M. Casimir energy in a curved background with a spherical boundary: An exactly solvable case. *Phys. Rev. D*, 1993, v. 48, 2806–2812.

12. Setare M. R., Saharian A. A. Casimir effect for a spherical shell in de Sitter space. *Class. Quantum Grav.*, 2001, v. 18, 2331–2338.

13. Setare M. R., Saharian A. A. Casimir effect in background of static domain wall. *Int. J. Mod. Phys. A*, 2001, v. 16, 1463–1470.

14. Birrell N. D., Davies P. C. W. Quantum fields in curved space. Cambridge University Press, Cambridge, 1994.

15. Weinberg S. Gravitation and Cosmology Wiley, New York, 1972.

Black Holes and Quantum Theory: The Fine Structure Constant Connection

Reginald T. Cahill

School of Chemistry, Physics and Earth Sciences, Flinders University, Adelaide 5001, Australia

E-mail: Reg.Cahill@flinders.edu.au

The new dynamical theory of space is further confirmed by showing that the effective "black hole" masses M_{BH} in 19 spherical star systems, from globular clusters to galaxies, with masses M, satisfy the prediction that $M_{BH} = \frac{\alpha}{2} M$, where α is the fine structure constant. As well the necessary and unique generalisations of the Schrödinger and Dirac equations permit the first derivation of gravity from a deeper theory, showing that gravity is a quantum effect of quantum matter interacting with the dynamical space. As well the necessary generalisation of Maxwell's equations displays the observed light bending effects. Finally it is shown from the generalised Dirac equation where the spacetime mathematical formalism, and the accompanying geodesic prescription for matter trajectories, comes from. The new theory of space is non-local and we see many parallels between this and quantum theory, in addition to the fine structure constant manifesting in both, so supporting the argument that space is a quantum foam system, as implied by the deeper information-theoretic theory known as Process Physics. The spatial dynamics also provides an explanation for the "dark matter" effect and as well the non-locality of the dynamics provides a mechanism for generating the uniformity of the universe, so explaining the cosmological horizon problem.

1 Introduction

Physics has had two distinct approaches to space. Newton asserted that space existed, but was non-dynamical and unobservable. Einstein, in contrast, asserted that space was merely an illusion, a perspective effect in that it is four-dimensional spacetime which is real and dynamical, and that the foliation into space and a geometrical model of time was observer dependent; there was no observer independent space. Hence also according to Einstein space was necessarily unobservable. However both approaches have been challenged by the recent discovery that space had been detected again and again over more than 100 years [1–11], and that the dynamics of space is now established*. The key discovery [2] in 2002 was that the speed of light is anisotropic — that it is c only with respect to space itself, and that the solar system has a large speed of some 400 km/s relative to that space, which causes the observed anisotropy. This discovery changes all of physics†. The problem had been that from the very beginning the various gas-mode Michelson interferometer experiments to detect this anisotropy had been incorrectly calibrated‡, and that the small fringe shifts actually seen corresponded to this high speed. As well it has been incorrectly assumed that the success of the Special Relativity formalism requires

that the speed of light be isotropic, that an actual 3-space be unobservable. Now that space is known to exist it must presumably also have a dynamics, and this dynamics has been discovered and tested by explaining various phenomena such as (i) gravity, (ii) the "dark matter" effect, (iii) the bore hole g anomalies, (iv) novel black holes, (v) light bending and gravitational lensing in general, and so on. Because space has been overlooked in physics as a dynamical aspect of reality all of the fundamental equations of physics, such as Maxwell's equations, the Schrödinger equation, the Dirac equation and so on, all lacked the notion that the phenomena described by these equations were excitations, of various kinds, of the dynamical space itself. The generalisation of the Schrödinger equation [12] then gave the first derivation and explanation for gravity: it is a quantum effect in which the wave functions are refracted by the inhomogeneities and time variations of the structured space. However the most striking discovery is that the internal dynamics of space is determined by the fine structure constant [13–16]. In this paper we report further observational evidence for this discovery by using a more extensive collection of "black hole" masses in spherical galaxies and globular clusters§. As well we give a more insightful explanation for the dynamics of space. We also show how this quantum-theoretic explanation for gravity leads to a derivation of the spacetime construct where, we emphasise, this is purely a mathematical construct and not an aspect of reality. This is important as it explains why the spacetime dynamics appeared to be successful, at

---

*At least in the limit of zero vorticity.

†Special Relativity does not require that the speed of light be isotropic, as is usually incorrectly assumed.

‡Special relativity effects and the presence of gas in the light paths both play critical roles in determining the calibration. In vacuum mode the interferometer is completely insensitive to absolute motion effects, i.e. to the anisotropy of light.

§The generic term "black hole" is used here to refer to the presence of a compact closed event horizon enclosing a spatial in-flow singularity.

least in those cases where the "dark matter" effect was not apparent. However in general the metric tensor of this induced spacetime does not satisfy the General Relativity (GR) equations.

2 Dynamics of space

At a deeper level an information-theoretic approach to modelling reality (Process Physics [1]) leads to an emergent structured "space" which is 3-dimensional and dynamic, but where the 3-dimensionality is only approximate, in that if we ignore non-trivial topological aspects of space, then it may be embedded in a 3-dimensional geometrical manifold. Here the space is a real existent discrete but fractal network of relationships or connectivities, but the embedding space is purely a mathematical way of characterising the 3-dimensionality of the network. This is illustrated in Fig. 1. This is not an ether model; that notion involved a duality in that both the ether and the space in which it was embedded were both real. Now the key point is that how we embed the network in the embedding space is very arbitrary: we could equally well rotate the embedding or use an embedding that has the network translating. These general requirements then dictate the minimal dynamics for the actual network, at a phenomenological level. To see this we assume at a coarse grained level that the dynamical patterns within the network may be described by a velocity field $\mathbf{v}(\mathbf{r}, t)$, where $\mathbf{r}$ is the location of a small region in the network according to some arbitrary embedding. For simplicity we assume here that the global topology of the network is not significant for the local dynamics, and so we embed in an E^3, although a generalisation to an embedding in S^3 is straightforward. The minimal dynamics then follows from the above by writing down the lowest order zero-rank tensors, with dimension $1/t^2$, that are invariant under translation and rotation, giving*

$$\nabla \cdot \left(\frac{\partial \mathbf{v}}{\partial t} + (\mathbf{v} \cdot \nabla) \, \mathbf{v} \right) +$$
$$+ \frac{\alpha}{8} \, (\mathrm{tr}\, D)^2 + \frac{\beta}{8} \, \mathrm{tr}\, (D^2) = -4\pi G\rho \,, \quad (1)$$

where ρ is the effective matter density, and where

$$D_{ij} = \frac{1}{2} \left(\frac{\partial v_i}{\partial x_j} + \frac{\partial v_j}{\partial x_i} \right). \quad (2)$$

In Process Physics quantum matter are topological defects in the network, but here it is sufficient to give a simple description in terms of an effective density, but which can also model the "dark energy" effect and electromagnetic energy effects, which will be discussed elsewhere. We see

---

*Note that then, on dimensional grounds, the spatial dynamics cannot involve the speed of light c, except on the RHS where relativistic effects come into play if the speed of matter relative to the local space becomes large, see [1]. This has significant implications for the nature and speed of so-called "gravitational" waves.
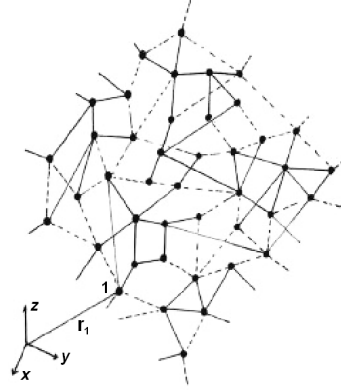

Fig. 1: This is an iconic graphical representation of how a dynamical network has its inherent approximate 3-dimensionality displayed by an embedding in a mathematical space such as an E^3 or an S^3. This space is not real; it is purely a mathematical artifact. Nevertheless this embeddability helps determine the minimal dynamics for the network, as in (1). At a deeper level the network is a quantum foam system [1]. The dynamical space is not an ether model, as the embedding space does not exist.

that there are only four possible terms, and so we need at most three possible constants to describe the dynamics of space: G, α and β. G will turn out to be Newton's gravitational constant, and describes the rate of non-conservative flow of space into matter. To determine the values of α and β we must, at this stage, turn to experimental data.

However most experimental data involving the dynamics of space is observed by detecting the so-called gravitational acceleration of matter, although increasingly light bending is giving new information. Now the acceleration $\mathbf{a}$ of the dynamical patterns in space is given by the Euler or convective expression

$$\mathbf{a}(\mathbf{r}, t) \equiv \lim_{\Delta t \to 0} \frac{\mathbf{v}(\mathbf{r} + \mathbf{v}(\mathbf{r}, t)\, \Delta t, t + \Delta t) - \mathbf{v}(\mathbf{r}, t)}{\Delta t} =$$
$$= \frac{\partial \mathbf{v}}{\partial t} + (\mathbf{v} \cdot \nabla) \mathbf{v} \quad (3)$$

and this appears in one of the terms in (1). As shown in [12] and discussed later herein the acceleration $\mathbf{g}$ of quantum matter is identical to this acceleration, apart from vorticity and relativistic effects, and so the gravitational acceleration of matter is also given by (3).

Outside of a spherically symmetric distribution of matter, of total mass M, we find that one solution of (1) is the velocity in-flow field given by†

$$\mathbf{v}(\mathbf{r}) = -\hat{\mathbf{r}} \sqrt{\frac{2GM(1 + \frac{\alpha}{2} + \ldots)}{r}} \quad (4)$$

but only when $\beta = -\alpha$, for only then is the acceleration of matter, from (3), induced by this in-flow of the form

$$\mathbf{g}(\mathbf{r}) = -\hat{\mathbf{r}} \frac{GM(1 + \frac{\alpha}{2} + \ldots)}{r^2} \quad (5)$$

which is Newton's Inverse Square Law of 1687, but with an effective mass that is different from the actual mass M.

---

†To see that the flow is inward requires the modelling of the matter by essentially point-like particles.

So Newton's law requires $\beta = -\alpha$ in (1) although at present a deeper explanation has not been found. But we also see modifications coming from the α-dependent terms.

A major recent discovery [13–16] has been that experimental data from the bore hole g anomaly has revealed that α is the fine structure constant, to within experimental errors: $\alpha = e^2/\hbar c \approx 1/137.04$. This anomaly is that g does not decrease as rapidly as predicted by Newtonian gravity or GR as we descend down a bore hole. The dynamics in (1) and (3) gives the anomaly to be

$$\Delta g = 2\pi \alpha G \rho d \qquad (6)$$

where d is the depth and ρ is the density, being that of glacial ice in the case of the Greenland Ice Shelf experiments, or that of rock in the Nevada test site experiment. Clearly (6) permits the value of α to be determined from the data, giving $\alpha = 1/(137.9 \pm 5)$ from the Greenland Ice Shelf data and, independently, $\alpha = 1/(136.8 \pm 3)$ from the Nevada test site data [16].

In general because (1) is a scalar equation it is only applicable for vorticity-free flows $\nabla \times \mathbf{v} = \mathbf{0}$, for then we can write $\mathbf{v} = \nabla u$, and then (1) can always be solved to determine the time evolution of $u(\mathbf{r}, t)$ given an initial form at some time t_0.*

The α-dependent term in (1) (with now $\beta = -\alpha$) and the matter acceleration effect, now also given by (3), permits (1) to be written in the form

$$\nabla \cdot \mathbf{g} = -4\pi G \rho - 4\pi G \rho_{DM}, \qquad (7)$$

where

$$\rho_{DM}(\mathbf{r}, t) \equiv \frac{\alpha}{32\pi G}\left((\mathrm{tr}\, D)^2 - \mathrm{tr}(D^2)\right), \qquad (8)$$

where ρ_{DM} is an effective matter density that would be required to mimic the α-dependent spatial self-interaction dynamics. Then (7) is the differential form for Newton's law of gravity but with an additional non-matter effective matter density. It has been shown [13–16] that this effect explains the so-called "dark matter" effect in spiral galaxies. As shown elsewhere it also explains, when used with the generalised Maxwell's equations, the gravitational lensing of light by this "dark matter" effect.

An intriguing aspect to the spatial dynamics is that it is non-local. Historically this was first noticed by Newton who called it action-at-a-distance. To see this we can write (1) as an integro-differential equation

$$\frac{\partial \mathbf{v}}{\partial t} = -\nabla\left(\frac{\mathbf{v}^2}{2}\right) + $$
$$+ G\int d^3 r' \frac{\rho_{DM}(\mathbf{r}', t) + \rho(\mathbf{r}', t)}{|\mathbf{r} - \mathbf{r}'|^3}(\mathbf{r} - \mathbf{r}'). \qquad (9)$$

This shows a high degree of non-locality and non-linearity,

and in particular that the behaviour of both ρ_{DM} and ρ manifest at a distance irrespective of the dynamics of the intervening space. This non-local behaviour is analogous to that in quantum systems. The non-local dynamics associated with the α dynamics has been tested in various situations, as discussed herein, and so its validity is well established. This implies that the minimal spatial dynamics in (1) involves non-local connectivities.

We term the dynamics of space in (1) as a "flowing space". This term can cause confusion because in normal language a "flow" implies movement of something relative to a background space; but here there is no existent background space, only the non-existent mathematical embedding space. So here the "flow" refers to internal relative motion, that one parcel of space has a motion relative to a nearby parcel of space. Hence the absolute velocities in (1) have no observable meaning; that despite appearances it is only the relative velocities that have any dynamical significance. Of course it is this requirement that determined the form of (1), and as implemented via the embedding space technique.

However there is an additional role for the embedding space, namely as a coordinate system used by a set of cooperating observers. But again while this is useful for their discourse it is not real; it is not part of reality.

3 Black holes

Eqn. (1) has "black hole" solutions. The generic term "black hole" is used because they have a compact closed event horizon where the in-flow speed relative to the horizon equals the speed of light, but in other respects they differ from the putative black holes of General Relativity[†] — in particular their gravitational acceleration is not inverse square law. The evidence is that it is these new "black holes" from (1) that have been detected. There are two categories: (i) an in-flow singularity induced by the flow into a matter system, such as, herein, a spherical galaxy or globular cluster. These black holes are termed minimal black holes, as their effective mass is minimal, (ii) primordial naked black holes which then attract matter. These result in spiral galaxies, and the effective mass of the black hole is larger than required merely by the matter induced in-flow. These are therefore termed non-minimal black holes. These explain the rapid formation of structure in the early universe, as the gravitational acceleration is approximately $1/r$ rather than $1/r^2$. This is the feature that also explains the so-called "dark matter" effect in spiral galaxies. Here we consider only the minimal black holes.

Consider the case where we have a spherically symmetric matter distribution at rest, on average with respect to distant space, and that the in-flow is time-independent and radially symmetric. Then (1) is best analysed via (9), which can now

---

*Eqn.(1) also has Hubble expanding space solutions.

[†]It is probably the case that GR has no such solutions — they do not obey the boundary conditions at the singularity, see Crothers [17].

Galaxy	Type	$M_{BH}(+,-)$	M	Ref
M87	E0	$3.4\,(1.0, 1.0){\times}10^9$	$6.2{\pm}1.7{\times}10^{11}$	1
NGC4649	E1	$2.0\,(0.4, 0.6){\times}10^9$	$8.4{\pm}2.2{\times}10^{11}$	2
M84	E1	$1.0\,(2.0, 0.6){\times}10^9$	$5.0{\pm}1.4{\times}10^{11}$	3
M32	E2	$2.5\,(0.5, 0.5){\times}10^6$	$9.6{\pm}2.6{\times}10^{8}$	4
NGC4697	E4	$1.7\,(0.2, 0.1){\times}10^8$	$2.0{\pm}0.5{\times}10^{11}$	2
IC1459	E3	$1.5\,(1.0, 1.0){\times}10^9$	$6.6{\pm}1.8{\times}10^{11}$	5
NGC3608	E2	$1.9\,(1.0, 0.6){\times}10^8$	$9.9{\pm}2.7{\times}10^{10}$	2
NGC4291	E2	$3.1\,(0.8, 2.3){\times}10^8$	$9.5{\pm}2.5{\times}10^{10}$	2
NGC3377	E5	$1.0\,(0.9, 0.1){\times}10^8$	$7.8{\pm}2.1{\times}10^{10}$	2
NGC4473	E5	$1.1\,(0.4, 0.8){\times}10^8$	$6.9{\pm}1.9{\times}10^{10}$	2
Cygnus A	E	$2.9\,(0.7, 0.7){\times}10^9$	$1.6{\pm}1.1{\times}10^{12}$	6
NGC4261	E2	$5.2\,(1.0, 1.1){\times}10^8$	$4.5{\pm}1.2{\times}10^{11}$	7
NGC4564	E3	$5.6\,(0.3, 0.8){\times}10^7$	$5.4{\pm}1.5{\times}10^{10}$	2
NGC4742	E4	$1.4\,(0.4, 0.5){\times}10^7$	$1.1{\pm}0.3{\times}10^{10}$	8
NGC3379	E1	$1.0\,(0.6, 0.5){\times}10^8$	$8.5{\pm}2.3{\times}10^{10}$	9
NGC5845	E3	$2.4\,(0.4, 1.4){\times}10^8$	$1.9{\pm}0.5{\times}10^{10}$	2
NGC6251	E2	$6.1\,(2.0, 2.1){\times}10^8$	$6.7{\pm}1.8{\times}10^{11}$	10
Globular cluster		$M_{BH}(+,-)$	M	Ref
M15		$1.7\,(2.7, 1.7){\times}10^3$	$4.9\ {\times}10^5$	10
G1		$1.8\,(1.4, 0.8){\times}10^4$	$1.35{\pm}0.5{\times}10^7$	11

Table 1. Black Hole masses and host masses for various spherical galaxies and globular clusters. References: (1) Macchetto *et al.* 1997; (2) Gebhardt *et al.* 2003; (3) average of Bower *et al.* 1998; Maciejewski & Binney 2001; (4) Verolme *et al.* 2002; (5) average of Verdoes Klein *et al.* 2000 and Cappellari *et al.* 2002; (6) Tadhunter *et al.* 2003; (7) Ferrarese *et al.* 1996; (8) Tremaine *et al.* 2002; (9) Gebhardt *et al.* 2000; (10) Ferrarese & Ford 1999; (11) Gerssen *et al.* 2002; (12) Gebhardt *et al.* 2002. Least squares best fit of this data to $\mathrm{Log}[M_{BH}] = \mathrm{Log}[\frac{\alpha}{2}] + x\mathrm{Log}[M]$ gives $\alpha = 1/137.4$ and $x = 0.974$. Data and best fit are shown in Fig. 2. Table adapted from Table 1 of [18].

be written in the form

$$|\mathbf{v}(\mathbf{r})|^2 = 2G \int d^3 r' \, \frac{\rho_{DM}(\mathbf{r}') + \rho(\mathbf{r}')}{|\mathbf{r} - \mathbf{r}'|} \qquad (10)$$

in which the angle integrations may be done to yield

$$v(r)^2 = \frac{8\pi G}{r} \int_0^r s^2 \left[\rho_{DM}(s) + \rho(s) \right] ds + $$
$$+ 8\pi G \int_r^\infty s \left[\rho_{DM}(s) + \rho(s) \right] ds, \qquad (11)$$

where with $v' = dv(r)/dr$,*

$$\rho_{DM}(r) = \frac{\alpha}{8\pi G} \left(\frac{v^2}{2r^2} + \frac{vv'}{r} \right). \qquad (12)$$

To obtain the induced in-flow singularity to $\mathrm{O}(\alpha)$ we substitute the non-α term in (11) into (12) giving the effective matter density that mimics the spatial self-interaction of

*Previous papers had a typo error in this expression. Thanks to Andree Blotz for noting that.

the in-flow,

$$\rho_{DM}(r) = \frac{\alpha}{2r^2} \int_r^\infty s\,\rho(s)\,ds + \mathrm{O}(\alpha^2). \qquad (13)$$

We see that the effective "dark matter" effect is concentrated near the centre, and we find that the total effective "dark matter" mass is

$$M_{DM} \equiv 4\pi \int_0^\infty r^2 \rho_{DM}(r)\,dr =$$
$$= \frac{4\pi\alpha}{2} \int_0^\infty r^2 \rho(r)\,dr + \mathrm{O}(\alpha^2) = \frac{\alpha}{2}\,M + \mathrm{O}(\alpha^2). \qquad (14)$$

This result applies to any spherically symmetric matter distribution, and is the origin of the α terms in (4) and (5). It is thus responsible for the bore hole anomaly expression in (6). This means that the bore hole anomaly is indicative of an in-flow singularity at the centre of the Earth. This contributes some 0.4% of the effective mass of the Earth, as defined by Newtonian gravity. However in star systems this minimal black hole effect is more apparent, and we label M_{DM} as M_{BH}. Table 1 shows the effective "black hole" masses attributed to various spherically symmetric star systems based upon observations and analysis of the motion of gases and stars in these systems. The prediction of the dynamics of space is that these masses should obey (14). The data from Table 1 is plotted in Fig. 2, and we see the high precision to which (14) is indeed satisfied, and over some 6 orders of magnitude, giving from this data that $\alpha \approx 1/137.4$.

The application of the spatial dynamics to spiral galaxies is discussed in [13–16] where it is shown that a complete non-matter explanation of the spiral galaxy rotation speed anomaly is given: there is no such stuff as "dark matter" — it is an α determined spatial self-interaction effect. Essentially even in the non-relativistic regime the Newtonian theory of gravity, with its "universal" Inverse Square Law, is deeply flawed.

4 Spacetime

The curved spacetime explanation for gravity is widely known. Here an explanation for its putative success is given, for there is a natural definition of a spacetime that arises from (1), but that is purely a mathematical construction with no ontological status — it is a mere mathematical artifact.

First consider the generalised Schrödinger [12]

$$i\hbar \frac{\partial \psi(\mathbf{r}, t)}{\partial t} = H(t)\,\psi(\mathbf{r}, t), \qquad (15)$$

where the free-fall hamiltonian is

$$H(t) = -i\hbar \left(\mathbf{v} \cdot \nabla + \frac{1}{2}\,\nabla \cdot \mathbf{v} \right) - \frac{\hbar^2}{2m}\,\nabla^2 \qquad (16)$$

As discussed in [12] this is uniquely defined by the requirement that the wave function be attached to the dynam-
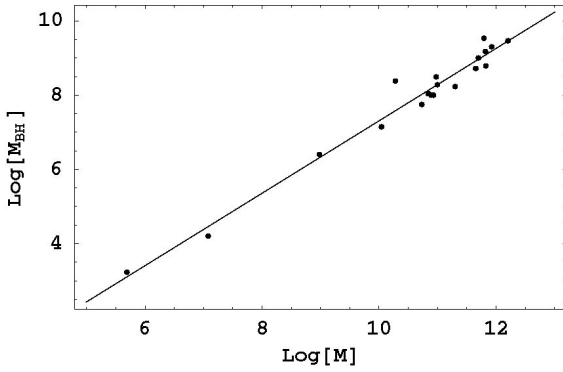
Fig. 2: Log-Log plot of black hole masses M_{BH} and host galaxy or globular cluster masses M (in solar units) from Table 1. Straight line is least squares best fit to $\text{Log}[M_{BH}] = \text{Log}[\frac{\alpha}{2}] + x\text{Log}[M]$, giving $\alpha = 1/137.4$ and $x = 0.974$. The borehole g-anomaly gives $\alpha = 1/(137.9 \pm 5)$ from the Greenland Ice Shelf data and $\alpha = 1/(136.8 \pm 3)$ from the Nevada test site data [16].

ical space, and not to the embedding space, which is a mere mathematical artifact. We can compute the acceleration of a localised wave packet according to

$$\mathbf{g} \equiv \frac{d^2}{dt^2} \left(\psi(t), \mathbf{r}\,\psi(t) \right) = $$
$$= \frac{\partial \mathbf{v}}{\partial t} + (\mathbf{v} \cdot \nabla)\mathbf{v} + (\nabla \times \mathbf{v}) \times \mathbf{v}_R \qquad (17)$$

where $\mathbf{v}_R = \mathbf{v}_0 - \mathbf{v}$ is the velocity of the wave packet relative to the local space, as $\mathbf{v}_0$ is the velocity relative to the embedding space. Apart from the vorticity term which causes rotation of the wave packet* we see, as promised, that this matter acceleration is equal to that of the space itself, as in (3). This is the first derivation of the phenomenon of gravity from a deeper theory: gravity is a quantum effect — namely the refraction of quantum waves by the internal differential motion of the substructure patterns to space itself. Note that the equivalence principle has now been explained, as this "gravitational" acceleration is independent of the mass m of the quantum system.

An analogous generalisation of the Dirac equation is also necessary giving the coupling of the spinor to the actual dynamical space, and again not to the embedding space as has been the case up until now,

$$i\hbar \frac{\partial \psi}{\partial t} = -i\hbar \left(c\vec{\alpha} \cdot \nabla + \mathbf{v} \cdot \nabla + \frac{1}{2} \nabla \cdot \mathbf{v} \right) \psi + \beta mc^2 \psi \quad (18)$$

where $\vec{\alpha}$ and β are the usual Dirac matrices. Repeating the analysis in (17) for the space-induced acceleration we obtain[†]

$$\mathbf{g} = \frac{\partial \mathbf{v}}{\partial t} + (\mathbf{v} \cdot \nabla)\mathbf{v} + (\nabla \times \mathbf{v}) \times \mathbf{v}_R - \frac{\mathbf{v}_R}{1 - \frac{\mathbf{v}_R^2}{c^2}} \frac{1}{2} \frac{d}{dt}\left(\frac{\mathbf{v}_R^2}{c^2}\right) \quad (19)$$

---
*This is the Lense-Thirring effect, and such vorticity is being detected by the Gravity Probe B satellite gyroscope experiment [33].

[†]Some details are incomplete in this analysis.

which generalises (17) by having a term which limits the speed of the wave packet relative to space to be $< c$. This equation specifies the trajectory of a spinor wave packet in the dynamical space.

We shall now show how this leads to both the spacetime mathematical construct and that the geodesic for matter worldlines in that spacetime is equivalent to trajectories from (19). First we note that (19) may be obtained by extremising the time-dilated elapsed time

$$\tau\left[\mathbf{r}_0\right] = \int dt \left(1 - \frac{\mathbf{v}_R^2}{c^2} \right)^{1/2} \qquad (20)$$

with respect to the particle trajectory $\mathbf{r}_0(t)$ [1]. This happens because of the Fermat least-time effect for waves: only along the minimal time trajectory do the quantum waves remain in phase under small variations of the path. This again emphasises that gravity is a quantum effect. We now introduce a spacetime mathematical construct according to the metric

$$ds^2 = dt^2 - \frac{\left(d\mathbf{r} - \mathbf{v}(\mathbf{r}, t)\,dt\right)^2}{c^2} = g_{\mu\nu}dx^\mu dx^\nu. \qquad (21)$$

Then according to this metric the elapsed time in (20) is

$$\tau = \int dt \sqrt{g_{\mu\nu} \frac{dx^\mu}{dt} \frac{dx^\nu}{dt}}, \qquad (22)$$

and the minimisation of (22) leads to the geodesics of the spacetime, which are thus equivalent to the trajectories from (20), namely (19). Hence by coupling the Dirac spinor dynamics to the space dynamics we derive the geodesic formalism of General Relativity as a quantum effect, but without reference to the Hilbert-Einstein equations for the induced metric. Indeed in general the metric of this induced spacetime will not satisfy these equations as the dynamical space involves the α-dependent dynamics, and α is missing from GR. So why did GR appear to succeed in a number of key tests where the Schwarzschild metric was used? The answer is provided by identifying the induced spacetime metric corresponding to the in-flow in (4) outside of a spherical matter system, such as the Earth. Then (21) becomes

$$ds^2 = dt^2 - \frac{1}{c^2}\left(dr + \sqrt{\frac{2GM(1+\frac{\alpha}{2}+\dots)}{r}}\,dt \right)^2 - $$
$$- \frac{1}{c^2}\, r^2\left(d\theta^2 + \sin^2\theta\, d\phi^2 \right). \qquad (23)$$

Making the change of variables[‡] $t \to t'$ and $\mathbf{r} \to \mathbf{r}' = \mathbf{r}$ with

$$t' = t - \frac{2}{c}\sqrt{\frac{2GM(1+\frac{\alpha}{2}+\dots)\,r}{c^2}} + $$
$$+ \frac{4GM(1+\frac{\alpha}{2}+\dots)}{c^3}\tanh^{-1}\sqrt{\frac{2GM(1+\frac{\alpha}{2}+\dots)}{c^2 r}} \qquad (24)$$

[‡]No unique choice of variables is required. This choice simply leads to a well-known form for the metric.

this becomes (and now dropping the prime notation)

$$ds^2 = \left(1 - \frac{2GM(1 + \frac{\alpha}{2} + \dots)}{c^2 r}\right) dt^2 -$$
$$- \frac{1}{c^2} r^2 (d\theta^2 + \sin^2\theta \, d\phi^2) - \frac{dr^2}{c^2 \left(1 - \frac{2GM(1 + \frac{\alpha}{2} + \dots)}{c^2 r}\right)} \quad (25)$$

which is one form of the the Schwarzschild metric but with the α-dynamics induced effective mass shift. Of course this is only valid outside of the spherical matter distribution, as that is the proviso also on (4). As well the above particular change of coordinates also introduces spurious singularities at the event horizon*, but other choices do not do this. Hence in the case of the Schwarzschild metric the dynamics missing from both the Newtonian theory of gravity and General Relativity is merely hidden in a mass redefinition, and so didn't affect the various standard tests of GR, or even of Newtonian gravity. Note that as well we see that the Schwarzschild metric is none other than Newtonian gravity in disguise, except for the mass shift. While we have now explained why the GR formalism appeared to work, it is also clear that this formalism hides the manifest dynamics of the dynamical space, and which has also been directly detected in gas-mode interferometer and coaxial-cable experiments.

One of the putative key tests of the GR formalism was the gravitational bending of light. This also immediately follows from the new space dynamics once we also generalise the Maxwell equations so that the electric and magnetic fields are excitations of the dynamical space. The dynamics of the electric and magnetic fields must then have the form, in 'empty' space,

$$\nabla \times \mathbf{E} = -\mu \left(\frac{\partial \mathbf{H}}{\partial t} + \mathbf{v} \cdot \nabla \mathbf{H}\right)$$
$$\nabla \times \mathbf{H} = \epsilon \left(\frac{\partial \mathbf{E}}{\partial t} + \mathbf{v} \cdot \nabla \mathbf{E}\right) \quad (26)$$
$$\nabla \cdot \mathbf{H} = \mathbf{0}, \qquad \nabla \cdot \mathbf{E} = \mathbf{0}$$

which was first suggested by Hertz in 1890 [34]. As discussed elsewhere the speed of EM radiation is now $c = 1/\sqrt{\mu\epsilon}$ with respect to the space, and in general not with respect to the observer if the observer is moving through space, as experiment has indicated again and again. In particular the in-flow in (4) causes a refraction effect of light passing close to the Sun, with the angle of deflection given by

$$\delta = 2\frac{v^2}{c^2} = \frac{4GM(1 + \frac{\alpha}{2} + \dots)}{c^2 d} \quad (27)$$

where v is the in-flow speed at the surface of the Sun, and d is the impact parameter, essentially the radius of the

Sun. Hence the observed deflection of 8.4×10^{-6} radians is actually a measure of the in-flow speed at the Sun's surface, and that gives $v = 615$ km/s. At the Earth distance the Sun induced spatial in-flow speed is 42 km/s, and this has been extracted from the 1925/26 gas-mode interferometer Miller data [1, 3]. These radial in-flows are to be vectorially summed to the galactic flow of some 400 km/s, but since that flow is much more uniform it does not affect the light bending by the Sun in-flow component†. Hence the deflection of light by the Sun is a way of directly measuring the in-flow speed at the Sun's surface, and has nothing to do with "real" curved spacetime. These generalised Maxwell equations also predict gravitational lensing produced by the large in-flows associated with new "black holes" in galaxies. So again this effect permits the direct observation of the these black hole effects with their non-inverse square law accelerations.

5 Conclusions

We have shown how minimal assumptions about the internal dynamics of space, namely how embeddability in a mathematical space such as an E^3 or an S^3, expressing its inherent 3-dimensionality, leads to various predictions ranging from the anisotropy of the speed of light, as expressed in the required generalisation of Maxwell' s equations, and which has been repeatedly observed since the Michelson-Morley experiment [5] of 1887, to the derivation of the phenomenon of gravity that follows after we generalise the Schrödinger and Dirac equations. This shows that the gravitational acceleration of matter is a quantum effect: it follows from the refraction of quantum waves in the inhomogeneities and time-dependencies of the flowing dynamical space. In particular the analysis shows that the acceleration of quantum matter is identical to the convective acceleration of the structured space itself. This is a non-trivial result. As well in the case of the Dirac equation we derive the spacetime formalism as well as the geodesic description of matter trajectories, but in doing so reveal that the spacetime is merely a mathematical construct. We note that the relativistic features of the Dirac equation are consistent with the absolute motion of the wave function in the dynamical 3-space. This emphasis yet again that Special Relativity does not require the isotropy of the speed of light, as is often incorrectly assumed.

Here we have further extended the observational evidence that it is the fine structure constant that determines the strength of the spatial self-interaction in this new physics by including data from black hole masses in 19 spherical star systems. Elsewhere we have already shown that the new space dynamics explains also the spiral galaxy rotation velocity anomaly; that it is not caused by a new form of matter, that the notion of "dark matter" is just a failure of

---

*The event horizon of (25) is at a different radius from the actual event horizon of the black hole solutions that arise from (1).

†The vector superposition effect for spatial flows is only approximate, and is discussed in more detail in [35]. The solar system has a galactic velocity of some 420±30 km/s in the direction RA=5.2 hr, Dec=−67°.

Newtonian gravity and GR. We have also shown that the space dynamics is non-local, a feature that Newton called action-at-a-distance. This is now extended to include the effects of the spatial self-interaction. The numerous confirmations of that dynamics, summarised herein, demonstrate the validity of this non-local physics. Of course since Newton we have become more familiar with non-local effects in the quantum theory. The new space dynamics shows that non-local effects are more general than just subtle effects in the quantum theory, for in the space dynamics this non-local dynamics is responsible for the supermassive black holes in galaxies. This non-local dynamics is responsible for two other effects: (i) that the dynamics of space within an event horizon, say enclosing a black hole in-flow singularity affects the space outside of the horizon, even though EM radiation and matter cannot propagate out through the event horizon, as there the in-flow speed exceeds the speed of light. So in this new physics we have the escape of information from within the event horizon, and (ii) that the universe overall is more highly connected than previously thought. This may explain why the universe is more uniform than expected on the basis of interactions limited by the speed of light, i. e. we probably have a solution to the cosmological horizon problem.

Elsewhere [1] we have argued that the dynamical space has the form of a quantum foam and so non-local quantum effects are to be expected. So it might be argued that the successful prediction of the masses of these black hole masses, and their dependence on the fine structure constant, is indicative of a grand unification of space and the quantum theory. This unification is not coming from the quantisation of gravity, but rather from a deeper modelling of reality as an information-theoretic system with emergent quantum-space and quantum matter.

References

1. Cahill R. T. Process Physics: From information theory to quantum space and matter. Nova Science, N.Y., 2005.

2. Cahill R. T. and Kitto K. Michelson-Morley experiments revisited. *Apeiron*, 2003, v. 10(2), 104–117.

3. Cahill R. T. Absolute motion and gravitational effects. *Apeiron*, 2004, v. 11(1), 53–111.

4. Cahill R. T. The Michelson and Morley 1887 experiment and the discovery of absolute motion. *Progress in Physics*, 2005, v. 3, 25–29.

5. Michelson A. A. and Morley E. W. *Philos. Mag.*, S. 5, 1887, v. 24, No. 151, 449–463.

6. Miller D. C. *Rev. Mod. Phys.*, 1933, v. 5, 203–242.

7. Illingworth K. K. *Phys. Rev.*, 1927, v. 3, 692–696.

8. Joos G. *Ann. der Physik*, 1930, Bd 7, 385.

9. Jaseja T. S. *et al. Phys. Rev.*, v. A133, 1964, 1221.

10. Torr D. G. and Kolen P. *Precision Measurements and Fundamental Constants*, ed. by Taylor B. N. and Phillips W. D. Nat. Bur. Stand. (U.S.), Spec. Pub., 1984, v. 617, 675.

11. Cahill R. T. The Roland DeWitte 1991 experiment. *Progress in Physics*, 2006, v. 3, 60–65.

12. Cahill R. T. Dynamical fractal 3-space and the generalised Schrödinger equation: Equivalence Principle and vorticity effects. *Progress in Physics*, 2006, v. 1, 27–34.

13. Cahill R. T. Gravity, "dark matter" and the fine structure constant. *Apeiron*, 2005, v. 12(2), 144–177.

14. Cahill R. T. "Dark matter" as a quantum foam in-flow effect. In: *Trends in Dark Matter Research*, ed. J. Val Blain, Nova Science, N.Y., 2005, 96–140.

15. Cahill R. T. Black holes in elliptical and spiral galaxies and in globular clusters. *Progress in Physics*, 2005, v. 3, 51–56.

16. Cahill R. T. 3-Space in-flow theory of gravity: Boreholes, blackholes and the fine structure constant. *Progress in Physics*, 2006, v. 2, 9–16.

17. Crothers S. J. A brief history of black holes. *Progress in Physics*, 2006, v. 2, 54–57.

18. Marconi A. and Hunt L. K. *ApJ*, 2003, v. 589, L21–L24, part 2.

19. Macchetto F. *et al. ApJ*, 1997, v. 489, 579.

20. Gebhardt K. *et al. ApJ*, 2003, v. 583, 92.

21. Bower G. A. *et al. ApJ*, 2001, v. 550, 75.

22. Maciejewski F. and Binney J. *MNRAS*, 2001, v. 323, 831.

23. Verolme E. K. *et al. MNRAS*, 2002, v. 335, 517.

24. Verdoes Klein G. A. *et al. AJ*, 2000, v. 120, 1221.

25. Cappellari M. *et al. ApJ*, 2002, v. 578, 787.

26. Tadhunter C. *et al. MNRAS*, 2003, v. 342, 861.

27. Ferrarese L. *et al. ApJ*, 1996, v. 470, 444.

28. Tremaine S. *et al. ApJ*, 2002, v. 574, 740.

29. Gebhardt K. *et al. ApJ*, 2000, v. 539, L13.

30. Ferrarese L. and Ford H. C. *ApJ*, 1999, v. 515, 583.

31. Gerssen J. *et al. Astron. J.*, 2002, v. 124, 3270–3288; Addendum 2003, v. 125, 376.

32. Gebhardt K. *et al. ApJ.*, 2002, v. 578, L41.

33. Cahill R. T. Novel Gravity Probe B frame-dragging effect. *Progress in Physics*, 2005, v. 3, 30–33.

34. Hertz H. On the fundamental equations of electro-magnetics for bodies in motion. *Wiedemann's Ann.*, 1890, v. 41, 369; Electric waves. Collection of scientific papers. Dover Publ., N.Y., 1962.

35. Cahill R. T. The dynamical velocity superposition effect in the quantum-foam in-flow theory of gravity. arXiv: physics/0407133.

Preferred Spatial Directions in the Universe: a General Relativity Approach

Larissa Borissova

E-mail: lborissova@yahoo.com

Herein is constructed, using General Relativity, the space metric along the Earth's trajectory in the Galaxy, where the Earth traces outs a complicated spiral in its orbital motion around the Sun and its concomitant motion with the solar system around the centre of the Galaxy. It is deduced herein that this space is inhomogeneous and anisotropic. The observable properties of the space, characterizing its gravitation, rotation, deformation, and curvature, are obtained. The theory predicts that the observable velocity of light is anisotropic, due to the anisotropy and inhomogeneity of space caused by the presence of gravitation and the space rotation, despite the world-invariance of the velocity of light remaining unchanged. It is calculated that two pairs of synchronised clocks should record a different speed of light for light beams travelling towards the Sun and orthogonal to this direction, of about $4 \times 10^{-4} c$ (i. e. 120 km/sec, 0.04% of the measured velocity of light c). This effect should have oscillations with a 12-hour period (due to the daily rotation of the Earth) and 6 month period (due to the motion of the Earth around the Sun). The best equipment for detecting the effect is that being used by R. T. Cahill (Flinders University, Australia) in his current experiments measuring the velocity of light in an RF coaxial-cable equipped with a pair of high precision synchronized Rb atomic clocks.

> *The geniality of geometry, its applicability to our real world, can be verified by observation or experiment, not logical deduction.*
>
> N. A. Kozyrev

1 Introduction

We construct herein, by General Relativity, a mathematical model for a space body moving around another body (the centre of attraction), both moving in an observer's reference space. The Earth rotates around the Sun, and orbits in common with it around the centre of the Galaxy; the Sun rotates around the centre of the Galaxy and orbits in common with the Galaxy around the centre of the Local Group of galaxies; etc. As a result there are preferred directions determined by orbital motions, so the real Universe is *anisotropic* (inequivalence of directions). Because there are billions of centres of gravitational attraction, the Universe is also *inhomogeneous* (inequivalence of points). Hence, for the real Universe, we cannot ignore the anisotropy of space and gravitation.

On the other hand, most cosmologists use the concept of a homogeneous isotropic Universe wherein all points and directions are equivalent. Such a model can be built only by an observer who, observing matter in the Universe from afar, doesn't see such details as stars and galaxies. Such conceptions lead to a vicious circle — most cosmologists are sure that our Universe is a homogeneous isotropic ball expanding from an initial point-like state (singularity); they ignore the anisotropy of space and gravitation in such models.

Relativistic models of a homogeneous isotropic universe (which include the Friedmann solutions) are only a few partial solutions to Einstein's equations. Besides, as shown during the last decade, many popular cosmological metrics (including the Friedmann solutions) are inadmissible, because the difference between the radial coordinate and the proper radius isn't taken into account there (see [1, 2] and References therein).

And so forth, we shall show that the homogeneous isotropic metric spaces contain no rotation and gravitation, and that they can only undergo deformation: no stars, galaxies or other space bodies exist in such a universe*. Why do the scientists use such solutions? The answer is clearly evident: such solutions are simple, and thereby easier to study.

We shall consider another problem statement, the case of an inhomogeneous anisotropic universe as first set up in 1944 by A. Zelmanov [4, 5]. Such a consideration is applicable to any local part of the Universe. We show in this paper that along such a preferred direction, caused by the orbital motion of a space body, an *anisotropy of the observable velocity of light* can be deduced, despite the world-invariance of the velocity of light remaining unchanged†. Using this result as a basis, we will show in a subsequent paper (now in preparation) that not only is the anisotropy of the velocity of light expected along a satellite's trajectory, but even its motion is permitted only in a non-empty space filled by a distribution of matter and a λ-field (both derived from the right side of Einstein's equations). This conclusion leads to

---

*This situation is similar to the standard solution of the gravitational wave problem, which considers them as space deformation waves in a space free of rotation and gravitation [3].

†The observable velocity of light is different to the world-invariant velocity of light if considered by means of the mathematical apparatus of physically observed quantities in General Relativity — so-called chronometric invariants [4, 5].

the possibility of a new source of energy working in a rotating (non-holonomic) space, and has a direct link to the conclusion that stars produce energy due to the background space non-holonomy (as recently derived by means of General Relativity in [6, 7]).

2 Observed characteristics of space in the Earth's motion in the Galaxy

How do the Earth and the planets move in space? The Earth rotates around its own axis at 465 m/sec at the equator, with an approximately 24-hour period, and moves at 30 km/sec around the Sun with a 365.25-day period (astronomical year). The Sun, in common with the planets, moves at 250 km/sec around the centre of the Galaxy with an ~ 200 million year period. And so the Earth's orbit traces a cylinder, the axis of which is the galactic trajectory of the Sun. As a result, the local space of the Earth draws a very stretched spiral, spanned over the "galactic" cylinder of the Earth's orbit. Each planet traces a similar spiral in the Galaxy.

We aim to build a metric for the space along the Earth's transit in the Galaxy. We do this in two steps. First, the metric along the Earth's transit in the gravitational field of the Sun. Second, using the Lorentz transformation to change to the reference frame moving (with respect to the first frame) along the axis coinciding with the direction in which the Earth moves in the Galaxy.

We use a reference frame which rotates and moves forwards in a weak gravitational field. We therefore use cylindrical coordinates. Then the metric along the Earth's transit in the gravitational field of the Sun has the form*

$$ds^2 = \left(1 - \frac{2GM}{c^2 r} - \frac{\omega^2 r^2}{c^2}\right) c^2 dt^2 - \frac{2\omega r^2}{c} c\, dt\, d\varphi - \left(1 + \frac{2GM}{c^2 r}\right) dr^2 - r^2 d\varphi^2 - dz^2, \tag{1}$$

where ω is the angular velocity of the Earth's rotation around the Sun: $\omega = \frac{v_{orb}}{r} = 2 \times 10^{-7}\ \text{sec}^{-1}$.

We now change to a reference frame that rotates in a weak gravitational field and moves uniformly with a velocity v (associated with the motion of the Sun in the Galaxy) along the z-axis. We apply the Lorentz transformations

$$\tilde{z} = \frac{z + \mathrm{v}t}{\sqrt{1 - \frac{\mathrm{v}^2}{c^2}}}, \qquad \tilde{t} = \frac{t + \frac{\mathrm{v}z}{c^2}}{\sqrt{1 - \frac{\mathrm{v}}{c^2}}}, \tag{2}$$

where $\tilde{z}$ and $\tilde{t}$ are corresponding coordinates in the new ref-

*See any textbook on relativity. Note that the gravitational field is included in the components of the fundamental metric tensor $g_{\alpha\beta}$ as $\frac{GM}{c^2 r}$. The mass of the Sun is $M_\odot = 2 \times 10^{33}$ g, the mass of the Earth is $M_\oplus = 6 \times 10^{27}$ g; the distance between the Sun and the Earth is 15×10^{11} cm, the Earth's radius is 6.37×10^8 cm. We obtain $\frac{GM_\odot}{c^2 r} = 10^{-8}$, $\frac{GM_\oplus}{c^2 r} = 10^{-10}$. So, in this consideration we mean the daily rotation of the Earth and its gravitational field neglected (quasi-Newtonian approximation).

erence frame. We differentiate $\tilde{z}$ and $\tilde{t}$, then substitute the resulting $d\tilde{z}^2$, $d\tilde{t}^2$ and $d\tilde{t}$ into (2). For v = 250 km/sec we have $\mathrm{v}^2/c^2 = 7 \times 10^{-7}$, hence $\frac{1}{\sqrt{1 - \mathrm{v}^2/c^2}} \approx 1 + \mathrm{v}^2/2c^2$. We ignore terms in powers higher than $\frac{1}{c^2}$. As a result we obtain the metric along the Earth's trajectory in the Galaxy (dropping the tilde from the formulae)

$$ds^2 = \left(1 - \frac{2GM}{c^2 r} - \frac{\omega^2 r^2}{c^2}\right) c^2 dt^2 - \frac{2\omega r^2}{c} c\, dt\, d\varphi - \left(1 + \frac{2GM}{c^2 r}\right) dr^2 - r^2 d\varphi^2 - \frac{2\omega \mathrm{v} r^2}{c^2} d\varphi\, dz - dz^2. \tag{3}$$

This metric differs from (1), because of a spatial term $2\omega r^2 \mathrm{v}/c^2$ depending upon the linear velocity v.

In order to obtain really observable effects expected in the metric (3), we use the mathematical method of physical observed quantities [4, 5], which considers a fixed spatial section connected to a real reference frame of an observer. For such an observer the fundamental metrical tensor[†] has the three-dimensional invariant form

$$h_{ik} = -g_{ik} + \frac{1}{c^2} v_i v_k, \qquad i, k = 1, 2, 3, \tag{4}$$

dependent upon the linear velocity of the space rotation $v_i = -\frac{cg_{0i}}{\sqrt{g_{00}}}$. In (3) the metric tensor has the components

$$h_{11} = 1 + \frac{2GM}{c^2 r}, \quad h_{22} = r^2\left(1 + \frac{\omega^2 r^2}{c^2}\right), \\ h_{23} = \frac{\omega r^2 \mathrm{v}}{c^2}, \qquad\qquad h_{33} = 1, \tag{5}$$

while its contravariant components are

$$h^{11} = 1 - \frac{2GM}{c^2 r}, \quad h^{22} = \frac{1 - \frac{\omega^2 r^2}{c^2}}{r^2}, \\ h^{23} = -\frac{\omega \mathrm{v}}{c^2}, \qquad\qquad h^{33} = 1. \tag{6}$$

According to the theory [4, 5], any reference space has principal observable (chronometrically invariant) characteristics: the chr.inv.-vector of gravitational inertial force

$$F_i = \frac{1}{1 - \frac{\mathrm{w}}{c^2}}\left(\frac{\partial \mathrm{w}}{\partial x^i} - \frac{\partial v_i}{\partial t}\right); \tag{7}$$

the chr.inv.-tensor of the angular velocity of the space rotation

$$A_{ik} = \frac{1}{2}\left(\frac{\partial v_k}{\partial x^i} - \frac{\partial v_i}{\partial x^k}\right) + \frac{1}{2c^2}\left(F_i v_k - F_k v_i\right); \tag{8}$$

and the chr.inv.-tensor of the rates of the space deformation

$$D_{ik} = \frac{1}{2}\frac{{}^* \partial h_{ik}}{\partial t}, \tag{9}$$

[†]The spatial indices $1, 2, 3$ are denoted by Roman letters, while the space-time indices $0, 1, 2, 3$ are denoted by Greek letters.

where $\mathrm{w} = c^2 \left(1 - \sqrt{g_{00}}\right)$, while $\frac{*\partial}{\partial t} = \frac{1}{\sqrt{g_{00}}} \frac{\partial}{\partial t}$ is the so-called chronometrically invariant time derivative.

Calculating these for the metric space (3), we obtain

$$F^1 = \left(\omega^2 r - \frac{GM}{r^2}\right)\left(1 + \frac{\omega^2 r^2}{c^2}\right); \qquad (10)$$

$$A^{12} = \frac{\omega}{r}\left(1 - \frac{2GM}{c^2 r} + \frac{\omega^2 r^2}{2c^2}\right), \qquad A^{31} = \frac{\omega^2 \mathrm{v} r}{c^2}. \qquad (11)$$

All components of D_{ik} equal zero. Hence the reference body gravitates, rotates, and moves forward at a constant velocity. Appropriate characteristics of the metrics (1) and (3) coincide, aside for A^{31}: $A^{31} = 0$ in (3).

The observable time interval $d\tau$ contains v_i [4, 5]:

$$d\tau = \left(1 - \frac{\mathrm{w}}{c^2}\right) dt - \frac{1}{c^2} v_i \, dx^i. \qquad (12)$$

Within an area wherein $A_{ik} = 0$ (holonomic space) the time coordinate $x^0 = ct$ can be transformed so that all $v_i = 0$. In other words, the time interval between two events at different points does not depend on the path of integration: time is *integrable*, so a global synchronization of clocks is possible. In such a space the spatial section $x^0 = \mathrm{const}$ is everywhere orthogonal to time lines $x^i = \mathrm{const}$. If $A_{ik} \neq 0$ (non-holonomic space), it is impossible for all v_i to be zero: the spatial section is not orthogonal to the time lines, and the time interval between two events at different points depends on the path of integration (time is *non-integrable*).

Zelmanov also introduced the chr.inv.-pseudovector of the angular velocity of the space rotation [4]

$$\Omega_i = \frac{1}{2} \varepsilon_{ijk} A^{jk}, \qquad (13)$$

where $\varepsilon_{ijk} = \frac{e_{ijk}}{\sqrt{h}}$ is the three-dimensional discriminant tensor, e_{ijk} is the completely antisymmetric three-dimensional tensor, $h = \det\|h_{ik}\|$. Hence, $\Omega_1 = A^{23}$, $\Omega_2 = A^{31}$, $\Omega_3 = A^{12}$.

In our statement we have two bodies, both rotating and gravitating. The first body is at rest with respect to the observer, whilst the second body moves with a linear velocity. As seen from (11), for the rest body only $\Omega_3 \neq 0$. For the moving body we also obtain $\Omega_2 \neq 0$ and $\Omega_3 \neq 0$.* In other words, any linear motion of an observer with respect to his reference body provides an additional degree of freedom to rotations of his reference space.

Besides the aforementioned observable "physical" characteristics F_i, A_{ik}, and D_{ik}, every reference space also has an observable geometric characteristic [4]: the chr.inv.-tensor of the three-dimensional space curvature

$$C_{lkij} = H_{lkij} - \frac{1}{c^2}\big(2A_{ki}D_{jl} + A_{ij}D_{kl} + {} \\ {} + A_{jk}D_{il} + A_{kl}D_{ij} + A_{li}D_{kj}\big), \qquad (14)$$

---

*This is because any linear motion leads to an additional term in the observable metric tensor h_{ik}: see formulae (5) and (6).

which possesses all the properties of the Riemann-Christoffel curvature tensor $R_{\alpha\beta\gamma\delta}$ in the spatial section. Here $H_{lkij} = h_{jm}H_{lki\cdot}^{\cdots m}$, where $H_{lki\cdot}^{\cdots m}$ is the chr.inv.-tensor similar to Schouten's tensor [8]:

$$H_{lki\cdot}^{\cdots j} = \frac{*\partial \Delta_{il}^j}{\partial x^k} - \frac{*\partial \Delta_{kl}^j}{\partial x^i} + \Delta_{il}^m \Delta_{km}^j - \Delta_{kl}^m \Delta_{im}^j. \qquad (15)$$

If all A_{ik} or D_{ik} are zero in a space, $C_{iklj} = H_{iklj}$. Zelmanov also introduced $H_{ik} = h^{mn}H_{imkn}$, $H = h^{ik}H_{ik}$, $C_{ik} = h^{mn}C_{imkn}$ and $C = h^{ik}C_{ik}$.

The chr.inv.-Christoffel symbols of the first and second kinds, by Zelmanov, are

$$\Delta_{ij}^k = h^{km}\Delta_{ij,m} = \frac{1}{2}\left(\frac{*\partial h_{im}}{\partial x^j} + \frac{*\partial h_{jm}}{\partial x^i} - \frac{*\partial h_{ij}}{\partial x^m}\right), \qquad (16)$$

where $\frac{*\partial}{\partial x^i} = \frac{\partial}{\partial x^i} - \frac{1}{c^2}\frac{*\partial}{\partial t}$ is the so-called chr.inv.-spatial derivative.

Calculating the components of Δ_{ij}^k for the metric (3), we obtain

$$\Delta_{22}^1 = -r\left(1 - \frac{2GM}{c^2 r} + \frac{2\omega^2 r^2}{c^2}\right),$$

$$\Delta_{11}^1 = \frac{GM}{c^2 r^2}, \qquad \Delta_{23}^1 = -\frac{\omega \mathrm{v} r}{c^2}, \qquad (17)$$

$$\Delta_{12}^2 = \frac{1}{r}\left(1 + \frac{\omega^2 r^2}{c^2}\right), \qquad \Delta_{13}^2 = \frac{\omega \mathrm{v}}{c^2 r},$$

while non-zero components of C_{iklj}, C_{ik} and C are

$$C_{1212} = -\frac{GM}{c^2 r} + \frac{3\omega^2 r^2}{c^2},$$

$$C_{11} = -\frac{GM}{c^2 r^3} + \frac{3\omega^2}{c^2}, \quad C_{22} = -\frac{GM}{c^2 r} + \frac{3\omega^2 r^2}{c^2}, \qquad (18)$$

$$C = 2\left(-\frac{GM}{c^2 r^3} + \frac{3\omega^2}{c^2}\right).$$

We have thus calculated by the theory of observable quantities, that:

> The observable space along the Earth's trajectory in the Galaxy is non-holonomic, inhomogeneous, and curved due to the space rotation and/or Newtonian attraction. This should be true for any other planet (or its satellite) as well, or any other body considered within the framework this analysis.

3 Deviation of light in the field of the Galactic rotation

We study how a light ray behaves in a reference body space described by the metric (3). Light moves along isotropic geodesic lines. Such geodesics are trajectories of the parallel transfer of the four-dimensional isotropic wave vector

$$K^\alpha = \frac{\Omega}{c}\frac{dx^\alpha}{d\sigma}, \qquad g_{\alpha\beta} K^\alpha K^\beta = 0, \qquad (19)$$

where Ω is the proper frequency of the radiation, $d\sigma = = h_{ik} dx^i dx^k$ is the three-dimensional observable interval*. The equations of geodesic lines in chr.inv.-form are [4, 5]

$$\frac{d\Omega}{d\tau} - \frac{\Omega}{c^2} F_i c^i + \frac{\Omega}{c^2} D_{ik} c^i c^k = 0,$$

$$\frac{d(\Omega c^i)}{d\tau} + 2\omega(D_k^i + A_{k\cdot}^{\cdot i}) c^k - \Omega F^i + \Omega \Delta_{kn}^i c^k c^n = 0,$$
(20)

where $c^i = \frac{dx^i}{d\tau}$ is the observable chr.inv.-velocity of light (its square is invariant $c_i c^i = h_{ik} c^i c^k = c^2$).

Substituting the chr.inv.-characteristics of the reference space (3) into equations (20), we obtain

$$\frac{1}{\Omega} \frac{d\Omega}{d\tau} - \frac{1}{c^2} \left(\omega^2 r - \frac{GM}{r^2} \right) \frac{dr}{d\tau} = 0,$$
(21)

$$\frac{d}{d\tau} \left(\Omega \frac{dr}{d\tau} \right) - 2\Omega\omega r \left(1 - \frac{2GM}{c^2 r} + \frac{3\omega^2 r^2}{2c^2} \right) \frac{d\varphi}{d\tau} -$$
$$- \Omega \left(\omega^2 r - \frac{GM}{r^2} \right) \left(1 + \frac{\omega^2 r^2}{c^2} \right) - \frac{2\Omega\omega v}{c^2} \frac{d\varphi}{d\tau} \frac{dz}{d\tau} -$$
$$- \Omega r \left(1 - \frac{2GM}{c^2 r} + \frac{2\omega^2 r^2}{c^2} \right) \left(\frac{d\varphi}{d\tau} \right)^2 = 0,$$
(22)

$$\frac{d}{d\tau} \left(\Omega \frac{d\varphi}{d\tau} \right) + \frac{2\Omega\omega}{r} \left(1 + \frac{GM}{2c^2 r} + \frac{\omega^2 r^2}{2c^2} \right) \frac{dr}{d\tau} +$$
$$+ \frac{2\omega}{r} \left(1 + \frac{\omega^2 r^2}{c^2} \right) \frac{dr}{d\tau} \frac{d\varphi}{d\tau} + \frac{2\Omega\omega v}{c^2 r} \frac{dr}{d\tau} \frac{dz}{d\tau} = 0,$$
(23)

$$\frac{d}{d\tau} \left(\Omega \frac{dz}{d\tau} \right) - \frac{2\Omega\omega^2 v r}{c^2} \frac{dr}{d\tau} = 0.$$
(24)

Integrating (21) we obtain the observable proper frequency of the light beam at the moment of observation

$$\Omega = \frac{\Omega_0}{\sqrt{1 - \frac{2GM}{c^2 r} - \frac{\omega^2 r^2}{c^2}}} \approx \Omega_0 \left(1 + \frac{GM}{c^2 r} + \frac{\omega^2 r^2}{2c^2} \right),$$
(25)

where Ω_0 is its "initial" proper frequency (in the absence of external affects). We integrate (22)–(24) with the use of (25).

Rewrite (24) as

$$\frac{d}{d\tau} \left(\Omega \frac{dz}{d\tau} \right) = \frac{\Omega\omega^2 v}{c^2} \frac{d}{d\tau} \left(r^2 \right),$$
(26)

integration of which gives

$$\Omega \frac{dz}{d\tau} = \frac{\Omega\omega^2 v r^2}{c^2} + Q, \qquad Q = \text{const},$$
(27)

where $\dot{z}_0 = \left(\frac{dz}{d\tau} \right)_0$ is the initial value of $\frac{dz}{d\tau}$, while the integration constant is $Q = \Omega_0 \left(\dot{z}_0 - \frac{\omega^2 v r_0^2}{c^2} \right)$.

Substituting (27) into (23) and (24) and using Ω from (25), we obtain the system of equations with respect to r and φ,

$$\frac{d}{d\tau} \left(\Omega \frac{d\varphi}{d\tau} \right) + \frac{2\Omega\omega}{r} \left(1 + \frac{GM}{2c^2 r} + \frac{\omega^2 r^2}{2c^2} \right) \frac{dr}{d\tau} +$$
$$+ \frac{2\omega}{r} \left(1 + \frac{\omega^2 r^2}{c^2} \right) \frac{dr}{d\tau} \frac{d\varphi}{d\tau} + \frac{2\Omega_0 \omega v \dot{z}_0}{c^2 r} \frac{dr}{d\tau} = 0,$$
$$\frac{d}{d\tau} \left(\Omega \frac{dr}{d\tau} \right) - 2\Omega\omega r \left(1 - \frac{2GM}{c^2 r} + \frac{3\omega^2 r^2}{2c^2} \right) \frac{d\varphi}{d\tau} -$$
$$- \Omega \left(\omega^2 r - \frac{GM}{r^2} \right) \left(1 + \frac{\omega^2 r^2}{c^2} \right) - \frac{2\Omega_0 \omega v \dot{z}_0 r}{c^2} \frac{d\varphi}{d\tau} -$$
$$- \Omega r \left(1 - \frac{2GM}{c^2 r} + \frac{2\omega^2 r^2}{c^2} \right) \left(\frac{d\varphi}{d\tau} \right)^2 = 0.$$
(28)

We are looking for an approximate solution to this system. The last term has the dimensionless factor $\frac{v\dot{z}_0}{c^2}$. For a light beam, $\dot{z}_0$ (the initial value of the light velocity along the z-axis) is c. Hence $\frac{v\dot{z}_0}{c^2} = \frac{v}{c}$. At 250 km/sec, attributed to the Earth moving in the Galaxy, $\frac{v}{c} = 8.3 \times 10^{-4}$. The terms $\frac{GM}{c^2 r}$ and $\frac{\omega^2 r^2}{c^2}$, related to the orbital motion of the Earth, are in order of 10^{-8}. We therefore drop these terms from consideration, so equations (28) become

$$\frac{d}{d\tau} \left(\Omega \frac{dr}{d\tau} \right) - 2\Omega\omega r \frac{d\varphi}{d\tau} - \Omega \left(\omega^2 r - \frac{GM_\odot}{r^2} \right) -$$
$$- \Omega r \left(\frac{d\varphi}{d\tau} \right)^2 - \frac{2\Omega_0 \omega v \dot{z}_0 r}{c^2} \frac{d\varphi}{d\tau},$$
(29)

$$\frac{d}{d\tau} \left(\Omega \frac{d\varphi}{d\tau} \right) + \frac{2\Omega\omega}{r} \frac{dr}{d\tau} + \frac{2\omega}{r} \frac{dr}{d\tau} \frac{d\varphi}{d\tau} + \frac{2\Omega_0 \omega v \dot{z}_0}{c^2 r} \frac{dr}{d\tau} = 0.$$
(30)

We rewrite (30) as

$$\ddot{\varphi} + 2(\dot{\varphi} + \tilde{\omega}) \frac{\dot{r}}{r} = 0,$$
(31)

where $\tilde{\omega} = \omega \left(1 + \frac{v\dot{z}_0}{c^2} \right)$, $\dot{\varphi} = \frac{d\varphi}{d\tau}$, $\ddot{\varphi} = \frac{d^2\varphi}{d\tau^2}$. This is an equation with separable variables, so its first integral is

$$\dot{\varphi} = \frac{B}{r^2} - \tilde{\omega}, \qquad B = \text{const} = (\dot{\varphi}_0 + \tilde{\omega}) r_0^2,$$
(32)

where $\dot{\varphi}_0$ and r_0 are the initial values of $\dot{\varphi}$ and r.

We rewrite (29) as

$$\ddot{r} - 2\tilde{\omega} r \dot{\varphi} + \frac{GM}{r^2} - \omega^2 r - r\dot{\varphi}^2 = 0,$$
(33)

where $\dot{r} = \frac{dr}{d\tau}$, $\ddot{r} = \frac{d^2 r}{d\tau^2}$. In our consideration, $\frac{GM}{r^2} - \omega^2 r$ is zero, so the motion of the Earth around the Sun satisfies the weightlessness condition [9, 10][†] — a balance between the

---

*So the space-time interval $ds^2 = g_{\alpha\beta} dx^\alpha dx^\beta$ in chr.inv.-form is $ds^2 = c^2 d\tau^2 - d\sigma^2 = 0$. Therefore, because $ds^2 = 0$ along isotropic trajectories by definition, there $d\sigma = c d\tau$.

[†]Each planet, in its orbital motion, should satisfy the *weightlessness condition* $w = v_i u^i$, where w is the potential of the field attracting the planet to a body around which this planet is orbiting, v_i is the linear velocity of the body's space rotation in this orbit, and $u^i = dx^i/dt$ is the coordinate velocity of the planet in its orbit. The orbital velocity is the same as the space rotation velocity. Hence the weightiness condition can be written as $GM/r = v^2 = v_i v^i$ [9, 10].

acting forces of gravity $\frac{GM}{r^2}$ and inertia $\omega^2 r$. Taking this into account, and substituting (32) into (33), we obtain

$$\ddot{r} + \tilde{\omega}^2 r - \frac{B^2}{r^3} = 0 \,. \tag{34}$$

We replace the variables as $\dot{r} = p$. So $\ddot{r} = p\frac{dp}{dr}$ and the equation (36) takes the form

$$p\frac{dp}{dr} = \frac{B^2}{r^3} - \tilde{\omega}^2 r^2 \,, \tag{35}$$

which can be easily integrated:

$$p^2 = \left(\frac{dr}{d\tau}\right)^2 = -\frac{B^2}{r^2} - \tilde{\omega}^2 r^2 + K \,, \qquad K = \text{const}, \tag{36}$$

where the integration constant is $K = \dot{r}_0^2 + (\dot{\varphi}_0 + \tilde{\omega})^2 r_0^2 + \tilde{\omega}^2 r_0^2$, so we obtain

$$\frac{dr}{d\tau} = \pm\sqrt{K - \tilde{\omega}^2 r^2 - \frac{B^2}{r^2}} \,. \tag{37}$$

Looking for τ as a function of r, we integrate (37) taking the positive time flow into account (positive values of τ). We obtain

$$\tau = \int_{r_0}^{r} \frac{r\,dr}{\sqrt{-\tilde{\omega}^2 r^4 + Kr^2 - B^2}} \,. \tag{38}$$

Introducing a new variable $u = r^2$ we rewrite (38) as

$$\tau = \frac{1}{2}\int_{u_0}^{u} \frac{du}{\sqrt{-\tilde{\omega}^2 u^2 + Ku - B^2}} \,, \tag{39}$$

which integrates to

$$\tau = -\frac{1}{2\tilde{\omega}}\left[\arcsin\left(\frac{-2\tilde{\omega}^2 r^2 + K}{\sqrt{K^2 - 4\tilde{\omega}^2 B^2}}\right) - \right.$$
$$\left. - \arcsin\left(\frac{-2\tilde{\omega}^2 r_0^2}{\sqrt{K^2 - 4\tilde{\omega}^2 B^2}}\right)\right] \tag{40}$$

where

$$K^2 - 4\tilde{\omega}^2 B^2 \equiv Q^2 =$$
$$= \left(\dot{r}_0^2 + r_0^2\dot{\varphi}_0^2\right)\left[\dot{r}_0^2 + 4\tilde{\omega}\left(\tilde{\omega} + \dot{\varphi}_0\right)r_0^2 + \dot{\varphi}_0^2 r_0^2\right], \tag{41}$$

so we obtain r^2 and r

$$r^2 = \frac{Q}{2\tilde{\omega}^2}\sin 2\tilde{\omega}\tau + r_0^2 \,, \qquad r = \sqrt{\frac{Q}{2\tilde{\omega}^2}\sin 2\tilde{\omega}\tau + r_0^2} \,, \tag{42}$$

where r_0 is the initial displacement in the r-direction.

Substituting (42) into (32) we obtain φ,

$$\varphi = \int_0^{\tau}\left(\frac{B}{r^2} - \tilde{\omega}\right)d\tau = -\tilde{\omega}\tau + \frac{\tilde{\omega}B}{\sqrt{Q^2 - 4\omega^4 r_0^4}} \times$$
$$\times \ln\left|\frac{\left(Q + \sqrt{Q^2 - 4\tilde{\omega}^4 r_0^4}\,\right)\tan\tilde{\omega}\tau + 2\tilde{\omega}^2 r_0^2}{\left(Q - \sqrt{Q^2 - 4\tilde{\omega}^4 r_0^4}\,\right)\tan\tilde{\omega}\tau + 2\tilde{\omega}^2 r_0^2}\right| + \varphi_0 \,, \tag{43}$$

where φ_0 is the initial displacement in the φ-direction.

Substituting Ω from (25) into (27), and eliminating the terms containing $\frac{GM}{c^2 r}$ and $\frac{\omega^2 r^2}{c^2}$, we obtain the observable velocity of the light beam in the z-direction

$$\dot{z} = \frac{\omega^2 \text{v} r^2}{c^2} + \dot{z}_0 - \frac{\omega^2 \text{v} r_0^2}{c^2} \,, \tag{44}$$

the integration of which gives its observable displacement

$$z = \dot{z}_0\tau + \frac{\omega^2 Q \text{v}}{4\tilde{\omega}^3 c^2}\left(1 - \cos 2\tilde{\omega}\tau\right) + z_0 \,, \tag{45}$$

which, taking into account that $\tilde{\omega} = \omega\left(1 + \frac{\text{v}\dot{z}_0}{c^2}\right)$, is

$$z = \dot{z}_0\tau + \frac{\text{v}Q}{4\tilde{\omega}c^2}\left(1 - \cos 2\tilde{\omega}\tau\right)\left(1 - \frac{\text{v}\dot{z}_0}{c^2}\right)^2 + z_0 \,. \tag{46}$$

We have obtained solutions for $\dot{r}$, $\dot{\varphi}$, $\dot{z}$ and r, φ, z. We see the galactic velocity of the Earth in only $\dot{z}$ and z.

Let's find corrections to the displacement of the light $\dot{z}$ and its displacement z caused by the motion of the Earth in the rotating and gravitating space of the Galaxy.

As follows from formula (41), Q doesn't include the initial velocity and displacement of the light beam in the z-direction. Besides, $Q = 0$ if $\dot{r}_0 = 0$ and $r_0 = 0$. In a real situation $\dot{r}_0 \neq 0$, because the light beam is emitted from the Earth so r_0 is the distance between the Sun and the Earth. Hence, in our consideration, $Q \neq 0$ always. If $\dot{\varphi}_0 = 0$, the light beam is directed strictly towards the Sun.

We calculate the correction to the light velocity in the r-direction $\Delta\dot{z}_0$ (we mean $\dot{\varphi}_0 = 0$, $\dot{z}_0 = 0$). Eliminating the term $1 - \frac{\text{v}\dot{z}_0}{c^2}$ we obtain

$$\Delta\dot{z} = \frac{Q\text{v}}{2c^2}\sin 2\tilde{\omega}\tau \,, \qquad Q = \dot{r}_0\sqrt{\dot{r}_0^2 + 4\tilde{\omega}^2 r_0^2} \,. \tag{47}$$

We see that the correction $\Delta\dot{z}_0$ is a periodical function, the frequency of which is twice the angular velocity of the Earth's rotation around the Sun; $2\tilde{\omega} = 4\times10^{-7}\,\text{sec}^{-1}$. Because the initial value of the light velocity is $\dot{r}_0 = c$, and also $4\tilde{\omega}^2 r_0^2 \ll c^2$, we obtain the amplitude of the harmonic oscillation

$$\frac{Q\text{v}}{2c^2} = \frac{\dot{r}_0^2}{2c^2}\sqrt{1 + \frac{4\tilde{\omega}^2 r_0^2}{c^2}} \approx \frac{\text{v}}{2} \,, \tag{48}$$

then the correction to the light velocity in the r-direction $\Delta\dot{z}_0$ is,

$$\Delta\dot{z} = \frac{\text{v}}{2}\sin 2\tilde{\omega}\tau = 4\times10^{-4}\left(\sin 2\tilde{\omega}\tau\right)c \,. \tag{49}$$

From this resulting "key formula" we have obtained we conclude that:

The component of the observable vector of the light velocity directed towards the Sun (the r-direction) gains an addition (correction) in the z-direction, because the Earth moves in common with the Sun in the

Galaxy. The obtained correction manifests as a harmonic oscillation added to the world-invariant of the light velocity c. The expected amplitude of the oscillation is $4 \times 10^{-4} c$, i.e. 120 km/sec; the period $T = \frac{1}{2\omega}$ is half the astronomical year. So the theory predicts an anisotropy of the observable velocity of light due to the inhomogeneity and anisotropy of space, caused by its rotation and the presence of gravitation.

In our statement the anisotropy of the velocity of light manifests in the z-direction. We therefore, in this statement, call the z-direction the *preferred direction*.

We can verify the anisotropy of the velocity of light by experiment. By the theory of observable quantities [4, 5], the invariant c is the length

$$c = \sqrt{h_{ik} c^i c^k} = \sqrt{\frac{h_{ik}\, dx^i dx^k}{d\tau}} = \frac{d\sigma}{d\tau} \qquad (50)$$

of the chr.inv.-vector $c^i = \frac{dx^i}{d\tau}$ of the observable light velocity. Let a light beam be directed towards the Sun, i.e. in the r-direction. According to our theory, the Earth's motion in the Galaxy deviates the beam away from the r-axis so that we should observe an additional z-component to the light velocity invariant. Let's set up two pairs of detectors (synchronised clocks) along the r-direction and z-direction in order to measure time intervals during which the light beams travel in these directions. Because the distances $\Delta\sigma$ between the clocks are fixed, and c is constant, the measured time in the z-direction is expected to have a dilation with respect to that measured in the r-direction: by formula (49) the light velocity measured in both directions is expected to be differ by ~ 120 km/sec at the maximum of the effect.

The most suitable equipment for such an experiment is that used by R. T. Cahill (Flinders University, Australia) in his current experiments on the measurement of the velocity of light in an RF coaxial-cable equipped with a pair of high precision synchronized Rb atomic clocks [11]. This effect probably had a good chance of being detected in similar experiments by D. G. Torr and P. Colen (Utah State University, USA) in the 1980's [12] and, especially, by Roland De Witte (Belgacom Laboratory of Standards, Belgium) in the 1990's [13]. However even De Witte's equipment had a measurement precision a thousand times lower than that currently used by Cahill.

Because the Earth rotates around its own axis we should observe a weak daily variation of this effect. In order to register the complete variation of this value, we should measure it at least during half the astronomical year (one period of its variation).

4 Inhomogeneity and anisotropy of space along the Earth's transit in the Galaxy

We just applied the metric (3) to the Earth's motion in the Galaxy. Following this approach, we can also employ this metric to other preferred directions in the Universe, connected to the motion of another space body, for instance — the motion of our Galaxy in the Local Group of galaxies.

Astronomical observations show that the Sun moves in common with our Galaxy in the Local Group of galaxies at the velocity 700 km/sec.* The metric (3) can take into account this aspect of the Earth's motion as well. In such a case we should expect two weak maximums in the time dilation measured in the above described experimental system during the 24-hour period, when the z-direction coincides with the direction of the apex of the Sun. The amplitude of the variation of the observable light velocity should be 2.8 times the variation caused by the Earth's motion in the Galaxy.

Swedish astronomers in the 1950's discovered that the Local Group of galaxies is a part of an compact "cloud" called the Supercluster of galaxies, consisting of galaxies, small groups of galaxies, and two clouds of galaxies. The Supercluster has a diameter of ~ 98 million light years, while our Galaxy is located at 62 million light years from the centre. The Supercluster rotates with a period of ~ 100 billion years in the central area and ~ 200 billion years at the periphery. As supposed by the Swedes, our Galaxy, located at $\sim 2/3$ of the Supercluster's radius, from its centre, rotates around the centre at a velocity of ~ 700 km/sec. (See Chapter VII, §6 in [14] for the details.)

In any case, in any large scale our metric (3) gives the same result, because any of the spaces is non-holonomic (rotates) around its own centre of gravity. All the spaces are included, one into the other, and cause bizarre spirals in their motions. The greater the number of the space structures taken onto account by our metric (3), the more complicated is the spiral traced out by the Earth observer in the space — the spiral is plaited into other space spirals (the fractal structure of the Universe [15]).

This analysis of our theoretical results, obtained by General Relativity, and the well-known data of observational astronomy leads us to the obvious conclusion:

> The main factors forming the observable structure of the space of the Universe are gravitational fields of bulky bodies and their rotations, not the space deformations as previously thought.

Many scientists consider homogeneous isotropic models as models of the real Universe. A homogeneous isotropic space-time is described by Friedmann's metric

$$ds^2 = c^2 dt^2 - R^2 \frac{dx^2 + dy^2 + dz^2}{\left[1 + \frac{k}{4}\left(x^2 + y^2 + z^2\right)\right]^2}, \qquad (51)$$

where $R = R(t)$; $k = 0, \pm 1$. For such a space, the main observable characteristics are $F^i = 0$, $A_{ik} = 0$, $D_{ik} \neq 0$. In other words, such a space can undergo deformation (expansion,

---

*The direction of this motion is pointed out in the sky as the apex of the Sun. Interestingly, the Sun has a slow drift of 20 km/sec in the same direction as the apex, but within the Galaxy with respect to its plane.

compression, or oscillation), but it is free of rotation and contains no gravitating bodies (fields). So the metric (51) is the necessary and sufficient condition for homogeneity and isotropy. This is a model constructed by an imaginary observer who is located so far away from matter in the real Universe that he sees no such details as stars and galaxies.

In contrast to them, we consider a cosmological model constructed by an Earth observer, who is carried away by all motions of our planet. Zelmanov, the pioneer of inhomogeneous anisotropic relativistic models, pointed out the mathematical conditions of a space's homogeneity and isotropy, expressed with the terms of physically observable characteristics of the space [4]. The conditions of isotropy are

$$F_i = 0, \quad A_{ik} = 0, \quad \Pi_{ik} = 0, \quad \Sigma_{ik} = 0, \qquad (52)$$

where $\Pi_{ik} = D_{ik} - \frac{1}{3} D h_{ik}$ and $\Sigma_{ik} = C_{ik} - \frac{1}{3} C h_{ik}$ are the factors of anisotropy of the space deformation and the three-dimensional (observable) curvature. In a space of the metric (3) we have $D_{ik} = 0$, hence there $\Pi_{ik} = 0$. However F_i and A_{ik} are not zero in such a space (see formulae 10 and 11). Besides these there are the non-zero quantities,

$$\Sigma_{11} = -\frac{1}{3} \frac{GM}{c^2 r^3} + \frac{\omega^2}{c^2};$$

$$\Sigma_{22} = -\frac{1}{3} \frac{GM}{c^2 r^2} + \frac{\omega^2 r}{c^2}; \qquad (53)$$

$$\Sigma_{33} = \frac{2}{3} \frac{GM}{c^2 r^3} - \frac{2\omega^2}{c^2}.$$

We see that a space of the metric (3) is anisotropic due to its rotation and gravitation.

The conditions of homogeneity, by Zelmanov [4], are

$$\nabla_j F_i = 0, \quad \nabla_j A_{ik} = 0, \quad \nabla_j D_{ik} = 0, \quad \nabla_j C_{ik} = 0. \quad (54)$$

Calculating the conditions for the metric (3), we obtain

$$\nabla_1 C_{11} = \frac{3GM}{c^2 r^4}, \qquad \nabla_1 C_{22} = \frac{3GM}{c^2 r^2},$$

$$\nabla_1 F_1 = \omega^2 \left(1 + \frac{3\omega^2 r^2}{c^2}\right) + \frac{2GM}{r^3} \left(1 + \frac{3GM}{c^2 r}\right), \quad (55)$$

$$\nabla_1 A_{12} = -\omega \left(\frac{2}{r^2} + \frac{\omega^2}{c^2} + \frac{3GM}{c^2 r^3}\right).$$

This means, a space of the metric (3) is inhomogeneous due to its rotation and gravitation.

The results we have obtained manifest thus:

> The real space of our Universe, where space bodies move, is inhomogeneous and anisotropic. Moreover, the space inhomogeneity and anisotropy determine the bizarre structure of the Universe which we observe: the preferred directions along which the space bodies move, and the hierarchial distribution of the motions.

5 Conclusions

By means of General Relativity we have shown that the space metric (3) along the Earth's trajectory in the Galaxy, where the Earth follows a complicated spiral traced out by its orbital motion around the Sun and its concomitant motion with the whole solar system around the centre of the Galaxy. We have shown that this metric space is: (a) globally non-holonomic due to its rotation and the presence of gravitation, as manifested by the non-holonomic chr.inv.-tensor A_{ik} (11) calculated in the metric space*; (b) inhomogeneous, because the chr.inv.-Christoffel symbols Δ_{ij}^k indicating inhomogeneity of space, being calculated in the metric space as shown by (17), contain gravitation and space rotation; (c) curved due to gravitation and space rotation, represented in the formulae for the three-dimensional chr.inv.-curvature C_{iklj} calculated in the metric space as shown by (18).

Consequently, in real space there exist "preferred" spatial directions along which space bodies undergo their orbital motions.

We have deduced that the observable velocity of light should be anisotropic in space due to the anisotropy and inhomogeneity of space, caused by the aforementioned factors of gravitation and space rotation, despite the world-invariance of the velocity of light. It has been calculated that two pairs of synchronised clocks should record different values for the speed of light in light beams directed towards the Sun and orthogonal to this direction, at about $4 \times 10^{-4} c$ (0.04% of the measured velocity of light c, i.e. ~ 120 km/sec). This effects should undergo oscillations with a 12-hour period (due to the daily rotation of the Earth) and with a 6-month period (due to the motion of the Earth around the Sun). Equipment most suitable for detecting the effect is that used by R. T. Cahill (Flinders University, Australia) in his current experiment on the measurement of the velocity of light in a one-way RF coaxial-cable equipped with a pair of high precision synchronized Rb atomic clocks.

The predicted anisotropy of the observable velocity of light has been deduced as a direct consequence of the geometrical structure of four-dimensional space-time. Therefore, if the predicted anisotropy is detected by experiment, it will be one more fact in support of Einstein's General Theory of Relativity.

The anisotropy of the observable velocity of light as a consequence of General Relativity was first pointed out by D. Rabounski in the editorial preface to [13], his papers [6, 7], and many private communications with the author, which commenced in Autumn, 2005. He has stated that the anisotropy results from the non-holonomity (rotation) of the

---

*Gravitation is represented by the mass of the Sun M, while the space rotation is represented by two factors: the angular velocity ω of the solar space rotation in the Earth's orbit (equal to the angular velocity of the Earth's rotation around the Sun), and also the linear velocity v of the rotation of the Sun in common with the whole solar system around the centre in the Galaxy.

local space of a real observer and/or the non-holonomity of the background space of the whole Universe. Moreover, the non-holonomic field of the space background can produce energy, if perturbed by a local rotation or oscillation (as this was theoretically found for stars [6, 7]).

Detailed calculations provided in the present paper show not only that the non-holonomity (rotation) of space is the source of the anisotropy of the observable velocity of light, but also gravitational fields.

This paper will be followed by a series of papers wherein we study the interaction between the fields of the space non-holonomity, and also consider these fields as new sources of energy. This means that we consider open systems. Naturally, given the case of an inhomogeneous anisotropic universe, it is impossible to study it as a closed system since such systems don't physically exist owing to the presence of space non-holonomity and gravitation*. In a subsequent paper we will consider the non-holonomic fields in a space of the metric (3) with the use of Einstein's equations. It is well known that the equations can be applied to a wide variety distributions of matter, even inside atomic nuclei. We can therefore, with the use of the Einstein equations, study the non-holonomic fields and their interactions in any scaled part of the Universe — from atomic nuclei to clusters of galaxies — the problem statement remains the same in all the considerations.

References

1. Crothers S. J. On the general solution to Einstein's vacuum field for the point-mass when $\lambda \neq 0$ and its implications for relativistic cosmology. *Progress in Physics*, 2005, v. 3, 7–18.

2. Crothers S. J. A brief history of black holes. *Progress in Physics*, 2006, v. 2, 54–57.

3. Borissova L. Gravitational waves and gravitational inertial waves in the General Theory of Relativity: a theory and experiments. *Progress in Physics*, 2005, v. 2, 30–62.

4. Zelmanov A. L. Chronometric invariants. Dissertation thesis, 1944. American Research Press, Rehoboth (NM), 2006.

5. Zelmanov A. L. Chronometric invariants and co-moving co-ordinates in the general relativity theory. *Doklady Acad. Nauk USSR*, 1956, v. 107(6), 815–818.

6. Rabounski D. Thomson dispersion of light in stars as a generator of stellar energy. *Progress in Physics*, 2006, v. 4, 3–10.

7. Rabounski D. A source of energy for any kind of star. *Progress in Physics*, 2006, v. 4, 19–23.

8. Schouten J. A., Struik D. J. Einführung in die neuren Methoden der Differentialgeometrie. *Zentralblatt für Mathematik*, 1935, Bd. 11 und Bd. 19.

9. Rabounski D., Borissova L. Particles here and beyond the Mirror. Editorial URSS, Moscow, 2001; arXiv: gr-qc/0304018.

10. Borissova L., Rabounski D. Fields, vacuum, and the mirror Universe. Editorial URSS, Moscow, 2001; CERN, EXT-2003-025.

11. Cahill R. T. A new light-speed anisotropy experiment: absolute motion and gravitational waves detected. *Progress in Physics*, 2006, v. 4, 73–92.

12. Torr D. G., Kolen P. An experiment to measure relative variations in the one-way velocity of light. *Precision Measurements and Fundamental Constants*, Natl. Bur. Stand. (U. S.), Spec. Publ., 1984, v. 617, 675–679.

13. Cahill R. T. The Roland De Witte 1991 experiment (to the memory of Roland De Witte). *Progress in Physics*, 2006, v. 3, 60–65.

14. Vorontsov-Velyaminov B. A. Extragalactic astronomy. Harwood Academic Publishers, N.Y., 1987.

15. Mandelbrot B. The fractal geometry of nature. W. H. Freeman, San Francisco, 1982.

16. Rabounski D. A theory of gravity like electrodynamics. *Progress in Physics*, 2005, v. 2, 15–29.

---

*According to the Copernican standpoint, the solar system should be a closed system, because that perspective doesn't take into account the fact that the solar system moves around the centre of the Galaxy, which carries it into other, more complicated motions.

Preferred Spatial Directions in the Universe. Part II. Matter Distributed along Orbital Trajectories, and Energy Produced from It

Larissa Borissova

E-mail: lborissova@yahoo.com

Using General Relativity we study the rotating space of an orbiting body (of the Earth in the Galaxy, for example). In such a space Einstein's equations predict that: (1) the space cannot be empty; (2) it abhors a vacuum (i. e. a pure λ-field), and so it must also possess a substantive distribution (e. g. gas, dust, radiations, etc.). In order for Maxwell's equations to satisfy Einstein's equations, it is shown that: (1) a free electromagnetic field along the trajectory of an orbiting body must be present, by means of purely magnetic "standing" waves; (2) electromagnetic fields don't satisfy the Einstein equations in a region of orbiting space bodies if there is no distribution of another substance (e. g. dust, gas or something else). The braking energy of a medium pervading space equals the energy of the space non-holonomic field. The energy transforms into heat and radiations within stars by a stellar energy mechanism due to the background space non-holonomy, so a star takes energy for luminosity from the space during the orbit. Employing this mechanism in an Earth-bound laboratory, we can obtain a new source of energy due to the fact that the Earth orbits in the non-holonomic fields of the space.

1 If a body undergoes orbital motion in a space, the space cannot be empty

This paper extends a study begun in *Preferred Spatial Directions in the Universe: a General Relativity Approach* [1]. We considered a space-time described by the metric[*]

$$ds^2 = \left(1 - \frac{2GM}{c^2 r} - \frac{\omega^2 r^2}{c^2}\right)c^2 dt^2 - \frac{2\omega r^2}{c} c\, dt\, d\varphi -$$
$$- \left(1 + \frac{2GM}{c^2 r}\right)dr^2 - r^2 d\varphi^2 - \frac{2\omega \mathrm{v} r^2}{c^2}\, d\varphi\, dz - dz^2, \tag{1}$$

where $G = 6.67 \times 10^{-8} \frac{\mathrm{cm}^3}{\mathrm{g} \times \mathrm{sec}^2}$ is Newton's gravitational constant, M is the value of an attracting mass around which a test-body orbits, ω is the cyclic frequency of the orbital motion, v is the linear velocity at which the body, in common with the gravitating mass, moves with respect to the observer and his references.

In fact, this metric describes (in quasi-Newtonian approximation) the space along the path of a body which orbits another body and moves in common with it with respect to the observer's reference frame (which determine his physical reference space), for instance, the motion of the Earth in the Galaxy. So this metric is applicable to bodies orbiting anywhere in the Universe.

Here we study, using Einstein's equations, a space described by the metric (1). This approach gives a possibility of answering this question: does some matter (substance and/or fields) exist along the trajectory of an orbiting body, and what is that matter (if present there)?

The general covariant Einstein equations are[†]

$$R_{\alpha\beta} - \frac{1}{2} g_{\alpha\beta} R = -\kappa T_{\alpha\beta} - \lambda g_{\alpha\beta}, \tag{2}$$

where $R_{\alpha\beta}$ is Ricci's tensor, $g_{\alpha\beta}$ is the fundamental metric tensor, R is the scalar (Riemannian) curvature, $\kappa = \frac{8\pi G}{c^2} = 1.86 \times 10^{-27} \frac{\mathrm{cm}}{\mathrm{g}}$ is Einstein's gravitational constant, $T_{\alpha\beta}$ is the energy-momentum tensor of a distributed matter, λ is the so-called cosmological term that describes non-Newtonian forces of attraction or repulsion[‡]. A space-time is *empty* if $R_{\alpha\beta} = 0$. In this case, $R = 0$, $T_{\alpha\beta} = 0$, $\lambda = 0$, i. e. no substance and no λ-fields. A space-time is pervaded by *vacuum* if $T_{\alpha\beta} = 0$ but $\lambda \neq 0$ and hence $R_{\alpha\beta} \neq 0$.

The Einstein equations can be applied to a wide variety of distributions matter, even inside atomic nuclei. We can therefore, with the use of the Einstein equations, study the distribution of matter in any scaled part of the Universe — from atomic nuclei to clusters of galaxies.

We use the Einstein equations in chronometrically invariant form, i. e. expressed in the terms of physical observed values (chronometric invariants, by A. Zelmanov [3, 4]). In such a form, the general covariant equations (2) are represented by the three sorts of their observable (chronometrically invariant) projections: the projection onto an observer's

---

[*]The metric is given in the cylindrical spatial coordinates r, φ, z. See [1] for the reason.

[†]The space-time (four-dimensional) indices are $\alpha, \beta = 0, 1, 2, 3$.

[‡]Depending upon the sign of λ: $\lambda > 0$ stands for repulsion, while $\lambda < 0$ stands for attraction. The *cosmological term* is also known as the λ-term. The forces described by λ (known as λ-forces) grow in proportional to distance and therefore reveal themselves in full at a "cosmological" distance comparable to the size of the Universe. Because the non-Newtonian gravitational fields (λ-fields) have never been observed, for our Universe in general the numerical value of λ is expected to be $\lambda < 10^{-56}$ cm^{-2}. Read Chapter 5 in [2] for the details.

time line, the mixed (space-time) projection, and the projection onto the observer's spatial section [3, 4]

$$\frac{^*\partial D}{\partial t} + D_{jl}D^{lj} + A_{jl}A^{lj} + {}^*\nabla_j F^j - \frac{1}{c^2}F_j F^j =$$
$$= -\frac{\kappa}{2}\left(\rho c^2 + U\right) + \widetilde{\lambda}c^2 ; \tag{3}$$

$${}^*\nabla_j\left(h^{ij}D - D^{ij} - A^{ij}\right) + \frac{2}{c^2}F_j A^{ij} = \kappa J^i ; \tag{4}$$

$$\frac{^*\partial D_{ik}}{\partial t} - \left(D_{ij} + A_{ij}\right)\left(D_k^j + A_{k\cdot}^{\cdot j}\right) + DD_{ik} -$$
$$- D_{ij}D_k^j + 3A_{ij}A_{k\cdot}^{\cdot j} + \frac{1}{2}\left({}^*\nabla_i F_k + {}^*\nabla_k F_i\right) -$$
$$- \frac{1}{c^2}F_i F_k - c^2 C_{ik} = \tag{5}$$
$$= \frac{\kappa}{2}\left(\rho c^2 h_{ik} + 2U_{ik} - Uh_{ik}\right) + \widetilde{\lambda}c^2 h_{ik} ,$$

where $\rho = \frac{T_{00}}{g_{00}}$ is the observable density of matter, $J^i = \frac{c\,T_0^i}{\sqrt{g_{00}}}$ is the vector of the observable density of impulse, $U^{ik} = c^2 T^{ik}$ is the tensor of the observable density of the impulse flow (the stress tensor), $U = h_{ik}U^{ik}$. We include $\widetilde{\lambda}$ in the equations because the metric (1) is applicable at any scale, not only the cosmological large scale*.

By the theory of physical observable quantities [3, 4], the quantities D_{ik}, F_i, A_{ik} and C_{ik} are the observable characteristics of the observer's reference space: the chr.inv.-tensor of the rates of the space deformation[†]

$$D_{ik} = \frac{1}{2}\frac{^*\partial h_{ik}}{\partial t} , \tag{6}$$

the chr.inv.-vector of the observable gravitational inertial force

$$F_i = \frac{c^2}{c^2 - w}\left(\frac{\partial w}{\partial x^i} - \frac{\partial v_i}{\partial t}\right) , \tag{7}$$

the chr.inv.-tensor of the angular velocity of the observable rotation of the space (the space non-holonomity tensor)

$$A_{ik} = \frac{1}{2}\left(\frac{\partial v_k}{\partial x^i} - \frac{\partial v_i}{\partial x^k}\right) + \frac{1}{2c^2}\left(F_i v_k - F_k v_i\right) , \tag{8}$$

where $h_{ik} = -g_{ik} + \frac{g_{0i}g_{0k}}{g_{00}} = -g_{ik} + \frac{1}{c^2}v_i v_k$ is the observable spatial chr.inv.-metric tensor, $v_i = -\frac{c\,g_{0i}}{\sqrt{g_{00}}}$ is the linear velocity of the rotation of the observer's space reference, $w = c^2(1 - \sqrt{g_{00}})$ is the gravitational potential. The quantity $C_{ik} = h^{mn}C_{imkn}$ is built on the tensor of the observable three-dimensional chr.inv.-curvature of the space

$$C_{imkn} = H_{imkn} - \frac{1}{c^2}\left(2A_{mi}D_{nk} + A_{in}D_{mk} + \right.$$
$$\left. + A_{nm}D_{ik} + A_{mk}D_{in} + A_{ki}D_{mn}\right) , \tag{9}$$

which possesses all the properties of the Riemann-Christoffel curvature tensor $R_{\alpha\beta\gamma\delta}$ in the observer's spatial section, and constructed with the use $H_{lkij} = h_{jm}H_{lki\cdot}^{\cdots m}$, where $H_{lki\cdot}^{\cdots m}$ is the chr.inv.-tensor similar to Schouten's tensor [5]

$$H_{lki\cdot}^{\cdots m} = \frac{^*\partial\Delta_{il}^j}{\partial x^k} - \frac{^*\partial\Delta_{kl}^j}{\partial x^i} + \Delta_{il}^m\Delta_{km}^j - \Delta_{kl}^m\Delta_{lm}^j , \tag{10}$$

while Δ_{ij}^k are the observable chr.inv.-Christoffel symbols

$$\Delta_{ij}^k = h^{km}\Delta_{ij,m} = \frac{1}{2}\left(\frac{^*\partial h_{im}}{\partial x^j} + \frac{^*\partial h_{jm}}{\partial x^i} - \frac{^*\partial h_{ij}}{\partial x^m}\right) . \tag{11}$$

In the formulae $\frac{^*\partial}{\partial x^i} = \frac{\partial}{\partial x^i} - \frac{1}{c^2}\frac{^*\partial}{\partial t}$ and $\frac{^*\partial}{\partial t} = \frac{1}{\sqrt{g_{00}}}\frac{^*\partial}{\partial t}$ are the chr.inv.-spatial derivative and the chr.inv.-time derivative respectively, while ${}^*\nabla_i$ is the spatial chr.inv.-covariant derivative, for instance, the chr.inv.-divergence of a chr.inv.-vector is ${}^*\nabla_i\,q^i = \frac{^*\partial q^i}{\partial x^i} + q^i\frac{^*\partial\ln\sqrt{h}}{\partial x^i} = \frac{^*\partial q^i}{\partial x^i} + q^i\Delta_{ji}^j$. See [3, 4] or [2] for the details.

We have obtained [1] for the metric (1) the non-zero components of the observable chr.inv.-metric tensor

$$h_{11} = 1 + \frac{2GM}{c^2 r} , \qquad h_{22} = r^2\left(1 + \frac{\omega^2 r^2}{c^2}\right) ,$$
$$h_{23} = \frac{\omega r^2 v}{c^2} , \qquad h_{33} = 1 ,$$
$$h^{11} = 1 - \frac{2GM}{c^2 r} , \qquad h^{22} = \frac{1 - \frac{\omega^2 r^2}{c^2}}{r^2} , \tag{12}$$
$$h^{23} = -\frac{\omega v}{c^2} , \qquad h^{33} = 1 ,$$

nonzero components of F^i and A_{ik}

$$F^1 = \left(\omega^2 r - \frac{GM}{r^2}\right)\left(1 + \frac{\omega^2 r^2}{c^2}\right) ,$$
$$A^{12} = \frac{\omega}{r}\left(1 - \frac{2GM}{c^2 r} + \frac{\omega^2 r^2}{2c^2}\right) , \quad A^{31} = \frac{\omega^2 v r}{c^2} , \tag{13}$$

and non-zero components of C_{ik}

$$C_{11} = -\frac{GM}{c^2 r^3} + \frac{3\omega^2}{c^2} , \quad C_{22} = -\frac{GM}{c^2 r} + \frac{3\omega^2 r^2}{c^2} . \tag{14}$$

Let's substitute the components of F_i, A_{ik}, C_{ik} and the chr.inv.-derivatives into the chr.inv.-Einstein equations (3), (4), and (5). We obtain

$$\omega^2 + \frac{GM}{r^3} + \frac{2\omega^4 r^2}{c^2} - \frac{3\omega^2 GM}{c^2 r} = -\frac{\kappa}{2}\left(\rho c^2 + U\right) + \widetilde{\lambda}c^2 ; \tag{15}$$

$$\kappa J^1 = 0 ; \quad \kappa J^2 = \frac{5\omega GM}{c^2 r^3} ; \quad \kappa J^3 = -\frac{2\omega^2 v}{c^2} ; \tag{16}$$

$$\frac{3GM}{r^3} + \frac{6\omega^4 r^2}{c^2} - \frac{\omega^2 GM}{c^2 r} + \frac{6G^2 M^2}{c^2 r^4} =$$
$$= \left[\frac{\kappa}{2}\left(\rho c^2 - U\right) + \widetilde{\lambda}c^2\right]\left(1 + \frac{2GM}{c^2 r}\right) + \kappa U_{11} ; \tag{17}$$

---

*As probable $\widetilde{\lambda} \sim \frac{1}{R^2}$, where R is the spatial radius of a given region, so the larger the size of a considered region, the smaller is λ. See [2].
[†]The spatial (three-dimensional) indices are $i, k = 1, 2, 3$.

$$\frac{9\omega^4 r^4}{c^2} - \frac{9\omega^2 GM}{c^2 r} + \frac{2G^2 M^2}{c^2 r^2} =$$
$$= \left[\frac{\kappa}{2}\left(\rho c^2 - U\right) + \widetilde{\lambda}c^2\right] r^2 \left(1 + \frac{\omega^2 r^2}{c^2}\right) + \kappa U_{22}; \qquad (18)$$

$$\frac{\omega^3 \mathrm{v} r^2}{c^2} - \frac{\omega\mathrm{v} GM}{c^2 r} = \left[\frac{\kappa}{2}\left(\rho c^2 - U\right) + \widetilde{\lambda}c^2\right]\frac{\omega\mathrm{v} r^2}{c^2} + \kappa U_{23}; \quad (19)$$

$$\frac{\kappa}{2}\left(\rho c^2 - U\right) + \widetilde{\lambda}c^2 + \kappa U_{33} = 0. \qquad (20)$$

Equations (15–20) are written for an arbitrary energy-momentum tensor $T_{\alpha\beta}$. As is well known, the left side of the Einstein equations must have a positive sign. We therefore conclude, from the first (scalar) chr.inv.-Einstein equation (15), that the cosmological term $\widetilde{\lambda}$ must be $\widetilde{\lambda} \geqslant 0$. (If $\widetilde{\lambda} > 0$, the non-Newtonian λ-force is the force of repulsion). So, in order to have the metric (1) satisfy the Einstein equations, we can have only the repulsive non-Newtonian forces in the given region described by the metric (1).

We express the right side of the general covariant Einstein equations (2) as the algebraic sum of two tensors

$$\kappa\widetilde{T}_{\alpha\beta} = \kappa T_{\alpha\beta} - \frac{\widetilde{\lambda}}{\kappa}g_{\alpha\beta}, \qquad (21)$$

where the first tensor describes a substance, while the second describes vacuum (λ-fields). We assume that the given space is permeated by only λ-fields, i. e. $T_{\alpha\beta} = 0$. In such a case the observable components of the energy-momentum tensor of vacuum are

$$\widetilde{\rho} = -\frac{\widetilde{\lambda}}{\kappa}, \qquad \widetilde{J}^i = 0, \qquad \widetilde{U}^{ik} = \frac{\widetilde{\lambda}c^2}{\kappa}. \qquad (22)$$

We see that the observable density of vacuum $\widetilde{\rho} = \mathrm{const}$ is $\widetilde{\rho} < 0$, if $\widetilde{\lambda} > 0$ and $\widetilde{J}^i = 0$. So the $\widetilde{\lambda}$-vacuum is a medium with a negative constant density, and also no flows of mass (energy) therein.

We obtain from the the second (vector) chr.inv.-Einstein equation (16): $J^1 = 0$, $J^2 \neq 0$, $J^3 \neq 0$ ($J^3 < 0$), so $J^i \neq 0$ in general. Because $J^i = 0$ in vacuum, we conclude that:

> Any region of space described by the metric specifically along the trajectory of any orbiting body in the Universe cannot be pervaded solely by vacuum, but must also be permeated by another distributed substance.
>
> Orbital motion is the main kind of motion in the Universe. We therefore conclude that the space of the Universe must be non-empty; necessarily filled by a substance (e. g. gas, dust, radiations, etc.). Being a direct deduction from the Einstein equations, this is one more fundamental fact predicted by Einstein's General Theory of Relativity.

Naturally, as astronomical observations in recent decades testify, such substances as gas, dust and radiations are found in any part of that region of the Universe that is accessible by modern astronomical techniques. We therefore aim

to describe the medium pervading space, by means of the algebraical sum of two energy-momentum tensors

$$T_{\alpha\beta} = T_{\alpha\beta}^{(\mathrm{g})} + T_{\alpha\beta}^{(\mathrm{em})}, \qquad (23)$$

where $T_{\alpha\beta}^{(\mathrm{em})}$ is set up for electromagnetic radiations as in [6], while $T_{\alpha\beta}^{(\mathrm{g})}$ describes an ideal liquid or gas

$$T_{\alpha\beta}^{(\mathrm{g})} = \left(\rho_{(\mathrm{g})} - \frac{p}{c^2}\right) b^\alpha b^\beta - \frac{p}{c^2}\, g^{\alpha\beta}, \qquad (24)$$

where $\rho_{(\mathrm{g})}$ is the observable density of the medium, p is the pressure within it, while $b^\alpha = \frac{dx^\alpha}{ds}$ is the four-dimensional velocity of the flow of the medium with respect to the reference space (reference body). Gas is a medium in which particles move chaotically with respect to each other, and also with respect to an observer's reference space. So a reference space doesn't accompany to flow of mass (energy) in the gas.

The observable components of $T_{\alpha\beta}^{(\mathrm{g})}$ are

$$\frac{T_{00}}{g_{00}} = \frac{\rho_{(\mathrm{g})} - \frac{p}{c^2}}{1 - \frac{*u^2}{c^2}} - \frac{p}{c^2}, \qquad J^i = \frac{\rho_{(\mathrm{g})} - \frac{p}{c^2}}{1 - \frac{*u^2}{c^2}}\,{}^*u^i,$$
$$U^{ik} = \frac{\left(\rho_{(\mathrm{g})} - \frac{p}{c^2}\right){}^*u^i {}^*u^k}{1 - \frac{*u^2}{c^2}} + p\,h^{ik}, \qquad (25)$$

while the trace of the stress-tensor U^{ik} is

$$U = \frac{\left(\rho_{(\mathrm{g})} - \frac{p}{c^2}\right){}^*u^2}{1 - \frac{*u^2}{c^2}} + 3p, \qquad (26)$$

where ${}^*u^i = \frac{dx^i}{d\tau}$ is the three-dimensional observable velocity of the flow of the medium (${}^*u^2 = {}^*u_i {}^*u^i = h_{ik}\,{}^*u^i {}^*u^k$).

A reference frame (space) where the flow stream of a mass is $q^i = c^2 J^i \neq 0$, doesn't accompany the medium. As seen from (16) and (25), given the case we are considering, ${}^*u^1 = 0$, while ${}^*u^2 \neq 0$ and ${}^*u^3 \neq 0$. Hence:

> If a body orbits at a radius r in the z-direction, a substantive medium that necessarily pervades the space has motions in the φ and z-directions (in the cylindrical spatial coordinates r, φ, z).

2 Maxwell's equations in a rotating space: a body can orbit only if there is a non-zero interplanetary or interstellar magnetic field along the trajectory

What structure is attributed to an electromagnetic field if the field fills the local space of an orbiting body? As is well known, the energy-momentum tensor of an electromagnetic field has the form [6]

$$T_{\alpha\beta}^{(\mathrm{em})} = \frac{1}{4\pi c^2}\left(-F_{\alpha\sigma}F_{\cdot\beta}^{\sigma} + \frac{1}{4}F_{\sigma\tau}F^{\sigma\tau}g_{\alpha\beta}\right), \qquad (27)$$

where $F_{\alpha\beta} = \frac{1}{2}\left(\frac{\partial A_\beta}{\partial x^\alpha} - \frac{\partial A_\alpha}{\partial x^\beta}\right)$ is Maxwell's electromagnetic field tensor, while A^α is the four-dimensional electromagnetic field potential given the observable chr.inv.-projections

$\varphi = \frac{A_0}{\sqrt{g_{00}}}$ and $q^i = A^i$ (the scalar and vector three-dimensional chr.inv-potentials). The observable chr.inv.-components of $T_{\alpha\beta}^{(\mathrm{em})}$ obtained in [2] are

$$\rho_{(\mathrm{em})} = \frac{E^2 + H^{*2}}{8\pi c^2}, \quad J_{(\mathrm{em})}^i = \frac{1}{4\pi c}\, \varepsilon^{ikm} E_k H_{*m}\,,$$

$$U_{(\mathrm{em})}^{ik} = \rho_{(\mathrm{em})} h^{ik} - \frac{1}{4\pi}\left(E^i E^k + H^{*i} H^{*k}\right), \qquad (28)$$

$$U_{(\mathrm{em})} = \rho_{(\mathrm{em})}\,,$$

where E_i and the H^{*i} are the observable chr.inv.-electric and magnetic field strengths, which are the chr.inv.-projections of the electromagnetic field tensor $F_{\alpha\beta}$ (read Chapter 3 in [2] for the details):

$$E_i = \frac{{}^*\partial\varphi}{\partial x^i} + \frac{1}{c}\frac{{}^*\partial q^i}{\partial t} - \frac{\varphi}{c^2} F^i, \qquad (29)$$

$$H^{*i} = \frac{1}{2}\varepsilon^{imn} H_{mn} = \frac{1}{2}\varepsilon^{imn}\left(\frac{{}^*\partial q_m}{\partial x^n} - \frac{{}^*\partial q_n}{\partial x^m} - \frac{2\varphi}{c} A_{mn}\right). \quad (30)$$

We consider electromagnetic fields that fill the space as electromagnetic waves — free fields without the sources that induced them. By the theory of fields, in such an electromagnetic field the electric charge density and the current density vector are zero. In such a case Maxwell's equations have the chr.inv.-form [2]:

$$\left.\begin{aligned}{}^*\nabla_i E^i - \frac{2}{c}\,\Omega_m H^{*m} &= 0 \\[4pt] \varepsilon^{ikm}\,{}^*\widetilde{\nabla}_k\left(H_{*m}\sqrt{h}\right) - \frac{1}{c}\frac{{}^*\partial}{\partial t}\left(E^i\sqrt{h}\right) &= 0\end{aligned}\right\}\mathrm{I} \quad (31)$$

$$\left.\begin{aligned}{}^*\nabla_i H^{*i} + \frac{2}{c}\,\Omega_m E^{*m} &= 0 \\[4pt] \varepsilon^{ikm}\,{}^*\widetilde{\nabla}_k\left(E_m\sqrt{h}\right) + \frac{1}{c}\frac{{}^*\partial}{\partial t}\left(H^{*i}\sqrt{h}\right) &= 0\end{aligned}\right\}\mathrm{II} \quad (32)$$

where $H_i = \frac{1}{2}\varepsilon_{imn}H^{mn}$, and ${}^*\widetilde{\nabla}_k = {}^*\nabla_k - \frac{1}{c^2}F_k$ denotes the chr.inv.-physical divergence.

Because of the ambiguity of the four-dimensional potential A^α, we can choose for $\varphi = 0$ [6]. A space wherein the metric (1) is stationary, gives $\frac{{}^*\partial q^i}{\partial t} = 0$. Because the components of $g_{\alpha\beta}$ depend solely on $x^1 = r$ of the spatial coordinates r, φ, z, the components of the energy-momentum tensor depend only on r. In such a case we obtain, from formulae (29) and (30), $E_i = 0$, $H^{*1} = H_{*1} = 0$, $H^{*2} = \frac{1}{\sqrt{h}}\frac{\partial q_3}{\partial r}$ and $H^{*3} = -\frac{1}{\sqrt{h}}\frac{\partial q_2}{\partial r}$, so the aforementioned chr.inv.-Maxwell equations take the form

$$\Omega_m H^{*m} = 0\,,$$
$$\varepsilon^{ikm}\,{}^*\widetilde{\nabla}_k\left(H_{*m}\sqrt{h}\right) = 0\,, \qquad (33)$$
$${}^*\nabla_i H^{*i} = 0\,.$$

We substitute into the first of these equations the values $\Omega_1 = 0$, $\Omega_2 = \frac{\omega^2 r \mathrm{v}}{c^2}$ and $\Omega_3 = \frac{\omega}{r}\left(1 - \frac{2GM}{c^2 r} + \frac{\omega^2 r^2}{2c^2}\right)$ we have

calculated for the metric (1). As a result we obtain a correlation between two components of the electromagnetic field vector chr.inv.-potential q^i, that is

$$q_2' = \frac{\omega \mathrm{v} r^2}{c^2}\, q_3'\,, \qquad (34)$$

where the prime denotes the differentiation with respect to r.

With the use of (30) we obtain H_{*2} and H_{*3}

$$H_{*2} = r\left(1 - \frac{GM}{c^2 r} + \frac{\omega^2 r^2}{2c^2}\right) q_3'\,, \quad H_{*3} = 0\,, \qquad (35)$$

so the second equation of (33) takes the form

$$rq_3''\left(1 - \frac{GM}{c^2 r} + \frac{\omega^2 r^2}{2c^2}\right) + q_3'\left(2 - \frac{GM}{c^2 r} + \frac{2\omega^2 r^2}{c^2}\right) = 0, \quad (36)$$

while the third equation of (33) is satisfied identically.

Equation (36) has separable variables, and so can be rewritten as follows

$$\frac{dy}{y} = -\frac{dr}{r}\left(1 + \frac{3\omega^2 r^2}{2c^2}\right), \qquad (37)$$

where $y = q_3'$. Integrating it, we obtain

$$y = q_3' = \frac{K}{r}\, e^{-\frac{3\omega^2 r^2}{4c^2}} \approx \frac{K}{r}\left(1 - \frac{3\omega^2 r^2}{4c^2}\right), \qquad (38)$$

where K is a constant of integration. Assuming $r = r_0$ and $y_0 = q_{3(0)}$ at the initial moment of time, we determine the constant: $K = y_0 r_0 \left(1 + \frac{3\omega^2 r_0^2}{4c^2}\right)$. Integrating (38), we have

$$q_3 = K\left(\ln r - \frac{3\omega^2 r^2}{8c^2}\right) + L\,, \quad L = \mathrm{const.} \qquad (39)$$

Determining the integration constant L from the initial conditions, we obtain the final expression for q_3:

$$q_3 = K\left[\ln\frac{r}{r_0} - \frac{3\omega^2}{8c^2}\left(r^2 - r_0^2\right)\right] + q_3(0)\,, \qquad (40)$$

where $q_3(0)$ is the initial value of q_3. Substituting (40) into (34) we obtain the equation

$$q_2' = \frac{\omega \mathrm{v} K r}{c^2}\,, \qquad (41)$$

which is easily integrated to

$$q_2 = \frac{\omega \mathrm{v} K}{2c^2}\left(r^2 - r_0^2\right). \qquad (42)$$

Finally, we calculate the non-zero components of the magnetic strength chr.inv.-vector H^{*i}. Substituting the obtained formulae for q_3' (38) and q_2' (41) into the definition of H^{*i} (30), we obtain

$$H^{*2} = \frac{1}{\sqrt{h}}H_{31} = q_3'(0)\left(1 - \frac{GM}{c^2 r} - \frac{\omega^2 r^2}{2c^2} + \frac{3\omega^2 r_0^2}{4c^2}\right),$$
$$\hspace{10cm} (43)$$
$$H^{*3} = \frac{1}{\sqrt{h}}H_{12} = -\frac{\omega \mathrm{v} r_0}{c^2}\, q_3'(0)\,.$$

This is the solution for H^{*i}, the magnetic strength chr. inv.-vector, obtained from the chr.inv.-Maxwell equations in the rotating space of an orbiting body. The solution we have obtained shows that:

> A free electromagnetic field along the trajectory of an orbiting body ($\omega \neq 0$, $v \neq 0$) cannot be zero, and is represented by purely magnetic "standing" waves (all components of the electric strength are $E^i = 0$).

This fundamental conclusion is easily obtained from the solution (43).

The linear velocity v of the orbiting body (the body moves in the $x^3 = z$-direction) produces effects in only the q_2-component of the three-dimensional observable vector potential (i. e. along the φ-direction).

The solution (43) exists only if the initial value of the derivative with respect to r of the z-component of the three-dimensional observable vector potential is $q_3'(0) \neq 0$.

The z-component $H^{*3} \neq 0$ if the reference body (in common with the observer) moves in the $x^3 = z$-direction at a linear velocity v and, at the same time, rotates orthogonally to it in the $x^2 = \varphi$-direction at an angular velocity ω. The component H^{*3} is positive, if v is negative. So H^{*3} is directed opposite to the motion of the observer (and his reference planet, the Earth for instance). The numerical value of H^{*3} is $\sim 8 \times 10^{-8}$ of H^{*2}. If the reference planet has its orbit "stopped" in the z-direction (a purely theoretical case), only $H^{*2} \neq 0$ is left because it depends on $\frac{GM}{c^2 r}$ and $\frac{\omega^2 r^2}{2c^2}$.

The stationary solution (43) of the chr.inv.-Maxwell equations describes standing magnetic waves in the φ- and z-directions. In such a case, as follows from the condition $E_i = 0$, the Pointing vector (the density of the impulse of the electromagnetic field) is $J_{(\text{em})}^i = 0$ (see formula 28). On the other hand the Einstein equations (15–20) we have obtained for the rotating space of an orbiting body (the same space as that used for the Maxwell equation) have the density of the impulse of matter $J^i \neq 0$ (see formula 16 in the Einstein equations), which should be applicable to any distribution of matter, including electromagnetic fields. This implies that:

> In the rotating space of an orbiting body, electromagnetic fields don't satisfy the Einstein equations if there is no distribution of another substance (dust, gas or something else) in addition to the fields.

As follows from (25) we have obtained in the metric considered, $J^i \neq 0$ for an ideal liquid or gas. So, if an electromagnetic field is added by a gaseous medium (for instance), they can together satisfy the Einstein equations in the rotating space of an orbiting body. We therefore conclude that:

> Interplanetary/interstellar space where space bodies are orbiting, must be necessarily pervaded by electromagnetic fields with a concomitant distribution of substantial matter, such as a gaseous medium, for instance.

We have actually shown that space bodies cannot undergo orbital motion in empty space, i. e. if electromagnetic fields and other substantive media (e. g. dust, gas, etc.) are not present. What a bizarre result!

It should be noted that we have obtained this startling conclusion using no preliminary proposition or hypothesis. This conclusion follows directly from the requirement for Maxwell's equations and Einstein's equations to be both satisfied in the rotating space of an orbiting body. So this is the *actual condition for orbital motion*, according to General Relativity.

3 Preferred spatial directions as a result of the interaction of the space non-holonomity fields

In this section we have to consider three problems arising from the specific space structure we have obtained for orbital motion.

First problem. Refer to the chr.inv.-Einstein equations (15–20) we have obtained in the rotating space of an orbiting body. The most significant terms in the left side of the scalar equation (15) are the first two. They both have a positive sign. Hence the right side of equation (15) must also be positive, i. e. the right side must satisfy the condition,

$$\widetilde{\lambda} c^2 > \frac{\kappa}{2} \left(\rho c^2 + U \right). \tag{44}$$

Let's apply this condition to a particular case of the orbiting body spaces: the space within the corridor along which the Earth orbits in the Galaxy. As a matter fact, this space is governed by the metric (1). In this space we have, $\omega^2 = 4 \times 10^{-14} \sec^{-2}$, $M = M_\odot = 2 \times 10^{33}$ g, $r = 15 \times 10^{12}$ cm. We obtain, $\omega^2 + \frac{GM}{r^3} \simeq 8 \times 10^{-14} \sec^{-2}$. Therefore

$$\widetilde{\lambda} c^2 > 8 \times 10^{-14} \, \text{cm}^{-2}, \qquad \widetilde{\lambda} > 10^{-34} \, \text{cm}^{-2}. \tag{45}$$

As a result $\widetilde{\lambda} > 10^{-34}$ cm^{-2} numerically equals $\frac{\omega^2}{2c^2}$ — the quantity which was proven in [7] to be the square of the dynamical "magnetic" strength of the field of the space non-holonomity. We therefore conclude that the $\widetilde{\lambda}$-field is connected to the non-holonomity field of the Earth's space.

We note that the Earth's space is non-holonomic due to the effect of a number of factors such as the daily rotation of the Earth, its yearly rotation around the Sun, its common rotation with the solar system around the centre of the Galaxy, etc. Each factor produces a field of non-holonomity, the algebraical sum of which gives the complete field of non-holonomity of the Earth.

Given the problem statement we are considering, the obtained numerical value $\widetilde{\lambda} > 10^{-34}$ cm^{-2} characterizing the non-Newtonian force of repulsion is attributed to the non-holonomity field of the Earth's space which is caused by the Earth's rotation around the Sun. If other problem statements are considered, we can calculate the numerical values of $\widetilde{\lambda}$ characterizing the other factors of the Earth's space non-holonomity. The non-Newtonian forces of repulsion obtained

therein are expected to be directed according to the acting factors (in different directions), so the numerical value of each $\widetilde{\lambda}$ has its own meaning, whilst their sum builds the common non-Newtonian repulsing force acting in the Earth's space.

Second problem. As follows from the scalar Einstein equation (16), the density of the impulse of the distributed matter in the $x^3 = z$-direction

$$J^3 = -\frac{2\omega^2 \mathrm{v}}{\kappa c^2} \qquad (46)$$

has a negative numerical value. So the flow of the distributed medium that fills the space is directed opposite to the orbital motion. In other words, according to the theory, the orbiting body should meet a counter-flow by the medium: a "relativistic braking" should be expected in orbital motions. Because the orbiting bodies, e. g. the stars, the planets and the satellites, show no such orbital braking, we propose a mechanism that refurbishes the braking energy of the medium into another sort of energy — heat or radiations, for instance.

This conclusion finds verification in recent theoretical research which, by means of General Relativity, indicates that stars produce energy due to the background space non-holonomity [8, 9]. It is shown in papers [8, 9], that General Relativity, in common with topology, predicts that the most probable configuration of the background space of the Universe is globally non-holonomic. The global anisotropic effect is expected to manifest as the anisotropy of the Cosmic Microwave Background Radiation and the anisotropy of the observable velocity of light. Moreover, if the global non-holonomic background is perturbed by a local rotation or oscillation (local non-holonomic fields), the background field produces energy in order to compensate for the perturbation in it. Such an energy producing mechanism is expected to be operating in stars, in the process of transfer of radiant energy from the central region to the surface, which has verification in the data of observational astrophysics [9].

From the standpoint of our theory herein, the aforementioned mechanism producing stellar energy [8, 9] is due to a number of factors that build the background space non-holonomity field in stars, not only the globally non-holonomic field of the Universe. By our theory, the substantive distribution is also connected to the space non-holonomity so that the braking energy of the medium is related to the space non-holonomity field. So a star, being in orbit in the Galaxy and the group of galaxies, meets the non-holonomity fields produced by the rotations of the Galactic space, the Local Group of galaxies, etc. Then the braking energy of the medium that fills the spaces (the same as for the energy of the space non-holonomic field) transforms into heat and radiations within the star by the stellar energy mechanism as shown in [8, 9]. In other words, a star "absorbs" the energy of the non-holonomity fields of the spaces wherein it is orbiting, then transforms the energy into heat and radiations.

Employing this mechanism in an Earth-bound laboratory, we can obtain a new source of energy due to the fact that the Earth orbits in the non-holonomic fields of the space.

Third problem. A relative variation of the observable velocity of light in the z-direction we have obtained in [1] is

$$\frac{\Delta \dot{z}}{c} = 2 \times 10^{-4} \sin 2\widetilde{\omega}\tau \,, \qquad (47)$$

where $\widetilde{\omega} = \omega \left(1 + \frac{\mathrm{v}}{c}\right)$, whilst given an Earth-bound laboratory the space rotation thereof is the sum of the Earth's rotations around the Sun and around the centre of the Galaxy. We see therefore, that we have a relative variation $\frac{\Delta \dot{z}}{c} \neq 0$ of the observable velocity of light only if both $\omega \neq 0$ and $\mathrm{v} \neq 0$. Hence the predicted anisotropy of the observable velocity of light depends on the interaction of two fields of non-holonomity that are represented in the laboratory space (within the framework of the considered problem statement).

The same is true for the flow of matter distributed throughout the space (46): $J^3 \neq 0$ only if both $\omega \neq 0$ and $\mathrm{v} \neq 0$. Thus the energy produced in a star due to the background space non-holonomity should be dependent not only on the absolute value of the non-holonomity (as the sum of all acting non-holonomic fields), but also on the interaction between the non-holonomic fields.

References

1. Borissova L. Preferred spatial directions in the Universe: a General Relativity approach. *Progress in Physics*, 2006, v. 4, 51–58.

2. Borissova L., Rabounski D. Fields, vacuum, and the mirror Universe. Editorial URSS, Moscow, 2001; CERN, EXT-2003-025.

3. Zelmanov A. L. Chronometric invariants. Dissertation thesis, 1944. American Research Press, Rehoboth (NM), 2006.

4. Zelmanov A. L. Chronometric invariants and co-moving co-ordinates in the general relativity theory. *Doklady Acad. Nauk USSR*, 1956, v. 107(6), 815–818.

5. Schouten J. A., Struik D. J. Einführung in die neuren Methoden der Differentialgeometrie. *Zentralblatt für Mathematik*, 1935, Bd. 11 und Bd. 19.

6. Landau L. D. and Lifshitz E. M. The classical theory of fields. Butterworth–Heinemann, 2003, 428 pages (4th final edition, revised and expanded).

7. Rabounski D. A theory of gravity like electrodynamics. *Progress in Physics*, 2005, v. 2, 15–29.

8. Rabounski D. Thomson dispersion of light in stars as a generator of stellar energy. *Progress in Physics*, 2006, v. 4, 3–10.

9. Rabounski D. A source of energy for any kind of star. *Progress in Physics*, 2006, v. 4, 19–23.

Multi-Spaces and Many Worlds from Conservation Laws

Giuseppe Basini* and Salvatore Capozziello†

*Laboratori Nazionali di Frascati, INFN, Via E. Fermi C.P. 13, I-0044 Frascati (Roma) Italy

‡Dipartimento di Scienze Fisiche, Università di Napoli "Federico II", and INFN, Sez. di Napoli
Complesso Universitario di Monte S. Angelo, Via Cinthia, Edificio N-I-80126 Napoli, Italy

Corresponding author, e-mail: capozziello@na.infn.it

Many Worlds interpretation of Quantum Mechanics can be related to a General Conservation Principle in the framework of the so called Open Quantum Relativity. Specifically, conservation laws in phase space of physical systems (e. g. minisuperspace) give rise to natural selection rules by which it is possible to discriminate among physical and unphysical solutions which, in the specific case of Quantum Cosmology, can be interpreted as physical and unphysical universes. We work out several examples by which the role of conservation laws is prominent in achieving the solutions and their interpretation.

1 Introduction

The issue to achieve a unified field theory cannot overcome to take into account the role and meaning of conservation laws and dynamical symmetries which have always had a fundamental role in physics. From a mathematical viewpoint, their existence allows to "reduce" the dynamics and then to obtain first integrals of motion, which often allow the exact solution of the problem of motion. Noether theorem is a prominent result in this sense, since it establishes a deep link between conservation laws and symmetries. Moreover, conservation laws can play a deep role in the definition of physical theories and, in particular, to define space-times which are of *physical interest*. The underlying philosophy is the fact that the violation of conservation laws (and then the symmetry breaking) could be nothing else but an artificial tool introduced in contemporary physics in order to solve phenomenologically some puzzles and problems, while effective conservation laws are never violated [1]. The absolute validity of conservation laws, instead, allows the solution of a wide variety of phenomena ranging from entanglement of physical systems [2], to the rotation curves of spiral galaxies [4]. Such results do not come from some *a priori* request of the theory, but is derived from the existence of a *General Conservation Law* (in higher dimensional space-time) where no violation is allowed [5]. This approach naturally leads to a dynamical unification scheme (the so called Open Quantum Relativity [1]) which can be, as a minimal extension, formulated in 5D [6]. In this context, it is worth stressing the deep relations among symmetries and first integrals of motion, conservation laws with the number and dimensionality of configuration spaces. In fact, phenomena, which in standard physics appear as due to symmetry breakings can be encompassed in a multi-space formulation as previously shown by Smarandache [7, 8]. On the other hand, the need of a multi-space formulation of the theory gives rise

to a direct application of the "Many Worlds" Interpretation of Quantum Mechanics [9, 10], in the sense that multi-spaces are nothing else but many worlds in the framework of Quantum Cosmology [11]. This is the argument of this paper: we want to show that configuration spaces derived from the request of integrability of the dynamical systems (and then from the presence of conservation laws) are physical universes, (i. e. observable universes) where cosmological parameters can be observed. On the other hand, if conservation laws are not present, in universes which come out in a Many Worlds interpretation are "unphysical" that is, it is not possible to label them by a set of observable cosmological parameters (technically they are "instanton-solutions"). In Sect. 2, we develop mathematical considerations on conservation laws showing how the presence of symmetries allows the integration of the dynamical systems, which means that the phase-space (and general solution) can be "split" in a multi-space of "integrated" components. Sect. 3 is devoted to the discussion of Many Worlds interpretation of Quantum Cosmology and, in particular, to the fact that multi-spaces related to the phase-space of conservation laws can be interpreted as "minisuperspaces" thanks to the Hartle criterion. Many Worlds-solutions from conservation laws are obtained in Sect. 4 by integrating the Wheeler-DeWitt (WDW) equation of Quantum Cosmology. Conclusions are drawn in Sect. 5.

2 Conservation laws and multi-spaces

Before considering multi-spaces and how they can be interpreted as the Many Worlds of Quantum Cosmology, let us discuss the reduction problem of dynamics connected symmetries and conservation laws. Our issue is to show that the total phase-space of a given dynamical system can be split in many subspaces, each of them related to a specific conserved quantity. As a general remark, it is possible to

show that if the Lie derivative of a given geometric quantity (e. g. vector, tensor, differential form) is zero, such a quantity is conserved. This property is *covariant* and specifies the number of dimensions and the nature of configuration space (and then of the phase-space) where the given dynamical system is defined. Furthermore, the existence of conserved quantities always implies a *reduction* of dynamics which means that the order of equations of motion is reduced thanks to the existence of first integrals. Before considering specific systems, let us remind some properties of the Lie derivative and how conservation laws are related to it. Let L_X be the Lie derivative

$$(L_X \omega)\,\xi = \frac{d}{dt}\,\omega\,(g^t_* \xi)\,, \tag{1}$$

where ω is a differential form of $\mathfrak{R}^n$ defined on the vector field ξ, g^t_* is the differential of the phase flux $\{g_t\}$ given by the vector field X on a differential manifold $\mathfrak{M}$. The discussion can be specified by considering a Lagrangian $\mathcal{L}$ which is a function defined on the tangent space of configurations $T\mathfrak{Q} \equiv \{q_i, \dot{q}_i\}$, that is $\mathcal{L} : T\mathfrak{Q} \to \mathfrak{R}$. In this case, the vector field X is

$$X = \alpha^i(q)\,\frac{\partial}{\partial q^i} + \dot{\alpha}^i(q)\,\frac{\partial}{\partial \dot{q}^i}\,, \tag{2}$$

where the dot denotes the derivative with respect to t, and we have

$$L_X \mathcal{L} = X\mathcal{L} = \alpha^i(q)\,\frac{\partial \mathcal{L}}{\partial q^i} + \dot{\alpha}^i(q)\,\frac{\partial \mathcal{L}}{\partial \dot{q}^i}\,. \tag{3}$$

It is important to note that t is simply a parameter which specifies the evolution of the system. The condition

$$L_X \mathcal{L} = 0 \tag{4}$$

implies that the phase flux is conserved along X: this means that a constant of motion exists for $\mathcal{L}$ and a conservation law is associated to the vector X. In fact, by taking into account the Euler-Lagrange equations, it is easy to show that

$$\frac{d}{dt}\left(\alpha^i\,\frac{\partial \mathcal{L}}{\partial \dot{q}^i}\right) = L_X \mathcal{L}\,. \tag{5}$$

If (4) holds, the relation $\Sigma_0 = \alpha^i \frac{\partial \mathcal{L}}{\partial \dot{q}^i}$ identifies a constant of motion. Alternatively, using a generalized differential for the Lagrangian $\mathcal{L}$, the Cartan one–form, $\theta_\mathcal{L} \equiv \frac{\partial \mathcal{L}}{\partial \dot{q}^i}\,dq^i$ and defining the inner derivative $i_X \theta_\mathcal{L} = \langle \theta_\mathcal{L}, X \rangle$, we get

$$i_X \theta_\mathcal{L} = \Sigma_0 \tag{6}$$

if, again, condition (4) holds. This representation identifies cyclic variables. Using a point transformation on vector field (2), it is possible to get

$$\tilde{X} = (i_X dQ^k)\,\frac{\partial}{\partial Q^k} + \left[\frac{d}{dt}(i_X dQ^k)\right]\frac{\partial}{\partial \dot{Q}^k}\,. \tag{7}$$

From now on, Lagrangians and vector fields transformed by the non–degenerate transformation

$$Q^i = Q^i(q)\,, \qquad \dot{Q}^i(q) = \frac{\partial Q^i}{\partial q^j}\,\dot{q}^j \tag{8}$$

will be denoted by a tilde. If X is a symmetry for the Lagrangian $\mathcal{L}$, also $\tilde{X}$ is a symmetry for the Lagrangian $\tilde{\mathcal{L}}$ giving rise to a conserved quantity, thus it is always possible to choose a coordinate transformation so that

$$i_X dQ^1 = 1\,, \qquad i_X dQ^i = 0\,, \qquad i \neq 1\,, \tag{9}$$

and then

$$\tilde{X} = \frac{\partial}{\partial Q^1}\,, \qquad \frac{\partial \tilde{\mathcal{L}}}{\partial Q^1} = 0\,. \tag{10}$$

It is evident that Q^1 is a cyclic coordinate because dynamics can be reduced. Specifically, the "reduction" is connected to the existence of the second of (10). However, the change of coordinates is not unique and an opportune choice of coordinates is always important. Furthermore, it is possible that more symmetries are existent. In this case more cyclic variables must exist. In general, a reduction procedure by cyclic coordinates can be achieved in three steps: (i) we choose a symmetry and obtain new coordinates as above and after this first reduction, we get a new Lagrangian $\tilde{\mathcal{L}}$ with a cyclic coordinate; (ii) we search for new symmetries in this new space and iterate the reduction technique until it is possible; (iii) the process stops if we select a pure kinetic Lagrangian where all coordinates are cyclic. In such a case, the dynamical system is *completely integrable* and integration can be achieved along every coordinate of configuration space (or every generalized coordinate-conjugate momentum couple of phase space). In this case, the total phase-space is split in subspaces, each one *labelled* by a conserved quantity. Technically, every symmetry selects a constant conjugate momentum since, by the Euler–Lagrange equations we get

$$\frac{\partial \tilde{\mathcal{L}}}{\partial Q^i} = 0 \Longleftrightarrow \frac{\partial \tilde{\mathcal{L}}}{\partial \dot{Q}^i} = \Sigma_i\,, \tag{11}$$

and the existence of a constant conjugate momentum means that a cyclic variable (a symmetry) exists.

However, The Lagrangian $\mathcal{L} = \mathcal{L}(q^i, \dot{q}^j)$ has to be non-degenerate, which means that the Hessian determinant has to be non-zero.

From the Lagrangian formalism, we can pass to the Hamiltonian one through the Legendre transformation

$$\mathcal{H} = \pi_j \dot{q}^j - \mathcal{L}(q^j, \dot{q}^j)\,, \qquad \pi_j = \frac{\partial \mathcal{L}}{\partial \dot{q}^j}\,, \tag{12}$$

defining, respectively, the Hamiltonian function and the conjugate momenta. In the Hamiltonian formalism, the conservation laws are obtained when $[\Sigma_j, \mathcal{H}] = 0$, $1 \leqslant j \leqslant m$ This is the relation for conserved momenta and, in order to obtain a symmetry, the Hamilton function has to satisfy the relation

$L_\Gamma \mathcal{H} = 0$, where the vector Γ is defined by

$$\Gamma = \dot{q}^i \, \frac{\partial}{\partial q^i} + \ddot{q}^i \, \frac{\partial}{\partial \dot{q}^i} \,. \qquad (13)$$

Let us now go to the specific formalism of Quantum Mechanics which we will use for the following Quantum Cosmology considerations. By the Dirac canonical quantization procedure, we have

$$\pi_j \longrightarrow \hat{\pi}_j = -i\partial_j \,, \qquad \mathcal{H} \longrightarrow \hat{\mathcal{H}}(q^j, -i\partial_{q^j}) \,. \qquad (14)$$

If $|\Psi\rangle$ is a *state* of the system (i. e. its wave function), dynamics is given by the Schrödinger eigenvalue equation

$$\hat{\mathcal{H}} |\Psi\rangle = E |\Psi\rangle \,, \qquad (15)$$

where, obviously, the whole wave-function is given by $|\phi(t, x)\rangle = e^{iEt/\hbar} |\Psi\rangle$. If a symmetry exists, the reduction procedure outlined above can be applied and then, from (11) and (12), we get

$$\pi_1 \equiv \frac{\partial \mathcal{L}}{\partial \dot{Q}^1} = i_{X_1} \theta_{\mathcal{L}} = \Sigma_1 \,,$$
$$\pi_2 \equiv \frac{\partial \mathcal{L}}{\partial \dot{Q}^2} = i_{X_2} \theta_{\mathcal{L}} = \Sigma_2 \,, \qquad (16)$$
$$\dots \quad \dots \quad \dots \,,$$

depending on the number of symmetry vectors. After Dirac quantization, we get

$$-i\partial_1 |\Psi\rangle = \Sigma_1 |\Psi\rangle, \quad -i\partial_2 |\Psi\rangle = \Sigma_2 |\Psi\rangle, \quad \dots \qquad (17)$$

which are nothing else but translations along the Q^j axis singled out by the corresponding symmetry. Eqs. (17) can be immediately integrated and, being Σ_j real constants, we obtain oscillatory behaviors for $|\Psi\rangle$ in the directions of symmetries, i. e.

$$|\Psi\rangle = \sum_{j=1}^m e^{i\Sigma_j Q^j} |\chi(Q^l)\rangle \,, \qquad m < l \leqslant n \,, \qquad (18)$$

where m is the number of symmetries, l are the directions where symmetries do not exist and n is the number of dimensions of configuration space. Vice-versa, dynamics given by (15) can be reduced by (17) if, and only if, it is possible to define constant conjugate momenta as in (16), *i.e.* oscillatory behaviors of a subset of solutions $|\Psi\rangle$ exist as a consequence of the fact that symmetries are present in the dynamics. The m symmetries give first integrals of motion. In one and two–dimensional configuration spaces, the existence of a symmetry allows the complete solution of the problem. Therefore, if $m = n$, the problem is completely solvable and a symmetry exists for every variable of configuration space. The reduction procedure of dynamics, connected to the existence of symmetries, allows to select a subset of the general solution of equations of motion, where oscillatory behaviors

of the wave functions are found. In other words, symmetries select exact solutions and reduce dynamics. In these cases, the general solution of a dynamical system can be split in a combination of functions each of them depending on a given variable. As a corollary, a Lagrangian (or a Hamiltonian) where only kinetic terms are present gives always rise to a full integrable dynamics. The total phase-space $\mathcal{M}$ of the system, thanks to conservation laws, can be split in the tensor product of phase-spaces (multi-spaces) assigned by conserved momenta, i. e. $\{q_i, \pi_i\} \to \{Q_i, \Sigma_i\}$, and then $\mathcal{M} = \Pi_{i=1}^n \{Q_i, \bigotimes \Sigma_i\}$. As we will see, this feature is relevant in minisuperspace Quantum Cosmology.

3 The "many-worlds" interpretation of Quantum Mechanics and the role of conservation laws

The above considerations acquire a fundamental role in Minisuperspace Quantum Cosmology since, as we will see, Conservation Laws give rise to an approach by which it is possible to "select" physical universes. Quantum Cosmology is one of the results of the efforts of last thirty years directed to the quantization of gravity [12]. The aim has been to obtain a scheme in which gravity is treated on the same ground of the other interaction of Nature. Such an approach (not a coherent theory yet) is the *canonical quantization of gravity*. In order to test the theoretical results, Planck's scales, which cannot be reached by the current physics, have to be considered, so the cosmology is the most reasonable area for the application of the observable predictions of quantum gravity. More properly, Quantum Cosmology is the quantization of dynamical systems which are "*universes*". In this context, supposed the Universe as a whole (the ensemble of all the possible universes), it has a quantum mechanical nature and that an observable universe is only a limit concept valid in particular regions of a manifold (*superspace*) composed by all the possible space-like 3-geometries and local configurations of the matter fields. The task of Quantum Cosmology is to relate all the measurable quantities of the observable universe* to the assigned boundary conditions for a wave function in the superspace. This wave function has to be connected to the probability to obtain typical universes (even if, in the standard approach, it is not a proper probability amplitude since a Hilbert space does not exist in the canonical formulation of quantum gravity) [11]. Quantum Cosmology has to solve, in principle, the problem of the initial conditions of the standard cosmology: *i.e.* it should explain the observed universe, specifying the physical meaning of the boundary conditions of the superspace wave function. In other words, the main issue of quantum cosmology is to search for boundary conditions in agreement with the

---

*An operative definition of "observable universe" could be a universe where cosmological parameters as the Hubble one H_0, the deceleration parameter q_0, the density parameters Ω_M, Ω_Λ, Ω_k and the age t_0 can be inferred by observations [3].

astronomical observations and these conditions have to be contained in the wave function of the universe $|\Psi\rangle$. The dynamical behavior of $|\Psi\rangle$ in the superspace is described by the Wheeler-DeWitt (WDW) equation [12] that is a second order functional differential equation hard to handle, because it has infinite degrees of freedom. Usually attention has been concentrated on finite dimensional models in which the metrics and the matter fields are restricted to particular forms (*minisuperspace models*), like homogeneous and isotropic spacetimes. With these choices, the WDW equation becomes a second order partial differential equation which, possibly, can be exactly integrated. However, by definition, there is no *rest outside of the Universe* in cosmology, so that boundary conditions must be considered as a *fundamental law of physics* [11]. Moreover, not only the conceptual difficulties, but also the mathematical ones, make Quantum Cosmology hard to handle. For example, the superspace of geometrodynamics [13] has infinite degrees of freedom so that it is technically impossible to integrate the full infinite dimensional WDW equation. Besides, a Hilbert space of states describing the universe is not available [12]. Finally, it is not well established how to interpret the solutions of WDW equation in the framework of probability theory. Despite these still unsolved shortcomings, several positive results have been obtained and Quantum Cosmology has become a sort of *paradigm* in theoretical physics researches. For example the infinite-dimensional superspace can be restricted to opportune finite-dimensional configuration spaces called *minisuperspaces*. In this case, the above mathematical difficulties can be avoided and the WDW equation can be integrated. The so called *no boundary condition* by Harte and Hawking [14] and the *tunneling from nothing* by Vilenkin [15] give reasonable laws for initial conditions from which our observable universe could be started. The *Hartle criterion* [11] is an interpretative scheme for the solutions of the WDW equation. Hartle proposed to look for peaks of the wave function of the universe: if it is strongly peaked, we have correlations among the geometrical and matter degrees of freedom; if it is not peaked, correlations are lost. In the first case, the emergence of classical relativistic trajectories (*i.e.* universes) is expected. The analogy to the quantum mechanics is immediate. If we have a potential barrier and a wave function, solution of the Schrödinger equation, we have an oscillatory regime upon and outside the barrier while we have a decreasing exponential behavior under the barrier. The situation is analogous in Quantum Cosmology: now potential barrier has to be replaced by the superpotential $U(h^{ij}, \varphi)$, where h^{ij} are the components of the three–metric of geometrodynamics and φ is a generic scalar field describing the matter content. More precisely, the wave function of the universe can be written as

$$\Psi\big[h_{ij}(x), \phi(x)\big] \sim e^{im_P^2 S}, \qquad (19)$$

where m_p is the Planck mass and

$$S \equiv S_0 + m_P^{-2} S_1 + \mathrm{O}(m_P^{-4}) \qquad (20)$$

is the action which can be expanded. We have to note that there is no normalization factor due to the lack of a probabilistic interpretative full scheme. Inserting S into the WDW equation and equating similar power terms of m_p, one obtains the Hamilton-Jacobi equation for S_0. Similarly, one gets equations for $S_1, S_2 \ldots$, which can be solved considering results of previous orders giving rise to the higher order perturbation theory. We need only S_0 to recover the semi-classical limit of Quantum Cosmology [10]. If S_0 is a real number, we get oscillating WKB modes and the Hartle criterion is recovered since $|\Psi\rangle$ is peaked on a phase-space region defined by

$$\pi_{ij} = m_P^2 \frac{\delta S_0}{\delta h^{ij}}, \qquad \pi_\varphi = m_P^2 \frac{\delta S_0}{\delta \varphi}, \qquad (21)$$

where π_{ij} and π_φ are classical momenta conjugates to h^{ij} and φ. It is worth stressing, at this point, that such a momenta are nothing else but Conservation Laws. The semi-classical region of superspace, where Ψ has an oscillating structure, is the Lorentz one otherwise it is Euclidean*. In the latter case, we have $S = iI$ and

$$\Psi \sim e^{-m_P^2 I}, \qquad (22)$$

where I is the action for the Euclidean solutions of classical field equations (*istantons*). This scheme, at least at a semi-classical level, solves the problem of initial conditions. Given an action S_0, Eqs. (21) imply n free parameters (one for each dimension of the configuration space $\mathcal{Q} \equiv \{h^{ij}, \varphi\}$) and then n first integrals of motion exactly as in the scheme proposed in the previous section. However the general solution of the field equations involves $2n - 1$ parameters (one for each Hamilton equation of motion except the energy constraint). Consequently, the wave function is peaked on a subset of the general solution. In this sense, the boundary conditions on the wave function imply initial conditions for the classical solutions. In other words, the issue is searching for some general method by which selecting such constants of motion related to the emergence of classical trajectories without arbitrarily choosing regions of the phase-space where momenta are conserved. In this sense, there is a deep connection between the conservation laws and the structure of the wave function of the universe. Using the results of the previous section (see Eq. 18), the oscillatory regime, and then the correlation among the variables in the framework of the Hartle criterion, is guaranteed only if conservation laws are present into dynamics. In this context, if conservation laws are absolutely valid, the above *reduction procedure* gives rise to subsets of the infinite dimensional general solution of

---

*It is important to note that we are using both symbols $|\Psi\rangle$ and Ψ depending on the interpretation which we want to give to the wave function. In the first case, the wave function is considered a "quantum-state", in the second one, it has a semi-classical interpretation.

the WDW equation where oscillating behaviors are recovered. Viceversa, the Hartle criterion is always connected to the presence of a conservation law and then to the emergence of classical trajectories which are *observable universes* where cosmological observations are possible. Then the above result can be given in the following way:

> *In minisuperspace quantum cosmology, the existence of conservation laws yields a reduction procedure of dynamics which allows to find out oscillatory behaviors for the general solution of WDW equation. Viceversa, if a subset of the solution of WDW equation has an oscillatory behavior, conserved momenta have to exist and conservation laws are present. If a conservation law exists for every configuration variable, the dynamical system is completely integrable and the general solution of WDW equation is a superposition of oscillatory behaviors. In other words, conservation laws allow and select observable universes.*

On the other hand, if conservation laws are not valid the WDW multi-space solution give rise to non-observable universes (instanton solutions).

4 Many worlds from conservation laws

In order to give concrete examples of the above results, we can show how, given a generic theory of gravity, it is possible to work out minisuperspace cosmological models where observable universes (classical trajectories) are obtained thanks to the existence of conserved quantities. We shall take into account the most general action in which gravity is nonminimally coupled to a scalar field:

$$\mathcal{A} = \int_{\mathcal{M}} d^4x \sqrt{-g} \left[F(\varphi)R + \frac{1}{2} g^{\mu\nu}\varphi_{;\mu}\varphi_{;\nu} - V(\varphi) + \mathcal{L}_m \right] \quad (23)$$

where the form and the role of $V(\varphi)$ are still general and $\mathcal{L}_m$ represents the standard fluid matter content of the theory. This effective action comes out in the framework of the Open Quantum Relativity [1, 6] a dynamical theory in which, asking for a General Conservation Principle [5], the unification of different interactions is achieved and several shortcomings of modern physics are overcome (see [1] and references therein). The state equation of fluid matter is $p = = (\gamma - 1)\rho$ and $1 \leqslant \gamma \leqslant 2$ where p and ρ are, respectively, the ordinary pressure and density. Now we have all the ingredients to develop a scalar-tensor gravity quantum cosmology. Using the transformations:

$$\varphi = e^{-\varphi}, \quad F(\varphi) = \frac{1}{8} e^{-2\varphi}, \quad V(\varphi) = U(\varphi)e^{-2\varphi}, \quad (24)$$

the action (23) can be recast in the form

$$\mathcal{A} = \int d^4x \sqrt{-g} \left\{ \exp\left[-2\varphi\right] \left[R + 4 g^{\mu\nu}\varphi_{;\mu}\varphi_{;\nu} + \right. \right.$$
$$\left. \left. - U(\varphi) \right] + \mathcal{L}_m \right\}, \quad (25)$$

always using Planck units $8\pi G = c = 1$. Let us now take into account a Friedman, Robertson, Walker (FRW) metric $ds^2 = dt^2 - a^2(t)d\Omega_3^2$, where $d\Omega_3^2$ is the 3–dimensional element of the spacelike manifold. With this assumption, the configuration space is $\mathcal{Q} \equiv \{a, \varphi\}$ and the tangent space is $T\mathcal{Q} \equiv \{a, \dot{a}, \varphi, \dot{\varphi}\}$. This is our minisuperspace. Clearly $p = p(a)$ and $\rho = \rho(a)$. Substituting the FRW metric and integrating by parts, the Lagrangian (25) becomes pointlike, that is:

$$\mathcal{L} = \frac{1}{8} a^3 e^{-2\varphi} \left[6\left(\frac{\dot{a}}{a}\right)^2 - 12\dot{\varphi}\left(\frac{\dot{a}}{a}\right) - 6\frac{k}{a^2} + \right.$$
$$\left. + 4\dot{\varphi}^2 - 8U(\varphi) \right] + a^3 \mathcal{L}_m. \quad (26)$$

At this point, it is worth noting that the scale–factor duality symmetry arises if the transformation of the scale factor of a homogeneous and isotropic space-time metric, $a(t) \to a^{-1}(-t)$, leaves the model invariant, taking into account also the form of the potential U.

Provided the transformations

$$\psi = \varphi - \frac{3}{2}\ln a, \qquad Z = \ln a, \quad (27)$$

the Lagrangian (26) becomes:

$$\mathcal{L} = e^{-2\psi} \left[4\dot{\psi}^2 - 3\dot{Z}^2 - 6ke^{-2Z} - 8W \right] + De^{3(1-\gamma)Z} \quad (28)$$

where the potential $W(\psi, Z)$, thanks to the transformations (27), is depending on both the variables of the minisuperspace. In the new variables, the duality invariance has become a parity invariance since Z and $-Z$ are both solutions of dynamics. The emergence of this feature is related to the presence of nonminimal coupling; it allows the fact that several solutions can be extended for $t \to -\infty$ without singularities [3]. Another important consideration is connected to the role of perfect fluid matter. It introduces two further parameters which are D (related to the bulk of matter) and γ (related to the type of matter which can be *e.g.* radiation $\gamma = 4/3$ or dust $\gamma = 1$). We shall see below that they directly determine the form of cosmological solutions. Two general forms of potential W preserving the duality symmetry

$$W(Z, \psi) = \frac{D}{4} e^{-3\gamma Z} e^{2\psi}, \qquad W(Z, \psi) = \Lambda, \quad (29)$$

where $\Lambda = $ const. These are all the ingredient we need in order to construct our minisuperspace quantum cosmology. Let us start with a simple but extremely didactic example of the above effective action (25) which is

$$\mathcal{A} = \int d^4x \sqrt{-g}\, e^{-2\varphi} \left[R + 4(\partial\varphi)^2 - \Lambda \right], \quad (30)$$

where $D = k = 0$ and $W = \Lambda$. This example is useful to show, as we shall see below, the way in which the full theory

G. Basini, S. Capozziello. Multi-Spaces and Many Worlds from Conservation Laws

works. The Lagrangian (28) becomes

$$\mathcal{L} = -3e^{-2\psi}\dot{Z}^2 + 4\dot{\psi}^2 e^{-2\psi} - 2\Lambda e^{-2\psi}, \qquad (31)$$

that is cyclic in Z. Due to the considerations in previous section, we have to derive a conserved quantity, relatively to the variable Z, and then an oscillatory behavior for the wave function of the universe Ψ. The Legendre transformation for the conjugate momenta gives

$$\pi_z = \frac{\partial \mathcal{L}}{\partial \dot{Z}} = -6\dot{Z}e^{-2\psi}, \quad \pi_\psi = \frac{\partial \mathcal{L}}{\partial \dot{\psi}} = 8\dot{\psi}e^{-2\psi}, \qquad (32)$$

and the Hamitonian is $\mathcal{H} = \pi_z \dot{Z} + \pi_\psi \dot{\psi} - \mathcal{L}$. From Dirac canonical quantization rules, it is possible to write $\pi_z \rightarrow -i\partial_z$ and $\pi_\psi \rightarrow -i\partial_\psi$, and then the WDW equation is

$$\left[\frac{1}{12}\partial_z^2 - \frac{1}{16}\partial_\psi^2 + 2\Lambda e^{-4\psi}\right]\Psi(Z,\psi) = 0, \qquad (33)$$

where a simple factor ordering choice is done [11]. This is a second order partial differential equation which can be solved by separation of variables $\Psi(Z,\psi) = A(Z)B(\psi)$ from which Eq. (33) can be split into two ordinary differential equations

$$\frac{d^2 B(\psi)}{d\psi^2} - \left(32\Lambda e^{-4\psi} + 16E\right)B(\psi) = 0, \qquad (34)$$

$$\frac{d^2 A(z)}{dz^2} = 12EA(z), \qquad (35)$$

where E is a arbitrary constant. For $E > 0$, the general solution of the WDW equation is

$$\Psi(Z,\psi) \propto \exp\left(\pm\sqrt{\frac{3}{2}}Z\right) \times$$
$$\times \left[c_0 \mp \frac{1}{8\sqrt{2\Lambda}}\exp\left(\pm 4\sqrt{2\Lambda}\,e^{-2\psi}\right)\right] \times \qquad (36)$$
$$\times \exp\left[\psi \mp 2\sqrt{2\Lambda}\,e^{-2\psi}\right].$$

For $E < 0$, Eq. (35) is a harmonic oscillator whose solutions are $A(Z) \propto \pm\sin(mZ)$ (we have put $|E| = m^2$). In this case the momentum $\pi_z = m$ is a constant of motion. Eq. (34) is solvable in terms of modified Bessel functions and the general solution of Eq. (33) is

$$\Psi(Z,\psi) \propto \pm\sin(mZ)\,K_{\frac{im}{2\Lambda}}\left(\sqrt{2\Lambda}\,e^{-2\psi}\right); \qquad (37)$$

with an evident oscillatory behavior. Finally, in the case $E = 0$, the solution is

$$\Psi(Z,\psi) \propto ZK_0\left(\sqrt{2\Lambda}\,e^{-2\psi}\right), \qquad (38)$$

where K_0 is the modified Bessel function of zero order. The absence of a positive defined scalar product in the superspace prevents the existence of a Hilbert space for the states

of the WDW equation; *i. e.* we cannot apply the full probability interpretation to the squared modulus of the wave function of the universe. This is the reason why we have to omit the normalization constants in front of the solutions (36), (37), (38). Various suggestions have been given in literature to interpret Ψ [11], although starting from different points of view, all these different interpretations arrive to the conclusion that, at least in the semiclassical limit, a notion of measure can be introduced considering $|\Psi|^2$. As we said above, the strong peaks of $|\Psi|^2$ (oscillatory behaviors) indicate classical correlations among the dynamical variables, whereas weak variations of $|\Psi|^2$ mean the absence of correlations [11]. In fact the presence of strong amplitude peaks of the wave function seems to be the common indicator of where the classical (in principle observable) universes enucleates in its configuration space. The classical limit of quantum cosmology can be recovered in the oscillation regime with great phase values of Ψ: in this region the wave function is strongly peaked on first integrals of motion related to conservation laws. In the case presented here, the solutions (36), (37), (38) give information on the nature and the properties of classical cosmological behavior: for the *vacuum state*, $E = 0$, we have

$$\Psi \sim \ln a\sqrt{\pi}\,e^\psi \exp\left(-\sqrt{2\Lambda}\,e^{-2\psi}\right) \to 0, \qquad (39)$$

for $\psi \to -\infty$ and

$$\Psi \sim 2\psi \ln a, \qquad (40)$$

for $\psi \to +\infty$. So $|\Psi|^2$ is exponentially small for $\psi \leqslant 0$, while it increases for great ψ. This fact tells us that is most probable a realization of a classical universe for great field configurations (for example see the prescriptions for chaotic inflation where the scalar field has to start with a mass of a few Planck masses [16]). Another feature which emerges from (36) and (37) is the following: as $Z = \ln a$, Ψ can be considered a superposition of states $\Psi(a)$ with states $\Psi(a^{-1})$, that is the wave function of the universe (and also the WDW equation) contains the scale factor duality. Furthermore, using the first integrals of motion (*i.e* the canonical momenta related to conservation laws), we get the classical solutions

$$a(t) = a_0 \left[\frac{\cos\lambda\tau + \sin\lambda\tau}{\cos\lambda\tau - \sin\lambda\tau}\right]^{\pm\sqrt{3}/3}, \qquad (41)$$

$$\varphi(t) = \frac{1}{4}\ln\left[\frac{\lambda^2}{k\cos^2 2\lambda\tau}\right] \pm$$
$$\pm \frac{\sqrt{3}}{2}\ln\left|\frac{\cos\lambda\tau + \sin\lambda\tau}{\cos\lambda\tau - \sin\lambda\tau}\right| + \varphi_0, \qquad (42)$$

and

$$a(t) = a_0 \exp\left\{\mp\frac{1}{\sqrt{6}}\arctan\left[\frac{1 - 2e^{4\lambda\tau}}{2e^{2\lambda\tau}\sqrt{1 - e^{4\lambda\tau}}}\right]\right\}, \qquad (43)$$

Λ	k	D	γ	Solution
$\neq 0$	0	$\neq 0$	1	CT
0	0	$\neq 0$	1	CT
0	± 1	$\neq 0$	$4/3$	I
$\neq 0$	0	0	$\forall \gamma$	CT
0	$k > 0$	$6k$	$\forall \gamma$	CT and I

Table 1: Main features of the solutions of WDW equation, Classical Trajectories (CT) and Instantons (I), for different values of parameter Λ, k, D, γ.

$$\varphi(t) = \frac{1}{4} \ln \left[\frac{2\lambda^2 e^{4\lambda\tau}}{k(1 - e^{4\lambda\tau})} \right] \mp$$
$$\mp \frac{1}{\sqrt{6}} \arctan \left[\frac{1 - 2e^{4\lambda\tau}}{2e^{2\lambda\tau}\sqrt{1 - e^{4\lambda\tau}}} \right] + \varphi_0 \,, \tag{44}$$

where $\tau = \pm t$, k is an integration constant and $\lambda^2 = \Lambda/2$. In (41), (42), we have $\Lambda > 0$, in (43), (44) $\Lambda < 0$. These "universes" are "observable" since, starting from these solutions, it is easy to construct all the cosmological parameters H_0, q_0, Ω_Λ, Ω_M and t_0. It is worth stressing that such solutions are found only if conservation laws exists. It is remarkable that the scalar factor duality emerges also for the wave function of the universe in a quantum cosmology context: that is the solutions for a have their dual counterpart a^{-1} in the quantum state described by Ψ. This fact, in the philosophy of quantum cosmology, allows to fix a law for the initial conditions (*e. g.* Vilenkin tunneling from nothing or Hartle-Hawking no-boundary conditions [11]) in which the duality is a property of the configuration space where our classical universe enucleates. This fact gives rise to cosmological solutions which can be consistently defined for $t \to \pm\infty$.

The approach can be directly extended to the Lagrangian (28), from which, by a Legendre transformation and a canonical quantization, we get the WDW equation

$$\left[\frac{1}{2} \partial_z^2 - \frac{1}{8} \partial_\psi^2 + 3ke^{-2Z-4\psi} + \right.$$
$$\left. + 4We^{-4\psi} - De^{3(1-\gamma)Z-2\psi} \right] \Psi(Z, \psi) = 0 \,, \tag{45}$$

whose solutions can be classified by the potential parameter Λ, the spatial curvature k, the bulk of matter D, and the adiabatic index γ. In the following Table, we give the main features of WDW solutions.

5 Discussion and conclusions

In this paper, we have shown that the reduction procedure of dynamics, related to conservation laws, can give rise to a splitting of the phase-space of a physical system, by which it is possible to achieve the complete solution of dynamics. This result can be applied to Quantum Cosmology, leading to the result that physical many worlds can be related to integrable multi-spaces of the above splitting. From a mathematical viewpoint, the above statement deserves some further discussion. As a first remark the general solution (18) can be interpreted as a superposition of particular solutions (the components in different directions) which result more *solved* (*i.e.* separated in every direction of configuration space) if more symmetries exist. Starting from such a consideration, as a consequence, we can establish a sort of *degree of solvability*, among the components of a given physical system, connected to the number of symmetries: (i) a system is *completely* solvable and separable if a symmetry exists for *every* direction of configuration space (in this case, the system is fully integrable and the relations among its parts can be exactly obtained); (ii) a system is *partially* solved and separated if a symmetry exists for *some* directions of configuration space (in this case, it is not always possible to get a general solution); (iii) a system is *not* separated at all and *no* symmetry exists, i. e. a necessary and sufficient condition to get the general solution does not exist. In other words, we could also obtain the general solution in the last case, but not by a straightforward process of separation of variables induced by the reduction procedure.

A further remark deserves the fact that the eigen-functions of a given operator (in our case the Hamiltonian $\hat{\mathcal{H}}$) define a Hilbert space. The above result works also in this case, so that we can define, for a quantum system whose eigen-functions are given by a set of commuting Hermitian operators, a *Hilbert Space of General Conservation Laws* (see also [5]). The number of dimensions of such a space is given by the components of superposition (18) while the number of symmetries is given by the oscillatory components. Vice-versa, the oscillatory components are *always* related to the number of symmetries in the corresponding Hilbert space. These results can be applied to minisuperspace quantum cosmology. The role of symmetries and conservation laws is prominent to interpret the information contained in the wave function of the universe which is solution of the WDW equation; in fact, the conserved momenta, related to some (or all) of the physical variables defining the minisuperspace, select oscillatory behaviors (*i.e.* strong peaks) in Ψ, which means "correlation" among the physical variables and then classical trajectories whose interpretation is that of "*observable universes*". In this sense, the so called Hartle criterion of quantum cosmology becomes a sufficient and necessary condition to select classical universes among all those which are possible. Working out this approach, we obtain the wave function of the universe Ψ depending on a set of physical parameter which are D, the initial bulk of matter, k, the spatial curvature constant, γ, the adiabatic index of perfect fluid matter, Λ, the parameter of the interaction potential.

The approach allows to recover several classes of interesting cosmological behaviors as De Sitter-like-singularity free solutions, power-law solutions, and pole-like solutions [3].

However, some points have to be considered in the interpretation of the approach. The Hartle criterion works in the context of an Everett-type interpretation of Quantum Cosmology [9, 17] which assumes the idea that the universe branches into a large number of copies of itself whenever a measurement is made. This point of view is the so called *Many Worlds* interpretation of Quantum Cosmology. Such an interpretation is an approach which gives a formulation of quantum mechanics designed to deal with correlations internal to individual, isolated systems. The Hartle criterion gives an operative interpretation of such correlations. In particular, if the wave function is *strongly peaked* in some region of configuration space, the correlations which characterize such a region can be, in principle, observed. On the other hand, if the wave function is *smooth* in some region, the correlations which characterize that region are precluded to the observations (that is, the cosmological parameters as H_0 or Ω_Λ cannot be neither calculated nor observed).

If the wave function is neither peaked nor smooth, no predictions are possible from observations. In conclusion, the analogy with standard quantum mechanics is straightforward. By considering the case in which the individual system consists of a large number of identical subsystems, one can derive, from the above interpretation, the usual probabilistic interpretation of Quantum Mechanics for the subsystems [11, 10]. If a conservation law (or more than one) is present for a given minisuperspace model, then strongly peaked (oscillatory) subsets of the wave function of the universe are found. Viceversa, oscillatory parts of the wave function can be always connected to conserved momenta and then to symmetries.

References

1. Basini G., Capozziello S. *Gen. Relativ. Grav.*, 2005, v. 37, 115.

2. Basini G., Capozziello S. *Europhys. Lett.*, 2003, v. 63, 166.

3. Basini G., Bongiorno F., Capozziello S. *Int. Journ. Mod. Phys.*, 2004, v. D13, 717.

4. Basini G., Bongiorno F., Capozziello S., Ricci M. *Int. Journ. Mod. Phys.*, 2004, v. D13, 359.

5. Basini G., Capozziello S., Longo G. *Phys. Lett.*, 2003, v. 311A, 465.

6. Basini G., Capozziello S. *Gen. Relativ. Grav.*, 2003, v. 35, 2217.

7. Smarandache F. A unifying field in logics: neutrosophic logic. Neutrosophy, neutrosophic set, neutrosophic probability. 3rd edition, American Research Press, Rehoboth, 2003.

8. Mao Linfan. Smarandache multi-space theory. Post-doctoral thesis. Hexis, Phoenix, 2005.

9. Everett H. *Rev. Mod. Phys.*, 1957, v. 29, 454.

10. Halliwell J. J. *Nucl. Phys.*, 1986, v. B266, 228.

11. Hartle J. B. In: *Gravitation in Astrophysics*, Cargese, 1986, eds. B. Carter and J. B. Hartle, Plenum Press, New York, 1986.

12. DeWitt B. S. *Phys. Rev.*, 1967, v. 160, 1113.

13. Misner C. W. *Phys. Rev.*, 1969, v. 186, 1319.

14. Hartle J. B. and Hawking S. W. *Phys. Rev.*, 1983, v. D28, 2960.

15. Vilenkin A. *Phys. Rev.*, 1986, v. D33, 3560.

16. Linde A. D. *Phys. Lett.*, 1982, v. B108, 389.

17. Finkelstein D. *Trans. N. Y. Acad. Sci.*, 1963, v. 25, 621.

SPECIAL REPORT

A New Light-Speed Anisotropy Experiment: Absolute Motion and Gravitational Waves Detected

Reginald T. Cahill

School of Chemistry, Physics and Earth Sciences, Flinders University, Adelaide 5001, Australia
E-mail: Reg.Cahill@flinders.edu.au; http://www.scieng.flinders.edu.au/cpes/people/cahill_r/

Data from a new experiment measuring the anisotropy of the one-way speed of EM waves in a coaxial cable, gives the speed of light as $300,000 \pm 400 \pm 20$ km/s in a measured direction RA$=5.5 \pm 2$ hrs, Dec$=70 \pm 10°$S, is shown to be in excellent agreement with the results from seven previous anisotropy experiments, particularly those of Miller (1925/26), and even those of Michelson and Morley (1887). The Miller gas-mode interferometer results, and those from the RF coaxial cable experiments of Torr and Kolen (1983), De Witte (1991) and the new experiment all reveal the presence of gravitational waves, as indicated by the last $\pm$ variations above, but of a kind different from those supposedly predicted by General Relativity. Miller repeated the Michelson-Morley 1887 gas-mode interferometer experiment and again detected the anisotropy of the speed of light, primarily in the years 1925/1926 atop Mt.Wilson, California. The understanding of the operation of the Michelson interferometer in gas-mode was only achieved in 2002 and involved a calibration for the interferometer that necessarily involved Special Relativity effects and the refractive index of the gas in the light paths. The results demonstrate the reality of the Fitzgerald-Lorentz contraction as an observer independent relativistic effect. A common misunderstanding is that the anisotropy of the speed of light is necessarily in conflict with Special Relativity and Lorentz symmetry — this is explained. All eight experiments and theory show that we have both anisotropy of the speed of light *and* relativistic effects, and that a dynamical 3-space exists — that absolute motion through that space has been repeatedly observed since 1887. These developments completely change fundamental physics and our understanding of reality. "Modern" vacuum-mode Michelson interferometers, particularly the long baseline terrestrial versions, are, by design flaw, incapable of detecting the anisotropy effect and the gravitational waves.

Contents

1 Introduction

Of fundamental importance to physics is whether the speed of light is the same in all directions, as measured say in a laboratory attached to the Earth. This is what is meant by *light speed anisotropy* in the title of this paper. The prevailing belief system in physics has it that the speed of light is isotropic, that there is no preferred frame of reference, that absolute motion has never been observed, and that 3-space does not, and indeed cannot exist. This is the essence of Einstein's 1905 postulate that the speed of light is independent of the choice of observer. This postulate has determined the course of physics over the last 100 years.

Despite the enormous significance of this postulate there has never been a direct experimental test, that is, in which the one-way travel time of light in vacuum over a set distance has been measured, and repeated for different directions. So how could a science as fundamental and important as physics permit such a key idea to go untested? And what are the consequences for fundamental physics if indeed, as reported herein and elsewhere, that the speed of light is anisotropic, that a dynamical 3-space does exist? This would imply that

if reality is essentially space and matter, with time tracking process and change, then physics has completely missed the existence of that space. If this is the case then this would have to be the biggest blunder ever in the history of science, more so because some physicists have independently detected that anisotropy. While herein we both summarise seven previous detections of the anisotropy and report a new experiment, the implications for fundamental physics have already been substantially worked out. It leads to a new modelling and comprehension of reality known as *Process Physics* [1].

The failure of mainstream physics to understand that the speed of light is anisotropic, that a dynamical 3-space exists, is caused by an ongoing failure to comprehend the operation of the Michelson interferometer, and also by theoretical physicists not understanding that the undisputed successes of special relativity effects, and even Lorentz symmetry, do not imply that the speed of light must be isotropic — this is a mere abuse of logic, as explained later.

The Michelson interferometer is actually a complex instrument. The problem is that the anisotropy of the speed of light affects its actual dimensions and hence its operation: there are actual length contractions of its physical arms. Because the anisotropy of the speed of light is so fundamental it is actually very subtle to design an effective experiment because the sought for effect also affects the instrument in more than one way. This subtlety has been overlooked for some 100 years, until in 2002 the original data was reanalysed using a relativistic theory for the calibration of the interferometer [2].

The new understanding of the operation of the Michelson interferometer is that it can only detect the light speed anisotropy when there is gas in the light paths, as there was in the early experiments. Modern versions have removed the gas and made the instrument totally unable to detect the light speed anisotropy. Even in gas mode the interferometer is a very insensitive device, being 2nd order in v/c and further suppressed in sensitivity by the gas refractive index dependency.

More direct than the Michelson interferometer, but still not a direct measurement, is to measure the one-speed of radio frequency (RF) electromagnetic waves in a coaxial cable, for this permits electronic timing methods. This approach is 1st order in v/c, and independent of the refractive index suppression effect. Nevertheless because it is one-way clocks are required at both ends, as in the Torr and Kolen, and De Witte experiments, and the required length of the coaxial cable was determined, until now, by the stability of atomic clocks over long durations.

The new one-way RF coaxial experiment reported herein utilises a new timing technique that avoids the need for two atomic clocks, by using a very special property of optical fibres, namely that the light speed in optical fibres is isotropic, and is used for transmitting timing information, while in the coaxial cables the RF speed is anisotropic, and is used as the

sensor. There is as yet no explanation for this optical fibre effect, but it radically changes the technology for anisotropy experiments, as well and at the same time that of gravitational wave detectors. In the near future all-optical gravitational wave detectors are possible in desk-top instruments. These gravitational waves have very different properties from those supposedly predicted from General Relativity, although that appears to be caused by errors in that derivation.

As for gravitational waves, it has been realised now that they were seen in the Miller, Torr and Kolen, and De Witte experiments, as they are again observed in the new experiment. Most amazing is that these wave effects also appear to be present in the Michelson-Morley fringe shift data from 1887, as the fringe shifts varied from day to day. So Michelson and Morley should have reported that they had discovered absolute motion, a preferred frame, and also wave effects of that frame, that the speed of light has an anisotropy that fluctuated over and above that caused by the rotation of the Earth.

The first and very successful attempt to look for a preferred frame was by Michelson and Morley in 1887. They did in fact detect the expected anisotropy at the level of ± 8 km/s [3], but only according to Michelson's Newtonian calibration theory. However this result has essentially been ignored ever since as they expected to detect an effect of at least ± 30 km/s, which is the orbital speed of the Earth about the Sun. As Miller recognised the basic problem with the Michelson interferometer is that the calibration of the instrument was then clearly not correctly understood, and most likely wrong [4]. Basically Michelson had used Newtonian physics to calibrate his instrument, and of course we now know that that is completely inappropriate as relativistic effects play a critical role as the interferometer is a 2nd order device ($\sim v^2/c^2$ where v is the speed of the device relative to a physical dynamical 3-space*), and so various effects at that order must be taken into account in determining the calibration of the instrument, that is, what light speed anisotropy corresponds to the observed fringe shifts. It was only in 2002 that the calibration of the Michelson interferometer was finally determined by taking account of relativistic effects [2]. One aspect of that was the discovery that only a Michelson interferometer in gas-mode could detect the light anisotropy, as discussed below. As well the interferometer when used in air is nearly a factor of 2000 less sensitive than that according to the inappropriate Newtonian theory. This meant that the Michelson and Morley anisotropy speed variation was now around 330km/s on average, and as high as 400km/s on some days. Miller was aware of this calibration problem, and resorted to a brilliant indirect method, namely to observe the fringe shifts over a period of a year, and to use the effect of the Earth's orbital speed upon the fringe shifts to arrive at

---

*In Michelson's era the idea was that v was the speed of light relative to an *ether*, which itself filled space. This dualism has proven to be wrong.

a calibration. The Earth's orbital motion was clearly evident in Miller's data, and using this effect he obtained a light speed anisotropy effect of some 200 km/s in a particular direction. However even this method made assumptions which are now known to be invalid, and correcting his earth-effect calibration method we find that it agrees with the new relativistic and gas effects calibration, and both methods now give a speed of near 400 km/s. This also then agrees with the Michelson-Morley results. Major discoveries like that of Miller must be reproduced by different experiments and by different techniques. Most significantly there are in total seven other experiments that confirm this Miller result, with four being gas-mode Michelson interferometers using either air, helium or a He/Ne mixture in the light path, and three experiments that measure variations in the one-way speed of EM waves travelling through a coaxial cable as the orientation of the cable is changed, with the latest being a high precision technique reported herein and in [5, 6]. This method is 1st order in v/c, so it does not require relativistic effects to be taken into account, as discussed later.

As the Michelson interferometer requires a gas to be present in the light path in order to detect the anisotropy it follows that vacuum interferometers, such as those in [7], are simply inappropriate for the task, and it is surprising that some attempts to detect the anisotropy in the speed of light still use vacuum-mode Michelson interferometers, some years after the 2002 discovery of the need for a gas in the light path [2].

Despite the extensive data collected and analysed by Miller after his fastidious testing and refinements to control temperature effects and the like, and most importantly his demonstration that the effects tracked sidereal time and not solar time, the world of physics has, since publication of the results by MIller in 1933, simply ignored this discovery. The most plausible explanation for this situation is the ongoing misunderstanding by many physicists, but certainly not all, that any anisotropy in the speed of light must necessarily by incompatible with Special Relativity (SR), with SR certainly well confirmed experimentally. This is misunderstanding is clarified. In fact Miller's data can now be used to confirm an important aspect of SR. Even so, ignoring the results of a major experiment simply because they challenge a prevailing belief system is not science — ignoring the Miller experiment has stalled physics for some 70 years.

It is clear that the Miller experiment was highly successful and highly significant, and we now know this because the same results have been obtained by later experiments which used *different* experimental techniques. The most significant part of Miller's rigorous experiment was that he showed that the effect tracked sidereal time and not solar time — this is the acid test which shows that the direction of the anisotropy velocity vector is relative to the stars and not to the position of the Sun. This difference is only some 4 minutes per day, but over a year amounts to a huge 24 hours

effect, and Miller saw that effect and extensively discussed it in his paper. Similarly De Witte in his extensive 1991 coaxial cable experiment [9] also took data for 178 days to again establish the sidereal time effect: over 178 days this effect amounts to a shift in the phase of the signal through some 12 hours! The sidereal effect has also been established in the new coaxial cable experiment by the author from data spanning some 200 days.

The interpretation that has emerged from the Miller and related discoveries is that space exists, that it is an observable and dynamical system, and that the Special Relativity effects are caused by the absolute motion of quantum systems through that space [1, 25]. This is essentially the Lorentz interpretation of Special Relativity, and then the spacetime is merely a mathematical construct. The new understanding has lead to an explanation of why Lorentz symmetry manifests despite there being a preferred frame, that is, a local frame in which only therein is the speed of light isotropic. A minimal theory for the dynamics of this space has been developed [1, 25] which has resulted in an explanation of numerous phenomena, such as gravity as a quantum effect [25, 8], the so-called "dark matter" effect, the black hole systematics, gravitational light bending, gravitational lensing, and so [21–25].

The Miller data also revealed another major discovery that Miller himself may not have understood, namely that the anisotropy vector actually fluctuates form hour to hour and day to day even when we remove the manifest effect of the Earth's rotation, for Miller may have interpreted this as being caused by imperfections in his experiment. This means that the flow of space past the Earth displays turbulence or a wave effect: basically the Miller data has revealed what we now call *gravitational waves*, although these are different to the waves supposedly predicted by General Relativity. These wave effects were also present in the Torr and Kolen [10] first coaxial cable experiment at Utah University in 1981, and were again manifest in the De Witte data from 1991. Analysis of the De Witte data has shown that these waves have a fractal structure [9]. The Flinders University Gravitational Waves Detector (also a coaxial cable experiment) was constructed to investigate these waves effects. This sees the wave effects detected by Miller, Torr and Kolen, and by De Witte. The plan of this paper is to first outline the modern understanding of how a gas-mode Michelson interferometer actually operates, and the nature, accuracy and significance of the Miller experiment. We also report the other seven experiments that confirm the Miller discoveries, particularly data from the new high-precision gravity wave detector that detects not only a light speed anisotropy but also the wave effects.

2 Special Relativity and the speed of light anisotropy

It is often assumed that the anisotropy of the speed of light is inconsistent with Special Relativity, that only one or the

other can be valid, that they are mutually incompatible. This misunderstanding is very prevalent in the literature of physics, although this conceptual error has been explained [1]. The error is based upon a misunderstanding of how the logic of theoretical physics works, namely the important difference between an *if* statement, and an *if and only if* statement. To see how this confusion has arisen we need to recall the history of Special Relativity (SR). In 1905 Einstein deduced the SR formalism by assuming, in part, that the speed of light is invariant for all relatively moving observers, although most importantly one must ask just how that speed is defined or is to be measured. The SR formalism then predicted numerous effects, which have been extensively confirmed by experiments over the last 100 years. However this Einstein derivation was an *if* statement, and not an *if and only if* statement. For an *if* statement, that *if A then B*, does not imply the truth of *A* if *B* is found to be true; only an *if and only if* statement has that property, and Einstein did not construct such an argument. What this means is that the validity of the various SR effects does *not* imply that the speed of light must be isotropic. This is actually implicit in the SR formalism itself, for it permits one to use any particular foliation of the 4-dimensional spacetime into a 3-space and a 1-space (for time). Most importantly it does not forbid that one particular foliation be actual. So to analyse the data from gas-mode interferometer experiments we must use the SR effects, and the fringe shifts reveal the preferred frame, an actual 3-space, by revealing the anisotropic speed of light, as Maxwell and Michelson had originally believed.

For "modern" resonant-cavity Michelson interferometer experiments we predict no rotation-induced fringe shifts, unless operated in gas-mode. Unfortunately in analysing the data from the vacuum-mode experiments the consequent null effect is misinterpreted, as in [7], to imply the absence of a preferred direction, of absolute motion. But it is absolute motion which causes the dynamical effects of length contractions, time dilations and other relativistic effects, in accord with Lorentzian interpretation of relativistic effects.

The detection of absolute motion is not incompatible with Lorentz symmetry; the contrary belief was postulated by Einstein, and has persisted for over 100 years, since 1905. So far the experimental evidence is that absolute motion and Lorentz symmetry are real and valid phenomena; absolute motion is motion presumably relative to some substructure to space, whereas Lorentz symmetry parameterises dynamical effects caused by the motion of systems through that substructure. To check Lorentz symmetry we can use vacuum-mode resonant-cavity interferometers, but using gas within the resonant-cavities would enable these devices to detect absolute motion with great precision. As well there are novel wave phenomena that could also be studied, as discussed herein and in [19, 20].

Motion through the structured space, it is argued, induces actual dynamical time dilations and length contractions in

agreement with the Lorentz interpretation of special relativistic effects. Then observers in uniform motion "through" the space will, on measurement of the speed of light using the special but misleading Einstein measurement protocol, obtain always the same numerical value c. To see this explicitly consider how various observers $P, P', \ldots$ moving with different speeds through space, measure the speed of light. They each acquire a standard rod and an accompanying standardised clock. That means that these standard rods would agree if they were brought together, and at rest with respect to space they would all have length Δl_0, and similarly for the clocks. Observer P and accompanying rod are both moving at speed v_R relative to space, with the rod longitudinal to that motion. P then measures the time Δt_R, with the clock at end A of the rod, for a light pulse to travel from end A to the other end B and back again to A. The light travels at speed c relative to space. Let the time taken for the light pulse to travel from $A \rightarrow B$ be t_{AB} and from $B \rightarrow A$ be t_{BA}, as measured by a clock at rest with respect to space*. The length of the rod moving at speed v_R is contracted to

$$\Delta l_R = \Delta l_0 \sqrt{1 - \frac{v_R^2}{c^2}} . \qquad (1)$$

In moving from A to B the light must travel an extra distance because the end B travels a distance $v_R t_{AB}$ in this time, thus the total distance that must be traversed is

$$c t_{AB} = \Delta l_R + v_R t_{AB} , \qquad (2)$$

similarly on returning from B to A the light must travel the distance

$$c t_{BA} = \Delta l_R - v_R t_{BA} . \qquad (3)$$

Hence the total travel time Δt_0 is

$$\Delta t_0 = t_{AB} + t_{BA} \quad = \quad \frac{\Delta l_R}{c - v_R} + \frac{\Delta l_R}{c + v_R} = \qquad (4)$$

$$= \quad \frac{2 \Delta l_0}{c \sqrt{1 - \frac{v_R^2}{c^2}}} . \qquad (5)$$

Because of the time dilation effect for the moving clock

$$\Delta t_R = \Delta t_0 \sqrt{1 - \frac{v_R^2}{c^2}} . \qquad (6)$$

Then for the moving observer the speed of light is defined as the distance the observer believes the light travelled $(2\Delta l_0)$ divided by the travel time according to the accompanying clock (Δt_R), namely $2\Delta l_0 / \Delta t_R = 2\Delta l_R / \Delta t_0$, from above, which is thus the same speed as seen by an observer at rest in the space, namely c. So the speed v_R of the observer through space is not revealed by this procedure, and the observer is erroneously led to the conclusion that the speed of light is always c. This follows from two or more

---

*Not all clocks will behave in this same "ideal" manner.

observers in manifest relative motion all obtaining the same speed c by this procedure. Despite this failure this special effect is actually the basis of the spacetime Einstein measurement protocol. That this protocol is blind to the absolute motion has led to enormous confusion within physics.

To be explicit the Einstein measurement protocol actually inadvertently uses this special effect by using the radar method for assigning historical spacetime coordinates to an event: the observer records the time of emission and reception of radar pulses ($t_r > t_e$) travelling through space, and then retrospectively assigns the time and distance of a distant event B according to (ignoring directional information for simplicity)

$$T_B = \frac{1}{2}\left(t_r + t_e\right), \qquad D_B = \frac{c}{2}\left(t_r - t_e\right), \qquad (7)$$

where each observer is now using the same numerical value of c. The event B is then plotted as a point in an individual geometrical construct by each observer, known as a spacetime record, with coordinates (D_B, T_B). This is no different to an historian recording events according to some agreed protocol. Unlike historians, who don't confuse history books with reality, physicists do so. We now show that because of this protocol and the absolute motion dynamical effects, observers will discover on comparing their historical records of the same events that the expression

$$\tau_{AB}^2 = T_{AB}^2 - \frac{1}{c^2}\, D_{AB}^2\,, \qquad (8)$$

is an invariant, where $T_{AB} = T_A - T_B$ and $D_{AB} = D_A - D_B$ are the differences in times and distances assigned to events A and B using the Einstein measurement protocol (7), so long as both are sufficiently small compared with the scale of inhomogeneities in the velocity field.

To confirm the invariant nature of the construct in (8) one must pay careful attention to observational times as distinct from protocol times and distances, and this must be done separately for each observer. This can be tedious. We now demonstrate this for the situation illustrated in Fig. 1.

By definition the speed of P' according to P is $v_0' = D_B/T_B$ and so $v_R' = v_0'$, where T_B and D_B are the protocol time and distance for event B for observer P according to (7). Then using (8) P would find that $\left(\tau_{AB}^P\right)^2 = T_B^2 - \frac{1}{c^2}D_B^2$ since both $T_A = 0$ and $D_A = 0$, and whence $\left(\tau_{AB}^P\right)^2 = \left(1 - \frac{v_R'^2}{c^2}\right)T_B^2 = (t_B')^2$ where the last equality follows from the time dilation effect on the P' clock, since t_B' is the time of event B according to that clock. Then T_B is also the time that P' would compute for event B when correcting for the time-dilation effect, as the speed v_R' of P' through space is observable by P'. Then T_B is the "common time" for event B assigned by both observers. For P' we obtain directly, also from (7) and (8), that $\left(\tau_{AB}^{P'}\right)^2 = (T_B')^2 - \frac{1}{c^2}(D_B')^2 = (t_B')^2$, as $D_B' = 0$ and $T_B' = t_B'$. Whence for this situation

$$\left(\tau_{AB}^P\right)^2 = \left(\tau_{AB}^{P'}\right)^2\,, \qquad (9)$$
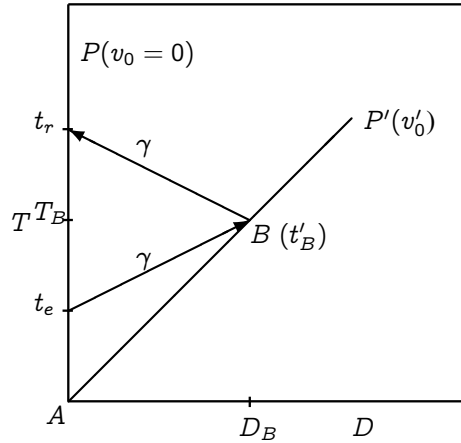
Fig. 1: Here $T - D$ is the spacetime construct (from the Einstein measurement protocol) of a special observer P *at rest* wrt space, so that $v_0 = 0$. Observer P' is moving with speed v_0' as determined by observer P, and therefore with speed $v_R' = v_0'$ wrt space. Two light pulses are shown, each travelling at speed c wrt both P and space. Event A is when the observers pass, and is also used to define zero time for each for convenience.

and so the construction (8) is an invariant.

While so far we have only established the invariance of the construct (8) when one of the observers is at rest in space, it follows that for two observers P' and P'' both in absolute motion it follows that they also agree on the invariance of (8). This is easily seen by using the intermediate step of a stationary observer P:

$$\left(\tau_{AB}^{P'}\right)^2 = \left(\tau_{AB}^{P}\right)^2 = \left(\tau_{AB}^{P''}\right)^2. \qquad (10)$$

Hence the protocol and Lorentzian absolute motion effects result in the construction in (8) being indeed an invariant in general. This is a remarkable and subtle result. For Einstein this invariance was a fundamental assumption, but here it is a derived result, but one which is nevertheless deeply misleading. Explicitly indicating small quantities by Δ prefixes, and on comparing records retrospectively, an ensemble of nearby observers agree on the invariant

$$\Delta\tau^2 = \Delta T^2 - \frac{1}{c^2}\,\Delta D^2, \qquad (11)$$

for any two nearby events. This implies that their individual patches of spacetime records may be mapped one into the other merely by a change of coordinates, and that collectively the spacetime patches of all may be represented by one pseudo-Riemannian manifold, where the choice of coordinates for this manifold is arbitrary, and we finally arrive at the invariant

$$\Delta\tau^2 = g_{\mu\nu}(x)\,\Delta x^\mu \Delta x^\nu, \qquad (12)$$

with $x^\mu = \{D_1, D_2, D_3, T\}$. Eqn. (12) is invariant under the Lorentz transformations

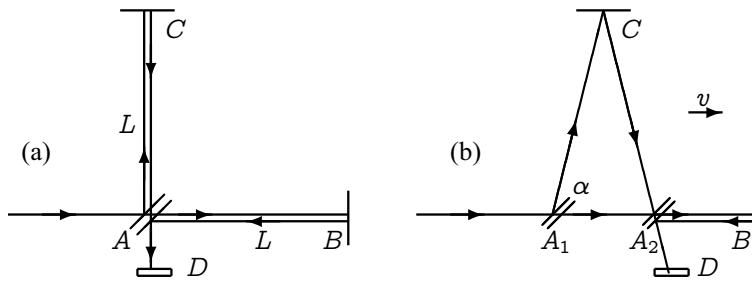$$x'^\mu = L^\mu_{\ \nu}\, x^\nu, \qquad (13)$$

Fig. 2: Schematic diagrams of the Michelson Interferometer, with beamsplitter/mirror at A and mirrors at B and C on arms from A, with the arms of equal length L when at rest. D is a screen or detector. In (a) the interferometer is at rest in space. In (b) the interferometer is moving with speed v relative to space in the direction indicated. Interference fringes are observed at the detector D. If the interferometer is rotated in the plane through $90°$, the roles of arms AC and AB are interchanged, and during the rotation shifts of the fringes are seen in the case of absolute motion, but only if the apparatus operates in a gas. By counting fringe changes the speed v may be determined.

where, for example for relative motion in the x direction, $L^\mu{}_\nu$ is specified by

$$
\begin{aligned}
x' &= \frac{x - vt}{\sqrt{1 - v^2/c^2}}\,,\\
y' &= y\,,\\
z' &= z\,,\\
t' &= \frac{t - vx/c^2}{\sqrt{1 - v^2/c^2}}\,.
\end{aligned}
\tag{14}
$$

So absolute motion and special relativity effects, and even Lorentz symmetry, are all compatible: a possible preferred frame is hidden by the Einstein measurement protocol.

So the experimental question is then whether or not a supposed preferred frame actually exists or not — can it be detected experimentally? The answer is that there are now eight such consistent experiments. In Sect. 4.7 we generalise the Dirac equation to take account of the coupling of the spinor to an actual dynamical space. This reveals again that relativistic effects are consistent with a preferred frame — an actual space. Furthermore this leads to the first derivation of gravity from a deeper theory — gravity turns out to be a quantum matter wave effect.

3 Light speed anisotropy experiments

We now consider the various experiments from over more than 100 years that have detected the anisotropy of the speed of light, and so the existence of an actual dynamical space, an observable preferred frame. As well the experiments, it is now understood, showed that this frame is dynamical, it exhibits time-dependent effects, and that these are "gravitational waves".

3.1 Michelson gas-mode interferometer

Let us first consider the new understanding of how the Michelson interferometer works. This brilliant but very subtle device was conceived by Michelson as a means to detect the anisotropy of the speed of light, as was expected towards the end of the 19th century. Michelson used Newtonian physics to develop the theory and hence the calibration for his device. However we now understand that this device detects 2nd order effects in v/c to determine v, and so we must use relativistic effects. However the application and analysis of data from various Michelson interferometer experiments using a relativistic theory only occurred in 2002, some 97 years after the development of Special Relativity by Einstein, and some 115 years after the famous 1887 experiment. As a consequence of the necessity of using relativistic effects it was discovered in 2002 that the gas in the light paths plays a critical role, and that we finally understand how to calibrate the device, and we also discovered, some 76 years after the 1925/26 Miller experiment, what determines the calibration constant that Miller had determined using the Earth's rotation speed about the Sun to set the calibration. This, as we discuss later, has enabled us to now appreciate that gas-mode Michelson interferometer experiments have confirmed the reality of the Fitzgerald-Lorentz length contraction effect: in the usual interpretation of Special Relativity this effect, and others, is usually regarded as an observer dependent effect, an illusion induced by the spacetime. But the experiments are to the contrary showing that the length contraction effect is an actual observer-independent dynamical effect, as Fitzgerald [27] and Lorentz had proposed [28].

The Michelson interferometer compares the change in the difference between travel times, when the device is rotated, for two coherent beams of light that travel in orthogonal directions between mirrors; the changing time difference being indicated by the shift of the interference fringes during the rotation. This effect is caused by the absolute motion of the device through 3-space with speed v, and that the speed of light is relative to that 3-space, and not relative to the apparatus/observer. However to detect the speed of the apparatus through that 3-space gas must be present in the light paths for purely technical reasons. The post relativistic-

effects theory for this device is remarkably simple. The relativistic Fitzgerald-Lorentz contraction effect causes the arm AB parallel to the absolute velocity to be physically contracted to length

$$L_{||} = L \sqrt{1 - \frac{v^2}{c^2}} . \qquad (15)$$

The time t_{AB} to travel AB is set by $Vt_{AB} = L_{||} + vt_{AB}$, while for BA by $Vt_{BA} = L_{||} - vt_{BA}$, where $V = c/n$ is the speed of light, with n the refractive index of the gas present (we ignore here the Fresnel drag effect for simplicity, an effect caused by the gas also being in absolute motion, see [1]). For the total ABA travel time we then obtain

$$t_{ABA} = t_{AB} + t_{BA} = \frac{2LV}{V^2 - v^2} \sqrt{1 - \frac{v^2}{c^2}} . \qquad (16)$$

For travel in the AC direction we have, from the Pythagoras theorem for the right-angled triangle in Fig. 1 that $(Vt_{AC})^2 = L^2 + (vt_{AC})^2$ and that $t_{CA} = t_{AC}$. Then for the total ACA travel time

$$t_{ACA} = t_{AC} + t_{CA} = \frac{2L}{\sqrt{V^2 - v^2}} . \qquad (17)$$

Then the difference in travel time is

$$\Delta t = \frac{(n^2 - 1) L}{c} \frac{v^2}{c^2} + O\left(\frac{v^4}{c^4}\right) . \qquad (18)$$

after expanding in powers of v/c. This clearly shows that the interferometer can only operate as a detector of absolute motion when not in vacuum ($n = 1$), namely when the light passes through a gas, as in the early experiments (in transparent solids a more complex phenomenon occurs). A more general analysis [1], including Fresnel drag, gives

$$\Delta t = k^2 \frac{Lv_P^2}{c^3} \cos\left(2(\theta - \psi)\right) , \qquad (19)$$

where $k^2 \approx n(n^2 - 1)$, while neglect of the relativistic Fitzgerald-Lorentz contraction effect gives $k^2 \approx n^3 \approx 1$ for gases, which is essentially the Newtonian theory that Michelson used.

However the above analysis does not correspond to how the interferometer is actually operated. That analysis does not actually predict fringe shifts for the field of view would be uniformly illuminated, and the observed effect would be a changing level of luminosity rather than fringe shifts. As Miller knew the mirrors must be made slightly non-orthogonal, with the degree of non-orthogonality determining how many fringe shifts were visible in the field of view. Miller experimented with this effect to determine a comfortable number of fringes: not too few and not too many. Hicks [29] developed a theory for this effect — however it is not necessary to be aware of this analysis in using the interferometer: the non-orthogonality reduces the symmetry of the device, and
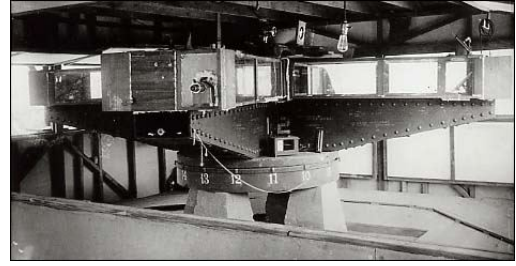
Fig. 3: Miller's interferometer with an effective arm length of $L = 32$ m achieved by multiple reflections. Used by Miller on Mt.Wilson to perform the 1925-1926 observations of absolute motion. The steel arms weighed 1200 kilograms and floated in a tank of 275 kilograms of Mercury. From Case Western Reserve University Archives.

instead of having period of $180°$ the symmetry now has a period of $360°$, so that to (19) we must add the extra term in

$$\Delta t = k^2 \frac{Lv_P^2}{c^3} \cos\left(2(\theta - \psi)\right) + a \cos\left(\theta - \beta\right) . \qquad (20)$$

Miller took this effect into account when analysing his data. The effect is apparent in Fig. 5, and even more so in the Michelson-Morley data in Fig. 4.

The interferometers are operated with the arms horizontal, as shown by Miller's interferometer in Fig. 3. Then in (20) θ is the azimuth of one arm relative to the local meridian, while ψ is the azimuth of the absolute motion velocity projected onto the plane of the interferometer, with projected component v_P. Here the Fitzgerald-Lorentz contraction is a real dynamical effect of absolute motion, unlike the Einstein spacetime view that it is merely a spacetime perspective artifact, and whose magnitude depends on the choice of observer. The instrument is operated by rotating at a rate of one rotation over several minutes, and observing the shift in the fringe pattern through a telescope during the rotation. Then fringe shifts from six (Michelson and Morley) or twenty (Miller) successive rotations are averaged to improve the signal to noise ratio, and the average sidereal time noted, giving the Michelson-Morley data in Fig. 4. or the Miller data like that in Fig. 5. The form in (20) is then fitted to such data by varying the parameters v_P, ψ, a and β, The data from rotations is sufficiently clear, as in Fig. 5, that Miller could easily determine these parameters from a graphical plot.

However Michelson and Morley implicitly assumed the Newtonian value $k = 1$, while Miller used an indirect method to estimate the value of k, as he understood that the Newtonian theory was invalid, but had no other theory for the interferometer. Of course the Einstein postulates, as distinct from Special Relativity, have that absolute motion has no meaning, and so effectively demands that $k = 0$. Using $k = 1$ gives only a nominal value for v_P, being some 8–9 km/s for the Michelson and Morley experiment, and some 10 km/s from Miller; the difference arising from the different latitu-
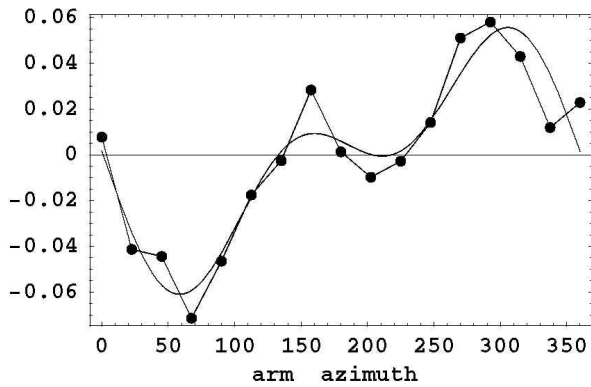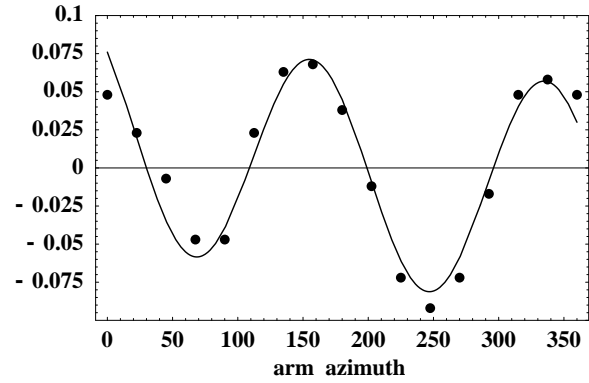
Fig. 4: Example of Michelson-Morley fringe shifts from average of 6 rotations measured every 22.5°, in fractions of a wavelength $\Delta\lambda/\lambda$, vs arm azimuth θ(deg), from Cleveland, Ohio, July 11, 1887 12:00 hrs local time or 7:00 hrs local sidereal time. This shows the quality of the fringe shift data that Michelson and Morley obtained. The curve is the best fit using the form in (20) which includes the Hick's $\cos(\theta - \beta)$ component that is required when the mirrors are not orthognal, and gives $\psi = 140°$, or 40° measured from South, compared to the Miller ψ for August at 7:00 hrs local sidereal time in Fig. 6, and a projected speed of $v_P = 400$ km/s. The Hick's effect is much larger in this data than in the Miller data in Fig. 5.

Fig. 5: Typical Miller rotation-induced fringe shifts from average of 20 rotations, measured every 22.5°, in fractions of a wavelength $\Delta\lambda/\lambda$, vs arm azimuth θ(deg), measured clockwise from North, from Cleveland Sept. 29, 1929 16:24 UT; 11:29 hrs average local sidereal time. The curve is the best fit using the form in (20) which includes the Hick's $\cos(\theta - \beta)$ component that is required when the mirrors are not orthognal, and gives $\psi = 158°$, or 22° measured from South, and a projected speed of $v_P = 351$ km/s. This process was repeated some 8,000 times over days throughout 1925/1926 giving, in part, the data in Fig. 6 and Fig. 18.

des of Cleveland and Mt. Wilson, and from Michelson and Morley taking data at limited times. So already Miller knew that his observations were consistent with those of Michelson and Morley, and so the important need for reproducibility was being confirmed.

3.2 Michelson-Morley experiment

The Michelson and Morley air-mode interferometer fringe shift data was based upon a total of only 36 rotations in July 1887, revealing the nominal speed of some 8–9 km/s when analysed using the prevailing but incorrect Newtonian theory which has $k = 1$ in (20), and this value was known to Michelson and Morley. Including the Fitzgerald-Lorentz dynamical contraction effect as well as the effect of the gas present as in (20) we find that $n_{air} = 1.00029$ gives $k^2 = 0.00058$ for air, which explains why the observed fringe shifts were so small. The example in Fig. 4 reveals a speed of 400 km/s with an azimuth of 40° measured from south at 7:00 hrs local sidereal time. The data is clearly very consistent with the expected form in (20). They rejected their own data on the sole but spurious ground that the value of 8 km/s was smaller than the speed of the Earth about the Sun of 30km/s. What their result really showed was that (i) absolute motion had been detected because fringe shifts of the correct form, as in (20), had been detected, and (ii) that the theory giving $k^2 = 1$ was wrong, that Newtonian physics had failed. Michelson and Morley in 1887 should have announced that the speed of light did depend of the direction of travel, that the speed was relative to an actual physical 3-space. However contrary to their own data they

concluded that absolute motion had not been detected. This bungle has had enormous implications for fundamental theories of space and time over the last 100 years, and the resulting confusion is only now being finally corrected, albeit with fierce and spurious objections.

3.3 Miller interferometer

It was Miller [4] who saw the flaw in the 1887 paper and realised that the theory for the Michelson interferometer must be wrong. To avoid using that theory Miller introduced the scaling factor k, even though he had no theory for its value. He then used the effect of the changing vector addition of the Earth's orbital velocity and the absolute galactic velocity of the solar system to determine the numerical value of k, because the orbital motion modulated the data, as shown in Fig. 6. By making some 8,000 rotations of the interferometer at Mt. Wilson in 1925/26 Miller determined the first estimate for k and for the absolute linear velocity of the solar system. Fig. 5 shows typical data from averaging the fringe shifts from 20 rotations of the Miller interferometer, performed over a short period of time, and clearly shows the expected form in (20) (only a linear drift caused by temperature effects on the arm lengths has been removed — an effect also removed by Michelson and Morley and also by Miller). In Fig. 5 the fringe shifts during rotation are given as fractions of a wavelength, $\Delta\lambda/\lambda = \Delta t/T$, where Δt is given by (20) and T is the period of the light. Such rotation-induced fringe shifts clearly show that the speed of light is different in different directions. The claim that Michelson interferometers, operating in gas-mode, do not produce fringe shifts under
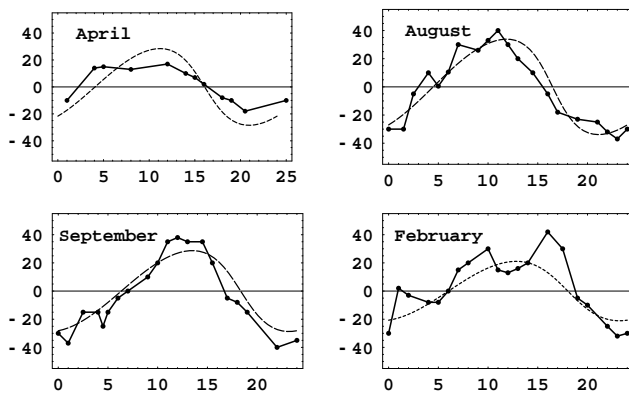
Fig. 6: Miller azimuths ψ, measured from south and plotted against sidereal time in hours, showing both data and best fit of theory giving $v_{cosmic} = 433$ km/s in the direction (RA $= 5.2^{hr}$, Dec $=-67°$), and using $n = 1.000226$ appropriate for the altitude of Mt. Wilson. The azimuth data gives a clearer signal than the speed data in Fig. 18. The data shows that the time when the azimuth ψ is zero tracks sidereal time, with the zero times being approximately 5 hrs and 17 hrs. However these times correspond to very different local times, for from April to August, for example, there is a shift of 8 hrs in the local time for these crossings. This is an enormous effect. Again this is the acid test for light speed anisotropy experiments when allowing the rotation of the Earth to change the orientation of the apparatus. The zero crossing times are when the velocity vector for absolute motion when projected onto the plane of the interferometer lines up with the local meridian. As well we see variations throughout these composite days with the crossing times changing by as much as ± 3 hrs, The same effect, and perhaps even larger, is seen in the Flinders data in Fig. 15. The above plots also show a distinctive signature, namely the change from month to month. This is caused by the vector addition of the Earth's orbital velocity of 30 km/s, the Sun's spatial in-flow velocity of 42 km/s at the Earth's distance and the cosmic velocity changing over a year. This is the effect that Miller used to calibrate his interferometer. However he did not know of the Sun in-flow component. Only after taking account of that effect does this calibration method agree with the results from the calibration method using Special Relativity, as in (20).

rotation is clearly incorrect. But it is that claim that lead to the continuing belief, within physics, that absolute motion had never been detected, and that the speed of light is invariant. The value of ψ from such rotations together lead to plots like those in Fig. 6, which show ψ from the 1925/1926 Miller [4] interferometer data for four different months of the year, from which the RA $= 5.2$ hr is readily apparent. While the orbital motion of the Earth about the Sun slightly affects the RA in each month, and Miller used this effect do determine the value of k, the new theory of gravity required a reanalysis of the data [1, 19], revealing that the solar system has a large observed galactic velocity of some 420 ± 30 km/s in the direction (RA $= 5.2$ hr, Dec $= -67°$). This is different from the speed of 369 km/s in the direction (RA $= 11.20$ hr, Dec $= -7.22°$) extracted from the Cosmic

Microwave Background (CMB) anisotropy, and which describes a motion relative to the distant universe, but not relative to the local 3-space. The Miller velocity is explained by galactic gravitational in-flows [1].

3.4 Other gas-mode Michelson interferometer experiments

Two old interferometer experiments, by Illingworth [11] and Joos [12], used helium, enabling the refractive index effect to be recently confirmed, because for helium, with $n = 1.000036$, we find that $k^2 = 0.00007$. Until the refractive index effect was taken into account the data from the helium-mode experiments appeared to be inconsistent with the data from the air-mode experiments; now they are seen to be consistent [1]. Ironically helium was introduced in place of air to reduce any possible unwanted effects of a gas, but we now understand the essential role of the gas. The data from an interferometer experiment by Jaseja *et al.* [13], using two orthogonal masers with a He-Ne gas mixture, also indicates that they detected absolute motion, but were not aware of that as they used the incorrect Newtonian theory and so considered the fringe shifts to be too small to be real, reminiscent of the same mistake by Michelson and Morley. The Michelson interferometer is a 2nd order device, as the effect of absolute motion is proportional to $(v/c)^2$, as in (20), but 1st order devices are also possible and the coaxial cable experiments described next are in this class. The experimental results and the implications for physics have been extensively reported in [1, 14, 15, 16, 17, 18].

3.5 Coaxial cable speed of EM waves anisotropy experiments

Rather than use light travel time experiments to demonstrate the anisotropy of the speed of light another technique is to measure the one-way speed of radio waves through a coaxial electrical cable. While this not a direct "ideal" technique, as then the complexity of the propagation physics comes into play, it provides not only an independent confirmation of the light anisotropy effect, but also one which takes advantage of modern electronic timing technology.

3.6 Torr-Kolen coaxial cable anisotropy experiment

The first one-way coaxial cable speed-of-propagation experiment was performed at the Utah University in 1981 by Torr and Kolen. This involved two rubidium clocks placed approximately 500 m apart with a 5 MHz radio frequency (RF) signal propagating between the clocks via a buried nitrogen-filled coaxial cable maintained at a constant pressure of 2 psi. Torr and Kolen found that, while the round speed time remained constant within 0.0001% c, as expected from Sect. 2, variations in the one-way travel time were observed. The maximum effect occurred, typically, at the times predicted using the Miller galactic velocity, although
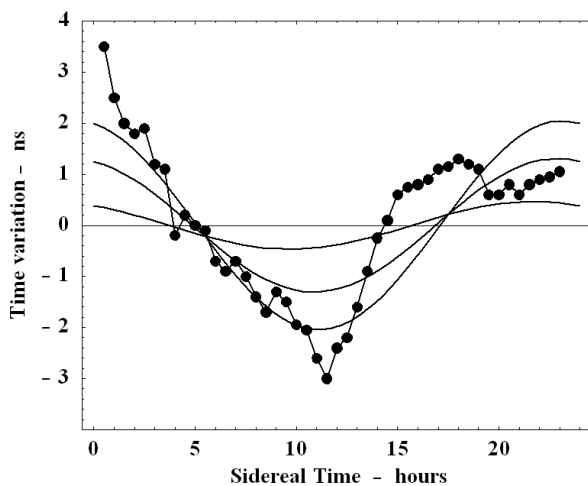
Fig. 7: Data from one day of the Torr-Kolen coaxial cable anisotropy experiment. Smooth curves show variations in travel times when the declination is varied by $\pm 10°$ about the direction (RA $= 5.2^{\text{hr}}$, Dec $= -67°$), for a cosmic speed of 433 km/s. Most importantly the dominant feature is consistent with the predicted local sidereal time.
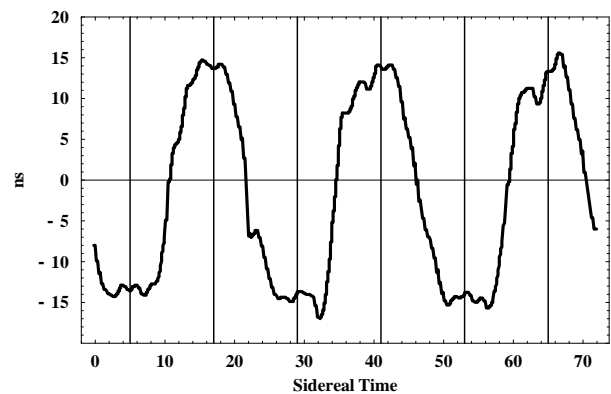

Fig. 8: Variations in twice the one-way travel time, in ns, for an RF signal to travel 1.5 km through a coaxial cable between Rue du Marais and Rue de la Paille, Brussels. An offset has been used such that the average is zero. The cable has a North-South orientation, and the data is $\pm$ difference of the travel times for NS and SN propagation. The sidereal time for maximum effect of ~ 5 hr and ~ 17 hr (indicated by vertical lines) agrees with the direction found by Miller. Plot shows data over 3 sidereal days and is plotted against sidereal time. The fluctuations are evidence of turbulence of gravitational waves.

Torr and Kolen appear to have been unaware of the Miller experiment. As well Torr and Kolen reported fluctuations in both the magnitude, from 1–3 ns, and the time of maximum variations in travel time. These effects are interpreted as arising from the turbulence in the flow of space past the Earth. One day of their data is shown in Fig. 7.

3.7 De Witte coaxial cable anisotropy experiment

During 1991 Roland De Witte performed a most extensive RF coaxial cable travel-time anisotropy experiment, accumulating data over 178 days. His data is in complete agreement with the Michelson-Morley 1887 and Miller 1925/26 interferometer experiments. The Miller and De Witte experiments will eventually be recognised as two of the most significant experiments in physics, for independently and using different experimental techniques they detected essentially the same velocity of absolute motion. But also they detected turbulence in the flow of space past the Earth — none other than gravitational waves. The De Witte experiment was within Belgacom, the Belgium telecommunications company. This organisation had two sets of atomic clocks in two buildings in Brussels separated by 1.5 km and the research project was an investigation of the task of synchronising these two clusters of atomic clocks. To that end 5MHz RF signals were sent in both directions through two buried coaxial cables linking the two clusters. The atomic clocks were caesium beam atomic clocks, and there were three in each cluster: A1, A2 and A3 in one cluster, and B1, B2, and B3 at the other cluster. In that way the stability of the clocks could be established and monitored. One cluster was in a building on Rue du Marais and the second cluster was due south in a building on Rue de la Paille. Digital phase comparators were used to measure changes in times between clocks within the same cluster and also in the one-way propagation times of the RF signals. At both locations the comparison between local clocks, A1-A2 and A1-A3, and between B1-B2, B1-B3, yielded linear phase variations in agreement with the fact that the clocks have not exactly the same frequencies together with a short term and long term phase noise. But between distant clocks A1 toward B1 and B1 toward A1, in addition to the same linear phase variations, there is also an additional clear sinusoidal-like phase undulation with an approximate 24 hr period of the order of 28 ns peak to peak, as shown in Fig. 8. The possible instability of the coaxial lines cannot be responsible for the observed phase effects because these signals are in phase opposition and also because the lines are identical (same place, length, temperature, etc...) causing the cancellation of any such instabilities. As well the experiment was performed over 178 days, making it possible to measure with an accuracy of 25 s the period of the phase signal to be the sidereal day (23 hr 56 min).

Changes in propagation times were observed over 178 days from June 3 to November 27, 1991. A sample of the data, plotted against sidereal time for just three days, is shown in Fig. 8. De Witte recognised that the data was evidence of absolute motion but he was unaware of the Miller experiment and did not realise that the Right Ascensions for minimum/maximum propagation time agreed almost exactly with that predicted using the Miller's direction (RA $= 5.2$ hr, Dec $= -67°$). In fact De Witte expected that the direction of absolute motion should have been in the CMB direction, but
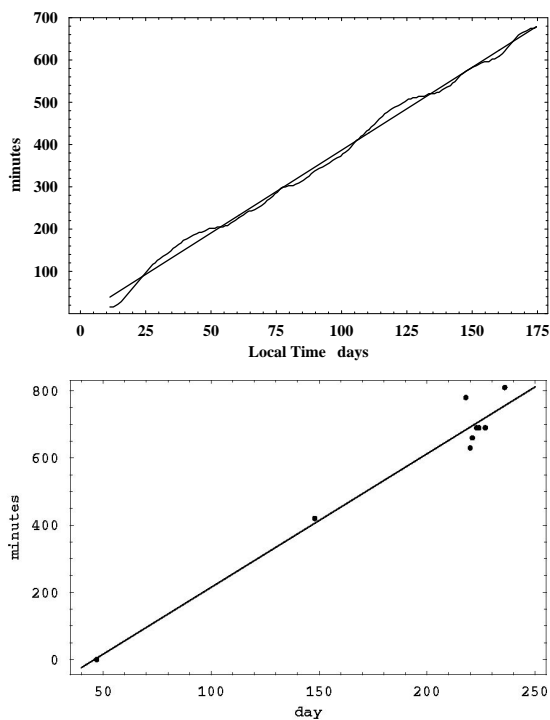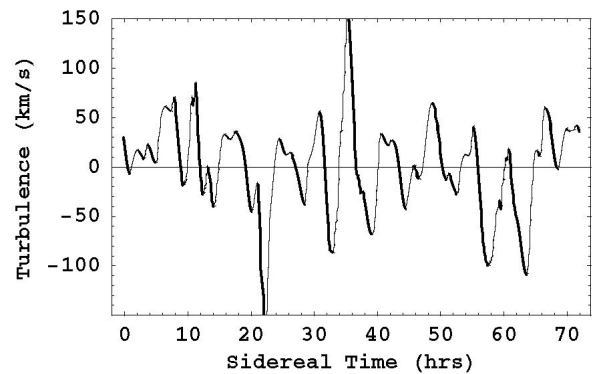
Fig. 10: Shows the speed fluctuations, essentially "gravitational waves" observed by De Witte in 1991 from the measurement of variations in the RF coaxial-cable travel times. This data is obtained from that in Fig. 8 after removal of the dominant effect caused by the rotation of the Earth. Ideally the velocity fluctuations are three-dimensional, but the De Witte experiment had only one arm. This plot is suggestive of a fractal structure to the velocity field. This is confirmed by the power law analysis in [8, 9].

Fig. 9: **Upper:** Plot from the De Witte data of the negative of the drift of the cross-over time between minimum and maximum travel-time variation each day (at $\sim 10\mathrm{hr}\pm 1\mathrm{hr}\,\mathrm{ST}$) versus local solar time for some 180 days. The straight line plot is the least-squares fit to the experimental data, giving an average slope of 3.92 minutes/day. The time difference between a sidereal day and a solar day is 3.93 minutes/day. This demonstrates that the effect is related to sidereal time and not local solar time. **Lower:** Analogous sidereal effect seen in the Flinders experiment. Due to on-going developments the data is not available for all days, but sufficient data is present to indicate a time shift of 3.97 minutes/day. This data also shows greater fluctuations than indicated by the De Witte data, presumably because De Witte used more extensive data averaging.

that would have given the data a totally different sidereal time signature, namely the times for maximum/minimum would have been shifted by 6 hrs. The declination of the velocity observed in this De Witte experiment cannot be determined from the data as only three days of data are available. The De Witte data is analysed in Sect. 4.7 and assuming a declination of $60°$ S a speed of 430 km/s is obtained, in good agreement with the Miller speed and Michelson-Morley speed. So a different and non-relativistic technique is confirming the results of these older experiments. This is dramatic.

De Witte did however report the sidereal time of the cross-over time, that is in Fig. 8 for all 178 days of data. That showed, as in Fig. 9, that the time variations are correlated with sidereal time and not local solar time. A least-squares best fit of a linear relation to that data gives that the cross-over time is retarded, on average, by 3.92 minutes per solar day. This is to be compared with the fact that a sidereal day

is 3.93 minutes shorter than a solar day. So the effect is certainly galactic and not associated with any daily thermal effects, which in any case would be very small as the cable is buried. Miller had also compared his data against sidereal time and established the same property, namely that the diurnal effects actually tracked sidereal time and not solar time, and that orbital effects were also apparent, with both effects apparent in Fig. 6.

The dominant effect in Fig. 8 is caused by the rotation of the Earth, namely that the orientation of the coaxial cable with respect to the average direction of the flow past the Earth changes as the Earth rotates. This effect may be approximately unfolded from the data leaving the gravitational waves shown in Fig. 10. This is the first evidence that the velocity field describing the flow of space has a complex structure, and is indeed fractal. The fractal structure, i. e. that there is an intrinsic lack of scale to these speed fluctuations, is demonstrated by binning the absolute speeds and counting the number of speeds within each bin, as discussed in [8, 9]. The Miller data also shows evidence of turbulence of the same magnitude. So far the data from three experiments, namely Miller, Torr and Kolen, and De Witte, show turbulence in the flow of space past the Earth. This is what can be called gravitational waves. This can be understood by noting that fluctuations in the velocity field induce ripples in the mathematical construct known as spacetime, as in (32). Such ripples in spacetime are known as gravitational waves.

4 Flinders University gravitational wave detector

In February 2006 first measurements from a gravitational wave detector at Flinders University, Adelaide, were taken. This detector uses a novel timing scheme that overcomes the limitations associated with the two previous coaxial cable
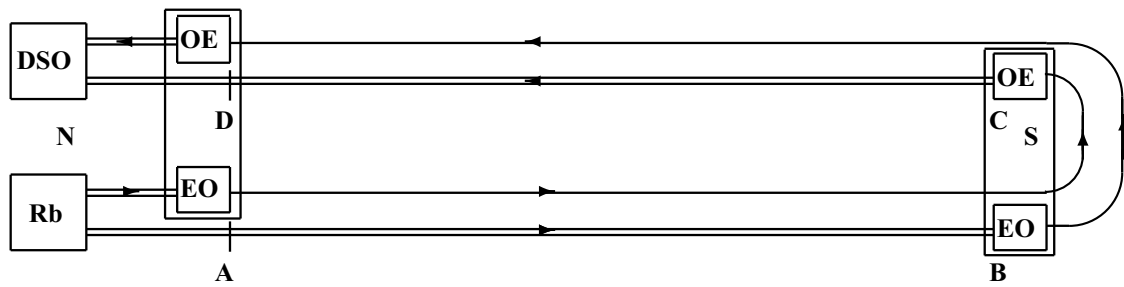
Fig. 11: Schematic layout of the Flinders University Gravitational Wave Detector. Double lines denote coaxial cables, and single lines denote optical fibres. The detector is shown in Fig. 12 and is orientated NS along the local meridian, as indicated by direction D in Fig. 16. Two 10 MHz RF signals come from the Rubidium atomic clock (Rb). The Electrical to Optical converters (EO) use the RF signals to modulate 1.3 μm infrared signals that propagate through the single-mode optical fibres. The Optical to Electrical converters (OE) demodulate that signal and give the two RF signals that finally reach the Digital Storage Oscilloscope (DSO), which measures their phase difference. Pairs of E/O and O/E are grouped into one box. Overall this apparatus measures the *difference* in EM travel time from A to B compared to C to D. All other travel times cancel in principle, though in practice small differences in cable or fibre lengths need to be electronically detected by the looping procedure. The key effects are that the propagation speeds through the coaxial cables and optical fibres respond differently to their absolute motion through space. The special optical fibre propagation effect is discussed in the text. Sections AB and CD each have length 5.0 m. The fibres and coaxial cable are specially manufactured to have negligible variation in travel speed with variation in temperature. The zero-speed calibration point can be measured by looping the arm back onto itself, as shown in Fig. 13, because then the 1st order in v/c effect cancels, and only 2nd order effects remain, and these are much smaller than the noise levels in the system. This detector is equivalent to a one-way speed measurement through a single coaxial cable of length 10 m, with an atomic clock at each end to measure changes in travel times. However for 10 m coaxial cable that would be impractical because of clock drifts. With this set-up the travel times vary by some 25 ps over one day, as shown in Figs.14 and 17. The detector was originally located in the author's office, as shown in Fig. 12, but was later located in an underground laboratory where temperature variations were very slow. The travel time variations over 7 days are shown in Fig. 15.

experiments. The intention in such experiments is simply to measure the one-way travel time of RF waves propagating through the coaxial cable. To that end one would apparently require two very accurate clocks at each end, and associated RF generation and detection electronics.

However the major limitation is that even the best atomic clocks are not sufficiently accurate over even a day to make such measurements to the required accuracy, unless the cables are of order of a kilometre or so in length, and then temperature control becomes a major problem. The issue is that the time variations are of the order of 25 ps per 10 meters of cable. To measure that requires time measurements accurate to, say, 1 ps. But atomic clocks have accuracies over one day of around 100 ps, implying that lengths of around 1 kilometre would be required, in order for the effect to well exceed timing errors. Even then the atomic clocks must be brought together every day to resynchronise them, or use De Witte's method of multiple atomic clocks. However at Flinders University a major breakthrough for this problem was made when it was discovered that unlike coaxial cables, the movement of optical fibres through space does not affect the propagation speed of light through them. This is a very strange effect and at present there is no explanation for it.

4.1 Optical fibre effect

This effect was discovered by Lawrance, Drury and the author, using optical fibres in a Michelson interferometer arrangement, where the effective path length in each arm was

4 metres of fibre. So rather than having light pass through a gas, and being reflected by mirrors, here the light propagates through fibres and, where the mirrors would normally be located, a 180 degree bend in the fibres is formed. The light emerging from the two fibres is directed to a common region on a screen, and the expected fringe shifts were seen. However, and most dramatically, when the whole apparatus was rotated no shift in the fringe shifts was seen, unlike the situation with light passing through a gas as above. This result implied that the travel time in each arm of the fibre was unaffected by the orientation of that arm to the direction of the spatial flow. While no explanation has been developed for this effect, other than the general observation that the propagation speed in optical fibres depends on refractive index profiles and transverse and longitudinal Lorentz contraction effects, as in solids these are coupled by the elastic properties of the solid. Nevertheless this property offered a technological leap forward in the construction of a compact coaxial cable gravitational wave detector. This is because timing information can be sent though the fibres in a way that is not affected by the orientation of the fibres, while the coaxial cables do respond to the anisotropy of the speed of EM radiation in vacuum. Again why they respond in this way is not understood. All we have is that fibres and coaxial cables respond differently. So this offers the opportunity to have a coaxial cable one-way speed measurement set up, but using only one clock, as shown in Fig. 11. Here we have one clock at one end of the coaxial cable, and the arrival time of the RF signal at the other end is used to

Fig. 12: The Flinders University Gravitational Wave Detector located in the author's office, showing the Rb atomic clock and Digital Storage Oscilloscope (DSO) at the Northern end of the NS 5 m cable run. In the foreground is one Fibre Optic Transceiver. The coaxial cables are black, while the optical fibres are tied together in a white plastic sleeve, except just prior to connecting with the transceiver. The second photograph shows the other transceiver at the Southern end. Most of the data reported herein was taken when the detector was relocated to an isolated underground laboratory with the transceivers resting on a concrete floor for temperature stabilisation.
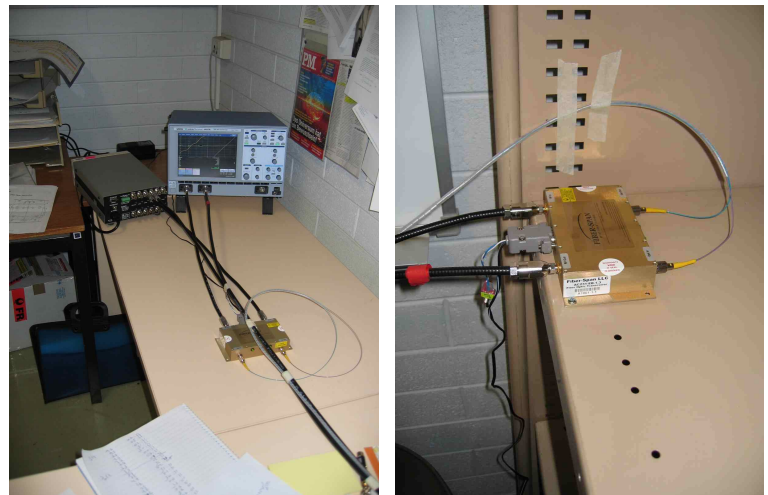
modulate a light signal that returns to the starting end via an optical fibre. The return travel time is constant, being independent of the orientation of the detector arm, because of this peculiar property of the fibres. In practice one uses two such arrangements, with the RF directions opposing one another. This has two significant advantages, (i) that the effective coaxial cable length of 10 meters is achieved over a distance of just 5 meters, so the device is more easily accommodated in a temperature controlled room, and (ii) temperature variations in that room have a smaller effect than expected because it is only temperature differences between the cables that have any net effect. Indeed with specially constructed phase compensated fibre and coaxial cable, having very low speed-sensitivity to temperature variations, the most temperature sensitive components are the optical fibre transceivers (E/O and O/E in Fig. 11).

4.2 Experimental components

Rubidium Atomic Clock: Stanford Research System FS725 Rubidium Frequency Standard. Multiple 10 MHz RF outputs. Different outputs were used for the two arms of the detector.

Digital Storage Oscilloscope: LeCroy WaveRunner WR6051A 500 MHz 2-channel Digital Storage Oscilloscope (DSO). Jitter Noise Floor 2 ps rms. Clock Accuracy $\leqslant 5$ pm. DSO averaging set at 5000, and generating time readings at 440/minute. Further averaged in DSO over 60 seconds, giving stored data stream at one data point/minute. The data was further running-averaged over a 60 minute interval. Connecting the Rb clock directly to the DSO via its two channels showed a long-term accuracy of ± 1 ps rms with this setup.

Fibre Optic Transceivers: Fiber-Span AC231-EB-1-3 RF/ Fiber Optic Transceiver (O/E and E/O). Is a linear extended band (5–2000 MHz) low noise RF fibre optic transceiver for single mode 1.3 μm fibre optic wireless systems, with independent receiver and transmitter. RF interface is a 50Ω connector and the optical connector is a low reflection FC/APC connector. Temperature dependence of phase delay is not

Fig. 13: The Flinders University Gravitational Wave Detector showing the cables formed into a loop. This configuration enables the calibration of the detector. The data from such a looping is shown in Fig. 14, but when the detector was relocated to an isolated underground laboratory.

measured yet. The experiment is operated in a uniform temperature room, so that phase delays between the two transceivers cancel to some extent.

Coaxial Cable: Andrews FSJ1-50A Phase Stabilised 50Ω Coaxial Cable. Travel time temperature dependence is 0.026 ps/m/°C. The speed of RF waves in this cable is $c/n = 0.84 c$, arising from the dielectric having refractive index $n = 1.19$. As well temperature effects cancel because the two coaxial cables are tied together, and so only temperature differences between adjacent regions of the cables can have any effect. If such temperature differences are < 1°C, then temperature generated timing errors from this source should be < 0.3 ps for the 10 m.

Optical Fibre: Sumitomo Electric Industries Ind. Ltd Japan Phase Stabilised Optical Fibre (PSOF) — single mode. Uses Liquid Crystal Polymer (LCP) coated single mode optical fibre, with this coating designed to make the travel time temperature dependence < 0.002 ps/m/°C very small compared

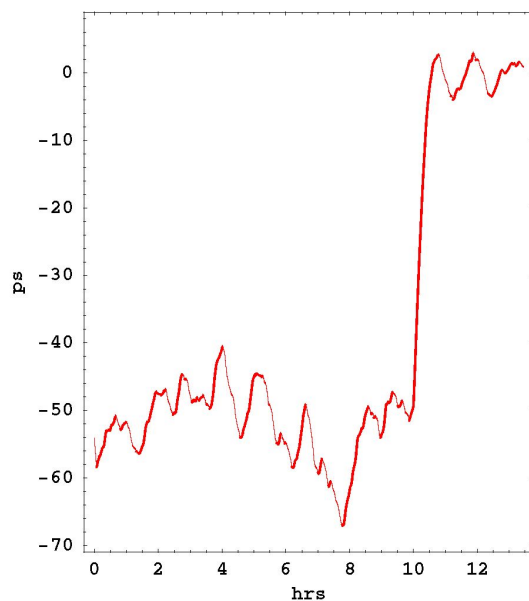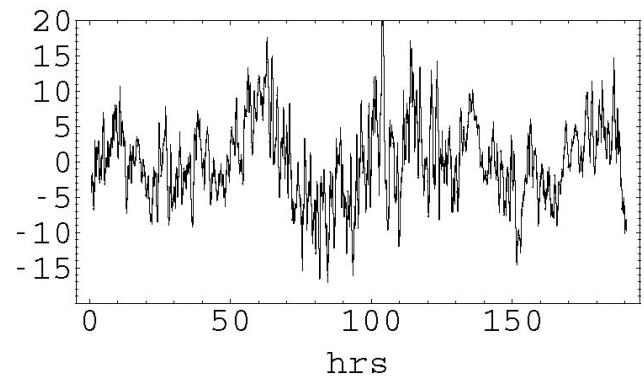Fig. 15: RF travel time variations in picoseconds (ps) for RF waves to travel through, effectively, 10 meters of coaxial cable orientated in a NS direction. The data is plotted against local Adelaide time for the days August 18–25, 2006. The zero of the travel time variations is arbitrary. The data shows fluctuations identified as earth rotation effect and gravitational waves. These fluctuations exceed those from timing errors in the detector.

Fig. 14: The detector arm was formed into a loop at approximately 10:00hrs local time. With the system still operating time averaging causes the trace to interpolate during this procedure, as shown. This looping effect is equivalent to having $\mathbf{v} = 0$, which defines the value of $\Delta\tau$. In plotting the times here the zero time is set so that then $\Delta\tau = 0$. Now the detector is calibrated, and the times in this figure are absolute times. The times are the N to S travel time subtracted from the shorter S to N travel time, and hence are negative numbers. This demonstrates that the flow of space past the Earth is essentially from south to north, as shown in Fig. 16. When the arms are straight, as before 10:00hrs we see that on average the two travel times differ by some 55 ps. This looping effect is a critical test for the detector. It clearly shows the effect of absolute motion upon the RF travel times. As well we see Earth rotation, wave and converter noise effects before 10:00hrs, and converter noise and some small signal after 10:00hrs, caused by an imperfect circle. From this data (24) and (25) give $\delta = 72°$ S and $v = 418$ km/s.

4.3 All-optical detector

The unique optical fibre effect permits an even more compact gravitational wave detector. This would be an all-optical system 1st order in v/c device, with light passing through vacuum, or just air, as well as optical fibres. The travel time through the fibres is, as above, unaffected by orientation of the device, while the propagation time through the vacuum is affected by orientation, as the device is moving through the local space.

In this system the relative time differences can be measured using optical interference of the light from the vacuum and fibre components. Then it is easy to see that the vacuum path length needs only be some 5 cm. This makes the construction of a three orthogonal arm even simpler. It would be a cheap bench-top box. In which case many of these devices could be put into operation around the Earth, and in space, to observe the new spatial-flow physics, with special emphasis on correlation studies. These can be used to observe the spatial extent of the fluctuations. As well space-probe based systems could observe special effects in the flow pattern associated with the Earth-Moon system; these effects are caused by the α-dependent dynamics in (26).

4.4 Results from the Flinders detector

Results from the detector are shown in Fig. 15. There the time variations in picoseconds are plotted against local Adelaide time. The times have an arbitrary zero offset. However most significantly we see ~ 24 hr variations in the travel time, as also seen by De Witte. We also see variations in the times and magnitudes from day to day and within each day. These are the wave effects although as well a component of these is probably also coming from temperature change
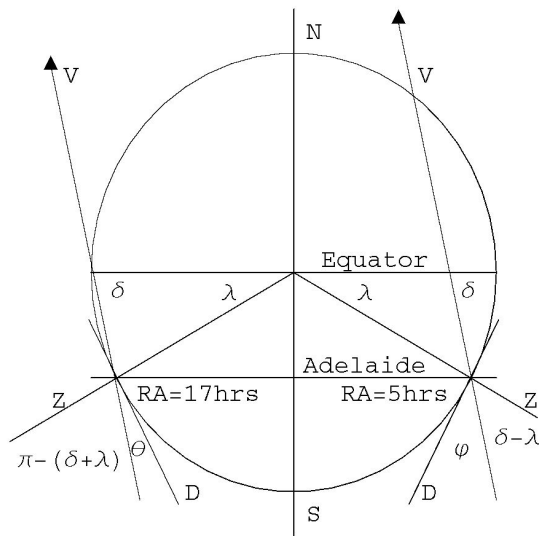
to normal fibres (0.07 ps/m/°C). As well temperature effects cancel because the two optical fibres are tied together, and so only temperature differences between adjacent regions of the fibres can have any effect. If such temperature differences are $<1°$C, then temperature generated timing errors from this source should be <0.02 ps for the 10 m. Now only Furukawa Electric Ind. Ltd Japan manufacturers PSOF.

Photographs of the Flinders detector are shown in Fig. 12. Because of the new timing technology the detector is now small enough to permit the looping of the detector arm as shown in Fig. 13. This enables a key test to be performed as in the loop configuration the signal should disappear, as then the device acts as though it were located at rest in space, because the actual effects of the absolute motion cancel. The striking results from this test are shown in Fig. 14. As well this key test also provides a means of calibrating the detector.

Fig. 16: Profile of Earth, showing NS axis, at Adelaide local sidereal time of RA ≈ 5 hrs (on RHS) and at RA ≈ 17 hrs (on LHS). Adelaide has latitude $\lambda = 38°$ S. Z is the local zenith, and the detector arm has horizontal local NS direction D. The flow of space past the Earth has average velocity **v**. The average direction, $-$**v**, of motion of the Earth through local 3-space has RA ≈ 5 hrs and Declination $\delta \approx 70°$ S. The angle of inclination of the detector arm D to the direction $-$**v** is $\phi = \frac{\pi}{2} - \delta + \lambda$ and $\theta = \delta + \lambda - \frac{\pi}{2}$ at these two RA, respectively. As the Earth rotates the inclination angle changes from a minimum of θ to a maximum of ϕ, which causes the dominant "dip" effect in, say, Fig. 17. The gravitational wave effect is the change of direction and magnitude of the flow velocity **v**, which causes the fluctuations in, say, Fig. 17. The latitude of Mt. Wilson is $34°$ N, and so its latitude almost mirrors that of Adelaide. This is relevant to the comparison in Fig. 18.
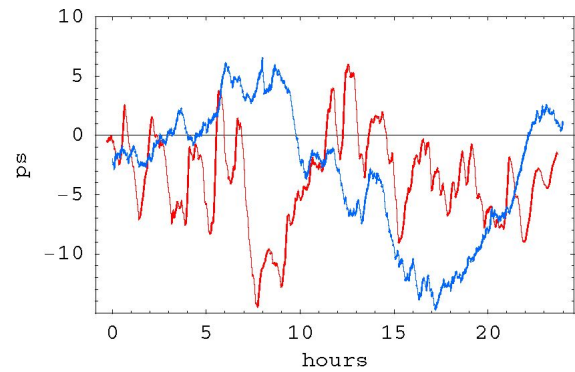

Fig. 17: The superimposed plots show the sidereal time effect. The plot (blue) with the minimum at approximately 17 hrs local Adelaide time is from June 9, 2006, while the plot (red) with the minimum at approximately 8 hrs local time is from August 23, 2006. We see that the minimum has moved forward in time by approximately 9 hrs. The expected shift for this 65 day difference, assuming no wave effects, is 4.3 hrs, but the wave effects shift the RA by some ± 2 hrs on each day as also shown in Fig. 9. This sidereal time shift is a critical test for the confirmation of the detector. Miller also detected variations of that magnitude as shown in Fig. 6. The August 23 data is also shown in Fig. 18, but there plotted against local sidereal time for comparison with the De Witte and Miller data.

effects in the optical fibre transceivers. In time the instrument will be improved and optimised. But we are certainly seeing the evidence of absolute motion, namely the detection of the velocity field, as well as fluctuations in that velocity. To understand the daily variations we show in Fig. 16 the orientation of the detector arm relative to the Earth rotation axis and the Miller flow direction, at two key local sidereal times. So we now have a very inexpensive gravitational wave detector sufficiently small that even a coaxial-cable three-arm detector could easily be located within a building. Three orthogonal arms permit a complete measurement of the spatial flow velocity. Operating such a device over a year or so will permit the extraction of the Sun in-flow component and the Earth in-flow component, as well as a detailed study of the wave effects.

4.5 Right ascension

The sidereal effect has been well established, as shown in Fig. 9 for both the De Witte and Flinders data. Fig. 6 clearly shows that effect also for the Miller data. None of the other anisotropy experiments took data for a sufficiently long

enough time to demonstrate this effect, although their results are consistent with the Right Ascension and Declination found by the Miller, De Witte and Flinders experiments. From some 25 days of data in August 2006, the local Adelaide time for the largest travel-time difference is approximately 10 ± 2 hrs. This corresponds to a local sidereal time of 17.5 ± 2 hrs. According to the Miller convention we give the direction of the velocity vector of the Earth's motion through the space, which then has Right Ascension 5.5 ± 2 hrs. This agrees remarkably well with the Miller and De Witte Right Ascension determinations, as discussed above. A one hour change in RA corresponds to a $15°$ change in direction at the equator. However because the declination, to be determined next, is as large as some $70°$, the actual RA variation of ± 2 hrs, corresponds to an angle variation of some $\pm 10°$ at that declination. On occasions there was no discernible unique maximum travel time difference; this happens when the declination is fluctuating near $90°$, for then the RA becomes ill-defined.

4.6 Declination and speed

Because the prototype detector has only one arm, rather than the ideal case of three orthogonal arms, to determine the declination and speed we assume here that the flow is uniform and time-independent, and use the changing difference in travel times between the two main coaxial cables. Consider Fig. 11 showing the detector schematic layout and Fig. 16
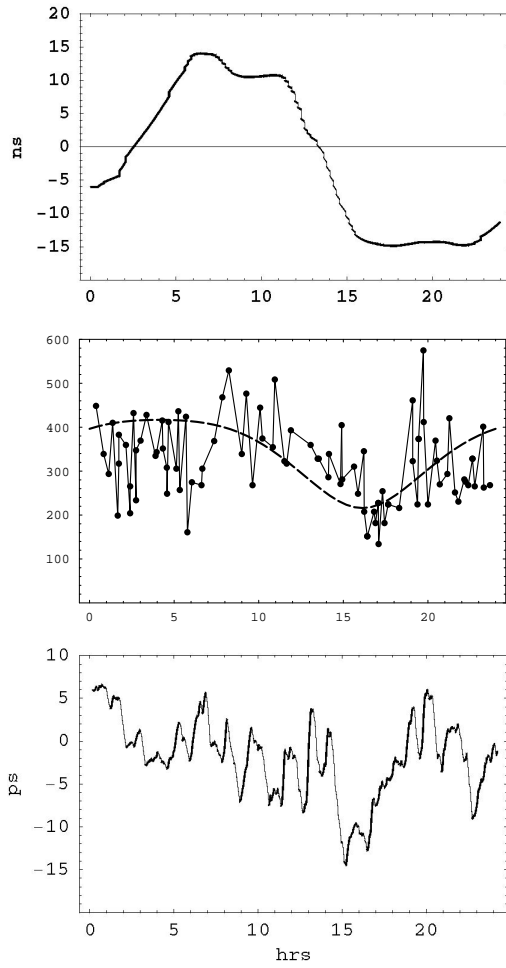
showing the various angles. The travel time in one of the circuits is given by

$$t_1 = \tau_1 + \frac{L_1}{v_c - v \cos(\Phi)} \qquad (21)$$

and that in the other arm by

$$t_2 = \tau_1 + \frac{L_1}{v_c + v \cos(\Phi)} \qquad (22)$$

where Φ is the angle between the detector direction and the flow velocity $\mathbf{v}$, v_c is the speed of radio frequency (RF) electromagnetic waves in the fibre when $\mathbf{v} = 0$, namely $v_c = c/n$ where n is the refractive index of the dielectric in the coaxial cable, and v is the change in that speed caused by the absolute motion of the coaxial cables through space, when the cable is parallel to $\mathbf{v}$. The factor of $\cos(\Phi)$ is just the projection of $\mathbf{v}$ onto the cable direction. The difference in signs in (21) and (22) arises from the RF waves travelling in opposite directions in the two main coaxial cables. The distance L_1 is the arm length of the coaxial cable from A to B, and L_2 is that from C to D. The constant times τ_1 and τ_2 are travel times arising from the optical fibres, the converters, and the coaxial cable lengths not included in L_1 and L_2, particularly the optical fibre travel times. which is the key to the new detector. The effect of the two shorter coaxial cable sections in each arm are included in τ_1 and τ_2 because the absolute motion effects from these arms is additive, as the RF travels in opposite directions through them, and so only contributes at 2nd order.

Now the experiment involves first the measurement of the difference $\Delta t = t_1 - t_2$, giving

$$\Delta t = \tau_1 - \tau_2 + \frac{L_1}{v_c - v \cos(\Phi)} - \frac{L_2}{v_c + v \cos(\Phi)} \approx$$
$$\approx \Delta \tau + (L_1 + L_2) \cos(\Phi) \frac{v}{v_c^2} + \dots \qquad (23)$$

on expanding to lowest order in v/v_c, and where $\Delta \tau \equiv$ $\equiv \tau_1 - \tau_2 + \frac{L_1 - L_2}{v_c}$. Eqn. (23) is the key to the operation of the detector. We see that the effective arm length is $L = $ $= L_1 + L_2 = 10$ m. Over time the velocity vector $\mathbf{v}$ changes, caused by the wave effects and also by the Earth's orbital velocity about the Sun changing direction, and as well the Earth rotates on its axis. Both of these effects cause v and the angle Φ to change. However over a period of a day and ignoring wave effects we can assume that v is unchanging. Then we can determine a declination δ and the speed v by (i) measuring the maximum and minimum values of Δt over a day, which occur approximately 12 hours apart, and (ii) determine $\Delta \tau$, which is the time difference when $v = 0$, and this is easily measured by putting the detector arm into a circular loop, as shown in Fig. 13, so that absolute motion effects cancel, at least to 1st order in v/v_c. Now from Fig. 16 we see that the maximum travel time difference Δt_{max} occurs

Fig. 18: **Top:** De Witte data, with sign reversed, from the first sidereal day in Fig. 8. This data gives a speed of approximately 430km/s. The data appears to have been averaged over more than 1hr, but still shows wave effects. **Middle:** Absolute projected speeds v_P in the Miller experiment plotted against sidereal time in hours for a composite day collected over a number of days in September 1925. Speed data like this comes from the fits as in Fig. 5 using the Special Relativity calibration in (20). Maximum projected speed is 417 km/s, as given in [3, 20, 9]. The data shows considerable fluctuations. The dashed curve shows the non-fluctuating variation expected over one day as the Earth rotates, causing the projection onto the plane of the interferometer of the velocity of the average direction of the space flow to change. If the data was plotted against solar time the form is shifted by many hours. Note that the min/max occur at approximately 5 hrs and 17 hrs, as also seen by De Witte and the new experiment herein. The corresponding variation of the azimuthal phase ψ from Fig. 5 is shown in Fig. 6. **Bottom:** Data from the new experiment for one sidereal day on approximately August 23. We see similar variation with sidereal time, and also similar wave structure. This data has been averaged over a running 1hr time interval to more closely match the time resolution of the Miller experiment. These fluctuations are believed to be real wave phenomena, predicted by the new theory of space [1]. The new experiment gives a speed of 418 km/s. We see remarkable agreement between all three experiments.

when $\Phi = \theta = \lambda + \delta - \frac{\pi}{2}$ in (23), and the minimum Δt_{min} when $\Phi = \phi = \lambda - \delta + \frac{\pi}{2}$, 12 hours later. Then the declination δ may be determined by numerically solving the transcendental equation which follows from these two times from (23)

$$\frac{\cos\left(\lambda + \delta - \frac{\pi}{2}\right)}{\cos\left(\lambda - \delta + \frac{\pi}{2}\right)} = \frac{\Delta t_{max} - \Delta\tau}{\Delta t_{min} - \Delta\tau}. \qquad (24)$$

Subsequently the speed v is obtained from

$$v = \frac{(\Delta t_{max} - \Delta t_{min})\, v_c^2}{L\left(\cos\left(\lambda + \delta - \frac{\pi}{2}\right) - \cos\left(\lambda - \delta + \frac{\pi}{2}\right)\right)}. \qquad (25)$$

In Fig. 14 we show the travel time variations for September 19, 2006. The detector arm was formed into a loop at approximately 10:00 hrs local time, with the system still operating: time averaging causes the trace to interpolate during this procedure, as shown. This looping effect is equivalent to having $\mathbf{v} = 0$, which defines the value of $\Delta\tau$. In plotting the times in Fig. 14 the zero time is set so that then $\Delta\tau = 0$. When the arms are straight, as before 10:00 hrs we see that on average the travel times are some 55 ps different: this is because the RF wave travelling S to N is now faster than the RF wave travelling from N to S. The times are negative because the longer S to N time is subtracted from the shorter N to S travel time in the DSO. As well we see the daily variation as the Earth rotates, showing in particular the maximum effect at approximately 8:00 hrs local time (approximately 15hrs sidereal time) as shown for the three experiments in Fig. 18, as well as wave and converter noise. The trace after 10:00 hrs should be flat — but the variations seen are coming from noise effects in the converters as well as some small signal arising from the loop not being formed into a perfect circle. Taking $\Delta t_{max} = -63$ ps and $\Delta t_{min} = -40$ ps from Fig. 14, (24) and (25) give $\delta = 72°$ S and $v = 418$ km/s. This is in extraordinary agreement with the Miller results for September 1925.

We can also analyse the De Witte data. We have $L = 3.0$ km, $v_c = 200,000$ km/s, from Fig. 8 $\Delta t_{max} - \Delta t_{min} \approx \approx 25$ ns, and the latitude of Brussels is $\lambda = 51°$ N. There is not sufficient De Witte data to determine the declination of $\mathbf{v}$ on the days when the data was taken. Miller found that the declination varied from approximately $60°$ S to $80°$ S, depending on the month. The dates for the De Witte data in Fig. 8 are not known but, for example, a declination of $\delta = 60°$ gives $v = 430$ km/s.

4.7 Gravity and gravitational waves

We have seen that as well as the effect of the Earth rotation relative to the stars, as previously shown by the data from Michelson-Morley, Illingworth, Joos, Jaseja *el al.*, Torr and Kolen, Miller, and De Witte and the data from the new experiment herein, there is also from the experimental data of Michelson-Morley, Miller, Torr and Kolen, De Witte and from the new experiment, evidence of turbulence in this flow of space past the Earth. This all points to the flow velocity field $\mathbf{v}(\mathbf{r}, t)$ having a time dependence over an above that caused simply because observations are taken from the rotating Earth. As we shall now show this turbulence is what is conventionally called "gravitational waves", as already noted [1, 19, 20]. To do this we briefly review the new dynamical theory of 3-space, following [25], although it has been extensively discussed in the related literature. In the limit of zero vorticity for $\mathbf{v}(\mathbf{r}, t)$ its dynamics is determined by

$$\nabla \cdot \left(\frac{\partial \mathbf{v}}{\partial t} + (\mathbf{v} \cdot \nabla)\mathbf{v}\right) + $$
$$+ \frac{\alpha}{8}\left((\mathrm{tr}\, D)^2 - \mathrm{tr}(D^2)\right) = -4\pi G\rho\,, \qquad (26)$$

where ρ is the effective matter/energy density, and where

$$D_{ij} = \frac{1}{2}\left(\frac{\partial v_i}{\partial x_j} + \frac{\partial v_j}{\partial x_i}\right). \qquad (27)$$

Most significantly data from the bore hole g anomaly and from the systematics of galactic supermassive black hole shows that $\alpha \approx 1/137$ is the fine structure constant known from quantum theory [21–24]. Now the Dirac equation uniquely couples to this dynamical 3-space, according to [25]

$$i\hbar \frac{\partial \psi}{\partial t} = -i\hbar\left(c\vec{\alpha}\cdot\nabla + \mathbf{v}\cdot\nabla + \frac{1}{2}\nabla\cdot\mathbf{v}\right)\psi + \beta mc^2\psi \quad (28)$$

where $\vec{\alpha}$ and β are the usual Dirac matrices. We can compute the acceleration of a localised spinor wave packet according to

$$\mathbf{g} \equiv \frac{d^2}{dt^2}\left(\psi(t), \, \mathbf{r}\,\psi(t)\right) \qquad (29)$$

With $\mathbf{v}_R = \mathbf{v}_0 - \mathbf{v}$ the velocity of the wave packet relative to the local space, as $\mathbf{v}_0$ is the velocity relative to the embedding space*, and we obtain

$$\mathbf{g} = \frac{\partial \mathbf{v}}{\partial t} + (\mathbf{v}\cdot\nabla)\mathbf{v} + (\nabla\times\mathbf{v})\times\mathbf{v}_R - \frac{\mathbf{v}_R}{1 - \frac{\mathbf{v}_R^2}{c^2}}\frac{1}{2}\frac{d}{dt}\left(\frac{\mathbf{v}_R^2}{c^2}\right) \quad (30)$$

which gives the acceleration of quantum matter caused by the inhomogeneities and time-dependencies of $\mathbf{v}(\mathbf{r}, t)$. It has a term which limits the speed of the wave packet relative to space to be $< c$. Hence we see that the phenomenon of gravity, including the Equivalence Principle, has been derived from a deeper theory. Apart from the vorticity[†] and relativistic terms in (30) the quantum matter acceleration is the same as that of the structured 3-space [25, 8].

We can now show how this leads to both the spacetime mathematical construct and that the geodesic for matter worldlines in that spacetime is equivalent to trajectories from (30). First we note that (30) may be obtained by extremising the time-dilated elapsed time

$$\tau[\mathbf{r}_0] = \int dt \left(1 - \frac{\mathbf{v}_R^2}{c^2}\right)^{1/2} \qquad (31)$$

---

*See [25] for a detailed explanation of the embedding space concept.
†The vorticity term explains the Lense-Thirring effect [30].

with respect to the particle trajectory $\mathbf{r}_0(t)$ [1]. This happens because of the Fermat least-time effect for waves: only along the minimal time trajectory do the quantum waves remain in phase under small variations of the path. This again emphasises that gravity is a quantum wave effect. We now introduce a spacetime mathematical construct according to the metric

$$ds^2 = dt^2 - \frac{\left(d\mathbf{r} - \mathbf{v}\left(\mathbf{r}, t\right) dt\right)^2}{c^2} = g_{\mu\nu} dx^\mu dx^\nu. \quad (32)$$

Then according to this metric the elapsed time in (31) is

$$\tau = \int dt \sqrt{g_{\mu\nu} \frac{dx^\mu}{dt} \frac{dx^\nu}{dt}}, \quad (33)$$

and the minimisation of (33) leads to the geodesics of the spacetime, which are thus equivalent to the trajectories from (31), namely (30). Hence by coupling the Dirac spinor dynamics to the space dynamics we derive the geodesic formalism of General Relativity as a quantum effect, but without reference to the Hilbert-Einstein equations for the induced metric. Indeed in general the metric of this induced spacetime will not satisfy these equations as the dynamical space involves the α-dependent dynamics, and α is missing from GR*.

Hence so far we have reviewed the new theory of gravity as it emerges within the new physics†. In explaining gravity we discover that the Newtonian theory is actually flawed: this happened because the motion of planets in the solar system is too special to have permitted Newtonian to model all aspects of the phenomenon of gravity, including that the fundamental dynamical variable is a velocity field and not an acceleration field.

We now discuss the phenomenon of the so-called "gravitational waves". It may be shown that the metric in (32) satisfies the Hilbert-Einstein GR equations, in "empty" space, but *only* when $\alpha \to 0$:

$$G_{\mu\nu} \equiv R_{\mu\nu} - \frac{1}{2} R g_{\mu\nu} = 0, \quad (34)$$

where $G_{\mu\nu}$ is the Einstein tensor, $R_{\mu\nu} = R^\alpha_{\mu\alpha\nu}$ and $R = g^{\mu\nu} R_{\mu\nu}$ and $g^{\mu\nu}$ is the matrix inverse of $g_{\mu\nu}$, and the curvature tensor is

$$R^\rho_{\mu\sigma\nu} = \Gamma^\rho_{\mu\nu,\sigma} - \Gamma^\rho_{\mu\sigma,\nu} + \Gamma^\rho_{\alpha\sigma} \Gamma^\alpha_{\mu\nu} - \Gamma^\rho_{\alpha\nu} \Gamma^\alpha_{\mu\sigma}, \quad (35)$$

where $\Gamma^\alpha_{\mu\sigma}$ is the affine connection

$$\Gamma^\alpha_{\mu\sigma} = \frac{1}{2} g^{\alpha\nu} \left(\frac{\partial g_{\nu\mu}}{\partial x^\sigma} + \frac{\partial g_{\nu\sigma}}{\partial x^\mu} - \frac{\partial g_{\mu\sigma}}{\partial x^\nu} \right). \quad (36)$$

Hence the GR formalism fails on two grounds: (i) it does not include the spatial self-interaction dynamics which has

---

*Why the Schwarzschild metric, nevertheless, works is explained in [25].

†Elsewhere it has been shown that this theory of gravity explains the bore hole anomaly, supermassive black hole systematics, the "dark matter" spiral galaxy rotation anomaly effect, as well as the putative successes of GR, including light bending and gravitational lensing.

coupling constant α, and (ii) it very effectively obscures the dynamics, for the GR formalism has spuriously introduced the speed of light when it is completely absent from (26), except on the RHS when the matter has speed near that of c relative to the space‡. Now when wave effects are supposedly extracted from (34), by perturbatively expanding about a background metric, the standard derivation supposedly leads to waves with speed c. This derivation must be manifestly incorrect, as the underlying equation (26), even in the limit $\alpha \to 0$, does not even contain c. In fact an analysis of (26) shows that the perturbative wave effects are fluctuations of $\mathbf{v}(\mathbf{r}, t)$, and travel at approximately that speed, which in the case of the data reported here is some $400\,\mathrm{km/s}$ in the case of earth based detections, i. e. 0.1% of c. These waves also generate gravitational effects, but only because of the α-dependent dynamical effects: when $\alpha \to 0$ we still have wave effects in the velocity field, but that they produce no gravitational acceleration effects upon quantum matter. Of course even in the case of $\alpha \to 0$ the velocity field wave effects are detectable by their effects upon EM radiation, as shown by various gas-mode Michelson interferometer and coaxial cable experiments. Amazingly there is evidence that Michelson-Morley actually detected such gravitational waves as well as the absolute motion effect in 1887, because fluctuations from day to day of their data shows effects similar to those reported by Miller, Torr and Kolen, De Witte, and the new experiment herein. Of course if the Michelson interferometer is operated in vacuum mode it is totally insensitive to absolute motion effects and to the accompanying wave effects, as is the case. This implies that experiments such as the long baseline terrestrial Michelson interferometers are seriously technically flawed as gravitational wave detectors. However as well as the various successful experimental techniques discussed herein for detecting absolute motion and gravitational wave effects a novel technique is that these effects will manifest in the gyroscope precessions observed by the Gravity Probe B satellite experiment [30, 31].

Eqn. (26) determines the dynamical time evolution of the velocity field. However that aspect is more apparent if we write that equation in the integro-differential form

$$\frac{\partial \mathbf{v}}{\partial t} = -\nabla \left(\frac{\mathbf{v}^2}{2} \right) + \\ + G \int d^3 r' \frac{\rho_{DM}(\mathbf{r}', t) + \rho(\mathbf{r}', t)}{|\mathbf{r} - \mathbf{r}'|^3} (\mathbf{r} - \mathbf{r}') \quad (37)$$

in which ρ_{DM} is velocity dependent,

$$\rho_{DM}(\mathbf{r}, t) \equiv \frac{\alpha}{32\pi G} \left((\mathrm{tr} D)^2 - \mathrm{tr}(D^2) \right), \quad (38)$$

and is the effective "dark matter" density. This shows several key aspects: (i) there is a local cause for the time de-

---

‡See [1] for a possible generalisation to include vorticity effects and matter related relativistic effects.

pendence from the ∇ term, and (ii) a non-local action-at-a-distance effect from the ρ_{DM} and ρ terms. This is caused by space being essentially a quantum system, so this is better understood as a quantum non-local effect. However (37) raises the question of where the observed wave effects come from? Are they local effects or are they manifestations of distant phenomena? In the latter case we have a new astronomical window on the universe.

5 Conclusions

We now have eight experiments that independently and consistently demonstrated (i) the anisotropy of the speed of light, and where the anisotropy is quite large, namely 300,000 $\pm$ 420 km/s, depending on the direction of measurement relative to the Milky Way, (ii) that the direction, given by the Right Ascension and Declination, is now known, being established by the Miller, De Witte and Flinders experiments*. The reality of the cosmological meaning of the speed was confirmed by detecting the sidereal time shift over 6 months and more, (iii) that the relativistic Fitzgerald-Lorentz length contraction is a real effect, for otherwise the results from the gas-mode interferometers would have not agreed with those from the coaxial cable experiments, (iv) that Newtonian physics gives the wrong calibration for the Michelson interferometer, which of course is not surprising, (v) that the observed anisotropy means that these eight experiments have detected the existence of a 3-space, (vi) that the motion of that 3-space past the Earth displays wave effects at the level of $\pm$ 30km/s, as confirmed by three experiments, and possibly present even in the Michelson-Morley data.

The Miller experiment was one of the most significant experiments of the 20th century. It meant that a substructure to reality deeper than spacetime had been revealed, that spacetime was merely a mathematical construct and not an aspect of reality. It meant that the Einstein postulate regarding the invariance of the speed of light was incorrect — in disagreement with experiment, and had been so from the beginning. This meant that the Special Relativity effects required a different explanation, and indeed Lorentz had supplied that some 100 years ago: in this it is the absolute motion of systems through the dynamical 3-space that causes SR effects, and which is diametrically opposite to the Einstein formalism. This has required the generalisation of the Maxwell equations, as first proposed by Hertz in 1888 [26]), the Schrödinger and Dirac equations [25, 8]. This in turn has lead to a derivation of the phenomenon of gravity, namely that it is caused by the refraction of quantum waves by the inhomogeneities and time dependence of the flowing patterns within space. That same data has also revealed the in-flow component of space past the Earth towards the Sun

[1], and which also is revealed by the light bending effect observed by light passing close to the Sun's surface [25]. This theory of gravity has in turn lead to an explanation of the so-called "dark matter" effect in spiral galaxies [22], and to the systematics of black hole masses in spherical star systems [25], and to the explanation of the bore hole g anomaly [21, 22, 23]. These effects have permitted the development of the minimal dynamics of the 3-space, leading to the discovery that the parameter that determines the strength of the spatial self-interaction is none other than the fine structure constant, so hinting at a grand unification of space and the quantum theory, along the lines proposed in [1], as an *information theoretic* theory of reality.

These developments demonstrate the enormous significance of the Miller experiment, and the extraordinary degree to which Miller went in testing and refining his interferometer. The author is proud to be extending the Miller discoveries by studying in detail the wave effects that are so apparent in his extensive data set. His work demonstrates the enormous importance of doing novel experiments and doing them well, despite the prevailing prejudices. It was a tragedy and an injustice that Miller was not recognised for his contributions to physics in his own lifetime; but not everyone is as careful and fastidious with detail as he was. He was ignored by the physics community simply because in his era it was believed, as it is now, that absolute motion was incompatible with special relativistic effects, and so it was accepted, without any evidence, that his experiments were wrong. His experiences showed yet again that few in physics actually accept that it is an evidence based science, as Galileo long ago discovered also to his great cost. For more than 70 years this experiment has been ignored, until recently, but even now discussion of this and related experiments attracts hostile reaction from the physics community.

The developments reported herein have enormous significance for fundamental physics — essentially the whole paradigm of 20th century physics collapses. In particular spacetime is now seen to be no more than a mathematical construct, that no such union of space and time was ever mandated by experiment. The putative successes of Special Relativity can be accommodated by the reality of a dynamical 3-space, with time a distinctly different phenomenon. But motion of quantum and even classical electromagnetic fields through that dynamical space explain the SR effects. Lorentz symmetry remains valid, but must be understood as applying only when the space and time coordinates are those arrived at by the Einstein measurement protocol, and which amounts to not making corrections for the effects of absolute motion upon rods and clocks on those measurements. Nevertheless such coordinates may be used so long as we understand that they lead to a confusion of various related effects. To correct the Einstein measurement protocol readings one needs only to have each observer use an absolute motion meter, such as the new compact all-optical devices, as well as a rod and

---

*Intriguingly this direction is, on average, perpendicular to the plane of the ecliptic. This may be a dynamical consequence of the new theory of space.

clock. The fundamental discovery is that for some 100 years physics has failed to realise that a dynamical 3-space exists — it is observable. This contradicts two previous assumptions about space: Newton asserted that it existed, was unchanging, but not observable, whereas Einstein asserted that 3-space did not exist, could not exist, and so clearly must be unobservable. The minimal dynamics for this 3-space is now known, and it immediately explains such effects as the "dark matter" spiral galaxy rotation anomaly, novel black holes with non-inverse square law gravitational accelerations, which would appear to offer an explanation for the precocious formation of spiral galaxies, the bore hole anomaly and the systematics of supermassive black holes, and so on. Dramatically various pieces of data show that the self-interaction constant for space is the fine structure constant. However unlike SR, GR turns out to be flawed but only because it assumed the correctness of Newtonian gravity. The self-interaction effects for space make that theory invalid even in the non-relativistic regime — the famous universal inverse square law of Newtonian gravity is of limited validity. Uniquely linking the quantum theory of matter with the dynamical space shows that gravity is a quantum matter wave effect, so we can't understand gravity without the quantum theory. As well the dynamics of space is intrinsically non-local, which implies a connectivity of reality that far exceeds any previous notions.

References

1. Cahill R. T. Process Physics: From information theory to quantum space and matter. Nova Science, N.Y., 2005.

2. Cahill R. T. and Kitto K. Michelson-Morley experiments revisited. *Apeiron*, 2003, v. 10(2), 104–117.

3. Michelson A. A. and Morley E. W. *Philos. Mag.*, S. 5, 1887, v. 24, No. 151, 449–463.

4. Miller D. C. *Rev. Mod. Phys.*, 1933, v. 5, 203–242.

5. Cahill R. T. Process Physics and Whitehead: the new science of space and time. Whitehead 2006 Conference, Salzburg, to be pub. in proceedings, 2006.

6. Cahill R. T. Process Physics: self-referential information and experiential reality. *To be pub*.

7. Müller H. *et al.* Modern Michelson-Morley experiment using cryogenic optical resonators. *Phys. Rev. Lett.*, 2003, v. 91(2), 020401-1.

8. Cahill R. T. Dynamical fractal 3-space and the generalised Schrödinger equation: Equivalence Principle and vorticity effects. *Progress in Physics*, 2006, v. 1, 27–34.

9. Cahill R. T. The Roland DeWitte 1991 experiment. *Progress in Physics*, 2006, v. 3, 60–65.

10. Torr D. G. and Kolen P. *Precision Measurements and Fundamental Constants*, ed. by Taylor B. N. and Phillips W. D. Nat. Bur. Stand. (U.S.), Spec. Pub., 1984, v. 617, 675–679.

11. Illingworth K. K. *Phys. Rev.*, 1927, v. 3, 692–696.

12. Joos G. *Ann. der Physik*, 1930, Bd. 7, 385.

13. Jaseja T. S. *et al. Phys. Rev.*, v. A133, 1964, 1221.

14. Cahill R. T. The Michelson and Morley 1887 experiment and the discovery of absolute motion. *Progress in Physics*, 2005, v. 3, 25–29.

15. Cahill R. T. The Michelson and Morley 1887 experiment and the discovery of 3-space and absolute motion. *Australian Physics*, Jan/Feb 2006, v. 46, 196–202.

16. Cahill R. T. The detection of absolute motion: from 1887 to 2005. *NPA Proceedings*, 2005, 12–16.

17. Cahill R. T. The speed of light and the Einstein legacy: 1905-2005. *Infinite Energy*, 2005, v. 10(60), 28–27.

18. Cahill R. T. The Einstein postulates 1905-2005: a critical review of the evidence. In: *Einstein and Poincaré: the Physical Vacuum*, Dvoeglazov V. V. (ed.), Apeiron Publ., 2006.

19. Cahill R. T. Quantum foam, gravity and gravitational waves. arXiv: physics/0312082.

20. Cahill R. T. Absolute motion and gravitational effects. *Apeiron*, 2004, v. 11(1), 53–111.

21. Cahill R. T. Gravity, "dark matter" and the fine structure constant. *Apeiron*, 2005, v. 12(2), 144–177.

22. Cahill R. T. "Dark matter" as a quantum foam in-flow effect. In: *Trends in Dark Matter Research*, ed. J. Val Blain, Nova Science, N.Y., 2005, 96–140.

23. Cahill R. T. 3-Space in-flow theory of gravity: Boreholes, blackholes and the fine structure constant. *Progress in Physics*, 2006, v. 2, 9–16.

24. Cahill R. T. Black holes in elliptical and spiral galaxies and in globular clusters. *Progress in Physics*, 2005, v. 3, 51–56.

25. Cahill R. T. Black holes and quantum theory: the fine structure constant connection. *Progress in Physics*, 2006, v. 4, 44–50.

26. Hertz H. On the fundamental equations of electro-magnetics for bodies in motion. *Wiedemann's Ann.*, 1890, v. 41, 369; Electric waves, collection of scientific papers. Dover, N.Y., 1962.

27. Fitzgerald G. F. *Science*, 1889, v. 13, 420.

28. Lorentz H. A. Electric phenomena in a system moving with any velocity less than that of light. In *The Principle of Relativity*, Dover, N.Y., 1952.

29. Hicks W. M. On the Michelson-Morley experiment relating to the drift of the ether. *Phil. Mag.*, 1902, v. 3, 9–42.

30. Cahill R. T. Novel Gravity Probe B frame-dragging effect. *Progress in Physics*, 2005, v. 3, 30–33.

31. Cahill R. T. Novel Gravity Probe B gravitational wave detection. arXiv: physics/0408097.